Luminant

Rafael Flores
Senior Vice President
& Chief Nuclear Officer
Rafael.Flores@Luminant.com

Luminant Power
P O Box 1002
6322 North FM 56
Glen Rose, TX 76043

T 254 897 5590
C 817 559 0403
F 254 897 6652

CP-201500430
TXX-15066

Ref. # 10CFR50.55a(z)(1)

April 22, 2015

U. S. Nuclear Regulatory Commission
ATTN: Document Control Desk
Washington, DC 20555

SUBJECT: COMANCHE PEAK NUCLEAR POWER PLANT
DOCKET NO. 50-445
RELIEF REQUEST 1B3-4 FOR UNIT 1 INSERVICE INSPECTION FOR APPLICATION OF AN ALTERNATIVE TO THE ASME BOILER AND PRESSURE VESSEL CODE SECTION XI EXAMINATION REQUIREMENTS FOR REACTOR PRESSURE VESSEL HEAD PENETRATON WELD INSPECTION FREQUENCY
(2007 EDITION OF ASME CODE, SECTION XI, 2008 ADDENDA
THIRD INTERVAL START DATE: AUGUST 13, 2010
THIRD INTERVAL END DATE: AUGUST 12, 2020)

Dear Sir or Madam:

Pursuant to 10 CFR 50.55a(z)(1), Luminant Generation Company, LLC (Luminant Power) is submitting Relief Request 1B3-4 (see attachment) for Comanche Peak Unit 1 for the third ten year inservice inspection interval. Luminant Power is requesting an alternative for the reactor pressure vessel head penetration weld inspection frequency as specified in Code Case N-729-1 from 10 calendar years to 15 calendar years. The alternative process provides an acceptable level of quality and safety.

Luminant Power requests approval of this relief request by December 15, 2015, to support the upcoming Comanche Peak Unit 1 refueling outage.

This communication contains no new licensing basis commitments regarding Comanche Peak Unit 1. Should you have any questions, please contact Mr. Jack Hicks at (254) 897-6725.

Sincerely,

Luminant Generation Company LLC

Rafael Flores

By: Fred W. Madden
Fred W. Madden
Director, External Affairs

A047
NRR

Attachment – Relief Request 1B3-4 for Code Case N-729-1 Reactor Pressure Vessel Head Penetration Weld Inspection Frequency Extension

c - Marc L. Dapas, Region IV (without Attachment 9.2, MRP-375)
Balwant K. Singal, NRR (without Attachment 9.2, MRP-375)
Resident Inspectors, Comanche Peak (without Attachment 9.2, MRP-375)
Robert Free, TDLR (without Attachment 9.2, MRP-375)
Jack Ballard, ANII, Comanche Peak (without Attachment 9.2, MRP-375)

COMANCHE PEAK NUCLEAR POWER PLANT UNIT 1
Relief Request Number 1B3-4
Code Case N-729-1 RPV Head Penetration Weld Inspection Frequency Extension
(Third 10-Year ISI Interval Start Date: August 13, 2010)

1. **ASME Code Component Affected:**

The affected components are American Society of Mechanical Engineers (ASME) Class 1 Pressurized Water Reactor (PWR) Reactor Vessel Upper Head (Closure Head) nozzles and partial-penetration welds fabricated with Primary Water Stress Corrosion Cracking (PWSCC) resistant materials. Comanche Peak Nuclear Power Plant Unit 1 (CPNPP1) penetration tubes and vent pipe are fabricated from Alloy 690 with Alloy 52/152 attachment welds.

2. **Applicable Code Edition and Addenda:**

CPNPP1 is currently using the 2007 Edition through 2008 Addenda of the ASME Section XI Boiler and Pressure Vessel Code. However, Code Case N-729-1 [Reference 1], as referenced in 10CFR50.55a(g)(6)(ii)(D), is the applicable code document for this Relief Request.

3. **Applicable Code Requirement:**

10CFR50.55a(g)(6)(ii)(D) required licensees of existing, operating pressurized water reactors (PWR) by December 31, 2008 to implement the requirements of ASME Code Case N-729-1. Code Case N-729-1, Inspection Item B4.40 for ASME Class 1 PWR Reactor Pressure Vessel Closure Head (RPVCH) nozzles and partial-penetration welds fabricated with PWSCC-resistant materials, requires volumetric and/or surface examination of essentially 100% of the required volume or equivalent surface of the nozzle tube each inspection interval (nominally 10 calendar years). A demonstrated volumetric or surface leak assessment through all J-groove welds is required.

4. **Reason for Request: Acceptable level of quality and safety (10CFR50.55a(z)(1)):**

Treatment of Alloy 690 RPVCH nozzles in Code Case N-729-1 was intended to be conservative and subject to reassessment once additional laboratory data and plant experience on the performance of Alloy 690 and Alloy 52/152 weld metals became available. Using plant and laboratory data, EPRI document MRP-375 [Reference 2] was developed to support a technically based volumetric/surface re-examination interval using appropriate analytical tools. This technical basis demonstrates that the re-examination interval can be extended to the requested interval length while maintaining an acceptable level of quality and safety. Therefore, Luminant is requesting approval of this alternative to allow the use of the ISI interval extension for the affected CPNPP1 components.

5. **Proposed Alternative and Basis for Use:**

In the Spring of 2007 (1RF12) the CPNPP1 RPVCH with Alloy 600/182/82 nozzles and partial-penetration welds was replaced with a new RPVCH utilizing Alloy 690/52/152 nozzles and partial-penetration welds. Luminant is requesting extension of the requirements of Code Case N-729-1, Inspection Item B4.40 for performing volumetric/surface examinations of the CPNPP1 RPVCH. Specifically, this would allow volumetric/surface examinations currently scheduled for the Spring of 2016 (1RF18) to be moved to the Spring of 2022 (1RF22). This request applies to the inspection frequencies not the inspection techniques, as the inspection techniques may change with later editions of ASME Section XI and 10CFR50.55a.

The basis for the inspection frequency for ASME Code Case N-729-1 comes, in part, from the analysis of laboratory and plant data presented in report MRP-111 [Reference 3], which was

COMANCHE PEAK NUCLEAR POWER PLANT UNIT 1
Relief Request Number 1B3-4
Code Case N-729-1 RPV Head Penetration Weld Inspection Frequency Extension
(Third 10-Year ISI Interval Start Date: August 13, 2010)

summarized in the safety assessment for RPVCHs in MRP-110 [Reference 4]. The material improvement factor for PWSCC of Alloy 690/52/152 materials over that of mill-annealed Alloys 600 and 182 was shown by this report to be on the order of 26 or greater.

Further evaluations were performed to demonstrate the acceptability of extending the inspection intervals for Code Case N-729-1, Inspection Item B4.40 components and were documented in MRP-375. In summary, the basis for extending the intervals from nominally 10 calendar years to nominally 15 calendar years is based on plant service experience, factor of improvement studies using laboratory data, deterministic study results, and probabilistic study results.

Per MRP-375, much of the laboratory data indicated a factor of improvement of 100 for Alloys 690/52/152 versus Alloys 600/182/82 (for equivalent temperature and stress conditions) in terms of crack growth rates (CGR). In addition, laboratory and plant data demonstrate a factor of improvement in excess of 20 in terms of the time to PWSCC initiation. This reduced susceptibility to PWSCC initiation and growth supports elimination of all volumetric exams throughout the plant service period. However, since work is still ongoing to determine the performance of Alloy 690/52/152 metals, the determination of the proposed inspection interval is based on conservatively smaller factors of improvement.

Deterministic calculations demonstrate that the alternative volumetric re-examination schedule is sufficient to detect any PWSCC before it could develop into a safety significant circumferential flaw that approaches the large size (i.e., more than 300°) necessary to produce a nozzle ejection. The deterministic calculations also demonstrate that any base metal PWSCC would likely be detected prior to a through-wall flaw occurring. Probabilistic calculations based on a Monte Carlo simulation model of the PWSCC process, including PWSCC initiation, crack growth, and flaw detection via ultrasonic testing show a substantially reduced effect on nuclear safety compared to a head with Alloy 600 nozzles examined per current requirements. [See Reference 2]

Service Experience

As documented in MRP-375, the resistance of Alloy 690 and corresponding weld metals Alloy 52 and 152 is demonstrated by the lack of PWSCC indications reported in these materials, in up to 24 calendar years of service for thousands of Alloy 690 steam generator tubes, and more than 20 calendar years of service for thick-wall and thin-wall Alloy 690 applications. This excellent operating experience includes service at pressurizer and hot-leg temperatures and includes Alloy 690 wrought base metal and Alloy 52/152 weld metal. This experience includes ISI volumetric/surface examinations performed in accordance with ASME Code Case N-729-1 on 13 of the 40 replacement RPVCHs currently operating in the U.S. fleet. This data supports a factor of improvement of at least 5 to 20 to detectable PWSCC when compared to service experience of Alloy 600 in similar applications.

Factors of Improvement (FOI) for Crack Initiation

Alloy 690 is highly resistant to PWSCC due to its approximate 30% chromium content. Per MRP-115 [Reference 5], it was noted that Alloy 82 CGR is 2.6 slower than Alloy 182. There is no strong evidence for a difference in Alloy 52 and 152 CGRs. Therefore, data used to develop factors of improvement for Alloy 52/152 were referenced against the base case Alloy 182, as Alloy 182 is more susceptible to crack initiation and growth when compared to Alloy 82. A simple factor of improvement approach was applied in a conservative manner in MRP-375 using multiple data. As

COMANCHE PEAK NUCLEAR POWER PLANT UNIT 1
Relief Request Number 1B3-4
Code Case N-729-1 RPV Head Penetration Weld Inspection Frequency Extension
(Third 10-Year ISI Interval Start Date: August 13, 2010)

discussed in MRP-375, laboratory and plant data demonstrate a factor of improvement in excess of 20 in terms of the time to PWSCC initiation.

Factors of Improvement (FOI) for Crack Growth

MRP-375 also assessed laboratory PWSCC crack growth rate data for the purpose of assessing FOI values for growth. Data analyzed to develop a conservative factor of improvement include laboratory specimens with substantial levels of cold work, which tends to increase the CGR. However, similar processing, fabrication, and welding practices apply to the original (Alloy 600) and replacement (Alloy 690) components. MRP-375 considered the most current worldwide set of available PWSCC CGR data for Alloy 690/52/152 materials.

Figure 3-2 of MRP-375, compares data from Alloy 690 specimens with less than 10% cold work and the statistical distribution from MRP-55 [Reference 6] describing the material variability in CGR for Alloy 600. Most of the laboratory comparisons were bounded by a factor of improvement of 20, and all were bounded by a factor of 10. Most data support a FOI of much larger than 20. This is similar for testing of the Alloy 690 Heat Affected Zone (HAZ) as shown in Figure 3-4 of MRP-375 and for the Alloy 52/152 weld metal as shown in Figure 3-6 of MRP-375. Based on the data, it is conservative to assume a FOI of between 10 and 20 for CGRs.

Design Features Further Increasing the Resistance of the CPNPP1 Replacement Heads to PWSCC

Methods were used to reduce residual stress caused by J-groove welding by applying a narrow gap for weld preparation (less weld deposit) and the use of automated welding to reduce residual stresses. These methods substantially reduce PWSCC susceptibility beyond that assumed in the generic MRP-375 study, resulting in additional assurances that the CPNPP1 head can be operated for 15 years prior to its next volumetric/surface examination with an acceptable level of quality and safety.

Deterministic Modeling

A deterministic crack growth evaluation is commonly applied to assess PWSCC risks for specific components and operating conditions. The deterministic evaluation is intended to demonstrate the time from an assumed initial flaw to some adverse condition. Deterministic crack modeling results were presented in MRP-375 for previous references in which both growth of part-depth surface flaws and through-wall circumferential flaws were evaluated and normalized to an adjusted growth of 613 degrees Fahrenheit (°F) to bound the PWR fleet. The time for through-wall crack growth in Alloy 600 nozzle tube material, when adjusted to a bounding temperature of 613°F, ranged between 1.9 and 3.8 Effective Full Power Years (EFPY). Assuming a growth FOI of 10 to 20 as previously established for Alloy 690/52/152 materials, the median time for through-wall growth was 37.3 EFPY. In a similar manner, crack growth results for through-wall circumferential flaws were tabulated and adjusted to a temperature of 613°F. Applying a growth FOI of 20 resulted in a median time of 176 EFPYs for growth of a through-wall circumferential flaw to 300 degrees of circumferential extent. The results of the generic evaluation are summarized in Table 4-1 of MRP-375. All cases were bounding and support an inspection interval greater than is being proposed. It is important to note that CPNPP1 RPVCH temperature is 561 °F (Use 562 °F in Table 6-1 of Reference 8) and well within the bounds of the assumptions.

Note that for a head with Alloy 600 nozzles and Alloy 82/182 attachment welds operating at a temperature of 562 °F, the re-inspection years (RIY) = 2.25 constraint on the volumetric/surface re-

COMANCHE PEAK NUCLEAR POWER PLANT UNIT 1
Relief Request Number 1B3-4
Code Case N-729-1 RPV Head Penetration Weld Inspection Frequency Extension
(Third 10-Year ISI Interval Start Date: August 13, 2010)

examination interval of ASME Code Case N-729-1 correspond to an interval of 6.034 EFPYs. Thus, a nominal interval of 15 calendar years for the CPNPP1 replacement head implies a FOI of approximately 2.5 versus the standard interval for heads with Alloy 600 nozzles. It is emphasized that the FOI of 2.5 (reference Attachment 1) implied by the requested extension period represents a level of reduction in PWSCC crack growth rate versus that for Alloys 600/82/182 that is completely bounded on a statistical basis by the laboratory data compiled in EPRI MRP-375. Given the lack of PWSCC cracks detected to date in any PWR plant applications of Alloys 690/52/152, the simple FOI assessment clearly supports the requested period of extension.

Deterministic calculations performed in MRP-375 demonstrate that the alternative volumetric re-examination interval is sufficient to detect PWSCC before it could develop into a safety significant circumferential flaw that approaches the large size necessary to produce a nozzle ejection. The deterministic calculations also demonstrate that any base metal PWSCC would likely be detected prior to a through-wall flaw occurring.

Probability of Cracking or Through-Wall Leaks

Probabilistic calculations are based on a Monte Carlo simulation model of the PWSCC process, including PWSCC initiation, PWSCC crack growth, and flaw detection via ultrasonic testing and visual examinations for leakage. The basic structure of the probabilistic model is similar to that used in the MRP-105 [Reference 7] technical basis report for inspection requirements for heads with Alloy 600 nozzles, but the current approach, as seen in MRP-375, includes more detailed modeling of surface flaws (including multiple flaw initiation for each nozzle on base metal and weld surfaces) and the initiation module has been calibrated to consider the latest set of experience for U.S. heads. The outputs of the probabilistic model are leakage frequency (i.e., frequency of through-wall cracking) and nozzle ejection frequency. Even assuming conservatively small factors of improvement for the crack growth rate for the replacement nickel-base alloys (with no credit for improved resistance to initiation), the probabilistic results with the alternative inspection regime show:

1. An effect on nuclear safety substantially within the acceptance criterion applied in the MRP-117 [Reference 8] technical basis for Alloy 600 heads, and

2. A substantially reduced effect on nuclear safety compared to that for a head with Alloy 600 nozzles examined per current requirements.

Furthermore, the results confirm a low probability of leakage if some modest credit is taken for improved resistance to PWSCC initiation compared to that for Alloys 600 and 182.

Conclusion

In summary, the basis for extending the intervals from nominally 10 calendar years to nominally 15 calendar years is based on plant service experience, factor of improvement studies using laboratory initiation and growth data, deterministic modeling, and probabilistic study results. The results of the analysis show that the alternative proposed frequency results in a substantially reduced effect on nuclear safety when compared to a head with Alloy 600 nozzles and examined per the current requirements. The proposed interval will continue to provide reasonable assurance of quality and safety.

COMANCHE PEAK NUCLEAR POWER PLANT UNIT 1
Relief Request Number 1B3-4
Code Case N-729-1 RPV Head Penetration Weld Inspection Frequency Extension
(Third 10-Year ISI Interval Start Date: August 13, 2010)

Additional assurance of structural integrity is provided by the design features of the CPNPP1 head such as the narrow weld preparation design, less residual stresses due to automated welding and the low operating temperature, and by the results from 2006 pre-service volumetric/surface examinations with no detectable defects. Furthermore, the visual examinations and acceptance criteria as required by Item B4.30 of Table 1 of ASME Code Case N-729-1 are not affected by this request and will continue to be performed on a frequency of every third refueling outage or 5 calendar years, whichever is less. As discussed in Section 5.2.3 of MRP-375, the visual examination requirement of the outer surface of the head for evidence of leakage supplements the volumetric/surface examination requirement and conservatively addresses the potential concern for boric acid corrosion of the low-alloy steel head due to PWSCC leakage. Visual examinations were completed on CPNPP1 head during the Fall 2011 refueling outage (1RF15) with no indication of leakage and must be conducted again by the Spring 2016 refueling outage (1RF18).

For the reasons noted above, it is requested that the NRC authorize this proposed alternative in accordance with 10CFR50.55a(z)(1) as the alternative provides an acceptable level of quality and safety.

6. Duration of Proposed Alternative:

The 3rd and 4th ISI Intervals, because utilizing the proposed examination frequency will require the examination to be performed in the 4th ISI Interval.

7. Precedents:

1. ML14283A045 supplemented by ML15069A227 - ASME Section XI Inservice Inspection Program Proposed Inservice Inspection Alternative N2-14 NDE-002, North Anna Power Station Unit 2.

8. Reference:

1. Code Case N-729-1 Alternative Examination Requirements for PWR Reactor Vessel Upper Heads With Nozzles Having Pressure-Retaining Partial-Penetration Welds Section XI, Division 1

2. MRP-375, Technical Basis for Re-examination Interval Extension for Alloy 690 PWR Reactor Vessel Top Head Penetration Nozzles

3. MRP-111, Materials Reliability Program: Resistance to Primary Water Stress Corrosion Cracking of Alloys 690, 52, and 152 in Pressurized Water Reactors

4. MRP-110, Materials Reliability Program: Reactor Vessel Closure Head Penetration Safety Assessment for U.S. Pressurized Water Reactor (PWR) Plants

5. MRP-115, Materials Reliability Program: Crack Growth Rates for Evaluating Primary Water Stress Corrosion Cracking (PWSCC) of Alloy 82, 182, and 132 Welds

6. MRP-55, Materials Reliability Program (MRP) Crack Growth Rates for Evaluating Primary Water Stress Corrosion Cracking (PWSCC) of Thick-Wall Alloy 600 Materials

COMANCHE PEAK NUCLEAR POWER PLANT UNIT 1
Relief Request Number 1B3-4
Code Case N-729-1 RPV Head Penetration Weld Inspection Frequency Extension
(Third 10-Year ISI Interval Start Date: August 13, 2010)

7. MRP-105, Materials Reliability Program: Probabilistic Fracture Mechanics Analysis of PWR Reactor Pressure Vessel Top Head Nozzle Cracking

8. MRP-117, Materials Reliability Program Inspection Plan for Reactor Vessel Closure Head Penetrations in U.S. PWR Plants

9. Attachments:

1. Minimum Factor of Improvement (FOI) Calculation for CPNPP1

2. MRP-375, Technical Basis for Re-examination Interval Extension for Alloy 690 PWR Reactor Vessel Top Head Penetration Nozzles

Attachment to TXX-15066
Attachment 9.1

Minimum Factor of Improvement (FOI) Calculation for CPNPP1

Minimum Factor of Improvement (FOI) Calculation for CPNPP1

Minimum FOI Implied by Requested Inspection Interval
ASME Code Case N-729-1 is based upon conclusions reached [Reference 3] that a re-examination interval between volumetric/surface examinations of one 24-month operating cycle is acceptable for a head with Alloy 600 nozzles and operating at a temperature of 605°F. The inspection period for heads with Alloy 690 nozzles in Code Case N-729-1 is a nominal 10 years, which represents a minimum implied factor of improvement (FOI) of 5 over Alloy 600.

Per the technical basis documents for ASME Code Case N-729-1 for heads with Alloy 600 nozzles ([Reference 2], [Reference 3], and [Reference 4]), the effect of differences in operating temperature on the required volumetric/surface re-examination interval for heads with Alloy 600 nozzles can be easily addressed on the basis of the Re-Inspection Years (RIY) parameter. The RIY parameter adjusts the effective full power years (EFPYs) of operation between inspections for the effect of head operating temperature using the thermal activation energy appropriate to PWSCC crack growth. For heads with Alloy 600 nozzles, ASME Code Case N-729-1 as conditioned by 10CFR50.55a(g)(6)(ii)(D)(2) limits the interval between subsequent volumetric/surface inspections to RIY= 2.25. The RIY parameter, when calculated for a head temperature of 562°F [Table 6-1 of Reference 3], limits the time available for potential crack growth between inspections to 6.034 EFPY.

U.S. PWR inspection experience for heads with Alloy 600 nozzles has confirmed that the RIY = 2.25 interval results in a suitably conservative inspection program. There have been no reports of nozzle leakage or of safety-significant circumferential cracking subsequent to the time that the Alloy 600 nozzles in a given head were first examined by non-visual inservice non-destructive examination ([Reference 8] and [Reference 9]).

Given that the allowed re-inspection interval for an original head with alloy 600/82/182 material operating at 562°F is 6.034 EFPY [Table 6-1 of Reference 3], the implied FOI needed to support a 15-yr inspection interval is equal to 15 divided by 6.034 which is approximately 2.5.

The necessary factor of improvement needed to support a 15-yr inspection interval for the CPNPP1 RPVCH nozzles is 2.5. As determined above, the minimum implied factor of improvement between Alloy 600 nozzles and Alloy 690 nozzles as deduced from Code Case N-729-1 is 5. Therefore, this simple factor of improvement comparison indicates that a 15-yr inspection interval for the CPNPP1 RPVCH Alloy 690/52/152 nozzles is acceptable.

References:

1. *ASME Code Case N-729-1*, "Alternative Examination Requirements for PWR Reactor Vessel Upper Heads With Nozzles l-laving Pressure-Retaining Partial-Penetration Welds, Section XI, Division 1," Approved March 28, 2006.

Minimum Factor of Improvement (FOI) Calculation for CPNPP

2. *MRP-110NP*, Materials Reliability Program: Reactor Vessel Closure Head Penetration Safety Assessment for U.S. PWR Plants, EPRI, Palo Alto, CA; 2004. 1009807-NP. [ML041680506]

3. *MRP*-117, Materials Reliability Program: Inspection Plan for Reactor Vessel Closure Head Penetrations in U.S. PWR Plants, EPRI, Palo Alto, CA: 2004. 1007830. [freely available at www.epri.com: NRC ADAMS Accession No. ML043570129]

4. *MRP*-105NP, Materials Reliability Program: Probabilistic Fracture Mechanics Analysis of PWR Reactor Pressure Vessel Top Head Nozzle Cracking, EPRI, Palo Alto, CA; 2004.1007834. [ML041680489]

5. *NUREG/CR-7137, ANL-10/36*, U.S. NRC, Stress Corrosion Cracking in Nickel-Base Alloys 690 and 152 Weld in Simulated PWR Environment - 2009, published June 2012. [ML12199A415]

6. *MRP-237 Rev.* 2, Materials Reliability Program: Resistance of Alloys 690, 152, and 52 to Primary Water Stress Corrosion Cracking: Summary of Findings between 2008 and 2012 from Completed and Ongoing Test Programs, EPRI, Palo Alto, CA: 2013. 3002000190. [freely available at www.epri.coml

7. M. B. Toloczko, M. J. Olszta, and S. M. Bruemmer, "One Dimensional Cold Rolling Effects on Stress Corrosion Crack Growth in Alloy 690 Tubing and Plate Materials," 15th International Conference on Environmental Degradation of Materials in Nuclear Power Systems - Water Reactors, TMS (The Minerals, Metals & Materials Society), 2011.

8. *EPRI MRP Letter 2011-034*, 'Tcold RV Closure Head Nozzle Inspection Impact Assessment," dated December 21, 2011. [ML12009A042]

9. G. White, V. Moroney, and C. Harrington, "PWR Reactor Vessel Top Head Alloy 600 CRDM Nozzle Inspection Experience," presented at EPRI International BWR and PWR Material Reliability Conference, National Harbor, Maryland, July 19, 2012.

EPRI | ELECTRIC POWER RESEARCH INSTITUTE

Materials Reliability Program: Technical Basis for Reexamination Interval Extension for Alloy 690 PWR Reactor Vessel Top Head Penetration Nozzles (MRP-375)

2014 TECHNICAL REPORT

Materials Reliability Program: Technical Basis for Reexamination Interval Extension for Alloy 690 PWR Reactor Vessel Top Head Penetration Nozzles (MRP-375)

3002002441

Final Report, February 2014

EPRI Project Manager
P. Crooker

All or a portion of the requirements of the EPRI Nuclear Quality Assurance Program apply to this product.

YES (NO)

ELECTRIC POWER RESEARCH INSTITUTE
3420 Hillview Avenue, Palo Alto, California 94304-1338 • PO Box 10412, Palo Alto, California 94303-0813 • USA
800.313.3774 • 650.855.2121 • askepri@epri.com • www.epri.com

DISCLAIMER OF WARRANTIES AND LIMITATION OF LIABILITIES

THIS DOCUMENT WAS PREPARED BY THE ORGANIZATION(S) NAMED BELOW AS AN ACCOUNT OF WORK SPONSORED OR COSPONSORED BY THE ELECTRIC POWER RESEARCH INSTITUTE, INC. (EPRI). NEITHER EPRI, ANY MEMBER OF EPRI, ANY COSPONSOR, THE ORGANIZATION(S) BELOW, NOR ANY PERSON ACTING ON BEHALF OF ANY OF THEM:

(A) MAKES ANY WARRANTY OR REPRESENTATION WHATSOEVER, EXPRESS OR IMPLIED, (I) WITH RESPECT TO THE USE OF ANY INFORMATION, APPARATUS, METHOD, PROCESS, OR SIMILAR ITEM DISCLOSED IN THIS DOCUMENT, INCLUDING MERCHANTABILITY AND FITNESS FOR A PARTICULAR PURPOSE, OR (II) THAT SUCH USE DOES NOT INFRINGE ON OR INTERFERE WITH PRIVATELY OWNED RIGHTS, INCLUDING ANY PARTY'S INTELLECTUAL PROPERTY, OR (III) THAT THIS DOCUMENT IS SUITABLE TO ANY PARTICULAR USER'S CIRCUMSTANCE; OR

(B) ASSUMES RESPONSIBILITY FOR ANY DAMAGES OR OTHER LIABILITY WHATSOEVER (INCLUDING ANY CONSEQUENTIAL DAMAGES, EVEN IF EPRI OR ANY EPRI REPRESENTATIVE HAS BEEN ADVISED OF THE POSSIBILITY OF SUCH DAMAGES) RESULTING FROM YOUR SELECTION OR USE OF THIS DOCUMENT OR ANY INFORMATION, APPARATUS, METHOD, PROCESS, OR SIMILAR ITEM DISCLOSED IN THIS DOCUMENT.

REFERENCE HEREIN TO ANY SPECIFIC COMMERCIAL PRODUCT, PROCESS, OR SERVICE BY ITS TRADE NAME, TRADEMARK, MANUFACTURER, OR OTHERWISE, DOES NOT NECESSARILY CONSTITUTE OR IMPLY ITS ENDORSEMENT, RECOMMENDATION, OR FAVORING BY EPRI.

THE FOLLOWING ORGANIZATION, UNDER CONTRACT TO EPRI, PREPARED THIS REPORT:

Dominion Engineering, Inc.

THE TECHNICAL CONTENTS OF THIS PRODUCT WERE **NOT** PREPARED IN ACCORDANCE WITH THE EPRI QUALITY PROGRAM MANUAL THAT FULFILLS THE REQUIREMENTS OF 10 CFR 50, APPENDIX B. THIS PRODUCT IS **NOT** SUBJECT TO THE REQUIREMENTS OF 10 CFR PART 21.

NOTE

For further information about EPRI, call the EPRI Customer Assistance Center at 800.313.3774 or e-mail askepri@epri.com.

ACKNOWLEDGMENTS

The following organization, under contract to the Electric Power Research Institute (EPRI), prepared this report:

Dominion Engineering, Inc.
12100 Sunrise Valley Drive, Suite 220
Reston, VA 20191

Principal Investigators
G. White
K. Schmitt
K. Fuhr
A. Olender

This report describes research sponsored by EPRI.

The contributions of the MRP utility participants are gratefully acknowledged. The MRP utility participants included Scott Boggs (FPL), Joseph Carrasco (PSEG), Guy DeBoo (Exelon), Glenn Gardner (Dominion), Christopher Koehler (Xcel Energy), Bernie Rudell (CENG), William Sims (Entergy), and Corey Thomas (SNC).

This publication is a corporate document that should be cited in the literature in the following manner:

Materials Reliability Program: Technical Basis for Reexamination Interval Extension for Alloy 690 PWR Reactor Vessel Top Head Penetration Nozzles (MRP-375). EPRI, Palo Alto, CA: 2014. 3002002441.

PRODUCT DESCRIPTION

This report presents a technical basis supporting an alternative reexamination interval for volumetric inspection of pressurized water reactor (PWR) reactor vessel top heads with Alloy 690 nozzles and Alloy 52/152 attachment welds.

Background

Due to concerns about primary water stress corrosion cracking (PWSCC), many PWR plants in the United States and overseas have replaced reactor vessel top heads containing Alloy 600 nozzles with heads containing Alloy 690 nozzles. Alloy 690 is considered highly resistant to PWSCC as a result of its approximately 30% chromium content. The resistance of Alloy 690 and corresponding weld metals Alloys 52 and 152 is demonstrated by the lack of any PWSCC indications reported in these materials, in up to 24 calendar years of service for many thousands of Alloy 690 steam generator tubes, and more than 22 calendar years of service for thick-wall Alloy 690 applications.

The current U.S. inspection regime for periodic volumetric and visual examinations in top heads with Alloy 690 nozzles and Alloy 52/152 attachment welds was established in 2004 as a conservative approach. Since that time, plant experience and laboratory testing have continued to demonstrate the much greater PWSCC resistance of those replacement alloys compared to Alloys 600/82/182 for the material conditions relevant to partial-penetration welded nozzles.

Objectives

- To develop an alternative inspection regime for PWR top heads with Alloy 690 nozzles.
- To develop a robust technical basis to support obtaining approval for implementation of the proposed alternative inspection regime, either through relief of current U.S. Nuclear Regulatory Commission (NRC) requirements, or revision of the American Society of Mechanical Engineers (ASME) Code inspection regime, followed by U.S. NRC acceptance.

Approach

This report presents deterministic and probabilistic calculations that assess the effect of the improved PWSCC resistance of Alloys 690/52/152. Much of the available laboratory data indicate a factor of improvement of 100 for Alloys 690/52/152 versus Alloys 600/182 (for equivalent temperature and stress conditions) in terms of crack growth rate. Moreover, existing laboratory and plant data demonstrate a factor of improvement in excess of 20 in terms of the time to PWSCC initiation. This much reduced susceptibility to PWSCC initiation and growth supports elimination of all volumetric examinations (as well as visual examinations for evidence of leakage) throughout the plant service period. However, since work is still ongoing to determine the performance of Alloys 690/52/152 in PWR replacement head applications, the determination of inspection intervals for reactor vessel heads with Alloy 690 nozzles was based on conservatively smaller factors of improvement.

The probabilistic calculations are based on a Monte Carlo simulation model of the PWSCC process, including PWSCC initiation, crack growth, and flaw detection via ultrasonic testing. The basic structure of the probabilistic model is similar to that used in the Electric Power Research Institute (EPRI) Materials Reliability Program (MRP) technical basis report on inspection requirements for heads with Alloy 600 nozzles (MRP-105, EPRI report 1007834). The current approach includes more detailed modeling of surface flaws (including multiple flaw initiation for each nozzle on base metal and weld surfaces), and calibration of the initiation module to consider the latest experience for U.S. heads. The outputs of the probabilistic model are leakage frequency (i.e., frequency of through-wall cracking) and nozzle ejection frequency.

Results

The deterministic calculations demonstrate that the alternative volumetric reexamination interval is sufficient to detect any PWSCC before it could develop into a safety-significant circumferential flaw that approaches the large size necessary to produce a nozzle ejection. The probabilistic results with the alternative inspection regime show (1) an effect on nuclear safety substantially within the acceptance criterion applied in the MRP-117 (EPRI 1007830) technical basis for Alloy 600 heads, and (2) a substantially reduced effect on nuclear safety compared to a head with Alloy 600 nozzles examined per current requirements, even assuming conservatively small factors of improvement for the crack growth rate for the replacement nickel-base alloys.

The proposed alternative inspection regime, which extends the volumetric re-examination interval of a nominal 10 years (per ASME Code Case N-729-1 and 10 CFR 50.55a(g)(6)(ii)(D)) to a nominal 20 years, removes excess conservatism while still maintaining a conservative approach. As a further conservatism, the proposed alternative inspection regime maintains the same periodic program of direct visual examinations for evidence of leakage, as defined by the current ASME requirement per Code Case N-729-1. Finally, analogous to the approach taken in Paragraph IWL-2421 of ASME Section XI for inspection of unbonded post-tensioning systems of concrete containments, this technical basis report also proposes a sample program of volumetric examinations for a pair of "sister" heads with a similar or identical design, same nozzle material supplier, and same head fabricator.

Applications, Value, and Use

This report is applicable to all PWRs with (or contemplating installing) a replacement reactor vessel head containing Alloy 690/52/152 materials. In the U.S., as of 2013, there are 40 PWRs operating with heads fabricated with Alloy 690 nozzles. Head replacement is a main option for addressing the potential for PWSCC in the remaining 25 currently operating U.S. PWRs. This study demonstrates that the frequency of volumetric inspections of the nozzles in replacement heads can be reduced while still maintaining a conservative inspection program for addressing the potential PWSCC concern for these materials.

Keywords

Alloy 690
Alloys 52/152
Primary water stress corrosion cracking
PWR reactor vessel head
Top head
Closure head
Reactor pressure vessel head penetration nozzles (RPVHPNs)

ABSTRACT

Due to concerns about primary water stress corrosion cracking (PWSCC), many pressurized water reactor (PWR) plants in the United States and overseas have replaced reactor vessel top heads containing Alloy 600 nozzles with heads containing Alloy 690 nozzles. Alloy 690 is considered highly resistant to PWSCC as a result of its approximately 30% chromium content. The resistance of Alloy 690 and corresponding weld metals Alloys 52 and 152 is demonstrated by the lack of any PWSCC indications reported in these materials, in up to 24 calendar years of service for many thousands of Alloy 690 steam generator tubes, and more than 22 calendar years of service for thick-wall Alloy 690 applications.

The current U.S. inspection regime for periodic volumetric and visual examinations in top heads with Alloy 690 nozzles and Alloy 52/152 attachment welds was established in 2004 as a conservative approach. Since that time, plant experience and laboratory testing have continued to demonstrate the much greater PWSCC resistance of these replacement alloys compared to Alloys 600/82/182 for the material conditions relevant to partial-penetration welded nozzles.

This report applies deterministic and probabilistic modeling to establish a technical basis for an alternative inspection regime for PWR top heads with Alloy 690 nozzles. It is intended to support obtaining approval for implementation of the proposed alternative inspection regime, either through the relief of current U.S. Nuclear Regulatory Commission (NRC) requirements or revision of the American Society of Mechanical Engineers (ASME) Code inspection regime, followed by U.S. NRC acceptance. The proposed alternative inspection regime, which extends the volumetric re-examination interval from a nominal 10 years to a nominal 20 years, removes excess conservatism while still maintaining a conservative approach. Much of the available laboratory data indicate a factor of improvement of 100 for Alloys 690/52/152 versus Alloys 600/182 (for equivalent temperature and stress conditions) in terms of crack growth rate. Moreover, existing laboratory and plant data demonstrate a factor of improvement in excess of 20 in terms of the time to PWSCC initiation. This much reduced susceptibility to PWSCC initiation and growth supports elimination of all volumetric examinations (as well as visual examinations for evidence of leakage) throughout the plant service period. As a further conservatism, the proposed alternative inspection regime maintains the same periodic program of direct visual examinations for evidence of leakage, as defined by the current ASME requirement per Code Case N-729-1. Finally, analogous to the approach taken in Paragraph IWL-2421 of ASME Section XI for inspection of unbonded post-tensioning systems of concrete containments, this technical basis report also proposes a sample program of volumetric examinations for a pair of "sister" heads with a similar or identical design, same nozzle material supplier, and same head fabricator.

ACRONYMS

AEF	Average Ejection Frequency
ALF	Average Leakage Frequency
ANL	Argonne National Laboratory
ASME	American Society of Mechanical Engineers
BMI	Bottom Mounted Instrumentation [Nozzle]
BMV	Bare Metal Visual [Examination]
BPVC	[ASME] Boiler & Pressure Vessel Code
CCDP	Conditional Core Damage Probability
CDF	Core Damage Frequency
CEA	Commissariat à l'énergie atomique
CEDM	Control Element Drive Mechanism
CFR	Code of Federal Regulations
CGR	Crack Growth Rate
CIEMAT	Centro de Investigaciones Energéticas, Medioambientales y Tecnológicas
CPE	Cumulative Probability of Ejection
CRDM	Control Rod Drive Mechanism
CW	Cold Work
DZ	Dilution Zone
EDF	Électricité de France
EDY	Effective Degradation Year
EFPY	Effective Full-Power Year
EPFM	Elastic-Plastic Fracture Mechanics
EPRI	Electric Power Research Institute
ET	Eddy Current Testing
FEA	Finite Element Analysis
FOI	Factor of Improvement

GE-GRC	General Electric Global Research Center
HAZ	Heat Affected Zone
ICI	Incore Instrumentation [Nozzle]
ID	Inside Diameter
IEF	Incremental Ejection Frequency
ILF	Incremental Leakage Frequency
ISI	Inservice Inspection
KAPL	Knolls Atomic Power Laboratory
MA	Mill-Annealed
MHI	Mitsubishi Heavy Industries
MRP	[EPRI] Materials Reliability Program
NDE	Non-Destructive Examination
NRC	U.S. Nuclear Regulatory Commission
NSC	Net Section Collapse
OD	Outside Diameter
PNNL	Pacific Northwest National Laboratory
POD	Probability of Detection
PWR	Pressurized Water Reactor
PWSCC	Primary Water Stress Corrosion Cracking
RFO	Refueling Outage
RIY	Reinspection Year [per ASME Code Case N-729-1]
RPV	Reactor Pressure Vessel
RPVH	Reactor Pressure Vessel Head
RPVHPN	Reactor Pressure Vessel Head Penetration Nozzle
RUB	Reverse U-Bend [Specimen]
SCC	Stress Corrosion Cracking
SIF	Stress Intensity Factor
TT	Thermally Treated
TW	Through-Wall
UT	Ultrasonic Testing
VE	Visual Examination [as defined in ASME Code Case N-729-1]

CONTENTS

LIST OF FIGURES

LIST OF TABLES

1
INTRODUCTION

This section introduces the need for a quantitative technical basis for the re-examination interval for PWR reactor vessel top heads with Alloy 690 nozzles. Included are the report objective, a description of the technical approach taken, and a summary of the report structure.

1.1 Background

1.1.1 Replacement RPV Heads with Alloy 690 Nozzles and Alloy 52/152 Attachment Welds

PWR reactor vessel top heads are designed with roughly between 40 and 100 penetration nozzles (i.e., reactor pressure vessel head penetration nozzles, or RPVHPNs) for various functions, such as connections of the control rod drive shafts to the control rod drives located above the head. Most RPVHPNs are attached to the head with a pressure-retaining partial-penetration (i.e., J-groove) weld. As documented in MRP-110 [1] and MRP 2011-034 [2], the Alloy 600 nozzles and Alloy 82/182 attachment welds of the original reactor vessel heads have shown a substantial susceptibility to primary water stress corrosion cracking (PWSCC). Due to this concern, many PWR reactor vessel top heads with Alloy 600 nozzles in U.S. and overseas plants have been replaced with heads having Alloy 690 nozzles.

1.1.2 Performance of Alloy 690 and Weld Metals Alloys 52 and 152

As a result of its chromium content of about 30%, Alloy 690 is considered highly resistant to PWSCC. The resistance of Alloy 690 and the corresponding weld metals Alloys 52 and 152 is demonstrated by the lack of any PWSCC indications reported in these materials, with up to 24 calendar years of service for many thousands of Alloy 690 steam generator tubes and more than 22 calendar years of service for thick-wall Alloy 690 applications. The high resistance to PWSCC of these alloys is further demonstrated by the general lack of PWSCC indications detected in laboratory PWSCC initiation studies for normal Alloys 690/52/152 in conditions representative of plant service.

1.1.3 Current Inspection Requirements for RPV Heads with Alloy 690 Nozzles and Alloy 52/152 Attachment Welds

The current inspection requirements for Alloy 690 RPVHPNs in U.S. PWRs are defined by ASME Code Case N-729-1 [3], which has been mandated with conditions by the U.S. NRC through 10 CFR 50.55a(g)(6)(ii)(D). The basic inspection requirements for partial-penetration welded Alloy 690 RPVHPNs are as follows:

- Volumetric/surface examination of all nozzles every ASME Section XI 10-year ISI interval (provided that flaws attributed to PWSCC have not previously been identified in the head)

- Direct visual examination (VE) of the outer surface of the head for evidence of leakage every third refueling outage or 5 calendar years, whichever is less

This current inspection regime was established in 2004 as a conservative approach and was intended to be subject to reassessment upon the availability of additional laboratory data and plant experience on the performance of Alloy 690 and Alloy 52/152 [4].[1] Since that time, plant experience and laboratory testing have continued to demonstrate the much greater resistance of these replacement alloys to PWSCC compared to that for Alloys 600/82/182 for the material conditions relevant to partial-penetration welded nozzles. Although laboratory research is ongoing to investigate and understand the times to crack initiation and the crack growth rates for these materials under various conditions, there are now sufficient data available to develop an improved technical basis for inspection of these components. As described below, a simple factor of improvement (FOI) approach is applied in a conservative manner.

1.2 Objective

This report develops an alternative inspection regime for PWR top heads with Alloy 690 nozzles and an associated robust technical basis. This report is intended to support obtaining approval to implement the proposed alternative inspection regime, either through relief of current U.S. NRC requirements or revision of the ASME Code inspection regime followed by U.S. NRC acceptance.

1.3 Scope

This report is applicable to all PWRs with (or contemplating installing) a replacement reactor vessel head containing Alloy 690/52/152 materials. In the U.S., as of 2013, there are 40 PWRs operating with heads fabricated with Alloy 690 nozzles. Head replacement is a main option for addressing the potential for PWSCC in the remaining 25 currently operating U.S. PWRs. This study demonstrates that the frequency of volumetric inspections of the nozzles in replacement heads can be reduced while still maintaining a conservative inspection program for addressing the potential PWSCC concern for these materials.

[1] The portion of the ASME technical basis document [4] for Code Case N-729 that addresses Alloy 690 RPVHPNs is as follows:

"**Guidance for Replacement Heads with Alloy 690 Nozzles**

The examination requirements for replacement heads with Alloy 690 nozzles are based on the results of the study presented in report MRP-111 [5] and summarized in the safety assessment (MRP-110 [1]). This study shows, on the basis of both laboratory test data and plant experience, that Alloy 690 base metal and Alloy 52/152 weld metals are much more resistant to PWSCC initiation than Alloy 600 base metal and Alloy 82/182 weld metals. The MRP-111 [5] evaluation of laboratory and plant experience indicates a material improvement factor of at least 26 for Alloy 690 versus mill-annealed Alloy 600, with larger improvement factors expected with more years of experience accumulated in the laboratory and field. Given that operating time has been shown by plant experience and laboratory testing to be a key parameter for determining the likelihood of cracking, the volumetric/surface NDE Interval of 10 years required in Table 1 [of N-729] for replacement heads with Alloy 690/52/152 materials is conservative. This interval corresponds to a fraction of a year in terms of time to PWSCC initiation for the original head materials.

After additional laboratory data and plant experience on the performance of Alloy 690 and Alloy 52/152 weld metals become available, revised examination requirements for replacement heads with Alloy 690 nozzles may be appropriate, but until then, the Code Case requires volumetric/surface examinations to be repeated each Interval (nominally 10 calendar years)."

1.4 Approach

This report presents deterministic and probabilistic calculations that assess the effect of the improved PWSCC resistance of Alloys 690/52/152. Much of the available laboratory data indicate a factor of improvement for Alloys 690/52/152 versus the performance of Alloys 600/182[2] (for equivalent temperature and stress conditions) on the order of 100 in terms of the crack growth rate. Moreover, existing laboratory and plant data demonstrate a factor of improvement in excess of 20 in terms of the time to PWSCC initiation. This much reduced susceptibility to PWSCC initiation and growth supports elimination of all volumetric examinations (as well as visual examinations for evidence of leakage) throughout the plant service period. However, since work is still ongoing to determine the performance of Alloys 690/52/152 in PWR replacement head applications, the determination of inspection intervals for reactor vessel heads with Alloy 690 nozzles was based on conservatively smaller factors of improvement. This conservative approach provides for continued monitoring of the status of the U.S. fleet of replacement heads. In the future, the situation may be re-assessed and excess conservatism removed from the technical basis for inspection.

The deterministic calculations demonstrate that the alternative volumetric re-examination interval is sufficient to detect any PWSCC before it could develop into a safety-significant circumferential flaw that approaches the large size necessary to produce a nozzle ejection. The deterministic calculations also demonstrate that any base metal PWSCC would likely be detected prior to a through-wall penetration occurring.

The probabilistic calculations are based on a Monte Carlo simulation model of the PWSCC process, including PWSCC initiation, PWSCC crack growth, and flaw detection via ultrasonic testing. The basic structure of the probabilistic model is similar to that used in the MRP-105 [6] technical basis report for inspection requirements for heads with Alloy 600 nozzles, but the current approach includes more detailed modeling of surface flaws (including multiple flaw initiation for each nozzle on base metal and weld surfaces) and the initiation module has been calibrated to consider the latest set of experience for U.S. heads. The outputs of the probabilistic model are leakage frequency (i.e., frequency of through-wall cracking) and nozzle ejection frequency. Even assuming conservatively small factors of improvement for the crack growth rate for the replacement nickel-base alloys (with no credit for improved resistance to initiation), the probabilistic results with the alternative inspection regime show:

1. An effect on nuclear safety substantially within the acceptance criterion applied in the MRP-117 [7] technical basis for Alloy 600 heads, and
2. A substantially reduced effect on nuclear safety compared to that for a head with Alloy 600 nozzles examined per current requirements.

Furthermore, the results confirm a low probability of leakage if some modest credit is taken for improved resistance to PWSCC initiation compared to that for Alloys 600 and 182.

[2] Alloy 600 wrought material is the appropriate reference for defining the FOI for Alloy 690 wrought material. As discussed in Section 3.1, Alloy 182 weld metal is chosen as the reference for defining the FOI for Alloys 52 and 152 weld metals because Alloy 182 is more susceptible to PWSCC initiation and growth than Alloy 82 (due to the higher Cr content of Alloy 82).

1.5 Report Structure

This technical basis report is organized as follows:

1. INTRODUCTION (SECTION 1)

   Section 1 introduces the need for a quantitative technical basis for the re-examination interval for PWR reactor vessel top heads with Alloy 690 nozzles. Included are the report objective, a description of the technical approach taken, and a summary of the report structure.

2. PLANT EXPERIENCE WITH ALLOYS 690/52/152 (SECTION 2)

   As documented in Section 2, Alloy 690 has been in PWR service for more than 24 years with no reports of detected PWSCC worldwide. Similarly, PWSCC has not been detected in Alloys 52 or 152 with initial PWR use starting in 1993-94. This excellent experience includes service at pressurizer and hot-leg temperatures, in thick-wall and thin-wall applications, and in Alloy 690 wrought base metal and Alloy 52/152 weld metal. This experience supports a factor of improvement in time to detectable PWSCC of at least 5 to 20, with the value increasing as additional service time with the replacement materials is accumulated.

3. FACTORS OF IMPROVEMENT FOR ALLOYS 690/52/152 VERSUS ALLOYS 600/182 (SECTION 3)

   As demonstrated in PWSCC crack growth rate testing, Alloy 690/52/152 material is not completely immune to PWSCC, with the level of susceptibility dependent on the particular material condition. A simple factor of improvement (FOI) approach is applied in a conservative manner in this study to model the increased resistance of Alloy 690 compared to Alloy 600 at equivalent temperature and stress conditions. Similarly, the PWSCC behavior in Alloys 52/152 is conservatively modeled through application of a FOI applied to the behavior expected for Alloy 182. Through application of available laboratory and plant data, Section 3 describes the development of conservatively small FOI values for modeling PWSCC initiation and PWSCC crack growth rates for the Alloy 690 nozzles and Alloy 52/152 attachment welds of PWR reactor vessel top heads.

4. DETERMINISTIC AND PROBABILISTIC PWSCC EVALUATIONS (SECTION 4)

   Section 4 gives an overview of the deterministic and probabilistic evaluations of the effect of inspection intervals on risks related to PWSCC degradation of Alloy 690 RPVHPNs, namely in comparison to the correspondent risks in Alloy 600 RPVHPNs. This overview includes an explanation of the evaluation approaches, a presentation of key results, and a statement of the conclusions drawn from these results. Section 4 is augmented by Appendix A and Appendix B, which comprise a comprehensive description of the probabilistic model and its constituent submodels, detailed input listings, and a comprehensive presentation of results.

5. CONCLUSIONS (SECTION 5)

   Section 5 presents the key conclusions of this technical basis report. Presented are alternative re-examination interval requirements for PWR reactor vessel top heads with Alloy 690 nozzles and Alloy 52/152 attachment welds that are justified by the available relevant plant and laboratory data. These alternative requirements maintain a conservative

approach while ensuring that the status of the replacement head fleet at U.S. PWRs is monitored over time. Section 5 concludes with a discussion of the modeling conservatisms that are included in the supporting deterministic and probabilistic analyses.

6. REFERENCES (SECTION 6)

   Section 6 lists the references cited in this report, including those cited in the two appendices.

7. DESCRIPTION OF PROBABILISTIC PWSCC MODEL (APPENDIX A)

   Appendix A introduces a probabilistic modeling framework developed to study top heads with Alloy 690 nozzles with emphasis on determining the effect of adjusting the inspection requirements of Code Case N-729-1 [3] on risks due to PWSCC degradation.

8. INPUTS AND RESULTS OF PROBABILISTIC PWSCC MODEL (APPENDIX B)

   Appendix B reports a set of results generated within the probabilistic framework to support alternative inspection regimes for top heads with RPVHPNs fabricated with Alloys 690/52/152. The probabilistic calculations presented in Appendix B are designed to bound the conditions for such heads, so conclusions drawn from the results are generically applicable to heads with Alloy 690 RPVHPNs.

2
PLANT EXPERIENCE WITH ALLOYS 690/52/152

Alloy 690 has been in PWR service for more than 24 years with no reports of detected PWSCC worldwide. Similarly, PWSCC has not been detected in Alloys 52 or 152 since initial PWR use starting in 1993-94. This excellent experience includes service at pressurizer and hot-leg temperatures, in thick-wall and thin-wall applications, and in Alloy 690 wrought base metal and Alloy 52/152 weld metal. This experience supports a factor of improvement in time to detectable PWSCC of at least 5 to 20, with the value increasing as additional service time with the replacement materials is accumulated.

2.1 Alloy 690 Steam Generator Tubing

Replacement steam generators with Alloy 690 tubing were put into operation in 1989 at Cook 2, Indian Point 3, and Ringhals 2. There have been no corrosion-induced flaws detected at these plants or at the many subsequent plants that have started up since that time with either replacement or original steam generators with Alloy 690 tubes [1]. In contrast, PWSCC was detected after one cycle of operation at several units with mill-annealed Alloy 600 (600MA) tubes, e.g., Doel 3, Tihange 2, and V. C. Summer, and after the second cycle at a number of other plants. This experience indicates that there is a service demonstrated factor of improvement of at least about 20, with the value increasing as the service time without detection of PWSCC of Alloy 690 tubes continues to accumulate.

The plants with original or replacement steam generators with Alloy 690 tubing in the U.S. and internationally are listed in Tables 10-4 and 10-5, respectively, of MRP-110 [1]. These tables provide basic data on the steam generator tubing at the 26 U.S. plants and 45 international plants with Alloy 690 tubing as of March 2004. The data include number of tubes, hot-leg operating temperature, estimated operating time, and an example inservice inspection scope. At U.S. and overseas PWRs, Alloy 690 steam generator tubing is subject to periodic examinations for PWSCC and other degradation modes. As of the date of this report, there have been no reports of PWSCC detected in the Alloy 690 tubing in any of the 71 plants listed in these tables nor in any other plants worldwide.

2.2 Steam Generator Tube-End Welds

Steam generator tubes are joined to the tubesheet using welds between the tube and cladding on the primary face of the tubesheet. Thus, each steam generator has thousands of welds and heat affected zones. There have been no reports of PWSCC being detected at these weld joints between Alloy 690 tubes and the cladding on the tubesheet (the cladding on early Alloy 690 steam generators was Alloy 82/182, while for later units it has been Alloy 52/152). While the Alloy 690 tube to tubesheet weld joints are not routinely inspected with sensitive methods, significant cracking would likely have been detected as result of leakage or visible cracks, as has occurred occasionally with Alloy 600 tube to tubesheet welds.

2.3 Alloy 690 Steam Generator Tube Plugs

Many steam generator tubes have used thermally treated Alloy 690 (690TT) tube plugs since the late 1980s. There have been no reports of PWSCC being detected in these plugs, which are subject to high tensile stresses and cold work. The plugs have been of two main kinds: mechanical plugs with an internal mandrel that expands and seals the plug envelope and tube to the tubesheet, and rolled-in thimble tubes. In both cases, the plugs are made from thick-wall rod material rather than from thin tubes. In contrast to the over 20 years of trouble-free service with Alloy 690TT plugs, plugs made of Alloy 600MA and even Alloy 600TT experienced PWSCC within one to two years of service. This experience indicates that there is a service demonstrated factor of improvement of at least about 20, with the value increasing as the service time without detection of PWSCC of Alloy 690 tube plugs continues to accumulate.

2.4 Alloy 690 Instrumentation Nozzles and Pressurizer Heater Sleeves

Many Alloy 600 pressurizer and hot-leg piping instrumentation nozzles and Alloy 600 pressurizer heater sleeves have been replaced with Alloy 690 in U.S. PWRs starting in 1990. The earliest such replacements with Alloy 690 nozzles used Alloy 82 and/or 182 as the weld material. Alloy 52 and 152 weld metals started to be used in repairs and in replacements beginning about 1993-94.

There have been no reports of PWSCC detected in these thick-wall Alloy 690 parts nor in Alloy 52/152 welds [8]. A comprehensive list of these components that were replaced using Alloy 690/52/152 materials as of 2004 is provided in Table 10-6 of MRP-110 [1]. As of this time the total number of such replacements in U.S. PWRs was roughly 400. Details on many of the replacement designs are available in MRP-87 [9]. Note that the pressurizers at four plants designed by Combustion Engineering were replaced in 2005-2006. However, the earliest cases of Alloy 600 pressurizer nozzle replacements were generally at plants for which the original pressurizer is still in service.

In one pressurizer where Alloy 690 nozzle base material and Alloy 82 weld material was utilized as replacement material in 1990 a leak developed in an Alloy 82 weld over 20 years later ([1] and [10]). Destructive examination of the Alloy 690 base material removed during the repair/replacement work showed no initiation of PWSCC in the Alloy 690 base material in the triple point region adjacent to where Alloy 82 PWSCC initiation was noted. The operating temperature at that location was approximately 630°F (332°C).

This experience demonstrates the substantial PWSCC resistance of thick-wall Alloy 690 components and Alloy 52/152 weld metal, including at temperatures substantially above the range of PWR hot-leg temperatures. Factors of improvement of at least 5 are readily apparent in this experience. Some of the original Alloy 600 components operated for as few as 6 years before PWSCC was reported.

2.5 Replacement Top Heads with Alloy 690 Nozzles

New and repaired reactor vessel top heads with Alloy 690 nozzles started to be used in the industry around 1992. Currently, more than 100 replacement and new heads with Alloy 690 nozzles and Alloy 52/152 attachment welds are in service worldwide. This includes 40 heads in

U.S. PWRs and all 58 PWR top heads in France. The current inspection status of these fleets of heads is as follows:

- As of the date of this report, the first 10-year inservice volumetric/surface examination per ASME Code Case N-729-1 [3] has been performed at nine of the 40 replacement heads in the U.S., representing more than 500 Alloy 690 RPVHPNs (based on the number of nozzles in each corresponding original head). Several of the replacement top heads in the U.S. that have had a volumetric/surface inservice examination already are known to operate at the upper end of the range of head operating temperatures, as high as 613°F (323°C) [2].
- In France, an NDE inspection of the Bugey 3 replacement head CRDM nozzles was performed in 2002 after 10 years of service [11]. EDF currently performs ISI every 10 years on three of its reactor vessel heads. Eddy current testing (ET) applied to the nozzle ID is the detection method, and ultrasonic testing (UT) and visual examination are applied as characterization methods if the ET threshold is reached. The three heads in the program are among the earliest placed into service. In 2013, the heads at Bugey 3 and Blayais 2 were inspected. The approach being applied in France is based on the existing knowledge regarding the resistance of Alloys 690/52/152 to PWSCC, including the latest set of inspection results.

As for all other Alloy 690/52/152 applications, there have been no reports of PWSCC detected for any of these replacement top head inspections.

In 2010, 24 nozzles in one Alloy 600 top head in the U.S. were repaired due to detection of possible PWSCC indications [2]. This head had operated for a period of 6 calendar years at a head temperature of about 613°F. It is likely based on the number of affected nozzles and the sizes of the detected indications that this head had detectable PWSCC as early as 1 or 2 calendar years after the start of its operation. This compares to the 10 calendar years of service at the time of inspection of each of the nine U.S. heads examined to date. Four of these nine heads operate at a temperature close to that for the head with Alloy 600 nozzles repaired in 2010. Thus, this subset of top head experience demonstrates a factor of improvement in PWSCC resistance of at least 5 to 10.

2.6 Implications

The wide range of plant experience with Alloys 690, 52, and 152 clearly demonstrates a substantial improvement in PWSCC resistance versus that for Alloys 600 and 182. Depending on the application, a factor of improvement in time to detectable PWSCC of at least 5 to 20 is apparent, with the value increasing as additional service time with the replacement materials is accumulated.

3
FACTORS OF IMPROVEMENT FOR ALLOYS 690/52/152 VERSUS ALLOYS 600/182

As a result of PWSCC susceptibility, many Alloy 600/82/182 components have been replaced with Alloy 690/52/152 components. The resistance to PWSCC of Alloys 690/52/152 is the result of their nominal chromium content of 30%. As demonstrated in PWSCC crack growth rate testing [12], Alloy 690/52/152 material is not completely immune to PWSCC, with the level of susceptibility dependent on the particular material condition. A simple factor of improvement (FOI) approach is applied in a conservative manner in this study to model the increased resistance of Alloy 690 compared to Alloy 600 at equivalent temperature and stress conditions. Similarly, the PWSCC behavior in Alloys 52/152 is conservatively modeled through application of a FOI applied to the behavior expected for Alloy 182. Through application of available laboratory and plant data, Section 3 describes the development of conservatively small FOI values for modeling PWSCC initiation and PWSCC crack growth rates for the Alloy 690 nozzles and Alloy 52/152 attachment welds of PWR reactor vessel top heads.

3.1 Relevant Material Conditions

Because of its high chromium content, Alloy 690 in its ideal material condition is generally recognized as being extremely resistant to PWSCC initiation and growth [12]. However, testing has also demonstrated the potential for increased susceptibility to PWSCC of Alloys 690, 52, and 152 depending on the material condition. Work is ongoing by researchers to investigate the effect of various material conditions on the susceptibility of these materials to PWSCC initiation and growth, including detailed screening and assessment of the international database of laboratory PWSCC crack growth rate testing data produced using controlled fracture mechanics specimens of these alloys.

Because work is still ongoing to investigate the performance of Alloys 690/52/152 in PWR plant applications, a conservative approach was taken in this report in which conservatively small factors of improvement were applied to credit the improved resistance to PWSCC compared to that for Alloys 600 and 182. The approach taken addresses the effect of the material conditions applicable to RPVHPNs in the following manner:

- The existing database of laboratory crack growth rate data includes data for Alloy 690 specimens with substantial levels of cold work, for Alloy 690 heat affected zone (HAZ) material, and for Alloy 52 and 152 material from various test welds. Thus, these material conditions are directly represented in the data conservatively used to support the crack growth FOI values applied in this report.
- The material conditions applicable to Alloy 690 RPVHPNs, including their Alloy 52/152 attachment welds, are similar to those applicable to the original Alloy 600 RPVHPNs and other PWR applications of thick-wall Alloy 600 wrought material and Alloy 82/182 weld

metals. Similar material processing, fabrication, and welding practices apply to the original and replacement components. Thus, the FOI approach implicitly addresses the material conditions applicable to Alloy 690/52/152 components.

- The conservatively small FOI values applied in this report tend to be supported on the basis of plant experience alone. The plant experience for Alloy 690/52/152 components directly reflects the effects of the material conditions applicable to these components.

The following material conditions are known to be potentially significant factors affecting PWSCC susceptibility:

- *Cold-worked Alloy 690 base metal material.* Material processing influences factors such as the microstructure, degree of cold work, and residual strain level. Relevant material processing parameters include heat treatment options (e.g., mill annealing (MA), thermal treatment (TT)) and possible material straightening. In particular, crack growth rate testing of Alloy 690 specimens has shown an increased susceptibility to crack growth when a high level of cold work is applied to the specimen [12].
- *HAZ of Alloy 690 base metal.* The weld heat affected zone (HAZ) of the Alloy 690 base metal may have a notably different microstructure and mechanical properties in comparison to the bulk base metal. The HAZ generally is expected to have higher plastic strain levels (up to 15% [13]) than those observed in the bulk Alloy 690 base metal. Because of the general concern that the HAZ material condition could lead to an increased susceptibility to PWSCC, the probabilistic model presented in this report includes the capability to apply a separate FOI to the Alloy 690 HAZ region of the RPVHPN.
- *Areas with high residual plastic strains and stresses, especially in and adjacent to welds.* In addition to producing substantial levels of plastic strain in the Alloy 690 base metal adjacent to the fusion line, the welding process can result in elevated levels of cumulative plastic strain in the weld metal [13]. It is expected that local regions with elevated plastic strain levels may have increased susceptibility to PWSCC crack growth.
- *Weld fabrication flaws including lack of fusion (LOF) defects.* Plant experience with Alloy 82/182 welds indicates that relatively large and sharp weld defects, such as some weld lack of fusion regions, may have the potential to promote PWSCC by creating a local stress concentrator and a significant local crack-tip stress intensity factor if they were to somehow become wetted ([14] and [15]).
- *Dilution zones of Alloy 52/152 weld metal at interfaces with lower-Cr metals such as Alloys 600/82/182, stainless steel, carbon steel, and low-alloy steel.* Another complexity is the change in elemental composition of the Alloy 52 or 152 weld metal in the local weld dilution zone (DZ) adjoining lower-Cr metals. The reduced chromium content in this region of the Alloy 52 or 152 weld metal might lead to an increase in PWSCC initiation or growth susceptibility. (However, there is a similar concern for Alloy 82 and 182 welds, and PWR plant experience has not revealed the DZ of Alloys 82/182 as a particular area of susceptibility.) Limited crack growth rate testing has been performed to date for Alloy 52/152 DZ material. However, laboratory analysis has indicated that the chromium content remains relatively high (i.e., >25%) throughout most of the Alloy 52/152 weld DZ adjoining Type 304 stainless steel [16]. Hence, the resistance to PWSCC in the DZ of the Alloy 52/152

weld butter layer adjoining the stainless steel cladding at the inside of the vessel head is expected to be substantially similar to that of the bulk Alloy 52/152 weld metal.[3]

- *Surface layers abused by grinding.* Finally, surface abuse by grinding or machining is a factor that is known to affect PWSCC initiation susceptibility (e.g., [19]). In the case of the Alloy 600 or Alloy 690 base metal, shrinkage due to the welding process can strain the surface cold-worked layer previously produced by machining, reaming, or grinding, and thus induce high tensile residual stresses in the surface layer [1].

An additional note related to PWSCC susceptibility of welds is that unlike for Alloys 82 and 182, there is no strong evidence for a difference in PWSCC susceptibility between Alloys 52 and 152.[4] Therefore, data for Alloys 52 and 152 are pooled for the development of a FOI with respect to Alloy 182. Alloy 182 is chosen as the reference for defining the FOI for Alloys 52 and 152 because Alloy 182 is more susceptible to PWSCC initiation and growth than Alloy 82 (due to the higher Cr content of Alloy 82). In terms of crack growth rate, MRP-115 [14] concludes that on average the crack growth rate for Alloy 82 is 2.6 times lower than that for Alloy 182. In terms of the susceptibility to crack initiation, very few cases of PWSCC in operating plants have been confirmed to have initiated within Alloy 82 weld metal ([10] and [18]).

For both the base and weld metals, the orientation of crack growth with respect to anisotropic microstructural characteristics of the material may have a considerable effect. For instance, in Alloy 690, crack growth parallel to the direction of unidirectional cold working (i.e., the rolling direction) exhibits higher CGRs than crack growth perpendicular to that direction. In weld metal, the most susceptible growth orientation is parallel to the dendrite solidification direction. Preference has been given to these more susceptible orientations in the testing compiled for this report.

3.2 Assessments of Laboratory Data

Several laboratories worldwide have allotted considerable time and resources to studying the PWSCC behavior of Alloys 690/52/152. The resistance to PWSCC of these materials has motivated more aggressive testing situations, including longer test durations, higher temperatures, severe specimen cold working, and occasionally more aggressive environment chemistry. This has led to wide variability in testing parameters, some of which are not representative of plant conditions. Thus, careful attention to testing parameters is required when evaluating the available data. Data assessment for specific testing is described in more detail in the following subsections.

[3] The chromium content specified for Type 304 stainless steel is 18.0–20.0%. This compares to 19.5 to 25.0% for the types of stainless steel weld metal commonly used for internal cladding of PWR reactor vessels (19.5–22.0% [17] for AWS ER308 weld metal and 23.0–25.0% [17] for AWS ER309 weld metal). The generally higher chromium content of the cladding weld metal would tend to result in a higher chromium content for the Alloy 52/152 dilution zone compared to that adjoining Type 304 stainless steel base metal.

[4] Testing by a single laboratory of Alloy 152 weld metal specimens has yielded several relatively high CGR data points (when compared to the average across laboratories for both Alloys 52 and 152). However, other laboratories have tested both Alloy 52 and Alloy 152 specimens and not reported a substantial difference in crack growth rates for the two alloys. Overall, there is no compelling evidence for concluding that there is a substantial difference in the PWSCC crack growth rate between Alloys 52 and 152.

3.2.1 PWSCC Initiation

3.2.1.1 Alloy 690 Crack Initiation

MRP-111 [5] is a compilation of the methodologies, results, and discussions of numerous crack initiation tests for Alloy 690 through 2004. As documented in this report, several different investigators have been able to initiate cracking in both Alloy 600 and Alloy 690, often under aggressive conditions. In many more cases, however, PWSCC could not be initiated in the Alloy 690 material. For specimens in which PWSCC could not be initiated, the test duration was reported in place of time to initiation. Two different techniques were used to estimate FOIs for PWSCC initiation in Alloy 690 versus Alloy 600:

- The first technique, based on the Weibull regression model [20], was applied to test sets that reported sufficient data. For this technique, a characteristic time based on the Alloy 600 data was estimated with a standard Weibull regression, and a characteristic time based on the Alloy 690 data was estimated with a Weibayes regression.[5] The FOI was calculated as the ratio of the estimated Alloy 690 and Alloy 600 characteristic times.
- The second technique simply calculated a FOI as the ratio of the first initiation time (or test duration if no initiation occurred in any specimens) across all Alloy 690 specimens to the first initiation time across all Alloy 600 specimens.

Overall FOIs were attained by averaging all test-specific FOIs. Table 3-1 presents the average FOIs determined in MRP-111.

Table 3-1
MRP-111 Factors of Improvement [5]

Method	Average FOI
Weibull/Weibayes: 690 vs. 600MA	>26.5
Weibull/Weibayes: 690 vs. 600TT	>13.3
Ratio of Time to First Initiation: 690 vs. 600MA/TT	>27.1

MRP-237 Revisions 1 [21] and 2 [12] describe the progress made in Alloy 690/52/152 crack initiation and growth tests up to 2008 and 2012, respectively. Several tests included Alloys 600/82/182 as control specimens, so FOIs can be determined from specimens under identical conditions[6]. Some tests did not use control specimens; in these cases, results are still presented as more evidence of long initiation times. The results described in this and the following sections are listed in alphabetical order by testing laboratory.

- Bettis tested several Alloy 690 heats for crack initiation and growth [12]. The most susceptible heat was tested in the fully annealed condition, and even after approximately 15,000 hours, no cracking was reported.

[5] The Weibayes regression treats non-failed specimens (suspended items) with an implicit assumption that initiation in the oldest specimen is imminent, and it therefore produces conservative times to initiation.

[6] FOIs were reported for some tests, in which case they are repeated here. If no FOI was reported, a FOI was calculated as the ratio of the time to first initiation for Alloy 690 specimens (or test duration if no initiation occurred) to the time to first initiation of Alloy 600 specimens.

- Commissariat à l'énergie atomique (CEA) tested several different types of Alloy 690 specimens, including reverse U-bend (RUB) and capsule configurations for both industrial-production heats and other experimental heats ([21] and [22]). A total of 40 different heats were used. No PWSCC was observed in any of the RUB specimens up through 90,000 hours, and there were no leaks in the capsules up to 100,000 hours. Alloy 600 capsule specimens cracked after 800 hours, giving a FOI of 125.
- Électricité de France (EDF) tested 48 C-ring specimens of Alloy 690, as well as several control specimens of Alloy 600 ([12] and [23]). The control specimens cracked after about 2000 hours, whereas the Alloy 690 specimens showed no signs of crack initiation through the end of the test at 3600 hours. The relatively short duration of these tests yields a very conservative FOI of 1.8.
- Knolls Atomic Power Laboratory (KAPL) performed tests on Alloy 690 that lasted up to 51,000 hours [24]. Of the 24 specimens tested, only two showed any indication of SCC occurrence at the end of the test, and these only had minor pockets of intergranular attack.
- Mitsubishi Heavy Industries (MHI) used mockups to test the PWSCC susceptibility of Alloy 690 ([12] and [25]). No cracking was detected in the Alloy 690 specimens after 40,000 hours. In contrast, Alloy 600 reference plugs showed leakage before 10,000 hours, giving a FOI of about 4. MHI also tested various forms of plant components. An Alloy 600MA steam generator tube (first rupture around 1000 hours) was compared to an Alloy 690TT CRDM nozzle (no rupture up to 95,000 hours) and an Alloy 690TT BMI nozzle (no rupture up to 80,000 hours). The FOIs calculated from these tests for Alloy 690TT over Alloy 600 MA are 95 and 80, respectively.
- Pacific Northwest National Laboratory (PNNL) recently started testing highly cold-worked material of Alloy 690 in conjunction with reference Alloy 600 material [26]. The Alloy 600 specimens cracked after about 1500 hours. The Alloy 690 tests are still ongoing, but as of November 2013, no cracking had been reported after 9200 hours of testing. The most recent information on these tests yields a minimum FOI of 6.1.
- Vattenfall tested the MA and TT treatments of both Alloy 600 and Alloy 690 ([21] and [27]). The number of RUB specimens and earliest times to initiation are shown in Table 3-2. For the MA condition, Alloy 690 has exhibited a FOI of over 49 versus Alloy 600. For the TT condition, the FOI is over 4.7. Both of these FOIs are limited by test duration.

Table 3-2
Vattenfall Data on the PWSCC Resistance of Alloys 600 and 690 [21]

Alloy	No. of Specimens	Time to Initiation (hours)
600MA	100	670
600TT	17	7000
690MA	41	>33,000
690TT	26	>33,000

3.2.1.2 Alloy 690 HAZ Crack Initiation

KAPL tested the HAZ region for Alloys 690 and 600 for both unconstrained and constrained (<14% plastic strain) welds [12]. It was determined that while the Alloy 600 HAZ cracked readily, the Alloy 690 HAZ did not show any initiation under the same conditions.

3.2.1.3 Alloy 52/152 Crack Initiation

EDF tested Alloys 52/152, 82, and 182 to determine relative improvement factors ([21] and [28]). Alloy 182 cracked after 95 hours, and Alloy 82 cracked after 570 hours. In comparison, Alloy 52/152 still had not cracked after >21,000 hours. This resulted in a FOI for Alloy 52/152 of 37 compared to Alloy 82 and over 150 compared to Alloy 182.

KAPL tested Alloy 52/152 welds for 2300 hours at 640°F (338°C) and 5300 hours at 680°F (360°C) [21]. The former tests showed no indications of SCC, while the latter only had a few, isolated "pockets." KAPL estimated the FOI of Alloy 52/152 over Alloy 82 to be approximately 100.

While MHI has not compared Alloy 52/152 to Alloy 82/182, they have had notable results in their PWSCC initiation tests [12]. Specimens of both Alloys 52 and 152 have not cracked after 107,000 hours, which are the longest tests yet reported.

Table 3-3 provides a summary of the crack initiation testing detailed throughout this section.

Table 3-3
Summary of FOIs for Crack Initiation for Alloys 690/52/152

Source	Material Comparison	Temperature [°F (°C)]	FOI
MRP-111	690:600MA	599-680 (315-360)	>26.5
MRP-111	690:600TT	599-680 (315-360)	>13.3
MRP-111	690:600	599-680 (315-360)	>27.1
CEA	690:600	680 (360)	>125
EDF	690:600	680 (360)	>1.8
MHI	690:600	680 (360)	>4
MHI	690TT:600MA	680 (360)	>95
MHI	690TT:600MA	680 (360)	>80
PNNL	690:600	617 (325)	>6.1
Vattenfall	690MA:600MA	689 (365)	>49
Vattenfall	690TT:600TT	689 (365)	>4.7
EDF	52/152:82	680 (360)	>37
EDF	52/152:182	680 (360)	>150
KAPL	52/152:82	680 (360)	~100

3.2.2 PWSCC Growth Rates

This section enumerates crack growth rate testing done by individual laboratories for different material conditions (Alloy 690 base metal, Alloy 690 HAZ, and Alloy 52/152). It is noted that much of the Alloy 690 CGR data was produced using specimens with significant amounts of cold work, while the database of laboratory CGRs applied to develop the MRP-55 [29] CGR equation did not include cold-worked specimens. The current effort of the authors to consolidate and interpret the latest set of available data is described in Section 3.3.

3.2.2.1 Alloy 690 Crack Growth Rates

Argonne National Laboratory (ANL) tested Alloy 690 specimens that had been subjected to a 26% thickness reduction by unidirectional cold rolling [21]. In this more susceptible condition, crack growth rates were reported to be 2×10-8 mm/s (S-L orientation[7]) and 3×10-8 mm/s (S-T orientation[7]). The MRP-55 [29] disposition curve for non-cold-worked Alloy 600 predicts CGRs on the order of 1×10^{-7} mm/s. Thus heavily cold-worked Alloy 690 still produced a crack growth FOI of about 5 over Alloy 600 in the S-L orientation and about 3 for the S-T orientation.

[7] Crack growth orientation is defined in Reference [21]:

- S-L: crack is located in the plane of the rolling/straining direction, with growth parallel to the rolling/straining direction (tending to produce the highest susceptibility to SCC growth)
- S-T: crack is located in the plane of the rolling/straining direction, with growth perpendicular to the rolling/straining direction (tending to produce intermediate susceptibility to SCC growth)

Bettis tested 186 Alloy 690 specimens from three heats under various conditions, including up to 33% cold work and temperatures between 600 and 680°F (316 and 360°C) [21]. A positive correlation between cold work and PWSCC susceptibility was determined, so Alloy 600 was also tested with matching levels of cold work. This work resulted in the conclusion that the crack growth FOI for Alloy 690 over Alloy 600 is between 5 and 10.

General Electric Global Research Center (GE-GRC) obtained CGRs of $<10^{-8}$ mm/s for Alloy 690 specimens with 25% cold work (CW) tested at 644°F (340°C) [21]. The FOI of the cold-worked Alloy 690 relative to Alloy 600 without cold work was determined to be at least 70; the FOI relative to Alloy 600 with similar levels of cold work was predicted to be closer to 400.

3.2.2.2 Alloy 690 HAZ Crack Growth Rates

There has only been minimal testing done to characterize the PWSCC susceptibility of the HAZ regions of Alloys 600 and 690. However, several laboratories have shown that the Alloy 690 HAZ exhibits similar, perhaps marginally larger, CGRs in comparison to Alloy 690 base metal, as shown in Table 3-4. This result indicates that the crack growth FOI for Alloy 690 base metal may also be applicable to the Alloy 690 HAZ.

Table 3-4
Average Crack Growth Rates for Alloy 690 HAZ [12]

Laboratory	Average CGR (mm/s)
ANL	$\leq 1\times10^{-8}$
CIEMAT	$<4\times10^{-9}$
GE	$<7\times10^{-9}$

3.2.2.3 Alloy 52/152 Crack Growth Rates

GE reported favorable results for Alloy 52/152 [21]. The measured CGRs were similar to those of Alloy 690 with 20% cold work. These resulted in FOIs of 150 compared to Alloy 82 and 400 compared to Alloy 182.

For other labs, CGRs were fairly low, with GE and PNNL reporting $<5\times10^{-9}$ mm/s. However, ANL did report somewhat higher CGRs in MRP-237 Rev. 1, at 5×10^{-8} mm/s ([12] and [21]).

Table 3-5 provides a summary of the base metal and weld metal crack growth testing detailed in this section.

Table 3-5
Summary of FOIs for Crack Growth for Alloys 690/52/152

Source	Material Comparison	Temperature (°C)	FOI
ANL	690:600 (S-L)	608 (320)	5
ANL	690:600 (S-T)	608 (320)	3
Bettis	690:600	600-680 (316-360)	5-10
GE	690 (CW):600	644-680 (340-360)	70
GE	690 (CW):600 (CW)	644-680 (340-360)	400
GE	52/152:82	644-680 (340-360)	150
GE	52/152:182	644-680 (340-360)	400

3.3 2013 EPRI Database of PWSCC Crack Growth Rates for Alloys 690/52/152

With the support of an international Expert Panel for PWSCC of Alloys 690/52/152, EPRI has collected a database with the most current set of available PWSCC crack growth rate data for these materials. The CGR database, with contributions from seven laboratories, includes over 500 data points for Alloy 690 and over 200 data points for Alloys 52/152 and derivations of these weld metals (e.g., 52i, 52M, etc.). The CGR data presented in this report represent the values reported by individual researchers, without any adjustment by the authors other than for temperature and stress intensity factor as discussed below. The data presented below represent essentially all of the data points reported by the various laboratories. No screening process was applied to the data on the basis of test characteristics such as minimum required crack extension or minimum required engagement to intergranular cracking. Instead, an inclusive process was applied to conservatively assess the factors of improvement apparent in the data for specimens with less than 10% added cold work. The only adjustments applied to the data were to normalize the data for the effect of temperature assuming the consensus activation energy for Alloy 600 of 130 kJ/mole, and the CGR was normalized to a common stress intensity factor using the K dependence assumed in the probabilistic modeling introduced in Section 4.3 (see Section B.2.3). Note that in the probabilistic modeling, the MRP-55 CGR equation for Alloy 600 [29] was conservatively modified to reflect a stress intensity factor threshold of zero. The modified MRP-55 equation was selected to have a very similar K dependence to that of the original MRP-55 equation over the range of stress intensity factors relevant to the laboratory CGR data collected for Alloys 690/52/152.

In Figure 3-1, the data for Alloy 690 specimens with less than 10% cold work are compared to the standard MRP-55 curve for thick-wall Alloy 600 material. For Alloy 690 CRDM/CEDM nozzles and other RPVHPNs, the effective cold-work level in the bulk Alloy 600 base metal is expected to be no greater than roughly 10% [55]. The MRP-55 curve [29] corresponds to the 75th percentile of the heat-to-heat variability in CGR for Alloy 600 (without intentionally introduced cold work to the tested specimens). Curves attained by scaling the MRP-55 curve by FOIs of 5, 10, and 20 are also shown for comparison with the data for Alloy 690. Additionally, Figure 3-2 shows the empirical distribution of (<10% cold work) Alloy 690 base metal data against several

hypothetical statistical distributions based on the FOI approach. These curves correspond to the nominal distributions used in the probabilistic modeling of this report (for equivalent temperature and stress intensity factor) for different assumed FOI values. Most of the laboratory CGR data are bounded by a FOI of 20, and all of the laboratory CGR data are bounded by a FOI of 10. Furthermore, most of the data support FOI values much larger than 20.

CGR data specific to the weld heat affected zone (HAZ) of the Alloy 690 base metal can also be compared to the MRP-55 curve, as shown in Figure 3-3. Figure 3-4 shows the empirical distribution of Alloy 690 HAZ data against several hypothetical statistical distributions based on the FOI approach. Again, these curves correspond to the nominal distributions used in the probabilistic modeling of this report (for equivalent temperature and stress intensity factor) for different assumed FOI values. Similar to the situation for the Alloy 690 bulk base metal, most of the laboratory CGR data are bounded by a FOI of 20, and all of the laboratory CGR data are bounded by a FOI of 10.

In Figure 3-5, the data for Alloy 52/152 specimens are compared to the standard MRP-115 curve for Alloy 182 weld metal. The MRP-115 curve [14] corresponds to the 75^{th} percentile of the weld-to-weld variability in CGR for Alloy 182 (with growth along the dendrite solidification direction). Curves attained by scaling the MRP-115 curve by FOIs of 5, 10, and 20 are shown for reference. It should be noted that there have been substantial differences in the CGR data reported between laboratories in some of the cases in which the same material was tested by multiple laboratories. This behavior accounts for the highest CGRs observed in Figure 3-5. Figure 3-6 shows the empirical distribution of Alloy 52/152 data against several hypothetical statistical distributions based on the FOI approach. Again, these curves correspond to the nominal distributions used in the probabilistic modeling of this report (for equivalent temperature and stress intensity factor) for different assumed FOI values. The full set of laboratory CGR data is virtually bounded by a FOI of 20, although most of the data support much larger FOI values. The wider distribution exhibited by the empirical data suggests more variability for crack growth rates in Alloys 52/152 compared to Alloy 182. This may be physically representative, but may also be an artifact of different testing procedures employed by different investigators.

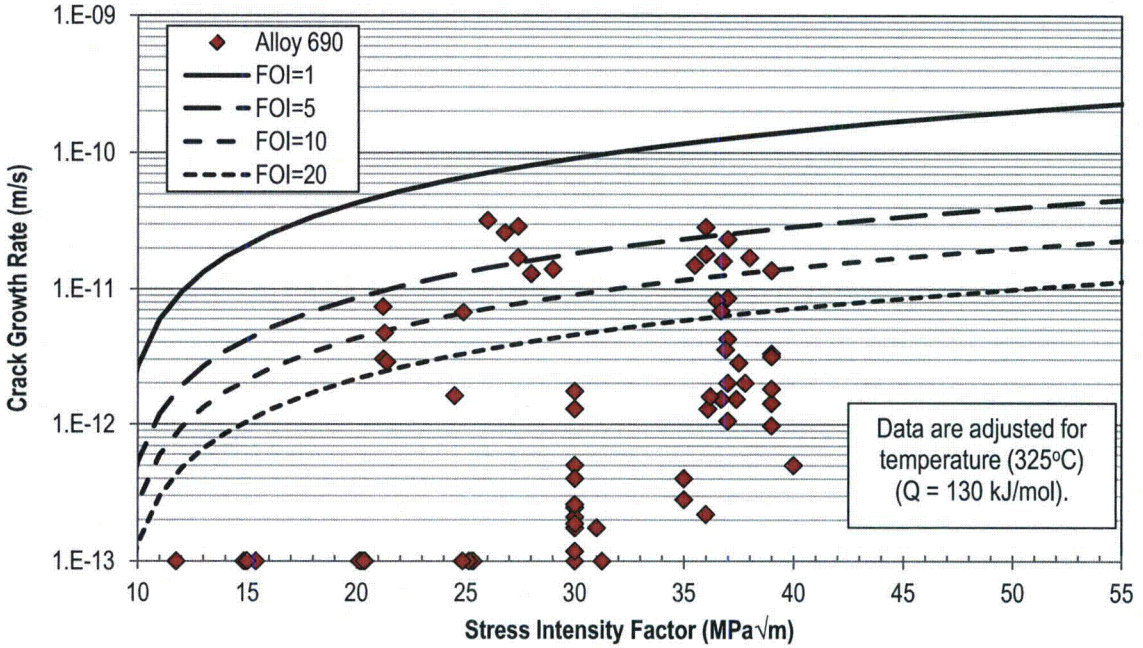

Figure 3-1
Alloy 690 Data with <10% Cold Work from the 2013 EPRI CGR Database, Shown with Variations on the MRP-55 (75th Percentile) Curve for Alloy 600

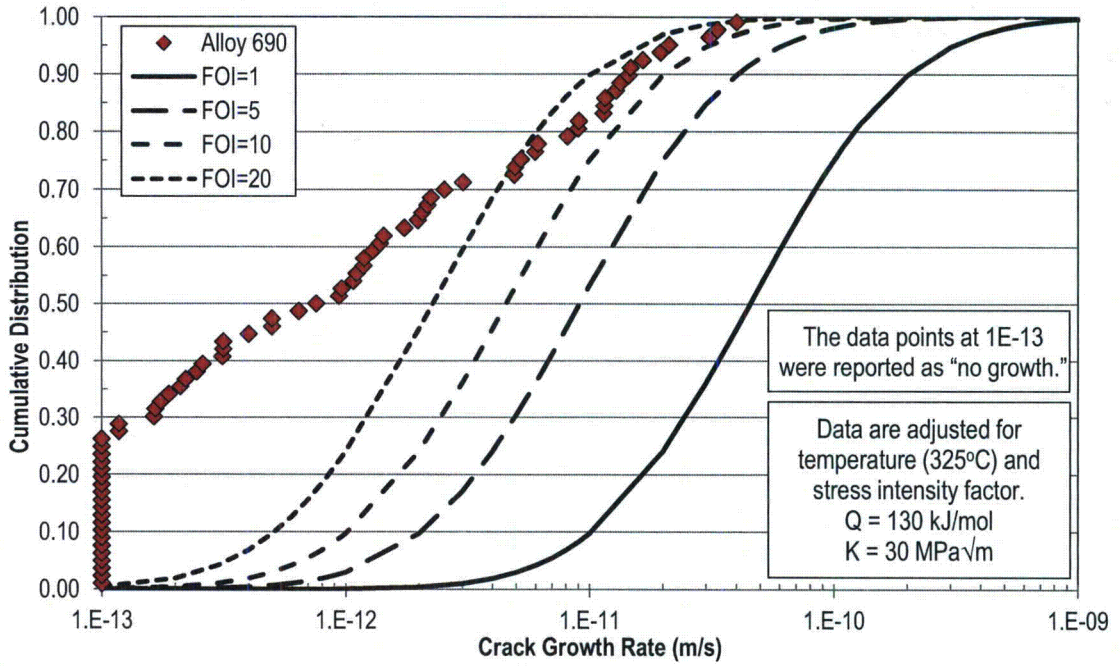

Figure 3-2
Empirical Cumulative Distribution Function of Alloy 690 Data with <10% Cold Work from the 2013 EPRI CGR Database, Shown with Variations on the Modified MRP-55 Distribution of CGRs Input to the Probabilistic Model

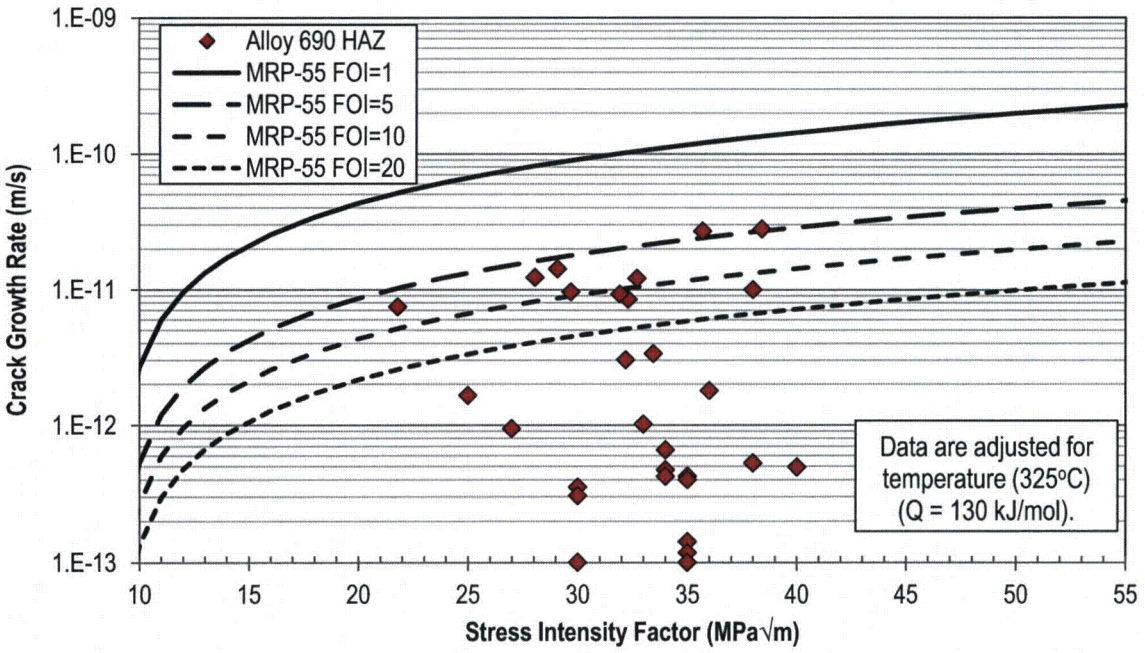

Figure 3-3
Alloy 690 HAZ Data from the 2013 EPRI CGR Database, Shown with Variations on the MRP-55 (75th Percentile) Curve for Alloy 600

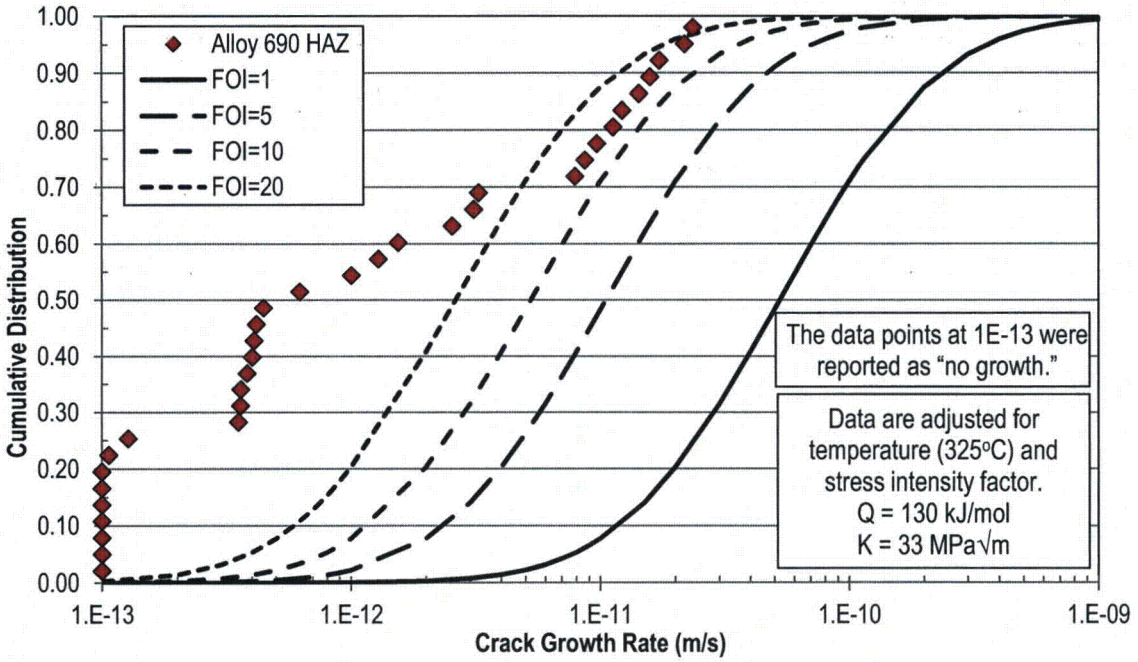

Figure 3-4
Empirical Cumulative Distribution Function of Alloy 690 HAZ Data from the 2013 EPRI CGR Database, Shown with Variations on the Modified MRP-55 Distribution of CGRs Input to the Probabilistic Model

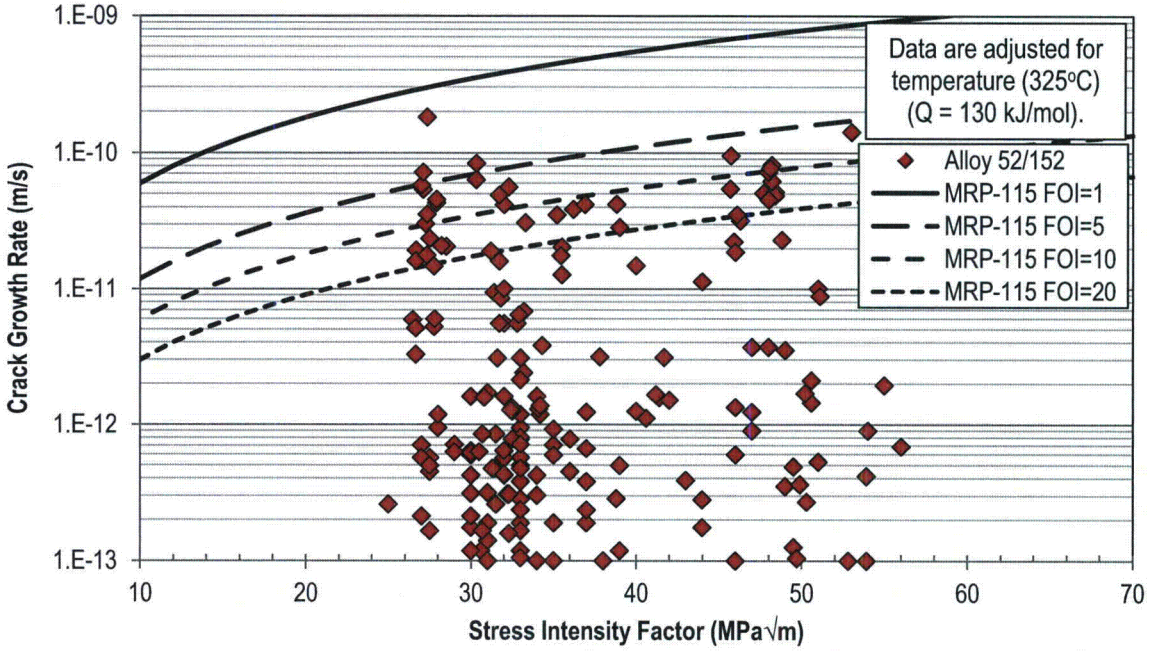

Figure 3-5
Alloy 52/152 Data from the 2013 EPRI CGR Database, Shown with Variations on the MRP-115 (75th Percentile) Curve for Alloy 182

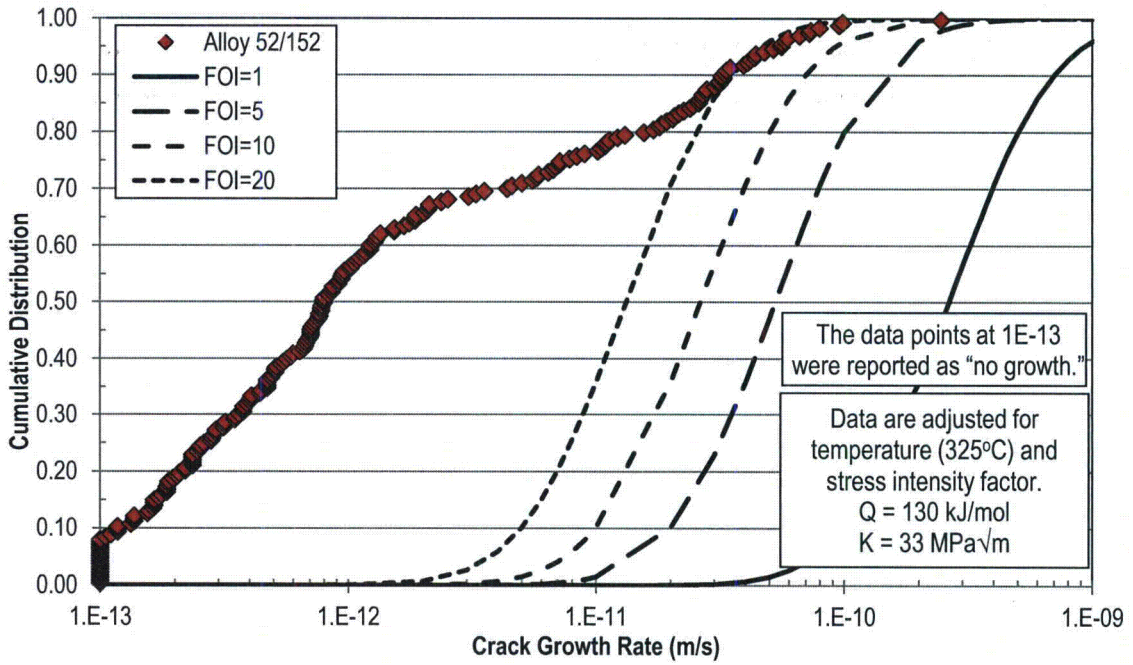

Figure 3-6
Empirical Cumulative Distribution Function of Alloy 52/152 Data from the 2013 EPRI CGR Database, Shown with Variations on the MRP-115 Distribution of CGRs Input to the Probabilistic Model

3.4 Conclusions Regarding Factors of Improvement

The authors of MRP-111 [5] and MRP-237 Rev. 1 [21] formulated conclusions about FOIs for Alloys 690/52/152 from the data that was included in their respective reports. These conclusions, as well as those estimated from the 2013 EPRI CGR database, are summarized in Table 3-6.

Table 3-6
Summary of FOIs Calculated From Tests Reported in MRP-111 [5] and MRP-237 Rev. 1 [21]

Source	Initiation		Growth Rate	
	Base Metal (690)	Weld Metal (52/152)	Base Metal (690)	Weld Metal (52/152)
MRP-111 (Weibull/Weibayes)	>26.5 (MA) >13.3 (TT)	NR(1)	NR	NR
MRP-111 (Ratio)	>27.1	NR	NR	NR
MRP-237 Rev. 1	>70 (MA) >40-100 (TT)	>60	~70	~400 (vs. Alloy 182)
2013 EPRI CGR Database (50th %tile)(2)	NR	NR	60 (<10%CW) 98 (HAZ)	331
2013 EPRI CGR Database (75th %tile)(2)	NR	NR	19 (<10%CW) 13 (HAZ)	58

(1) NR = not reported.
(2) The 50th percentile FOI is calculated as the ratio between the 50th percentile of the laboratory CGR data and the 50th percentile of the CGR per the modified MRP-55 distribution or per the MRP-115 distribution, as applicable. Similarly, the 75th percentile FOI is calculated as the ratio between the analogous 75th percentile values.

For crack initiation, FOIs presented in this section are conservatively small because, in many cases, crack initiation of Alloys 690/52/152 was not observed during testing; instead, the initiation time was assumed to be equivalent to the test duration. Additionally, many of the Alloy 690 crack growth rate tests were performed on specimens with considerable amounts of cold work (up to 40%), which is known to accelerate CGRs (by this same reasoning, CGR FOIs from MRP-237 Rev. 1 [21] may also be conservative).

Because work is still ongoing to determine the performance of Alloys 690/52/152 in PWR replacement head applications, conservatively small factors of improvement were applied in the technical basis calculations presented in Section 4:

- The technical basis calculations apply growth FOIs varying from 10 to 20 for Alloy 690 base metal and from 5 to 10 for Alloy 52/152 weld metal and Alloy 690 HAZ material. The lower assumed growth FOI values for the weld metal and HAZ material reflect the general concern for potentially elevated crack growth rates in the weld metal and base metal HAZ in comparison to that for bulk base metal. It is noted that the currently available laboratory data

for Alloy 690 HAZ material do not show a substantially elevated crack growth rate in comparison to that for Alloy 690 bulk base metal.

- The technical basis calculations investigating the nuclear safety concern of nozzle ejection do not take any credit for an improved resistance to PWSCC initiation of the Alloy 690 RPVHPNs (i.e., an initiation FOI of 1 is assumed). Based on the plant and laboratory data presented in Sections 2 and 3, additional cases apply a conservatively small initiation FOI of 5 for the purpose of investigating the benefit of the improved performance of Alloys 690/52/152 for the probability of leakage due to through-wall PWSCC.

Based on the work presented in Sections 2 and 3, there is high confidence that the actual FOI values for Alloy 690 RPVHPNs are substantially greater than the values assumed in the inspection technical basis calculations. In the future, the situation may be re-assessed and excess conservatism removed from the technical basis for inspection.

4
DETERMINISTIC AND PROBABILISTIC PWSCC EVALUATIONS

This section gives an overview of the deterministic and probabilistic evaluations of the effect of inspection intervals on risks related to PWSCC degradation of Alloy 690 RPVHPNs, namely in comparison to the correspondent risks in Alloy 600 RPVHPNs. This overview includes an explanation of the evaluation approaches, a presentation of key results, and a statement of the conclusions drawn from these results.

This section is augmented by Appendix A and Appendix B, which together comprise a comprehensive description of the probabilistic model and its constituent submodels, detailed input listings, and a comprehensive presentation of results.

4.1 Approach

This section compiles both deterministic and probabilistic technical bases for establishing a recommended inspection interval for Alloy 690 top heads. The deterministic technical basis applies industry-standard crack growth calculation procedures (e.g., relief requests, techniques developed in earlier MRP reports) to predict time to certain adverse conditions under various conservative assumptions. These deterministic results provide a conservative bound on the recommended inspection interval for Alloy 690 top heads.

Probabilistic evaluation is then applied to make predictions for leakage and ejection risk generally using best-estimate inputs and assumptions. This evaluation is conducted for both Alloy 600 and Alloy 690 top heads and for various different inspection intervals. The objective is to provide a technical basis for an Alloy 690 top head inspection interval based on absolute and relative risk assessment, the latter in comparison to correspondent risks in Alloy 600 RPVH with inspection internals simulated in accordance with current industry standards. This probabilistic evaluation gives consideration to complex and potentially risk-limiting processes aside from growth, like PWSCC initiation, UT flaw detection prior to leakage, and UT or visual detection prior to nozzle ejection. The probabilistic model is similar to those applied in MRP-105 [6] and MRP-335 Rev. 1 [30].

Evaluation is conducted using initiation and growth models reflective of Alloy 600 and, separately, Alloy 690. The Alloy 690 models are based on the FOI approach substantiated in Section 3, wherein established Alloy 600 initiation time model predictions are scaled (shifted into the future) by some value greater than or equal to one (the FOI for initiation) and established Alloy 600 crack growth rate model predictions are scaled by some value less than or equal to one (the reciprocal of the FOI for growth). Given the current lack of precise and substantiated FOIs, simulation experiments are conducted with various assumed FOIs yielding a set of results (each bearing different degrees of conservatism with respect to available data) from which conclusions may be refined.

4.2 Deterministic Crack Growth Evaluations

Deterministic crack growth evaluation is commonly applied to assess PWSCC risks for specific components and operating conditions. In general, such deterministic evaluations quantify the time between a certain initial condition—a known or hypothetical flaw size—to some adverse condition—through-wall growth, a prescribed stability margin, etc.—under a set of assumptions. This time is then used to inform options for inspection intervals, mitigation, and repair. Often, deterministic evaluations rely on conservative assumptions to allow margin for error.

Deterministic crack growth evaluation is provided in this section as a precursor to probabilistic evaluation to illustrate directly the relationship between the improved PWSCC growth resistance of Alloys 690/52/152 and the average time to certain adverse conditions. These evaluations rely on conservative crack growth rate predictions and the assumption of an existing flaw (which is replaced with a PWSCC initiation model for probabilistic evaluation). The evaluations are therefore considered to provide a reasonable *lower bound* on the average time to adverse conditions, from which a *conservative* inspection interval may be recommended.

The probabilistic evaluation replaces these conservatisms with best estimates, incorporating distributed inputs to reflect uncertainty and variability. The probabilistic evaluation returns predictions in the form of probabilities, based upon which examination intervals may be adjusted to achieve an acceptable level of risk.

4.2.1 Existing Calculations

This evaluation draws upon existing crack growth calculations for Alloy 600/82/182 RPVHPNs. Results of these existing calculations are summarized in Table 4-1. As described in the next subsection, these calculations are adjusted to be representative of Alloy 690/52/152 RPVHPNs.

The following list describes each cited crack growth calculation and states key underlying conservatisms:

- **General:** The following conservatisms apply to all crack growth calculations presented in this section:
  - All calculations use a 75th percentile crack growth rate curve derived from Alloy 600 data, as developed in MRP-55 [29].
  - For estimating crack stress intensity factors, all calculations assume residual stresses that are bounding of those predicted in the vicinity of the location of interest. That is, there is no credit taken for a drop in residual stress as flaws grow in length away from stress concentrations.
  - Time to leakage results for surface cracks are reported from 10%TW (e.g., ~1.6 mm). There is some likelihood of detecting cracks with UT or eddy current examination techniques before they reach this size.
  - Growth results for through-wall circumferential cracks along the J-groove weld are reported from 30° to 300°. Leakage is expected to manifest through cracks less than 30° around the circumference, such that there is some likelihood of visually detecting cracks before they reach this size.

  - Calculations are usually performed for uphill and downhill RPVHPN locations. Time for growth results are reported for the more conservative location in all cases.

- **MRP-105 Deterministic Calculations:** Section 6 of MRP-105 [6] provides deterministic crack growth analyses for the time to grow from 30° to 300° for through-wall circumferential flaws along the top edge of J-groove welds. Several conservatisms are applied including the use of stress intensity factors that bound those predicted across all penetration angles for a given crack length, and a factor of two applied to all crack growth rates to account for environmental uncertainties.

  MRP-105 studies four distinct RPVHPN geometries, each the outermost penetration associated with one of four distinct reactor vessel top head designs.

- **Examination Frequency Relief Request:** AM-2007-011 (Section 5.2 of Attachment 3 of the 10 CFR 50.55a Alternate Examination Frequency Relief Request for Byron 2) [31] provides time to leakage calculations for nozzle OD axial flaws, ID axial flaws, and OD circumferential flaws. Several conservatisms are applied including the assumption that growth is driven by the stress profile for the location of maximum residual stress and the assumption that crack growth rates for OD circumferential flaws exposed to the annulus environment are scaled by a factor of two.

  AM-2007-011 studies cracks present in nozzles with different penetration angles, each with different predicted residual stress fields. Results for time to leakage are reported for the 42.8° penetration. These results are similar to or lower than those for other penetration angles investigated in the report.

- **Technical Basis for CRDM Inspection Interval:** Appendix B of R-3515-00-1-NP [32] provides calculations for the time to leakage for nozzle ID and OD axial flaws and the time to grow from 30° to 300° for through-wall circumferential flaws along the top edge of J-groove welds.

  R-3515-00-1-NP studies cracks present in nozzles with different penetration angles, each with different predicted residual stress fields. Results for growth times are reported for the 27.1° penetration. These results are similar to or lower than those for other penetration angles investigated in the report.

- **MRP-375 Deterministic Calculations:** The deterministic calculations of this report are based on those described in Section 5-2 of MRP-335 Rev. 1 [30]. This includes deterministic calculations for the time to leakage for nozzle ID and OD axial flaws and the time to grow from 30° to 300° for through-wall circumferential flaws along the top edge of J-groove welds. Several conservatisms are applied, including the use of stress intensity factors that bound those predicted across all penetration angles for a given circumferential crack length, a zero stress intensity factor threshold for growth, and a factor of two applied to all circumferential crack growth rates to account for environmental uncertainties.

  The assumed residual stress profile at each location is derived as an average of residual stress results across various different penetration angles. The average penetration angle in the underlying data set is roughly 20°.

Table 4-1
Summary of Deterministic Crack Growth Calculations (Factor of Improvement of 10 to 20 Assumed)

Crack Type	Case Name and Table Reference Number	Flaw Orientation and Location	Penetration Angle (°)	Initial Flaw Size	Initial Aspect Ratio	End Condition	Operating Temperature (°F)	Time for Growth from Initial to End Conditions (EFPY)	Time for Growth Adjusted to 613°F (EFPY)	Time for Growth Conservatively Adjusted to Alloy 690 (EFPY)
Surface Crack	Examination Frequency Relief Request [1]	OD Circumferential Crack (Downhill)	42.8	~10%TW	6	100%TW	558	8.2	2.0	39.7
		ID Axial Crack (Uphill)	42.8	~10%TW	6	100%TW	558	7.7	1.9	37.3
		OD Axial Crack (Uphill)	42.8	~10%TW	2	to top of weld	558	9.4	2.3	22.8
	Inspection Interval Technical Basis [2]	ID Axial Crack (Downhill)	27.1	~10%TW	6	100%TW	599.7	2.8	2.0	40.3
		OD Axial Crack (Downhill)	27.1	~10%TW	2	to top of weld	599.7	5.1	3.7	36.7
	Deterministic Calculation of This Report	ID Axial Crack (Downhill)	~20	~10%TW	4.5	100%TW	600	5.3	3.8	76.8
		OD Axial Crack (Downhill)	~20	~10%TW	4.5	to top of weld	600	4.1	3.0	29.7
	Conservative Time Between Detectable Flaw and Leakage (Median of Cases)								**2.3**	**37.3**
Through-Wall Circumferential Crack	MRP-105 Deterministic Calculations [3]	Circumferential Crack along the J-groove Weld (Downhill)	38	30°	N/A	300°	600	22.1	16.0	320.3
			43.5	30°	N/A	300°	600	10.8	7.8	156.5
			48.8	30°	N/A	300°	600	9.3	6.7	134.8
			49.7	30°	N/A	300°	600	18.8	13.6	272.5
	Inspection Interval Technical Basis [2]		27.1	30°	N/A	300°	599.7	8.4	6.0	120.8
	Deterministic Calculation of This Report		~20	30°	N/A	300°	600	13.5	9.8	195.7
	Conservative Time Between Leakage and Stability Risks (Median of Cases)								**8.8**	**176.1**

[1] *Byron Unit 2 - Technical Basis for Reactor Pressure Vessel Head Inspection Relaxation*, AM-2007-011 Revision 1, Exelon Nuclear, 2007.
[2] *Technical Basis for RPV Head CRDM Nozzle Inspection Interval - H. B. Robinson Steam Electric Plant, Unit No. 2*, R-3515-001-NP, Dominion Engineering, Inc., 2003.
[3] *Materials Reliability Program: Probabilistic Fracture Mechanics Analysis of PWR Reactor Vessel Top Head Nozzle Cracking (MRP 105)*, EPRI, Palo Alto, CA: 2004. 1007834.

4.2.2 Approach to Using Existing Calculations

Existing crack growth calculations for Alloy 600/82/182 RPVHPNs are selected and adjusted to be representative of Alloy 690/52/152 RPVHPNs.

First, to allow consistent interpretation of the results, the initial and end conditions for each crack type are made uniform. Surface flaw results are estimated from an initial condition of 10% through-wall[8]. The end condition for ID axial and OD circumferential flaws is through-wall growth; the end condition for OD axial flaws is growth to the top (or heel) of the J-groove weld. Through-wall circumferential crack results are estimated from an initial condition of 30° around the nozzle to an end condition of 300° around the nozzle (suggestive of net section collapse risk).

Then, to further allow consistent interpretation, all results are adjusted[9] to an operating temperature of 613°F (323°C) using the Arrhenius relationship with an activation energy of 130 kJ/mol. This operating temperature is believed to be an upper bound for operating Alloy 690 top heads in service today.

Finally, the results of the Alloy 600 deterministic calculations are scaled by a FOI for PWSCC growth. Consistent (if not conservative) with respect to laboratory data presented in Section 3, a FOI of 20 is assumed for ID axial cracks, OD circumferential cracks, and through-wall circumferential cracks. These cracks are expected to reside predominantly in wrought Alloy 690 material. The leakage concern for OD axial cracks is due to growth upward from the initiation location below the weld. Because such OD axial cracks are expected to reside partially in the HAZ of the Alloy 690 material, a FOI of only 10 is conservatively assumed.

4.2.3 Conclusions Regarding Deterministic Results

The deterministic calculation results applicable to Alloy 600 and Alloy 690 nozzles adjusted to a common temperature of 613°F (323°C) are given in the two rightmost columns of Table 4-1. As detailed in Sections 4.2.1 and 4.2.2, these calculations compound various conservatisms and should thus be interpreted as reasonable lower bounds on the times to adverse conditions on reactor vessel top heads, i.e., these times are not considered best estimates.

The conservative time between detectable flaw size (assumed to be 10% through-wall) and leakage varies between 1.9 and 3.8 EFPY at 613°F (or between RIY = 2.6 and 5.2 via the N-729-1 definition) for a range of different crack types on an Alloy 600 RPVH. This is consistent with the N-729-1 requirement of volumetric examination before RIY = 2.25. Because inspections occur after fewer RIYs than it takes a detectable flaw to grow through-wall, an inspection would occur and provide an opportunity to detect a given flaw before leakage results.

The conservative time between evident leakage and risk of net section collapse varies between 6 and 16 EFPY at 613°F (i.e., between RIY = 8 and 22) for the Alloy 600 RPVH. These results demonstrate that considerable time is required for an assumed through-wall circumferential flaw

[8] Most reports assumed an initial depth somewhat less than 10% through-wall; however, time to leakage from 10% through-wall could generally be estimated with depth versus time plots.

[9] In place of being able to reproduce results at different temperatures or with different FOIs on growth, adjustments to growth predictions are made simply by scaling time spans linearly. This is believed to be a reasonable approximation for the purposes of this deterministic evaluation.

to grow to the size that nozzle ejection may occur, even in the case of crack growth rates applicable to Alloy 600 material.

For different analyses and different crack types on an Alloy 690 RPVH, the conservative time between detectable flaw size and leakage varies between 23 and 77 EFPY at 613°F (or between RIY = 31 and 106). This result is supportive of an extension of the UT inspection interval to 20 calendar years.

The conservative time between evident leakage and risk of net section collapse varies between 121 and 320 EFPY at 613°F (i.e., between RIY = 167 and 441) for the Alloy 690 RPVH. These results suggest an extremely low risk of Alloy 690 RPVHPN ejection, even if inspections are assumed to be neglected. The purpose of the probabilistic analyses discussed next is to quantify this risk through simulation of the PWSCC degradation process, with conservatively small credit for the improved performance of Alloys 690/52/152 versus Alloys 600/82/182.

4.3 Summary of Probabilistic Model

The following sections provide an overview of the probabilistic model for evaluating the effect of UT inspection interval extension on leakage and nozzle ejection risk for reactor vessel top heads. The model underlying the probabilistic evaluation is modified from the model presented in Appendix B of MRP-335 Rev. 1 [30]. The probabilistic model is capable of accepting plant- and industry-specific inputs (distributed or deterministic), conducting lifetime analyses of PWSCC manifesting in various forms at various locations, and returning statistics to describe the risks of key failure modes (e.g., leakage and ejection).

The integrated probabilistic model includes submodels for simulating component and crack stress conditions, PWSCC initiation, PWSCC growth, and flaw examination. In comparison to the prior version used in MRP-335 Rev. 1, the crack initiation and crack growth submodels have been augmented to include FOIs to scale the results of established Alloy 600/82/182 models to be more representative of Alloy 690/52/152 components.

Appendix A provides a more comprehensive description of the probabilistic model.

The key results generated for this study are summarized in Section 4.4.

4.3.1 Factor of Improvement (FOI) Framework

The submodels used for crack initiation and growth prediction for Alloy 600 RPVHPNs in MRP-335 Rev. 1 have been adapted for Alloy 690 RPVHPNs by applying FOIs to account for superior PWSCC resistance of the material. This approach is based on:

- Approaches often applied to model the susceptibility to SCC of Alloy 600TT and Alloy 690 steam generator tubing [33].
- Previous relief request submissions to the NRC [31].
- MRP-237 Rev. 2 [12], which poses the superior performance of Alloy 690 to Alloy 600 in terms of FOI, as described in Section 3.

PWSCC Initiation FOI: Statistical Weibull models are developed for the PWSCC initiation process in Alloy 600 top heads. This development is enabled by an expansive data set quantifying Alloy 600 top head operating and inspection experience, including many incidences

of flaw detection. Given the relatively limited operating experience with Alloy 690 top heads, it is considered premature to develop specific statistical PWSCC initiation models. Since no incidences of flaw detection have been observed, such development would rely on necessarily conservative assumptions about the imminence of PWSCC in Alloy 690 top heads. Instead, this study applies a simple FOI approach to adjust established Alloy 600 initiation predictions to be better representative of Alloy 690.

To apply the Alloy 600 initiation experience to Alloy 690, initiation time predictions for Alloy 600 locations—based on a Weibull model developed from Alloy 600/82/182 top head data—are multiplied by a defined FOI (greater than or equal to one) to account for the superior resistance to cracking. Likewise, initiation time predictions for Alloy 52/152 locations—also, based on a Weibull model developed from Alloy 600/82/182 top head data—are multiplied by a defined, potentially different, FOI.

Based on the available data presented in Section 3, initiation FOIs of at least 20 are demonstrated by existing data. Such factors on the time to initiation result in a negligible probability of nozzle ejection (i.e., less than about 10^{-8} per head per year) and very low probability of leakage. The detailed calculations of this report apply conservatively low initiation FOIs varying from 1 to 5 in order to conservatively credit the improved initiation performance of Alloys 690/52/152 relative to Alloys 600/82/182.

PWSCC Growth FOI: Statistical models for PWSCC crack growth rates in Alloy 600 and Alloy 82/182 were developed in MRP-55 [29] and MRP-115 [14], respectively. At the time of this report, work is ongoing to develop CGR equations for Alloys 690/52/152 based on a detailed screening and assessment of the available data for CGR testing in these alloys. Therefore, to account for the increased PWSCC growth resistance of Alloys 690/52/152, the FOI approach is applied to adjust predictions based on the established Alloy 600 and Alloy 82/182 models.

The FOI for crack growth is applied by dividing the Alloy 600/82/182 flaw depth and flaw length growth rates by a FOI. Different FOIs may also be applied to crack locations residing in different RPVHPN locations to reflect variation in the susceptibility of wrought Alloy 690 base metal, Alloy 52/152 weld material, and Alloy 690 material located in the J-groove weld heat affected zone (HAZ).

Similar to the initiation FOIs above, taking credit for a growth FOI such as 100 results in a negligible probability of nozzle ejection. However, since work is still ongoing to determine the performance of Alloys 690/52/152 in PWR replacement head applications, conservatively smaller factors of improvement were applied in the technical basis calculations. The studies presented in this section use growth FOIs varying from 10 to 20 for Alloy 690 base metal and from 5 to 10 for Alloy 52/152 weld metal and Alloy 690 HAZ material. In the future, the situation may be re-assessed and excess conservatism removed from the technical basis for inspection.

4.3.2 Key Modeling Assumptions

Several assumptions and simplifications are embedded in the probabilistic model used for this evaluation. Knowledge of the following simplifications is key when interpreting the results given in this section and in Appendix B; however, the conclusions drawn in this report are not expected to be dependent on these simplifications. It is noted that each of these key modeling assumptions

is shared with the RPVHPN model described in the peening topical report, MRP-335 Rev. 1 [30].

- *Possible flaw locations.* It is assumed that multiple crack initiation on a single RPVHPN can be adequately represented through six possible initiation sites: an axial flaw at the nozzle ID, an axial flaw at the nozzle OD below the weld, and a radial flaw in the weld material (each at the greatest uphill and greatest downhill locations, i.e., the locations of largest tensile residual stresses). To determine risks representative of an entire top head, many RPVHPNs at different angles of incidence relative to the RPV head are modeled. The probability of initiation at any given site is assumed to be equal (i.e., the surface stress dependency of PWSCC initiation is not explicitly modeled).
- *Circumferential flaw initiation.* If any nozzle or weld flaw grows into the annulus above the J-groove weld[10], a circumferential flaw is assumed to initiate with an initial circumferential extent of 30°. This assumption is consistent with MRP-105 [6].
- *Nozzle ejection threshold.* Ejection of a given RPVHPN is assumed to occur once the through-wall circumferential flaw reaches a specified threshold length. Cases presented in this section assume a conservative threshold length equivalent to 300° around the penetration, which is the same value used in MRP-105 [6] and is based on net section collapse (NSC) calculations presented in Appendix D of that report. The difference in ASME BPVC Section II-D material properties between Alloy 600 and Alloy 690 only changes the results of NSC calculations by approximately 1°. Consequently, this value remains valid and conservative irrespective of the top head alloy. Additional details are provided in Section A.8.

4.3.3 Individual Submodels

The submodels of the probabilistic framework have been adapted from Appendix B of MRP-335 Rev. 1 [30] for use with Alloy 690 RPVHPNs. The submodel enabling the consideration of peening effects has been disabled in this version of the probabilistic model while additional inspection scheduling options have been added. The individual submodels incorporated into the probabilistic model of RPVHPN PWSCC are detailed in Appendix A and summarized below:

- *Load and stress calculation.* The total stress profile along each line of potential flaw growth is approximated as a second-order polynomial. Polynomial coefficients are fit based on the results of FEA studies spanning different nozzle geometries, welding parameters, etc. The crack stress intensity factors at the deepest point and at the surface tips are calculated with the standard influence coefficient method [34]. Further details are provided in Section A.5.
- *Flaw initiation.* The flaw initiation model sets an initiation time and an initial depth and length for flaws. To adjust established Alloy 600/82/182 Weibull-based PWSCC initiation models for use on Alloy 690 RPVHPNs, the calculated initiation times are multiplied by FOIs as described in Section 4.3.1. Details are provided in Section A.4.

[10] Flaw growth into the annulus is presumed to occur if an axial ID flaw or radial weld flaw grows to a depth exceeding the material thickness or if an axial OD flaw grows to a length such that its uppermost tip extends to the J-groove weld root.

- *PWSCC flaw growth.* The standard PWSCC growth models of MRP-55 [29] for Alloy 600 and of MRP-115 [14] for Alloy 82/182 are adopted in this study. These models account for growth rate dependencies with respect to stress intensity factor and temperature and probabilistically capture the range of growth rates observed in laboratory experiments. To adapt these models for use on Alloy 690 and Alloy 52/152, respectively, the crack growth rates are divided by FOIs. Details are provided in Section A.6.

  Fatigue flaw growth is not considered in this study given that PWSCC crack growth is expected to dominate based on crack growth analyses and as confirmed by plant experience [1].

- *Flaw detection.* UT and BMV inspections are simulated at specified intervals which are guided by the inspection requirements of ASME Code Case N-729-1 [3] as well as the inspection interval extensions sought in this technical basis report.

  The UT inspection model and inputs of MRP-335 Rev. 1 [30] are adopted in this study to express probability of detection as a function of through-wall percentage. UT examinations are assumed to be unable to detect flaws growing in the weld material. Visual detection is modeled probabilistically based on a probability of leakage detection that is assumed constant, irrespective of leak rate. Details are provided in Section A.7.

4.4 Probabilistic Model Results

The probabilistic model described in the previous sections is integrated within a Monte Carlo simulation framework allowing for the statistical prediction of possible outcomes such as nozzle leakage and ejection. The primary statistics used to assess and compare the results of the probabilistic model are defined below and are more thoroughly explained in Section A.8:

- Incremental leakage frequency (ILF) is defined as the average number of new leaking nozzles per year on a RPV top head. This statistic is derived for any given operational cycle by averaging the predicted number of new leaking nozzles for that operational cycle across all Monte Carlo realizations and dividing by the number of calendar years per cycle. Average leakage frequency (ALF) is the average of the ILFs across all cycles in the total operational service period of the plant.

- Likewise, incremental ejection frequency (IEF) is defined as the average number of nozzle ejections per year on a RPV top head. This statistic is derived for any given operational cycle by averaging the predicted number of ejections for that operational cycle across all Monte Carlo realizations and dividing by the number of years per cycle. Average ejection frequency (AEF) is the average of the IEFs across all cycles in the total operational service period of the plant.

For three base cases,[11] the IEF and ILF are plotted in Figure 4-1 and Figure 4-2 , respectively. Table 4-2 provides a listing of key statistics for each of the base cases. A summary discussion of the base case results is provided in Section 4.4.1, and key trends from other studies (in which inspection interval or assumed FOIs are varied) are discussed in Sections 4.4.2 through 4.4.4.

[11] The term "base case" is used here to identify the cases with best-approximation inputs from the cases used to explore parametric model sensitivity or model convergence.

The assumed FOIs for initiation and growth are varied among the cases presented in this section in order to investigate the effect of the assumed degree of improved PWSCC performance of Alloys 690/52/152.[12] To simplify presentation, a naming convention for FOI is used:

$$\text{FOI Identifer} = g\left(FOI_{wrought}\right)/\left(FOI_{HAZ\&weld}\right)\, i\left(FOI_{wrought}\right)/\left(FOI_{HAZ\&weld}\right)$$

where *g* indicates growth FOIs and *i* indicates initiation FOIs. $FOI_{wrought}$ is applied to the wrought nozzle material (with respect to the Alloy 600 predictions), and $FOI_{HAZ\&weld}$ is applied to the HAZ nozzle material (with respect to the Alloy 600 predictions) and the weld material (with respect to the Alloy 182 predictions).[13] For example, g10/5 i2/1 indicates a growth FOI of 10 on the wrought material and of 5 on the HAZ and weld material with an initiation FOI of 2 on the wrought material and of 1 on the HAZ and weld material.

4.4.1 Base Case Results

For direct comparison and comparison with the results other cases presented later, three base cases are defined. In general, each case considers a RPVH operating period of 40 calendar years, a 613°F (323°C) operating temperature, and a refueling cycle length of two calendar years (the cycle length resulting in the maximum time between UT inspections under current requirements). A summary of the FOI and inspection inputs for each base case follows while the remaining inputs are defined in Table B-1 through Table B-9 of Appendix B:

- *Alloy 600 with inspections per N-729-1 (all FOIs are 1)*
- This case provides a benchmark with which to compare the relative change in risk predictions for various inspection regimes and FOIs. UT inspections are simulated to occur on the most frequent schedule that has been applied in the U.S. for top heads with Alloy 600 nozzles, i.e., every fuel cycle, or 2 calendar years in the assumed case.[14] BMV inspections are simulated to occur every other refueling cycle (i.e., every 4 years) for the first 8 EDY of top head operation and then occur every cycle.
- *Alloy 690 case with BMV inspections every 4 years, UT inspections every 20 years, and FOI of g10/5 i1/1*

  The inspection intervals and FOIs selected for this case are used to justify extending the UT inspection interval to 20 years, even with no assumed initiation improvement and modest assumed growth FOIs.

[12] The use of deterministic instead of distributed FOIs is considered superior in this work as it provides a more direct relationship between risks and PWSCC resistance, i.e., it eliminates a layer of abstraction in the presentation of the results.

[13] The use of the same FOI for the Alloy 690 HAZ and weld material was a conservative modeling choice given the general concern for potentially elevated crack growth rates in the base metal HAZ in comparison to that for bulk Alloy 690 base metal.

[14] For the assumed head temperature of 613°F (323°C) and an assumed capacity factor of 0.92, the RIY accumulated between simulated UT inspections is RIY = 2.54. This is slightly greater than the RIY = 2.25 interval of Code Case N-729-1 [3].

- *Alloy 690 case with BMV inspections every 4 years, no modeled UT inspections, and FOI of g20/10 i1/1*

  The inspection intervals and FOIs selected for this case are used to justify extending the UT inspection interval beyond the expected replacement head operating period, with no assumed initiation improvement but a growth resistance for Alloys 690/52/152 that is considered more representative (in comparison to the previous base case) of available information.

As demonstrated in Figure 4-1 and Figure 4-2, UT inspection as modeled is predicted to have a modest effect on leakage risk but a dramatic effect on ejection risk, the latter indicated by the sharp decrease in IEF between the operating cycle preceding UT inspection (at 18.4 EFPY) and the operating cycle following UT inspection (at 20.2 EFPY). The modesty in leakage prevention is due in part to the assumption that UT inspection cannot detect flaws initiating and growing the weld material; the effectiveness for ejection prevention is due to the high probability of detecting through-wall circumferential flaws above the J-groove weld. Since BMV inspections can only detect flaws after leakage, BMV inspection has no effect on the frequency of leakage. On the other hand, the benefit of each BMV inspection (as well as of each UT inspection) is visible in the nozzle ejection frequency results of Figure 4-1.

As shown in Table 4-2, eliminating the UT inspection interval while doubling the FOI for crack growth is predicted to result in a 51% reduction in the AEF (from 6.2E-6 to 3.1E-6). Both of these results are a significant improvement over the Alloy 600 base case, for which the predicted AEF is 5.1E-5 (a factor of 8 or 17 higher than the Alloy 690 base cases).

The ALFs for the three base cases—0.200, 0.196, and 0.146 respectively—are similar. The decreasing trend indicates that ALF is reduced to a greater extent by the higher assumed FOIs than by the more frequent UT examinations (this trade-off being at the heart of this study). Additionally, as detailed in Section 4.4.4, taking credit for a modest FOI on initiation further reduces the probability of leakage.

For greater detail about the results of the base cases, refer to Section B.3.2.1 in Appendix B.

4.4.2 Varying Inspection Intervals

In addition to the inspection strategies of the two Alloy 690 base cases, two additional inspection strategies were considered: the first in accordance with Code Case N-729-1 for PWSCC resistant materials and the second an extension of the BMV interval to 10 years in addition to the extension of the UT interval to 20 years.

As expected at the onset of this study, the inspection of Alloy 690 heads per N-729-1 (with either set of FOIs assumed in the base cases) is predicted to result in a much reduced frequency of nozzle ejection versus that for Alloy 600 heads inspected per N-729-1. However, as discussed in the previous subsection, extending the UT inspection interval to 20 years is predicted to maintain a substantial risk benefit relative to the Alloy 600 case.

For the second base case (g10/5), extending the BMV inspection interval from every other cycle to every five cycles (i.e., from every 4 to every 10 years) with UT inspections every 20 years is predicted to increase the AEF by a factor of two. Under the assumption of g20/10 FOIs, the resultant AEF prediction is still over two orders of magnitude lower than the Alloy 600 base

case; under the assumption of g10/5 FOIs, the resultant AEF prediction is over four times lower than the Alloy 600 base case.

Finally, the g10/5 base case was rerun without UT inspection. Forgoing the UT examination at 20 years resulted in an AEF approximately 16 times larger than the base case and nearly twice that of the Alloy 600 base case.

For greater detail about the results for varying inspection strategies, refer to Section B.3.2.2 in Appendix B.

4.4.3 Factor of Improvement on Crack Growth Rates

Applying FOIs on growth leads to significant reductions in the AEF prediction (typically an order of magnitude greater than the factor of change in the FOI) because both the rate of surface flaw growth and through-wall circumferential crack growth are reduced.

Because leakage is predicted to primarily result from flaws growing through the weld, giving credit for growth improvement solely in the wrought material (e.g., from g20/10 to g100/10) provides limited benefit with regard to leakage reduction.

For greater detail about the results for varying FOIs on growth, refer to Section B.3.2.3 in Appendix B.

4.4.4 Factor of Improvement on Crack Initiation

Crediting initiation improvement leads to smaller relative benefits with regard to ejection than crediting growth improvement. However, initiation improvement does greatly reduce the likelihood of leakage. These results suggest that nozzle leakage is limited by initiation while ejection may be more limited by circumferential growth around the nozzle than by flaw initiation.

The leakage predictions made crediting only growth improvement are generally high in comparison to the low rate of Alloy 690 component leakage that has been observed in practice. Applying a modest FOI of 5 for PWSCC initiation in Alloy 690 and Alloy 52/152 reduces the frequency of leakage predictions to be more consistent with the current observed performance of Alloy 690 RPVHPNs.

For greater detail about the results for varying FOIs on initiation, refer to Section B.3.2.3 in Appendix B.

4.4.5 Probabilistic Model Sensitivity, Convergence, and Benchmarking Results

In addition to varying the inspection and FOI parameters, a variety of sensitivity cases were run to understand the sensitivity of model results and dependent conclusions to variation of inputs or model assumptions, e.g., changing the mean RPVH temperature or correlating crack growth rates and initiation times. The results of these model sensitivity cases are discussed in Section B.3.3.

With the exception of one case[15], the risk of ejection across all sensitivity cases remained below that of the Alloy 600 base case.

Monte Carlo convergence testing comprised ten independent runs of the Alloy 690 (g20/10) base case with the number of realizations per run equivalent to that used for all other cases presented in this section. The results of these runs confirmed a Monte Carlo convergence band with a standard deviation less than 1% for ALF and 5% for AEF predictions.

As additional validation, the probabilistic model results were benchmarked against two case studies presented in MRP-105 [6]. When the key model inputs were matched, the benchmarking effort revealed reasonable agreement between the two probabilistic models in view of the differences in the detailed modeling approaches and assumptions. The benchmarking exercise provides continuity between the MRP-105 technical basis for heads with Alloy 600 nozzles and the present study.

Table 4-2
Key Statistics for Results of the Base Cases for 40 Calendar Year Simulations

Base Case Description	Average Yearly Frequency		Cumulative Probability of Ejection on Head
	Leaking Penetrations (ALF)	Ejected Penetrations (AEF)	
Alloy 600 with Examinations per N-729-1	0.200	5.13E-05	1.95E-03
Alloy 690 (g10/5) with UT Inspection at 20 Years and BMV Inspection every Two Cycles	0.196	6.24E-06	2.39E-04
Alloy 690 (g20/10) with No UT Inspection and BMV Inspection every Two Cycles	0.146	3.07E-06	1.14E-04

[15] The one exception used a modest correlation (-0.8) between the sampled time of initiation and sampled growth rates. Still, the equivalent sensitivity case (with correlated initiation and growth) for Alloy 600 resulted in a predicted ejection risk more than twice that for the analogous sensitivity case for Alloy 690. This is considered an acceptable result because there is no technical basis to assume that the relationship between initiation and growth in Alloy 690 would be starkly different for Alloy 600.

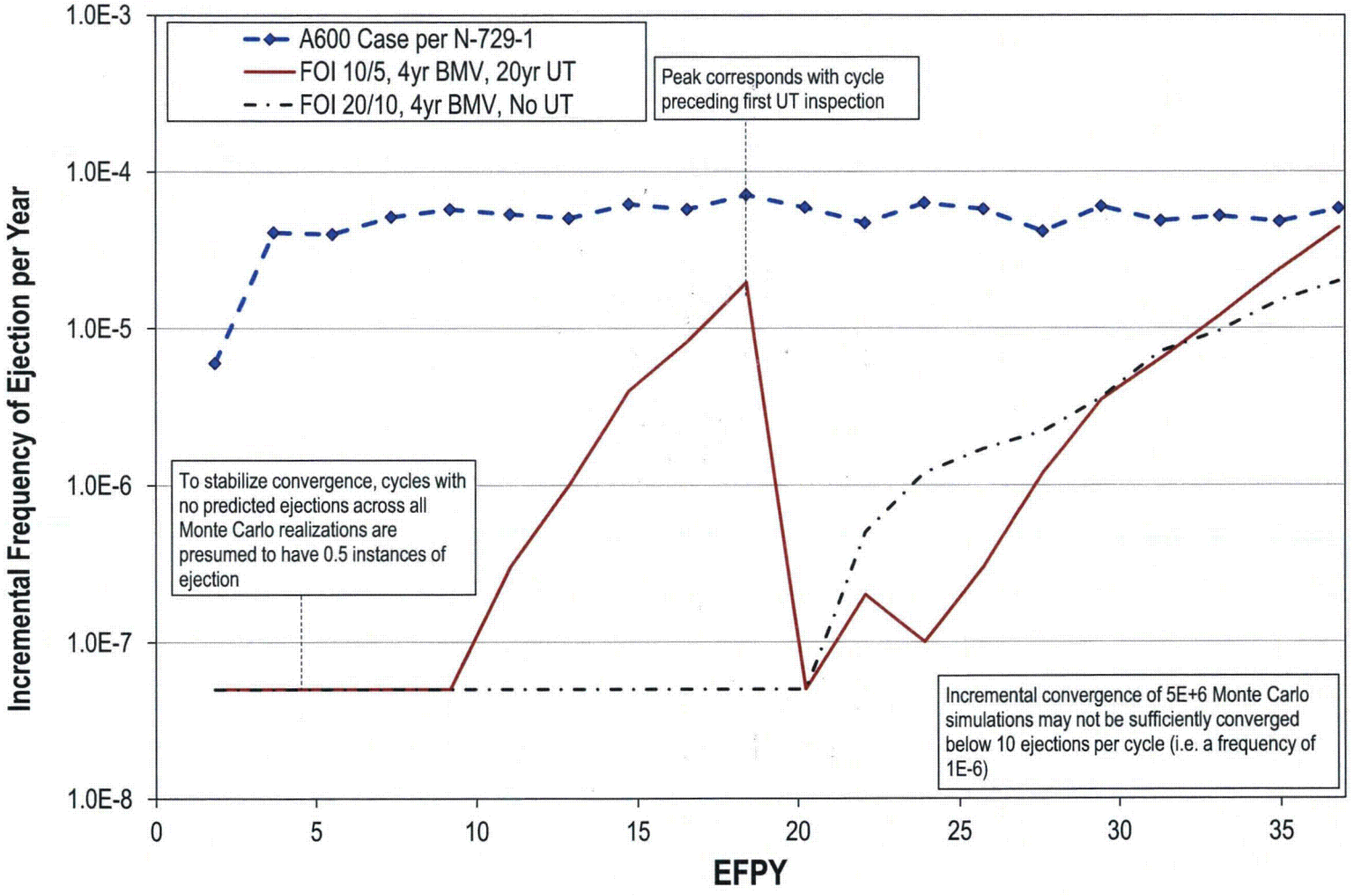

Figure 4-1
Comparison of Incremental Risk of Ejection Versus Time Among the Three Base Cases

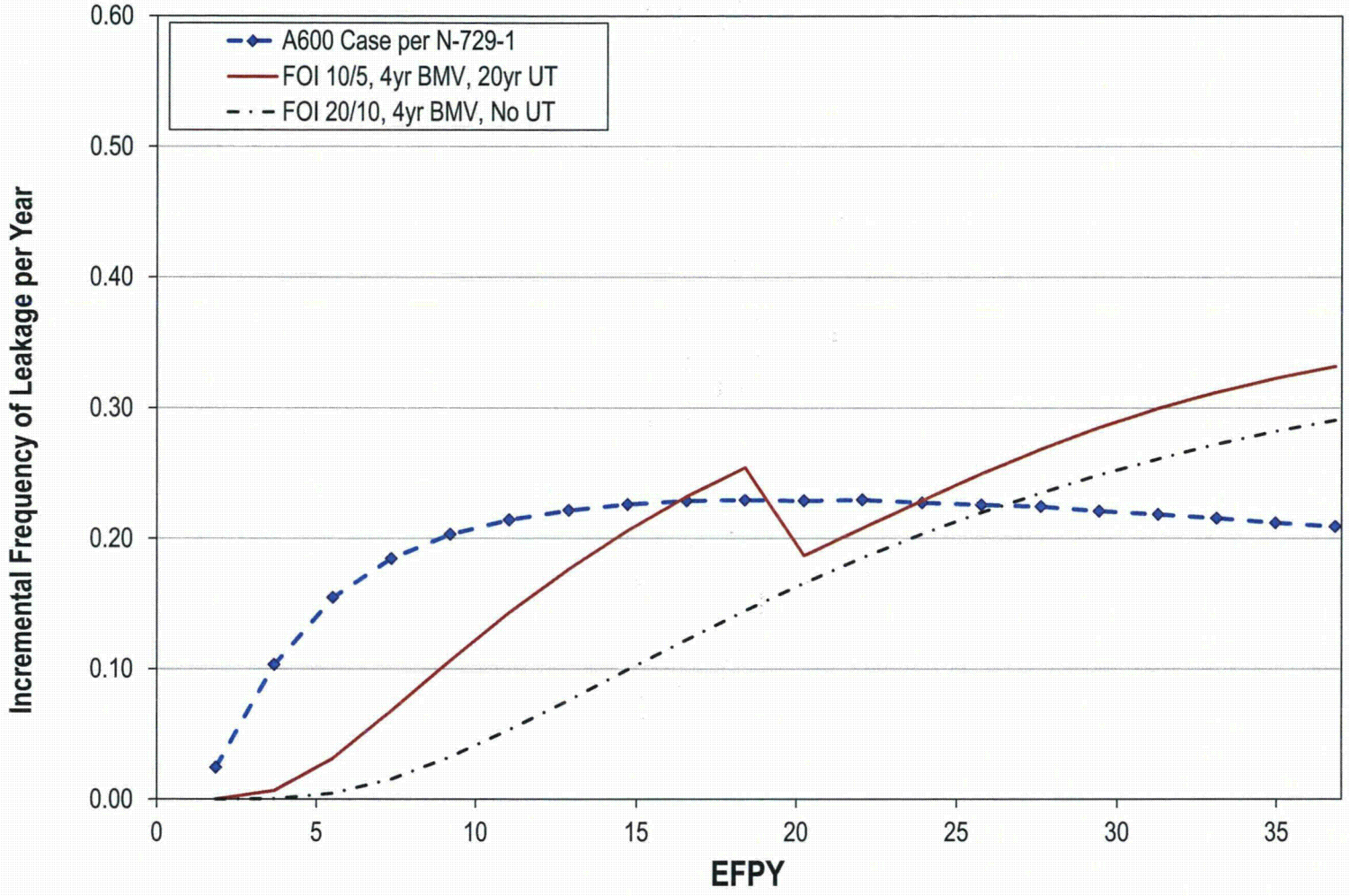

Figure 4-2
Comparison of Incremental Risk of Leakage Initiation Versus Time Among the Three Base Cases

4.5 Conclusions Regarding Probabilistic Results

The efficacy of a reexamination interval extension for Alloy 690 top heads is studied probabilistically as follows:

- A probabilistic model has been developed to allow prediction of PWSCC degradation and its associated risks in reactor pressure vessel top heads. The model is parameterized to allow specification of various inspection options, including BMV and UT inspection intervals.
- A FOI is specified for PWSCC initiation in wrought Alloy 690 relative to wrought Alloy 600. A second independent FOI is specified for PWSCC initiation in Alloy 690 HAZ relative to wrought Alloy 600 and Alloy 52/152 weld material relative to Alloy 182. Based on the material condition of each modeled RPVHPN location, a nominal initiation time is calculated via an established Weibull model (either developed from Alloy 600 or Alloy 82/182 data). This nominal initiation time is multiplied by the appropriate FOI to simulate initiation resistance in Alloy 690 or Alloys 52/152.
- An independent FOI is specified for PWSCC growth in each of the same materials and material conditions as for PWSCC initiation. Based on local material condition at each active crack tip, a nominal CGR is calculated via established models (either MRP-55 or MRP-115). The nominal CGR is divided by the appropriate FOI to simulate growth resistance in Alloy 690 or Alloys 52/152.
- Independent test cases are run to simulate different inspection intervals and degrees of resistance to PWSCC (via FOI parameters). To develop conclusions about the extension of reexamination intervals for Alloy 690 top heads, results are contrasted against those for an Alloy 600 top head examined in accordance with Code Case N-729-1 requirements.

The following conclusions can be drawn based on the results presented in Section 4.4 and Appendix B:

- The risks of ejection support the extension of the UT reexamination interval to 20 years for an assumed growth FOI of 10 for wrought Alloy 690 material and of 5 for nozzle HAZ and weld materials.
- The risks of ejection support the eliminating the UT reexamination requirement for an assumed growth FOI of 20 for wrought Alloy 690 material and of 10 for nozzle HAZ and weld materials.
- For the base cases, in which no credit is taken for superior resistance to PWSCC initiation, the rate of leak initiation is not significantly improved with respect to the Alloy 600 baseline. Applying a modest FOI of 5 for PWSCC initiation in Alloy 690 and Alloy 52/152—in addition to either combination of the growth FOI and the inspection interval specified the previous two bullets—reduces the frequency of leakage to values that are much lower than the Alloy 600 baseline and are more consistent with the current observed performance of Alloy 690 RPVHPNs.

5
CONCLUSIONS

Section 5 presents the key conclusions of this technical basis report. Presented are alternative re-examination interval requirements for PWR reactor vessel top heads with Alloy 690 nozzles and Alloy 52/152 attachment welds that are justified by the available relevant plant and laboratory data as described in Sections 2 and 3. These alternative requirements maintain a conservative approach while ensuring that the status of the replacement head fleet at U.S. PWRs is monitored over time. Section 5 concludes with a discussion of the modeling conservatisms that are included in the supporting deterministic and probabilistic analyses.

5.1 Implications of Plant and Laboratory Data

As presented in Sections 2 and 3, the experience with Alloys 690, 52, and 152 has been excellent, with no reports of PWSCC indications from PWR service and no cases of PWSCC initiation for laboratory testing with normal Alloys 690/52/152 in conditions representative of plant service. This favorable laboratory experience has included smooth wall test specimens, notched test specimens, and weld flaws. Much of the available laboratory data indicate a factor of improvement for Alloys 690/52/152 versus the performance of Alloys 600/182 (for equivalent temperature and stress conditions) on the order of 100 in terms of the crack growth rate. Moreover, existing laboratory and plant data demonstrate a factor of improvement in excess of 20 in terms of the time to PWSCC initiation. This much reduced susceptibility to PWSCC initiation and growth supports elimination of all volumetric examinations (as well as visual examinations for evidence of leakage) throughout the plant service period. However, since work is still ongoing to determine the performance of Alloys 690/52/152 in PWR replacement head applications, the deterministic and probabilistic assessments of this technical basis report (Section 4) were implemented with conservatively smaller factors of improvement. In the future, the situation may be re-assessed and excess conservatism removed from the technical basis for inspection.

As discussed in Section 3.1, data are available on the level of chromium dilution of Alloys 52/152 adjacent to stainless steel base metal. This work indicates modest levels of reduction in the nominal 30% chromium content within the weld dilution zone. Thus, the resistance to PWSCC in the dilution zone of the Alloy 52/152 weld butter layer adjoining the stainless steel cladding at the inside of the vessel head is expected to be substantially similar to that of the bulk Alloy 52/152 weld metal.

For modeling the crack growth rate, conservatively small FOI values in the range between 5 and 20 were applied, with the largest of these FOI values applied for the Alloy 690 RPVHPN base metal condition. The deterministic crack growth calculations demonstrated that the alternative volumetric re-examination interval is sufficient to detect any PWSCC before it could develop into a safety-significant circumferential flaw that approaches the large size necessary to produce a nozzle ejection. The deterministic calculations also demonstrated that any base metal PWSCC

would likely be detected prior to a through-wall penetration occurring. Furthermore, experience has shown that axial cracking and detectable pressure boundary leakage precede the possibility of safety-significant circumferential cracking in RPVHPNs. Thus, the periodic visual examinations currently required by ASME Code Case N-729-1 [3] are also effective in precluding nozzle ejection given the substantial time required for flaw growth in Alloy 690 RPVHPNs.

For the probabilistic calculations directly relevant to nuclear safety (i.e., for the calculation of nozzle ejection frequency), it was not necessary to take any credit for increased resistance to PWSCC initiation to demonstrate an acceptably small effect on nuclear safety of the PWSCC concern. This was demonstrated both in terms of an absolute acceptance criterion for ensuring nuclear safety, as well as through a relative comparison versus predictions for a head with Alloy 600 nozzles examined per the applicable inspection frequencies. Only modest credit for improved resistance to PWSCC initiation (e.g., FOI of 5 or 10) was necessary to demonstrate a suitably low probability of pressure boundary leakage.

Finally, it is emphasized that the analyses presented in this report are bounding of all U.S. PWRs:

- A bounding nominal operating temperature of 613°F (323°C) was assumed.
- The variability in the resistance to PWSCC initiation was addressed in a conservative manner. Conservatively small FOI values were applied versus the demonstrated performance for heads with Alloy 600 nozzles. A wide distribution of times to first PWSCC initiation in a head was assumed prior to application of the assumed FOI. The conclusions of the probabilistic analyses were confirmed for sensitivity cases biasing the time to first initiation toward earlier initiation and correlating the time to first initiation with the crack growth rate, resulting in higher crack growth rates applied over the plant service period.
- Growth of safety-significant circumferential flaws was modeled based on the bounding stress intensity factors calculated for any circumferential plane of crack growth above the top of the weld. A substantial uncertainty distribution was applied to the calculated stress intensity factor in the probabilistic calculations.
- A relatively large number of top head nozzles (89) was assumed in the probabilistic analyses. This assumption readily covers the entire PWR fleet given that the precise number of nozzles assumed has a minor effect on the probabilistic calculations.

5.2 Alternative Inspection Regime for Heads Fabricated with Alloy 690 Nozzles and Alloy 52/152 Attachment Welds

5.2.1 Interval for Periodic Volumetric/Surface Examinations

As demonstrated in this report, the volumetric/surface re-examination interval per ASME Code Case N-729-1 [3] for heads with Alloy 690 nozzles and Alloy 52/152 attachment welds is appropriately extended to a nominal 20 years:

- Volumetric/surface examination of all nozzles every second ASME Section XI inspection interval (nominally 20 calendar years) (provided that flaws attributed to PWSCC have not previously been identified in the head).

This change to the re-examination interval of ASME Code Case N-729-1 [3] removes excess conservatism while still maintaining a conservative approach. This revised interval ensures an acceptably small effect of the PWSCC concern on nuclear safety, and it ensures that information on the status of the U.S. fleet of heads with Alloy 690 nozzles continues to be collected. The proposed revised interval continues to provide reasonable assurance of structural integrity and thus an acceptable level of quality and safety.

5.2.2 Options for Sample Program of Volumetric/Surface Examinations

This report also demonstrates the adequacy of substantially longer volumetric/surface re-examination intervals, i.e., 30 or 40 years. Based on these results, it is concluded that a sample program is also an acceptable alternative, in which a pair of "sister" heads is examined in combination. This approach is analogous to that taken in Paragraph IWL-2421 of ASME Section XI [35] for inspection of unbonded post-tensioning systems of concrete containments. IWL-2421 recognizes the value of coordinating inspections of items of identical or similar design at multiple plants. Before applying this sample option, the licensee shall confirm that each of the two "sister" heads has a similar or identical design, same nozzle material supplier, and same head fabricator. The two "sister" heads may be located in two different plants at the same site, or in two plants at different sites whether operated by the same or different utilities.

The following three sample program options are acceptable in lieu of the volumetric/surface re-examination interval per ASME Code Case N-729-1 [3] for heads with Alloy 690 nozzles and Alloy 52/152 attachment welds:

- Sample Option 1. Volumetric/surface examination of all nozzles in "Sister Head A" or "Sister Head B" nominally every 15 calendar years. The volumetric/surface examination shall be alternated between the "sister" heads, with "Sister Head A" the first head to be examined.
- Sample Option 2. Volumetric/surface examination of all nozzles in "Sister Head A" or "Sister Head B" every second ASME Section XI inspection interval (nominally 20 calendar years). The volumetric/surface examination shall be alternated between the "sister" heads, with "Sister Head A" the first head to be examined.
- Sample Option 3. Volumetric/surface examination of all nozzles in "Sister Head A" every second ASME Section XI inspection interval (nominally 20 calendar years). Volumetric/surface examination of all nozzles in "Sister Head B" every fourth ASME Section XI inspection interval (nominally 40 calendar years).

If there is more than a 10°F (5.6°C) difference in nominal head operating temperature between "Sister Head A" and "Sister Head B" (as evaluated at the time the sample program is established for the pair of heads), the head with the higher nominal head operating temperature shall be designed as "Sister Head A," and the head with the lower nominal head operating temperature shall be designed as "Sister Head B." If there is no more than a 10°F (5.6°C) difference in nominal head operating temperature, the designations may be made at the choice of the licensee or licensees at the time of the first examination. Finally, neither sample option shall be implemented any longer if flaws attributed to PWSCC are identified in either "sister" head.

This change to the re-examination interval of ASME Code Case N-729-1 [3] removes excess conservatism while still maintaining a conservative approach. These revised intervals ensure an

acceptably small effect of the PWSCC concern on nuclear safety, and they ensure that information on the status of the U.S. fleet of heads with Alloy 690 nozzles continues to be collected. The proposed sample programs continue to provide reasonable assurance of structural integrity and, thus, an acceptable level of quality and safety.

5.2.3 Interval for Periodic Direct Visual Examinations (VEs) for Leakage

As a further conservatism,[16] no change is proposed to the program of direct visual examinations for evidence of leakage defined by ASME Code Case N-729-1 [3]:

- Direct visual examination (VE) of the outer surface of the head for evidence of leakage every third refueling outage or 5 calendar years, whichever is less.

This requirement supplements the volumetric/surface examination requirement and conservatively addresses the potential concern for boric acid corrosion of the low-alloy steel head due to PWSCC leakage.

The VE interval of no more than 5 calendar years conservatively addresses the boric acid corrosion concern given the following:

- As described in Section 3.4 of MRP-117 [7], the boric acid corrosion concern for PWR reactor vessel top heads is principally addressed through the requirement for periodic direct visual examinations. Adequate protection against structurally significant boric acid corrosion through periodic visual examinations at appropriate intervals is supported by plant experience [56] and by deterministic and probabilistic models of the boric acid corrosion process, including those presented in MRP-110 [1]. Since MRP-110 was published in 2004, the MRP sponsored an extensive program of boric acid corrosion testing and additional analysis work ([57], [58], [59], [60], [61], [62]),[17] including full-scale mockups of leaking CRDM nozzles with careful attention to obtaining thermal-hydraulic conditions representative of a leaking CRDM nozzle in an operating PWR. This test program, which is now complete, confirms the previous conclusions based on plant experience and analytical work [1] that structurally significant volumes of material loss (1) require a reasonably long period of time to develop and (2) are preceded by evidence of leakage and corrosion that is readily visible.
- The deterministic crack growth calculations presented in Section 4.2 demonstrate the substantial time required for a part-depth flaw to grow through-wall, and the probabilistic calculations introduced in Section 4.3 confirm that the risk of leakage occurring is largely due to PWSCC located exclusively in the J-groove weld. (As discussed in Section B.3.2, the main probabilistic cases predict that more than 90% of the leakage frequency as modeled is due to flaws exclusively located in the weld metal.) Relatively small leak rates are expected for through-wall flaws located exclusively in the J-groove weld metal. Such small leak rates

[16] The evaluations of this report would support an extension of the interval for direct visual examinations in addition to an extension of the interval for volumetric examinations. For example, as discussed in Section B.3.2.2, an extension of the interval for direct visual examinations to 6 calendar years is shown to result in an acceptably small effect on the nozzle ejection frequency.

[17] ANL [63] has also completed boric acid corrosion testing under sponsorship of NRC with results consistent with those for the MRP program.

are unlikely to be sufficient to produce the amount of local cooling necessary for substantial boric acid corrosion to occur.

- Relatively little credit for an improved PWSCC initiation resistance of Alloys 690/52/152 is necessary to demonstrate a rather low probability of leakage occurring, including for Alloy 690 RPVHPNs operating at the upper end of reactor vessel head operating temperatures.
- The low PWSCC crack growth rates applicable to Alloy 690 RPVHPNs results in a much increased time for an initial leak to increase to the point that there is the possibility of significant boric acid corrosion occurring (in comparison to the times calculated for Alloy 600 RPVHPNs [1]).

5.3 Modeling Conservatisms

These conclusions are maintained despite the following key conservatisms applicable to the analyses presented for Alloy 690 RPVHPNs:

- Base cases give no credit to reduced susceptibility to PWSCC initiation in Alloy 690/52/152 RPVHPNs. While this is in part to account for localized material conditions that may be susceptible to initiation, there is strong theoretical, experimental, and operational evidence that Alloy 690/52/152 RPVHPNs are generally less susceptible to PWSCC initiation than their Alloy 600/82/182 predecessors.
- Base cases give only modest credit (FOIs between 5 and 20) to reduced susceptibility to PWSCC growth in Alloy 690/52/152 RPVHPNs. While this is in part to account for localized material conditions that may be susceptible to growth, there is strong theoretical, experimental, and operational evidence that Alloy 690/52/152 RPVHPNs may be up to 100 times or more resistant to PWSCC growth than their Alloy 600/82/182 predecessors.

Furthermore, the conclusions are maintained despite the following key conservatisms applicable to the probabilistic analyses presented for both Alloy 600 and Alloy 690 RPVHPNs:

- A through-wall 30° circumferential flaw located at the top of the weld is assumed to be produced immediately upon nozzle leakage (i.e., through-wall cracking to the nozzle annulus). This assumption was maintained from the approach taken in MRP-105 [6] as part of the technical basis for the inspection requirements for unmitigated RPVHPNs in N-729-1 [3]. In most cases, circumferential cracking in the nozzle tube at or near the top of the weld has not been detected for leaking RPVHPNs [1].
- The overall likelihood of flaw detection is conservatively low due to several modeling decisions including:
  - Surface ET inspection is not modeled.
  - UT inspection is not credited for flaws growing through the J-groove weld.
  - A POD of 0.9 is assumed to model bare metal visual examinations for evidence of leakage of RPVHPNs. A higher POD is typically expected based on plant experience.
  - No credit is taken for the UT leak path exam for the case of RPVHPNs.
- An environmental factor greater than 1 is assumed to increase the growth rate of circumferential cracks in contact with the OD annulus of RPVHPNs. This is assumed

because of the possibility of an accelerating effect of the chemical environment on the nozzle OD.

- A zero stress intensity factor threshold is assumed for growth.
- Axial ID flaws on RPVHPN tubes are assumed to always initiate at the elevation having the highest hoop stresses.
- Bounding high K solutions are used to predict crack growth of circumferential cracks above the J-groove weld.

6
REFERENCES

1. *Materials Reliability Program: Reactor Vessel Closure Head Penetration Safety Assessment for U.S. PWR Plants (MRP-110): Evaluations Supporting the MRP Inspection Plant*, EPRI, Palo Alto, CA: 2004. 1009807.
2. T_{cold} *RV Closure Head Nozzle Inspection Impact Assessment*, EPRI, Palo Alto, CA: 2011. MRP 2011-034.
3. ASME Code Case N–729-1, "Alternative Examination Requirements for PWR Reactor Vessel Upper Heads With Nozzles Having Pressure-Retaining Partial-Penetration Welds," Section XI, Division 1, American Society of Mechanical Engineers, New York, Approved March 28, 2006.
4. ASME Section XI, Code Case N-729, "Technical Basis Document," dated September 14, 2004.
5. *Materials Reliability Program (MRP), Resistance to Primary Water Stress Corrosion Cracking of Alloys 690, 52, and 152 in Pressurized Water Reactors (MRP-111)*, EPRI, Palo Alto, CA, U.S. Department of Energy, Washington, DC: 2004. 1009801.
6. *Materials Reliability Program: Probabilistic Fracture Mechanics Analysis of PWR Reactor Vessel Top Head Nozzle Cracking (MRP-105)*, EPRI, Palo Alto, CA: 2004. 1007834.
7. *Materials Reliability Program: Inspection Plan for Reactor Vessel Closure Head Penetrations in U.S. PWR Plants (MRP-117)*, EPRI, Palo Alto, CA: 2004. 1007830.
8. *Materials Handbook for Nuclear Pressure Boundary Applications (2010)*, EPRI, Palo Alto, CA: 2010. 1022344.
9. *Materials Reliability Program: PWSCC of Alloy 600 Type Materials in Non-Steam Generator Tubing Applications - Survey Report Through June 2002, Part 1: PWSCC in Components Other Than CRDM/CEDM Penetrations (MRP-87)*, EPRI, Palo Alto, CA: 2003. 1007832.
10. Calvert Cliffs Nuclear Power Plant Unit No. 2, Docket No. 50-318, License No. DPR 69, Licensee Event Report 2011-001, "Pressure Boundary Leakage Caused by Primary Water Stress Corrosion Cracking," Report Date April 15, 2011.
11. G. Turluer, et al., "The French Regulatory Experience and Views on Nickel-Base Alloy PWSCC Prevention and Treatment," *Conference on Vessel Head Penetration Inspection, Cracking and Repairs* Sponsored by U.S. Nuclear Regulatory Commission and Argonne National Laboratory, Gaithersburg, MD, Sept. 29 to Oct. 2, 2003.
12. *Materials Reliability Program: Resistance of Alloys 690, 152, and 52 to Primary Water Stress Corrosion Cracking (MRP-237, Rev. 2): Summary of Findings Between 2008 and*

2012 from Completed and Ongoing Test Programs. EPRI, Palo Alto, CA: 2013. 3002000190.

13. P. Andresen, M. Morra, and A. Ahluwalia, "SCC Growth Rates of Alloy 152/52/52i Welds," *EPRI Alloy 690/52/152 Primary Water Stress Corrosion Cracking Research Collaboration Meeting,* Nov. 27-29, 2012.
14. *Materials Reliability Program Crack Growth Rates for Evaluating Primary Water Stress Corrosion Cracking (PWSCC) of Alloy 82, 182, and 132 Welds (MRP-115)*, EPRI, Palo Alto, CA: 2004. 1006696.
15. Letter from D. M Hoots (Exelon) to U.S. Nuclear Regulatory Commission, "Licensee Event Report (LER) 455-2007-001-00, Reactor Pressure Vessel Head Control Drive Mechanism Penetration Nozzle Weld Indication Due to an Initial Construction Weld Defect Allowing the Initiation of Primary Water Stress Corrosion Cracking," dated June 8, 2007.
16. S. M. Bruemmer, M. B. Toloczko, M. J. Olszta, R. Seffens, and P. Efsing, "Characterization of Defects in Alloy 152, 52 and 52M Welds," *14th Int. Conf. on Environmental Degradation of Materials in Nuclear Power Systems – Water Reactors*, Aug. 2009.
17. AWS Specification A5.9/A5.9M:2006, "Specification for Bare Stainless Steel Welding Electrodes and Rods."
18. P. Efsing, B. Forssgren, and R. Kilian, "Root Cause Failure Analysis of Defected J-Groove Welds in Steam Generator Drainage Nozzles," *12th Int. Conf. on Environmental Degradation of Materials in Nuclear Power System – Water Reactors*, TMS, 2005.
19. M. Foucault, et al., "PWSCC of Ni base Alloy : Surface mastering and crack initiation," Quantitative Micro-Nano (QMN-2) Approach to Predicting SCC of Fe-Cr-Ni Alloys – Initiation of SCC, June 12-17, 2011, Sun Valley Resort, Staehle Consulting, 2012.
20. R. B. Abernethy, *The New Weibull Handbook, Second Edition*, Robert B. Abernethy, North Palm Beach, Florida, 1996.
21. *Materials Reliability Program: Resistance of Alloys 690, 52 and 152 to Primary Water Stress Corrosion Cracking (MRP-237, Rev. 1): Summary of Findings From Completed and Ongoing Test Programs Since 2004.* EPRI, Palo Alto, CA: 2008. 1018130.
22. O. Raquet et al., "Assessment of the PWSCC resistance of Alloy 690TT – Overview of The Laboratory Results," *EPRI Alloy 690/52/152 Primary Water Stress Corrosion Cracking Expert Panel Meeting*, Oct. 2006.
23. K. Tsutsumi and T. Couvant, "Evaluation of the Susceptibility to SCC Initiation of Alloy 690 in Simulated PWR Primary Water," *15th Int. Conf. on Environmental Degradation of Materials in Nuclear Power Systems –Water Reactors*, Aug. 2011.
24. D. Morton, J. Mullen, and R. Etien, "SCC Growth Rate Testing of Alloy 690 and EN52i in Aerated and Deaerated Water," *EPRI Alloy 690/52/152 Primary Water Stress Corrosion Cracking Expert Panel Meeting,* Nov. 30-Dec. 3, 2010.
25. T. Maeguchi, Y. Nagoshi, and S. Hirano, "Effect of Cold Work and Grain Boundary Carbides on PWSCC Susceptibility of Alloy 690," *EPRI Alloy 690/52/152 Primary Water Stress Corrosion Cracking Research Collaboration Meeting,* Nov. 27-29, 2012.

26. M. Toloczko, et al., "Update on SCC Initiation Testing of Cold-Worked Alloy 690 in PWR Primary Water," *EPRI Alloy 690/52/152 Primary Water Stress Corrosion Cracking Research Collaboration Meeting*, Dec. 3-6, 2013.

27. P. Efsing, "Alloy 690 Issue from a Utility Perspective," *EPRI Alloy 690/52/152 Primary Water Stress Corrosion Cracking Expert Panel Meeting*, Nov. 2007.

28. F. Vaillant, et al., "Assessment of PWSCC Resistance of Alloy 690: an Overview of Laboratory Results and Field Experience," *EPRI Alloy 690/52/152 Primary Water Stress Corrosion Cracking Expert Panel Meeting*, Nov. 2007.

29. *Materials Reliability Program (MRP) Crack Growth Rates for Evaluating Primary Water Stress Corrosion Cracking (PWSCC) of Thick-Wall Alloy 600 Materials (MRP-55) Revision 1*, EPRI, Palo Alto, CA: 2002. 1006695.

30. *Materials Reliability Program: Topical Report for Primary Water Stress Corrosion Cracking Mitigation by Surface Stress Improvement (MRP-335, Revision 1)*, EPRI, Palo Alto, CA: 2013. 3002000073. [available on www.epri.com]

31. *Byron Unit 2 - Technical Basis for Reactor Pressure Vessel Head Inspection Relaxation*, AM-2007-011 Revision 1, Exelon Nuclear, September 27, 2007.

32. *Technical Basis for RPV Head CRDM Nozzle Inspection Interval - H. B. Robinson Steam Electric Plant, Unit No. 2*, DEI Report R-3515-00-1-NP, Dominion Engineering, Inc., 2003.

33. *Steam Generator Management Program: Pressurized Water Reactor Generic Tube Degradation Predictions Update: Recirculating Steam Generators with Alloy 600TT, Alloy 690TT, and Alloy 800NG Tubing*, EPRI, Palo Alto, CA: 2013. 3002000475.

34. T. L. Anderson, et al., "Development of Stress Intensity Factor Solutions for Surface and Embedded Cracks in API 579," *Welding Research Council Bulletin 471,* May 2002.

35. 2007 ASME Boiler & Pressure Vessel Code, Section XI, Paragraph IWL-2421, "Sites With Multiple Plants," 2008a Addenda, American Society of Mechanical Engineers, New York, July 1, 2008.

36. *Materials Reliability Program: Technical Basis for Change to ASME Section XI Appendix VII RMSE Requirement for Qualification of Depth-Sizing for UT Performed from the ID of Large-Diameter Thick-Wall Supplement 2, 10, and 14 Piping Welds (MRP-373).* EPRI, Palo Alto, CA: 2013. 3002000612. [available on www.epri.com]

37. I. A. Papazoglou, et al., *Probabilistic Safety Analysis Procedures Guide,* US NRC NUREG/CR-2815, Brookhaven National Laboratory, January 1984.

38. *Westinghouse Structural Reliability and Risk Assessment (SRRA) Model for Piping Risk-Informed Inservice Inspection*, WCAP-14572, Rev. 1-NP-A, Supplement 1, February 1999, ADAMS Accession No. ML042610375.

39. 2007 ASME Boiler & Pressure Vessel Code, Section XI, Non-Mandatory Appendix R, Risk-Informed Inspection Requirements for Piping, 2008a Addenda, American Society of Mechanical Engineers, New York, July 1, 2008.

40. *Models and Inputs Selected for Use in the xLPR Pilot Study,* EPRI, Palo Alto, CA. 2010, 1022528. [available on www.epri.com]

41. R. Y. Rubinstein, "Simulation and the Monte Carlo Method," John Wiley & Sons, 1981.

42. D. Rudland, J. Broussard, et al., "Comparison of Welding Residual Stress Solutions for Control Rod Drive Mechanism Nozzles," *Proceedings of the ASME 2007 Pressure Vessels & Piping Division Conference: PVP2007*, San Antonio, Texas, July 2007.

43. S. Marie, et al., "French RSE-M and RCC-MR code appendices for flaw analysis: Presentation of the fracture parameters calculation – Part III: Cracked Pipes," *International Journal of Pressure Vessels and Piping*, 84, pp. 614-658, 2007.

44. *Farley CRDM Through-Wall Circumferential Crack Fracture Mechanics*. Dominion Engineering Inc.: Reston, VA: 2003. C-7781-00-1.

45. US NRC, Regulatory Guide 1.174, "An Approach for Using Probabilistic Risk Assessment in Risk-Informed Decisions on Plant-Specific Changes to the Licensing Basis," Revision 2, May 2011.

46. *PWR Materials Reliability Program Response to NRC Bulletin 2001-01 (MRP-48)*, EPRI, Palo Alto, CA: 2001. 1006284.

47. D. Montgomery, G. Runger, and N. Hubele. *Engineering Statistics*. John Wiley & Sons, Inc., New York, NY 1994.

48. *PWSCC Prediction Guidelines*, EPRI, Palo Alto, CA: 1994. TR-104030.

49. *Validation of Stress Corrosion Cracking Initiation Model for Stainless Steel and Nickel Alloys – Effects of Cold Work*. EPRI, Palo Alto, CA: 2012. 1025121.

50. C. Amzallag, et al., "Stress Corrosion Life Assessment of Alloy 600 PWR Components," *Ninth Int. Symposium on Environmental Degradation of Materials in Nuclear Power Systems – Water Reactors*, TMS, 1999.

51. *Statistical Analysis of Steam Generator Tube Degradation*, EPRI, Palo Alto, CA: 1991. NP-7493.

52. J. A. Gorman, et al., "Correlation of Temperature with Steam Generator Tube Corrosion Experience," *Fifth International Symposium on Environmental Degradation of Materials in Nuclear Power Systems – Water Reactors*, American Nuclear Society, 1992.

53. *Materials Reliability Program: Technical Bases for the Chemical Mitigation of Primary Water Stress Corrosion Cracking in Pressurized Water Reactors (MRP-263)*, EPRI, Palo Alto, CA: 2009. 1019082.

54. G. White, V. Moroney, and C. Harrington, "PWR Reactor Vessel Top Head Alloy 600 CRDM Nozzle Inspection Experience," presented at EPRI International BWR and PWR Material Reliability Conference, National Harbor, Maryland, July 19, 2012.

55. *Materials Reliability Program: Material Production and Component Fabrication and Installation Practices for Alloy 690 Replacement Components in Pressurized Water Reactor Plants (MRP-245)*, EPRI, Palo Alto, CA: 2008. 1016608.

56. *Materials Reliability Program: Boric Acid Corrosion Guidebook, Revision 2: Managing Boric Acid Corrosion Issues at PWR Power Stations (MRP-058, Rev 2)*, EPRI, Palo Alto, CA: 2012. 1025145.

57. *Reactor Vessel Head Boric Acid Corrosion Testing (MRP-163),Task 1: Stagnant and Low Flow Primary Water Test*, EPRI, Palo Alto, CA: 2005. 1013030.

58. *Reactor Vessel Head Boric Acid Corrosion Testing (MRP-164) – Task 2: Jet Impingement Studies*, EPRI, Palo Alto, CA: 2005. 1010089.

59. *Materials Reliability Program, Reactor Vessel Head Boric Acid Corrosion Testing: Task 3 – Separate Effects Testing (MRP-165)*, EPRI, Palo Alto, CA: 2005. 1011807.

60. *Materials Reliability Program: Reactor Vessel Head Boric Acid Corrosion Testing (MRP-266) – Task 4: Full-Scale Mockup Testing*, EPRI, Palo Alto, CA: 2009. 1019085.

61. *Materials Reliability Program: Reactor Vessel Head Boric Acid Corrosion Testing (MRP-199): Task 4: Full-Scale CRDM Mockup Testing, Phase 1: Design and Analysis*, EPRI, Palo Alto, CA: 2007. 1015006.

62. *Materials Reliability Program: Boric Acid Corrosion Testing: Implications and Assessment of Test Results (MRP-308)*, EPRI, Palo Alto, CA: 2011. 1022853.

63. U.S. Nuclear Regulatory Commission, *Boric Acid Corrosion of Light Water Reactor Pressure Vessel Materials*, NUREG/CR-6875, ANL-04/08, 2005.

A
DESCRIPTION OF PROBABILISTIC PWSCC MODEL

This appendix introduces a probabilistic modeling framework developed to study top heads with Alloy 690 nozzles with emphasis on determining the effect of adjusting the inspection requirements of Code Case N-729-1 [3] on risks due to PWSCC degradation.

A.1 Introduction to Probabilistic Risk Assessment

This section is adapted from MRP-373 [36] and provides an overview of probabilistic risk assessment.

Probabilistic risk assessment is a comprehensive methodology for evaluating risks associated with complex systems. Unlike deterministic assessment, in which an event always occurs or never occurs, probabilistic risk assessment allows predictions of event risks or probabilities. Probabilistic assessment seeks to incorporate variation in conditions (e.g., from plant to plant or from component to component) and uncertainties due to lack of understanding in physical processes or inherent randomness. Well-designed probabilistic assessment can provide valuable insight beyond that of deterministic analysis.

In a deterministic assessment, each input is often set at a conservative value to address uncertainty and variability. This practice can compound various conservative margins in a fashion that can lead to unrealistic results and often masks the true extent of conservatism in the final calculation results. A probabilistic assessment, however, provides a statistical estimate for key outputs so that a specific degree of conservatism can be selected.

Probabilistic assessment has a long-standing institution for studying failure risks in nuclear plant components ([37] and [38]). One code precedent for the use of risk-informed assessment in place of deterministic assessment is ASME Section XI Appendix R [39]. A recent example of probabilistic assessment for studying failure risks in nuclear component weldments is the xLPR program [40].

One appropriate and commonly used method for conducting probabilistic assessment is the Monte Carlo simulation method [41]. Monte Carlo simulation involves the use of many individual realizations, each considered representative of the modeled process. For each realization, inputs are determined by randomly sampling from distributions that are developed to be representative of available information, e.g., variability in data, known physical constraints, observed correlations, etc. After establishing the inputs, each realization is carried out deterministically. After many realizations (e.g., up to 10^9), the results of individual realizations are combined to describe outputs in a statistical sense. For instance, an event likelihood is calculated by dividing the number of realizations in which the event occurred by the total number of realizations. The statistics predicted by a set of Monte Carlo realizations gradually converge to the true statistics of the system given the set of defined input distributions.

Convergence analysis methods can be used to roughly quantify the degree of convergence for an estimated statistical quantity (e.g., see Section B.3.3.2).

Monte Carlo simulation is used to generate the results presented in this document. The next sections describe the submodels that execute a single Monte Carlo realization. Information about model inputs is given in Appendix B.

A.2 Probabilistic Model Framework

The probabilistic model framework allows the study of the effect of PWSCC resistance and varying inspection regimes on PWSCC degradation of RPVHPNs fabricated from Alloy 690. The framework combines the individual submodels discussed in Sections A.3 through A.7 to predict leakage and ejection statistics based on the criteria in Section A.8. Results generated with this model are given in Section B.3 using the inputs and uncertainties discussed in Section B.2.

Section A.2.1 gives a point-by-point description of the elements of the probabilistic model framework, which are depicted graphically in Figure A-1 and Figure A-2. A higher level summary of the framework implementation is given below:

- Uncertainty is incorporated for each Monte Carlo realization by sampling input and parameter values from appropriately selected probability distributions. The frequency of sampling (e.g., once per top head, once per penetration, once per crack) established based on the dominant source(s) of variation for each uncertainty. Important sampling bounds for and correlations between distributed variables may be included.
- The model accounts for several diverse mechanisms of PWSCC initiation and growth on RPVHPNs (as detailed in Section A.3) to reflect the range of crack locations and geometries that may occur in service. Loads and stresses are derived specific to each location.
- Each initiated flaw is allowed to grow until its penetration nozzle is repaired, its penetration nozzle is ejected, or the end of the top head service period is reached without repair or ejection.
  - When leakage occurs due to a flaw at any location, it is assumed that this flaw immediately transitions to a through-wall circumferential crack along the J-groove weld.
  - Inspections are simulated at scheduled intervals. If a UT inspection detects a flaw in the nozzle material or if a BMV inspection detects a leak, the offending penetration is repaired and no future flaw growth can occur on it.
  - Each penetration on a RPVH is modeled independently.
- Initiations, leaks, ejections, and repairs are tracked as a function of operating cycle for each Monte Carlo realization and summary statistics are compiled at the end of each Monte Carlo run. Statistics are compiled as penetration frequencies (i.e., all penetration events are counted) or head frequencies (i.e., only first-of-its-kind event is counted on each head). The availability of both types of statistics indicates whether risk is concentrated in a small number of heads with more aggressive sampled parameters or whether risk is more uniformly distributed across heads.

A.2.1 Structure of Probabilistic Model Framework

A high level presentation of the main loop of the probabilistic model for a given weld is presented in Figure A-1 and a more detailed presentation of the embedded time looping structure is given in Figure A-2. The remainder of this section provides an end-to-end description to accompany these figures.

Initialization: Several conditions for the run are defined prior to entering the main (Monte Carlo) loop. These conditions include operating parameters that remain constant throughout the run, such as the number and length of operating cycles, the frequency of inspections, and weld geometry attributes.

Main loop: Next, the main loop is entered. Each loop constitutes a Monte Carlo realization of a RPV top head.

At the beginning of each Monte Carlo realization, deterministic values for distributed inputs that are applicable over the entire RPVH are determined by random sampling (the distribution associated with each distributed input is user-defined). Event scheduling for a given top head, including operating, inspection, and PWSCC initiation times, is developed in the main loop prior to entering the penetration looping and time looping structures. The initiation time submodel (detailed in Section A.4) is called to predict a reference initiation time for the reactor vessel head. This reference initiation time is used to determine initiation times for multiple instances of PWSCC spread over multiple penetrations.

The main loop is cycled for each Monte Carlo realization and is exited once all of the Monte Carlo realizations are completed. After exiting the main loop, the program evaluates the results of the run, outputs information relevant to the study, and terminates the run.

Penetration loop: Following the definition of characteristics that apply to the entire top head, the penetration loop is entered. Each loop constitutes the consideration of a single RPVHPN.

At the beginning of each penetration loop, deterministic values for penetration-specific distributed inputs are determined by random sampling. Then, the program invokes the multiple-flaw initiation submodel (see Section A.4) to predict initiation times at six distinct potential flaw sites (see Section A.3). The PWSCC initiation FOIs are applied respective to the material condition of each initiation site.

The current penetration cycle is terminated without entering the time loop if all of the predicted initiation times exceed the duration of operation. If not, the initiation submodel assigns initial conditions to each flaw that is predicted to initiate during the RPVH service period.

A load submodel (see Section A.5) is used to determine the operational and residual stresses at the various crack locations. The RPVHPN model does not incorporate the known dependence of initiation time versus surface stress, i.e., it is assumed that all locations are equally likely to initiate PWSCC. After loads are assigned, the time looping structure is entered.

This penetration loop is cycled until PWSCC initiation and growth has been simulated for each penetration in the reactor vessel head. Upon exiting the penetration loop, the penetration results are cumulated to estimate risks on a per-penetration and a per-head basis.

Time loops: After establishing initiated cracks and stress conditions, the program enters the time looping structure for the current penetration.

The time looping structure is composed of an outer cycle-by-cycle loop (where each loop constitutes an operating period between RFOs) and a nested within-cycle loop (where each loop constitutes a fraction of an operating cycle). The cycle-by-cycle loop is terminated if the penetration is repaired at an outage. The within-cycle loop is terminated if penetration ejection occurs. Within-cycle loops are skipped if there are no active flaws throughout their duration.

If one or more flaw is active, the stress intensity factor for each active flaw is calculated based on its location, geometry, and stress profile at the beginning of the within-cycle loop. All active flaws are grown in accordance with the flaw propagation submodel (see Section A.6). Growth rates are calculated and adjusted by a FOI respective to the material condition of the crack tip. The flaw depth and length are integrated at a constant rate for the duration of the within-cycle loop (i.e., forward Euler integration).

Before completing a given within-cycle loop, any flaw that has breached the nozzle OD annulus above the weld is considered to cause a leak and this is catalogued for the calculation of statistical outcomes outside of the main loop. When a flaw causes a leak, it is assumed to transition immediately to a circumferential through-wall crack that grows along the top of the J-groove weld contour.

At the end of each within-cycle loop, any through-wall circumferential flaws are evaluated cumulatively to determine if they occupy enough of the nozzle circumference to cause ejection (see Section A.8). If ejection is predicted to occur, the penetration is removed from service (i.e., the current penetration simulation is terminated), the result is catalogued, and the penetration loop is cycled. This is equivalent to returning the head to operation with a repaired penetration considered unsusceptible to PWSCC.

At the end of each operating cycle, the inspection scheduling inputs are consulted to determine if an examination is to be performed and if the examination is to be ultrasonic (UT), bare-metal visual (BMV), or both. As needed, the inspection submodels (see Section A.7) are called. If any flaw is detected, its penetration is removed from service (i.e., the current penetration simulation is terminated), the result is catalogued, and the penetration loop is cycled. If a flaw is not detected, it remains active and continues to grow. After all scheduled inspections, the simulation proceeds to the next operating cycle.

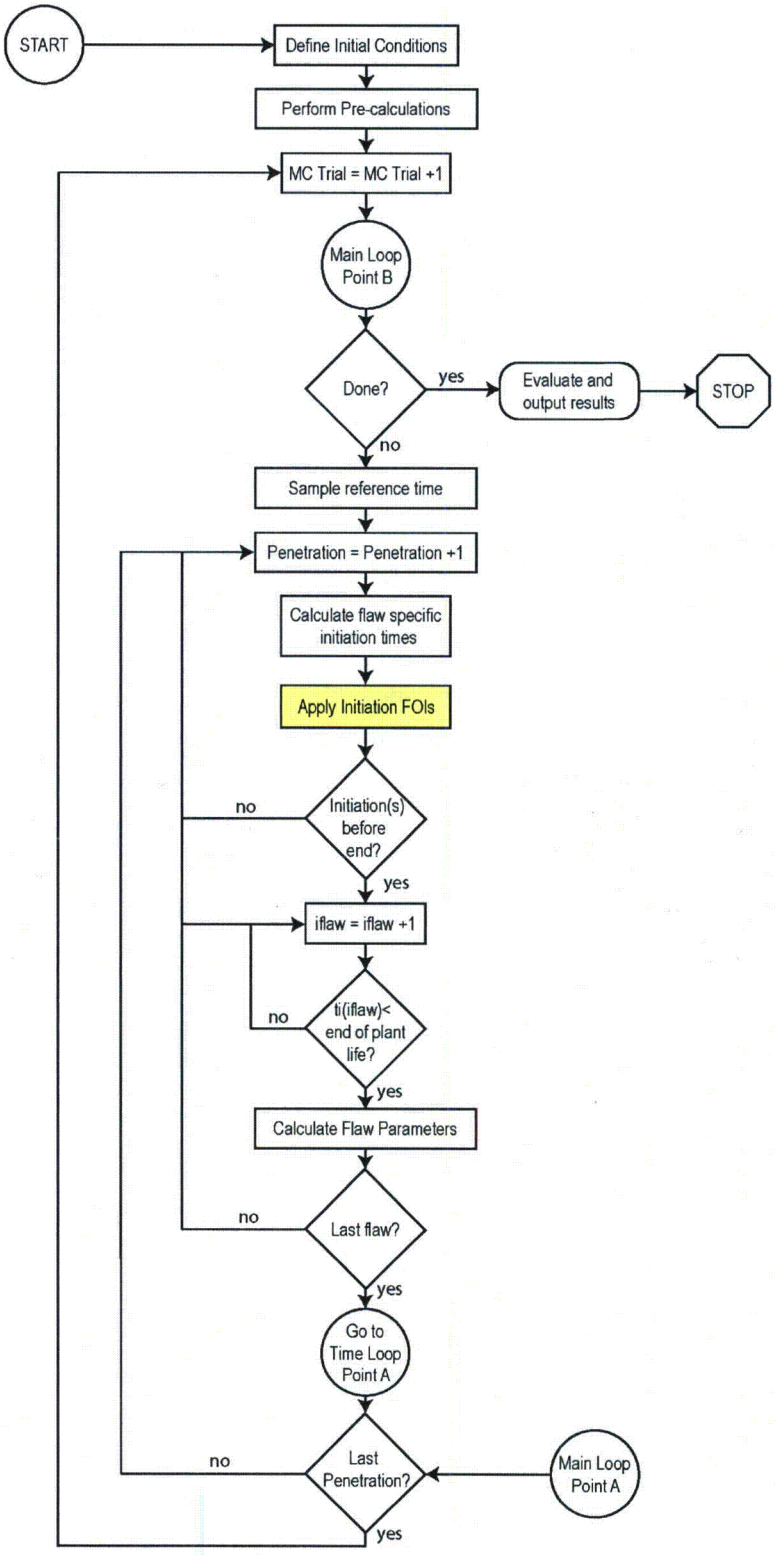

Figure A-1
RPVHPN Probabilistic Model Flow Chart: Main Loop

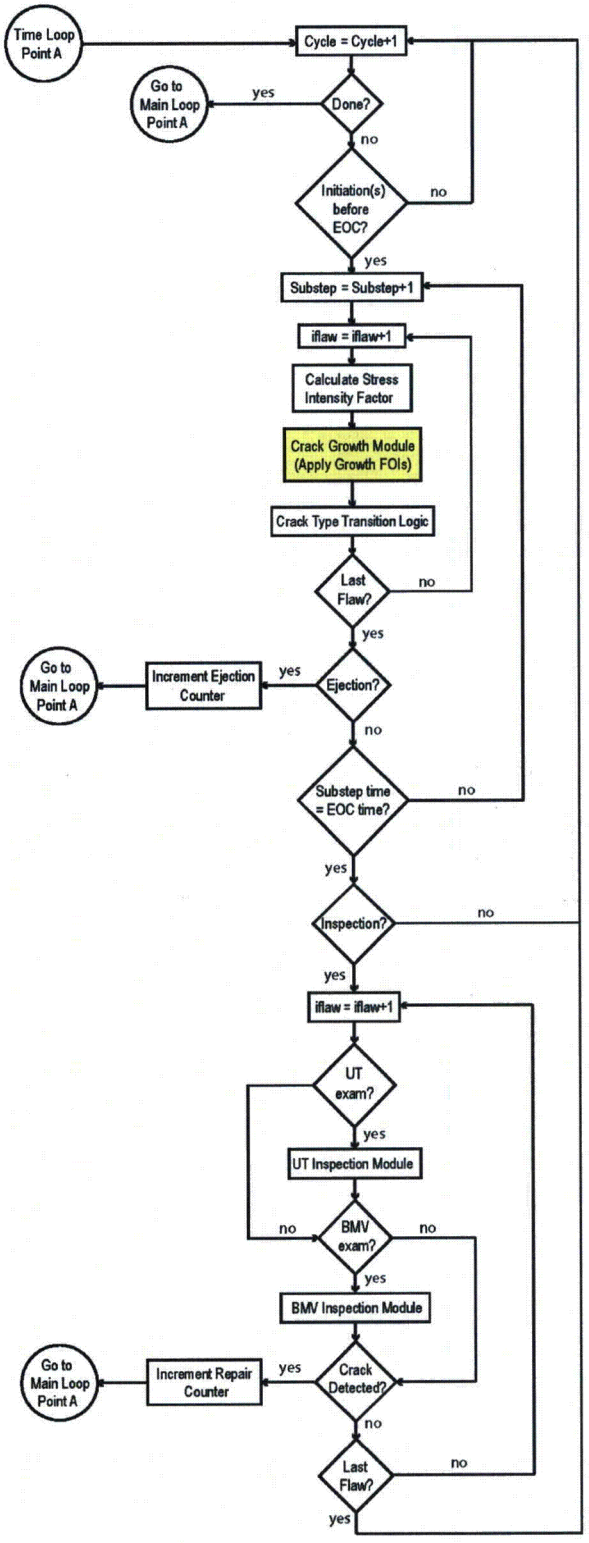

Figure A-2
RPVHPN Probabilistic Model Flow Chart: Detail of Time Loop

A.3 Spatial Discretization of Flaws

This section introduces the spatial discretization used to model PWSCC in RPVHPNs and, subsequently, the different cracking mechanisms modeled at the various locations. Each cracking mechanism reflects a cracking type observed for RPVHPNs. Due to varying geometry, accessibility, material condition, etc., each mechanism is modeled with a unique set of initiation, load, growth, and examination techniques. It is important to distinguish each mechanism, as they will be referenced frequently throughout this appendix. Table A-1 summarizes each mechanism. Figure A-3 provides a schematic of a general RPVHPN, indicates the primary growth direction (i.e., the direction that leads to leakage) of each modeled PWSCC mechanism, and identifies the assumed material condition at each simulated crack tip.

For the purpose of this study, each RPVHPN is divided into an uphill and downhill side. Each cracking mechanism may form on either the uphill or downhill sides, each having a unique loading condition. This convention is based on the fact that the downhill and uphill locations are generally the locations of highest tensile weld residual stresses (due to nozzle ovalization) [42]. This convention was also used in MRP-105 [6].

The key characteristics of the cracking mechanisms modeled in this study are given below:

Initial flaws

- **Radially-oriented weld cracks** initiate at the J-groove weld surface and grow toward the weld toe. These cracks cause leakage if they reach the weld root. These cracks are opened by hoop stresses in the J-groove weld.

  Naturally, the initiation site and crack tips associated with radially-oriented weld cracks are in the weld material. Initiation time and crack growth rates are therefore adjusted by the FOIs for Alloy 52/152 relative to Alloy 182.

- **ID axial cracks** are partial through-wall cracks that initiate and grow through-wall on the penetration nozzle ID. These cracks are conservatively assumed to initiate in the region above the weld such that they immediately result in leakage if they penetrate through-wall into the OD nozzle annulus. These cracks are opened by hoop stresses in the penetration nozzle.

  The initiation site and crack tips associated with ID axial cracks are assumed to lie in the bulk Alloy 690 material. Initiation time and crack growth rates are therefore adjusted by the FOIs for wrought Alloy 690 relative to Alloy 600.

- **OD axial cracks** are partial through-wall cracks that initiate and grow through-wall on the penetration nozzle OD located below the weld. These cracks cause leakage if they grow in length to reach the nozzle OD annulus; they may transition to through-wall axial cracks if they grow to the ID before reaching the annulus. OD axial cracks are assumed to initiate uniformly between the weld toe and the point where the residual surface stresses tend to fall below 80% of yield. These cracks are opened by hoop stresses in the penetration nozzle.

  The initiation site associated with OD axial cracks are assumed to lie in the Alloy 690 HAZ. Initiation time is adjusted by the initiation FOI for Alloy 690 HAZ relative to Alloy 600.

  The upper crack tip of OD axial cracks are also assumed to lie in the Alloy 690 HAZ. Crack growth rate at the upper crack tip is adjusted by the growth FOI for Alloy 690 HAZ relative

to Alloy 600. The deepest point and the lower crack tips of OD axial cracks are assumed to lie in the bulk Alloy 690 material so their crack growth rates are adjusted by the growth FOI for wrought Alloy 690 relative to Alloy 600.[18]

Resultant flaws

- **Through-wall axial cracks** are located below the weld. These cracks form if an OD axial crack reaches through-wall before reaching the nozzle OD annulus and cause leakage if they grow in length to reach the nozzle OD annulus. These cracks are opened by hoop stresses in the penetration nozzle.

  For through-wall axial cracks as with part-depth OD flaws, the growth rate of the lower crack tip is adjusted by the growth FOI for wrought Alloy 690 relative to Alloy 600 and the growth rate of the upper tip is adjusted by the growth FOI for Alloy 690 HAZ relative to Alloy 600 (see prior footnote for further modeling details).

- **Circumferential through-wall cracks** are located on the weld contour above the weld. Consistent with conventions of MRP-105 [6], these cracks are assumed to occur immediately following leakage caused by any of the preceding crack mechanisms, either by branching of the flaw that caused the leakage or by initiation of a new flaw on the OD surface of the nozzle by the leaking primary coolant. These cracks are opened by a complex stress field acting orthogonally to the weld contour.

  For circumferential through-wall cracks, the growth rate is adjusted by the growth FOI for wrought Alloy 690 relative to Alloy 600.

Table A-1
Summary of PWSCC Mechanisms Modeled on RPVHPNs

ID of Crack Mechanism	Orientation	Shape	Material Characteristics	Location	Transitions to...
ID Axial Flaw	Axial	Semi-elliptical, partially through-wall	Alloy 690	Top of weld, inner diameter	Circumferential TW flaw upon growing through-wall
OD Axial Flaw	Axial	Semi-elliptical, partially through-wall	Alloy 690	Bottom of weld, outer diameter	Circumferential TW flaw upon growing to weld root, or TW axial flaw upon growing through-wall
Weld Flaw	Radially-oriented	Semi-elliptical, partially through-weld	Alloy 52/152	In weld	Circumferential TW flaw upon growing to weld root
TW Axial Flaw	Axial	Rectangular, through- wall	Alloy 690	Bottom of weld	Circumferential TW flaw upon growing to weld root
Circumferential TW Flaw	Circumferential	Through-wall	Alloy 690	Along upper weld contour	Ejection upon growing past stability threshold

[18] As a result of the above modeling conventions, growth of OD axial cracks is inherently asymmetric when the degree of PWSCC resistance is considered different between bulk and HAZ Alloy 690. As an approximation, a symmetric, semi-elliptical crack shape is assumed to be recovered after each integration time step. The length of the resultant crack is determined by the sum of the CGRs at the lower and upper tips; the center of the resultant crack is shifted in accordance with the difference between the CGRs at the lower and upper tips.

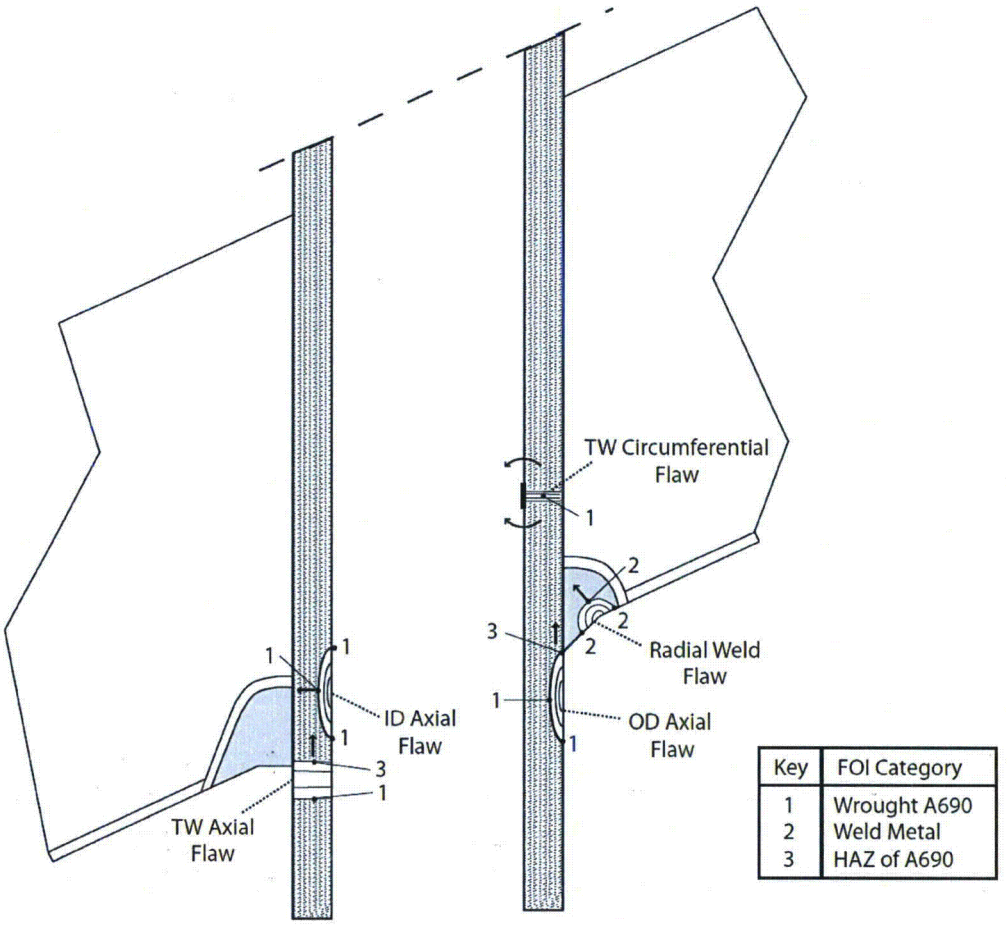

Figure A-3
Schematic of Modeled Cracking Mechanisms and Assumed Material Conditions for RPVHPN Probabilistic Assessment (Arrows Indicate Direction of Growth Toward Leakage)

A.4 Flaw Initiation

This study employs a statistical Weibull approach for predicting crack initiation that is based on the approach used by MRP-335 Rev. 1 [30]. In each realization, the initiation submodel predicts PWSCC initiation across all initiation sites (see Section A.3) and all penetrations in a single head.

A.4.1 Head Initiation Model

The head initiation reference time is used to correlate the initiation time for all penetrations and flaws on a given head. It is determined by fitting a Weibull distribution to the operating experience for the time to first detected cracking on Alloy 600 RPVHs. FOIs are applied to the individual flaw initiation times (described in Section A.4.2), not the head reference time. The head initiation reference time, t_{ref}, roughly corresponds to the time of first flaw initiation on an Alloy 600 head.

The general two-parameter Weibull cumulative distribution function is given as follows:

$$F(t) = 1 - e^{-\left(\frac{t}{\theta}\right)^{\beta}} \qquad \text{[A-1]}$$

where F is the cumulative fraction of components with PWSCC initiation and t is the corresponding operating time. The Weibull slope, or shape parameter, β, is related to the rate at which degradation spreads through a given component population such as steam generator tubing. The Weibull characteristic time parameter, θ, provides a measure of the time scale for the degradation mode of interest. Specifically, the Weibull characteristic time is the time required to reach a cumulative failure fraction of 0.632 (i.e., the time required for 63.2% of the items in a given population to fail).

The Weibull slope, β, a user-selected failure fraction, F_1, (e.g., 0.1%, 1%, 10%, etc.), and the time at which this user-selected failure fraction is reached, t_1, are provided as inputs to the probabilistic model and are based on operating experience. The process by which β, F_1, and t_1 are determined by fitting to existing data for first crack initiation in Alloy 600 RPVHPN welds is discussed in Section B.2.2. The value of θ is then determined from β, F_1, and t_1 during runtime using Equation [A-1].

Once β and θ are known for the current Monte Carlo realization, they can be used to sample a reference initiation time in EDY. In this study, the initiation time is adjusted for temperature (to convert to EFPY) using the widely accepted Arrhenius relationship:

$$t_{ref} = t_{ref,EDY} \times e^{\left(\frac{Q_i}{R}\right)\left(\frac{1}{T} - \frac{1}{T_{ref}}\right)} \qquad \text{[A-2]}$$

where T is the absolute operating temperature, Q_i is the apparent thermal activation energy for crack initiation, R is the universal gas constant, and T_{ref} is the Arrhenius model absolute reference temperature.

The result of the above equation, t_{ref}, is considered to be the average time of the first PWSCC initiation on a head with Alloy 600 nozzles for the current Monte Carlo realization. This time is not applied to any specific location, but it is used by the multiple crack initiation model, which is discussed next.

A.4.2 Initiation Times of Multiple Cracks

Another Weibull model is utilized to predict times of initiation of multiple PWSCC cracks on a head. The use of this statistical model reflects systematic and statistical variations in material properties and environmental conditions from location to location, and from penetration to penetration, on a single head.

The multiple crack initiation Weibull model uses a new Weibull slope, $\beta_{mult,i}$, to reflect a new rate at which PWSCC degradation spreads to multiple sites on a head after the first crack initiation. This Weibull slope is sampled for each penetration to reflect the premise that each penetration has unique conditions relevant to multiple flaw initiation. It is noted that sampling the multiple flaw Weibull slope for each penetration results in the clustering of flaws on affected

penetrations. Sensitivity studies in MRP-335 Rev. 1 [30] showed that sampling the multiple-crack Weibull slope once for a top head slightly decreased ejection frequency relative to sampling at each penetration. The distribution selected for $\beta_{mult,i}$ is discussed in Section B.2.2.

Based on the spatial discretization resulting in six flaw sites per penetration, the initiation time returned by Equation [A-2] is indicative of the average time of the first PWSCC initiation across all $6N_{pen}$ crack sites on an Alloy 600 head. This time is therefore associated with the cumulative probability ($F_{1_{st}}$) given by Benard's approximation in Equation [A-3] below:

$$F_{1st} = \frac{1-0.3}{6N_{pen}+0.4} \qquad [A\text{-}3]$$

For each penetration, the characteristic time parameter for the multiple flaw Weibull model, $\theta_{mult,i}$, is calculated from $\beta_{mult,i}$, t_{ref}, and $F_{1_{st}}$ above using Equation [A-1]. Then, an initiation time for each crack site, $t_{ref,i,loc}$, is sampled from the resulting Weibull distribution. Based on the material condition of the initiation site, $t_{ref,i,loc}$ is multiplied by the relevant FOI as discussed in Section A.4.3.

The above approach allows for the initiation of multiple cracks and it can be shown that, on average, a single initiation across all initiation sites is expected prior to t_{ref}, the average time of first initiation based on Alloy 600 industry experience.

A.4.3 Factor of Improvement on Initiation

Statistical Weibull models have been developed for the PWSCC initiation process in Alloy 600 top heads. This development has been enabled by an expansive data set quantifying Alloy 600 top head operating and inspection experience, including many incidences of flaw detection. Given the relatively limited fleet-wide operating experience with Alloy 690 top heads, it is considered premature to develop specific statistical PWSCC initiation models. Since no incidences of flaw detection have been observed, such development would rely on necessarily conservative assumptions about the imminence of PWSCC in Alloy 690 top heads. Instead, this study applies a simple FOI approach to adjust established Alloy 600 initiation predictions to be better representative of Alloy 690.

Three different FOI parameters are implemented in the initiation submodel:

- A FOI for wrought Alloy 690 material is applied to initiation time predictions for ID axial flaws
- A FOI for Alloy 690 HAZ, which is believed to be more susceptible to PWSCC than the bulk base metal, is applied to initiation time predictions for OD axial flaws
- A FOI for Alloy 52/152 material is applied to initiation time predictions for radial flaws in the J-groove weld

All cases presented in this report use deterministic values for the FOI parameters, which reflects that the uncertainties derived in the Alloy 600 and Alloy 82/182 models are representative of the uncertainties in Alloy 690 and Alloy 52/152 initiation behavior. The extent to which there is more uncertainty in the advanced alloy initiation times is treated by examining a range of FOIs in

different cases, as detailed in Section B.2.5. The use of a deterministic FOI is considered superior to using a distributed one because it does not hide the effect of the FOI behind a layer of abstraction. The presumption that the scaled uncertainty of the Alloy 600 (182) model is representative of Alloy 690 (52/152) initiation time uncertainty is considered appropriate given the available information.

The FOI effects are implemented by scaling the value of $t_{ref,i,loc}$ determined from the Alloy 600 or Alloy 82/182 initiation models, as appropriate. In all cases presented in this report, the initiation FOI for all material conditions are set equal. This conforms to the assumed uniform probability of initiation at each potential flaw site.

A.4.4 Crack Initialization

Crack initialization refers here to assigning initial conditions to each crack at its initiation time. These initial conditions include size and location. Orientation is predetermined by the initiation site (see Section A.3).

Initial crack depth is sampled from a distribution of positive, non-zero, value. This reflects both that the Weibull initiation models discussed above were fit to industry data recording first detection of crack indications and that crack detection may occur for a range of different flaw sizes. Initial crack lengths are attained by scaling the initial depth by a sampled aspect ratio. The distributions selected for initial depth and aspect ratio are detailed in Section B.2.2.2.

Initiation location is not tracked for ID cracks. ID cracks are assumed to initiate at an arbitrary axial location near the weld top. Similarly, weld cracks are assumed to initiate at the weld center.

Initiation location is tracked for OD cracks. The variability in OD crack axial location affects the crack's susceptibility to leakage; i.e., the initial OD crack location together with the initial OD crack length gives a distance for growth to the OD annulus. For OD cracks, the initial axial location is attained by taking a uniform sample between the weld toe and the axial location where the weld residual surface stress falls below 80% of yield stress. The location of 80% of yield is derived from results of J-groove welding residual stress FEA results for Alloy 600 nozzles [42], which are expected to be comparable to the analogous locations for Alloy 690 nozzles.

A.5 Loads and Stress Intensity Factors

A.5.1 Loads and Component Stress

The load model incorporated to establish RPVHPN operational and residual stresses is adapted from MRP-335 Rev. 1 Appendix Section B.3 [30]. While the MRP-335 Rev. 1 models were developed for Alloy 600 top heads, the model forms are considered generally applicable to Alloy 690 top heads. Input selection for this model is discussed in Section B.2.1.4.

The load model calculates stresses at the different locations of interest for PWSCC on RPVHPNs. The load model accounts for welding residual stresses as well as operational loads. Ultimately, the RPVHPN load model returns through-wall (or through-weld) stress profiles on the different vectors that are attributed to the growth of the various cracking mechanisms considered in this study (see Figure A-4).

The total stress profiles at the six locations/directions (vectors) of interest are derived from the results of various J-groove weld finite element analyses (the general methodology of such RPVHPN FEA studies is outlined in [42]). The six vectors of interest for predicting the crack growth mechanisms are depicted in Figure A-4 and described below:

- Hoop stress from the penetration nozzle ID to the OD above the weld (uphill/downhill)
- Hoop stresses from the penetration nozzle OD to the ID below the weld (uphill/downhill)
- Hoop stresses from the weld surface to the weld root (uphill/downhill)

For all six vectors, a second-order polynomial function of through-wall (or through-weld) fraction is used to model the total stress profile. This is considered sufficient for capturing the essential gradient and curvature characteristics observed in RPVHPN FEA results [42]. The resulting general equation form is:

$$\sigma_{tot,loc}\left(\frac{x}{D}\right)=\sigma_{0,tot,loc}+\sigma_{1,tot,loc}\left(\frac{x}{D}\right)+\sigma_{2,tot,loc}\left(\frac{x}{D}\right)^2 \qquad \text{[A-4]}$$

Instead of fitting the polynomial coefficients to FEA results directly, a more robust probabilistic fit is achieved by estimating distributions for the following parameters:

- ID stress ($\sigma_{ID,loc}$)
- The ratio of OD to ID stress ($R_{1,loc}$)
- The ratio of the mid-through-wall stress and the average of the ID and OD stresses ($R_{0.5,loc}$).

The estimation of these parameter distributions is detailed in Section B.2.1.4.

For each penetration, the parameters above are sampled from their fitted distribution. Then, the parameters are related to the polynomial coefficients, allowing solution:

$$\begin{aligned}\sigma_{ID,loc}&=\sigma_{0,tot,loc}\\ R_{1,loc}\sigma_{ID,loc}&=\sigma_{0,tot,loc}+\sigma_{1,tot,loc}+\sigma_{2,tot,loc}\\ \left(\frac{\sigma_{ID,loc}+R_{1,loc}\sigma_{ID,loc}}{2}\right)R_{0.5,loc}&=\sigma_{0,tot,loc}+0.5\sigma_{1,tot,loc}+0.25\sigma_{2,tot,loc}\end{aligned} \qquad \text{[A-5]}$$

Because the FEA studies used to develop the total stress model described above were for an uncracked component, the crack face pressure (equivalent to the operating pressure) is appended for stress intensity factor evaluation.

Finally, residual stress relaxation due to temperature and load cycling that can occur at penetration locations is conservatively not included in this probabilistic model.

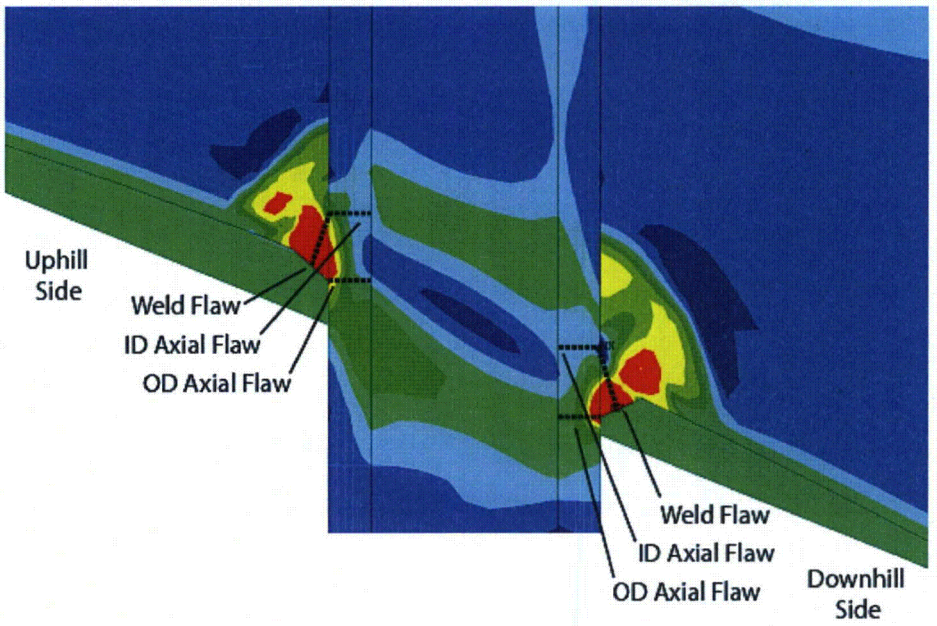

Figure A-4
Depiction of Stress Profile Vectors for Each Crack Mechanism Location (six bold dotted lines) and Stress Contour Plot [30]

A.5.2 Stress Intensity Factor

Methods for stress intensity factor calculation are adapted from MRP-335 Rev. 1 [30]. The methods are based in structural mechanics principles that are considered generally applicable to cracks in Alloy 600 and Alloy 690.

Section 3 in Reference [34] describes the calculation of stress intensity factor, K, for a circumferentially or axially oriented surface crack on a pipe of arbitrary size using the influence coefficient method. The method described may be applied to a crack subjected to: a) a stress profile acting orthogonally to the crack face (i.e., axial stresses for circumferential cracks and hoop stresses for axial cracks) that is defined by a polynomial function in the direction of the crack depth and is uniform along the crack length, and/or b) stresses due to global bending loads, which are by definition not uniform over the crack length.

The general form of the stress intensity factor calculation (for a surface crack with depth a on a pipe with thickness t) by way of the influence coefficient method is:

$$K = \left[\sigma_0 G_0 + \sigma_1 G_1 \left(\frac{a}{t}\right) + \sigma_2 G_2 \left(\frac{a}{t}\right)^2 + \sigma_3 G_3 \left(\frac{a}{t}\right)^3 + \sigma_4 G_4 \left(\frac{a}{t}\right)^4 + G_{gb}\sigma_{gb} \right] \sqrt{a\pi} \qquad \text{[A-6]}$$

where the G terms are the influence coefficients specific to the crack and component geometries and the point on the crack, σ_0 through σ_4 are the polynomial coefficients of the through-wall stress profile (in units of stress), and σ_{gb} is the nominal bending stress (which is assumed to be negligible). In this study, only the σ_0 through σ_2 terms are used because the through-wall stress

profile is modeled as a second order polynomial in Equation [A-4] without global bending moments.

The condition of stress profile uniformity along the crack length is not upheld in RPVHPNs due to the rapidly changing residual stress distributions near the J-groove weld. However, for modeling purposes, the stress results extracted from FEA on the approximate vectors shown in Figure A-4 are assumed uniform over the crack face. As can be observed from the hoop stress contour plot, the vectors used to estimate stresses tend to lie over more severe stress magnitudes for the respective crack types.

The influence coefficients are interpolated from tables built by way of linear-elastic finite element parametric analyses. Tables 15 and 39 in Reference [43] provide such look-up tables for the surface tip and deepest points of cracks with the following morphology: semi-elliptical, axial or circumferential surface cracks on the inner diameter of a pipe. Higher order influence coefficients (e.g., G_2, G_3, and G_4) may be calculated with weight function coefficients as discussed in Section 6.3 in Reference [34].

The calculation of stress intensity factors for weld cracks is not as clear as for the ID or OD crack locations. This is because there are no pre-determined influence coefficient lookup tables for cracks with the geometry and boundary conditions of the J-groove weld. As an approximation, cracks at the weld locations are treated as being on a flat plate with a thickness equal to the head thickness, t_{head}. Under this assumption, the influence coefficients are interpolated from either the ID or OD lookup tables, using an R_i/t lookup value of 1000 and a through-wall fraction lookup value of a/t_{head}. For the R_i/t ratio value of 1000, both the ID and OD solutions have asymptotically converged to the solution for a flat plate.

A.5.2.1 Stress Intensity Factor Calculation for Through-Wall Axial Cracks

If an axial OD crack goes through-wall prior to reaching the nozzle OD annulus, growth continues in the length direction. In this case, the semi-elliptical crack shape assumed in Section A.5.2 breaks down and a through-wall model is required to accurately predict stress intensity factor at the crack tips.

Reference [43] provides an influence coefficient method for the prediction of stress intensity factor of a rectangular through-wall crack. The influence coefficient equation is:

$$K = \sigma_m F_m \sqrt{c\pi} \qquad [A\text{-}7]$$

where c is the half-length of the through-wall crack, σ_m is the membrane elastic stress, and F_m is the lone influence coefficient.

In this study, the membrane elastic stress is considered to be well-approximated by the through-wall average of the total stress profile, attained by taking the integral of the total stress polynomial. The influence coefficient is interpolated from a lookup table as a function of non-dimensional length (see Reference [43] for details).

A.5.2.2 Stress Intensity Factor Calculation for Circumferential Through-Wall Cracks on the Weld Contour

As previously discussed, any crack predicted to leak is assumed to transition immediately to a through-wall crack along the J-groove weld contour. The growth of such cracks is modeled until the nozzle ejection criterion is reached.

Because of the spiral geometry of these cracks, and the complex stress profile along the length of the crack, there exists no parameterized method for predicting stress intensity factors at the crack tips as a function of the stress distribution characteristics (as has been done for all previous K calculations). Instead, stress intensity factors are predicted as a function of crack length exclusively, based on FEA results for representative RPVHPN geometries.

References [32] and [44] describe FEA performed to predict stress intensity factors at the tips of through-wall cracks growing along the contour of RPVHPN J-groove welds, from both the uphill and downhill sides of the nozzle, at various elevations. These analyses include effects of welding residual stress and operational loads. Both analyses use the geometry of the outermost nozzle at the subject plant, resulting in a generally bounding welding residual stress profile along the crack face.

Across these studies, the most bounding average K versus crack length curves have been selected for use in this probabilistic analysis (i.e., those from Reference [44]). Figure A-5 shows these K curves, for the uphill and downhill sides of the nozzle. Linear interpolation is used between FEA evaluated points. (Extrapolation is never necessary because these cracks initiate at 30°, by convention, and ejection of the nozzle occurs at or less than 330°, as will be discussed in forthcoming sections.) To address the uncertainty in stress intensity factor due primarily to crack and component geometrical variation, a random scaling factor is applied to the curve-predicted K values. The distribution selected for this variable is discussed in Section B.2.3.2.

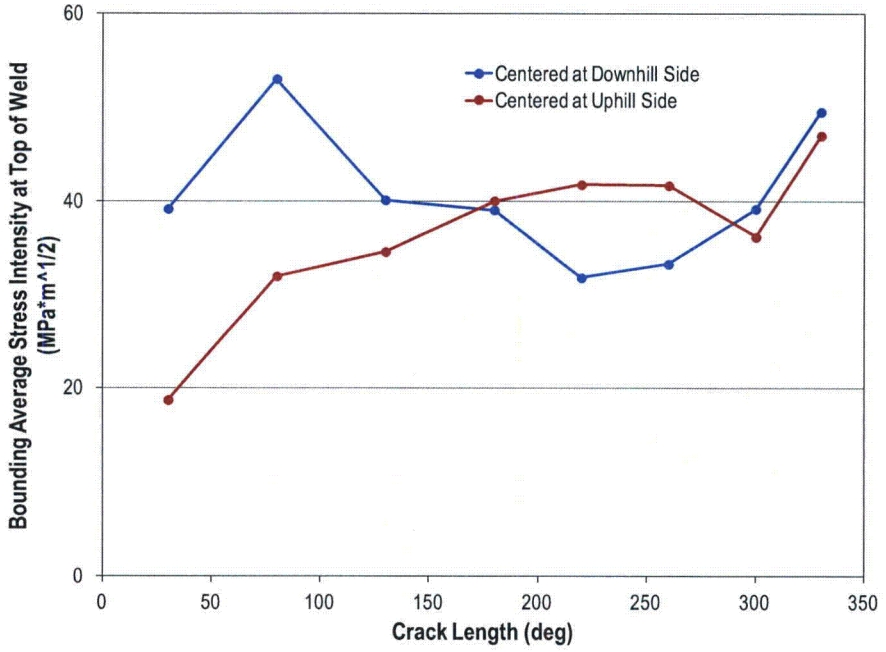

Figure A-5
Modeled Average Stress Intensity Factor vs. Crack Length for a Through-Wall Crack along the J-Groove Weld of a RPVHPN [44]

A.6 Treatment of Flaw Growth Rate

The general crack growth rate model forms for weld metals and base metals, respectively, are given in Equation [A-8]. Temperature effects are incorporated through a widely accepted Arrhenius term and stress intensity factor effects are incorporated through a standard power-law dependence. Model parameters (and associated uncertainties) are estimated from data (Section B.2.3 presents the derivation of these parameters based on Alloy 600 data). The model dependencies, parameters, and uncertainties derived from Alloy 600 data are assumed to apply to Alloy 690 after scaling by a FOI; similarly, model dependencies, parameters, and uncertainties derived from Alloy 82/182/132[19] data are assumed to apply to 52/152 after scaling.

$$\frac{\delta}{\delta t}(d) = e^{\frac{Q_g}{R}\left(\frac{1}{T}-\frac{1}{T_{ref}}\right)} \frac{\alpha_w}{FOI_w} f_{weld} f_{ww} \left(K_I - K_{Ith,w}\right)^{b_w}$$

$$\frac{\delta}{\delta t}(d) = e^{\frac{Q_g}{R}\left(\frac{1}{T}-\frac{1}{T_{ref}}\right)} \frac{\alpha_b}{FOI_b} f_{heat} f_{wh} \left(K_I - K_{Ith,b}\right)^{b_b} \qquad \text{[A-8]}$$

[19] The MRP-115 model includes an alloy factor to account for the generally larger CGRs in Alloy 182 versus Alloy 82 due to differences in nominal chromium content. This alloy factor is not applied in this work, effectively recovering the Alloy 182 model.

where

d	=	general crack dimension (e.g., depth or length)
Q_g	=	thermal activation energy for crack growth
R	=	universal gas constant
T	=	absolute temperature at location of crack
T_{ref}	=	absolute reference temperature used to normalize data
α	=	power-law coefficient
FOI	=	FOI applicable for material condition at location of interest
f_{weld}	=	"weld-to-weld" factor applied to all specimens fabricated from the same weld to account for weld wire/stick heat processing and for weld fabrication
f_{ww}	=	"within weld" factor that accounts for the variability in crack growth rate for different specimens fabricated from the same weld
K_I	=	crack-tip stress intensity factor at location of interest
$K_{I_{th}}$	=	crack-tip stress intensity factor threshold
b	=	stress intensity factor exponent

The subscripts w and b indicate different parameters for the weld metal and base metal, respectively.

This model is applied to make predictions for depth growth rate by substituting the K_{90} stress intensity factor term for the K_I term above and for length growth rate by substituting the K_0 stress intensity factor term for the K_I term.

The uncertainty in the crack growth rate models is incorporated through the weld-to-weld and within-weld factors, f_{weld} and f_{ww}, or the heat-to-heat and within-heat factors, f_{heat} and f_{wh}. The within-weld and within-heat factors are sampled for each flaw site from a distribution reflective of the growth rate variation observed in laboratory studies of cracks in a controlled set of specimens. Similarly, the weld-to-weld and heat-to-heat factors are sampled once for each head from a distribution reflective of the growth rate variation observed in laboratory studies across different specimens, after averaging the within-weld or within-heat variation.

The sampled weld-to-weld (or heat-to-heat) factors may be correlated with the average time of first initiation to simulate the premise that heads that are more susceptible to PWSCC initiation tend to have higher flaw propagation rates.

In general, the estimation of crack growth versus time requires the solution of the above ordinary differential equation. This is achieved numerically by discretizing each plant operating cycle into many sub-cycles (referred to as "within-cycle loops" in Section A.2) and advancing growth linearly over each sub-cycle, using the crack geometry and stress profile at the beginning of each sub-cycle to predict growth rate—a forward Euler method. Four (4) sub-cycles per calendar year are used to produce Alloy 690 results in this study; this is demonstrated to yield solutions that are sufficiently converged in comparison to the true solution to Equation [A-8] (see Section B.3.3.2). Consistent with MRP-335 Rev. 1 [30], 12 sub-cycles per calendar year are used to produce Alloy 600 results due to the characteristically higher growth rates.

A.6.1 Special Considerations for Crack Growth on RPVHPNs

This section discusses the special model constraints and interactions applied to capture the essential growth characteristics of complex cracking in RPVHPNs.

- Axial OD cracks are assumed to initiate below the weld, somewhere between the weld toe and the point where surface stress falls below 80% of yield. If the crack depth penetrates through-wall prior to reaching the nozzle OD annulus, the crack transitions to a through-wall axial crack (and the applicable growth model is henceforth used). If the upper crack tip of an axial OD crack reaches the weld root, i.e., the nozzle OD annulus, the crack transitions to the weld contour (i.e., circumferential) through-wall growth model.
- Radially orientated cracks in the J-groove weld are prevented from growing in length past the half-width of the weld—the width of the weld half-way along the weld path line as demonstrated in Figure B-2. This is done to approximate the premise that weld cracks would arrest in length growth upon reaching either the penetration nozzle or Alloy 52 weld butter material interface.
- As mentioned several times previously, leakage of any crack is immediately followed by the formation of a through-wall crack growing along the J-groove weld contour. The crack is assumed to initiate with a length equivalent to 30° around the weld contour. This assumption has a precedent in MRP-105 [6] and, together with the immediate transition to through-wall growth on the weld contour after leakage, is expected to result in conservative estimates for the time to ejection following leakage.
- For circumferential through-wall cracks growing along the weld contour, a random factor ($C_{mult,circ}$) is applied to scale the growth rate predicted using the second line of Equation [A-8]. This random factor is intended to capture the possibility of the growth rate being accelerated by the concentrated chemical environment that may develop in the annulus on the nozzle OD above the weld. The potential for chemical concentration in the annulus is discussed in MRP-55 [29]. The distribution selected for this variable is discussed in Section B.2.3.2.
- The program considers the rare case where through-wall crack growth along the weld contour initiates on both the uphill and downhill sides of the penetration nozzle. In this case, the lengths of the uphill and downhill cracks are combined to assess for nozzle ejection (as detailed in Section A.8).

A.6.2 Factor of Improvement on Growth

The models selected in this study to estimate PWSCC crack growth in the Alloy 690/52/152 nozzle and weld material are based on the statistical models established for Alloy 600 in MRP-55 [29] and Alloy 82/182 model in MRP-115 [14]. These models are relatively simple and incorporate mathematical dependencies for two major factors affecting flaw growth rate: temperature and stress intensity factor. At the time of this report, the magnitude and quality of available data for CGR testing in Alloys 690/52/152 is not sufficient to allow independent statistical model development. Therefore, to account for the increased PWSCC growth resistance of Alloys 690/52/152, a factor of improvement (FOI) approach is applied to adjust predictions based on the established Alloy 600 and Alloy 82/182 models.

There are three FOI parameters implemented to account for differences in PWSCC resistance between the Alloy 600 and Alloy 690 families of materials (which apply as indicated in Figure A-3):

1. **A FOI for wrought Alloy 690 material** is applied to axial flaws in the nozzle except the cases covered by item 3 below.

2. **A FOI for the J-groove weld material** is applied to radial flaws in the J-groove weld.
3. **A FOI for Alloy 690 HAZ** is applied to the upper crack tip of through-wall and part-depth OD axial cracks.

Crack depth and crack length growth rates are calculated as described in Section A.6. The FOI effect is implemented by dividing the nominal CGRs by the FOI relevant to the crack tip location.

For axial OD cracks, the upper tip of the crack grows through the HAZ material while the lower crack tip grows in wrought material. In cases where the FOI for these regions is different, asymmetric crack growth would be expected. Instead, however, the crack is assumed to remain symmetrical and semi-elliptical; the axial location of the crack tip is shifted each sub-cycle by an amount specified in Equation [A-9]:

$$\Delta H = \frac{FOI_{wr} - FOI_{HAZ}}{FOI_{wr} + FOI_{HAZ}} \Delta c \quad (+ \text{ is upward}) \qquad [A\text{-}9]$$

where

ΔH = change in crack axial position over the cycle
FOI_{wr} = FOI on the wrought material
FOI_{HAZ} = FOI on the HAZ material
Δc = change in crack half-length over the sub-cycle

A.7 Inspection and Detection

This section describes the models applied to simulate ultrasonic and visual examinations of RPVHPNs and is very similar to the methodology applied in MRP-335 Rev. 1 [30]. In the absence of contradictory evidence, it is assumed that the efficacy of ultrasonic and visual examinations for Alloy 690 top heads is consistent with that for Alloy 600 top heads.

In this study, no credit is taken for performance of ET examinations.

Section A.7.1 discusses how examinations are scheduled, Section A.7.2 describes the inspection models, and Section A.7.3 describes the detection and repair modeling rules.

A.7.1 Examination scheduling

The base case inspection intervals are guided by ASME Code Case N-729-1 [3]. This Code Case specifies the following:

- Requirements for the maximum number of operating cycles that are currently permitted between non-visual non-destructive examinations (NDEs) as a function of operating head temperature, cycle length, and capacity factor. Inputs for UT inspection scheduling are given in Section B.2.4.1.
- Requirements for bare metal visual (BMV) scheduling interval as a function of the plant's effective degradation years (EDY). Inputs for BMV inspection scheduling are given in Section B.2.4.1.

The central goal of this probabilistic modeling effort is to provide a technical basis demonstrating the efficacy of extending the ISI inspection interval for RPVHs with Alloy 690 penetration nozzles beyond those specified by current N-729-1 requirements. The technical basis aims to demonstrate that ISI intervals can be extended while maintaining a significant improvement versus Alloy 600 in terms of the risk of ejection over the entire plant operating period. The inspection interval effectiveness is demonstrated by investigating cases with ISI intervals that are extended in comparison to N-729-1 requirements and comparing their results with cases simulated to have ISI intervals in accordance with N-729-1 (see Section B.3.2).

A.7.2 Inspection modeling

This section describes the inspection models (i.e., the determination of POD) for UT and BMV inspections. It also defines the coverage of each examination technique. No credit is taken for ET examinations in this work.

As in MRP-335 Rev. 1 [30], UT inspection of RPVHPNs is based on the general POD equation described in Equation [A-10], where through-wall fraction is used as the independent variable to incorporate the dependence of UT performance on both the depth of the crack and the thickness of the component.

$$POD_{UT}\left(\frac{a}{t}\right)=\frac{e^{\beta_{1,UT}+\beta_{2,UT}\ln\left(\frac{a}{t}\right)}}{1+e^{\beta_{1,UT}+\beta_{2,UT}\ln\left(\frac{a}{t}\right)}} \qquad \text{[A-10]}$$

Given the lack of qualified inspection data from which to perform a detailed model regression, a simplified approach is adopted. The POD model form in Equation [A-10] is fit twice to provide a lower bound and an upper bound for POD versus through-wall crack percentage. Section B.2.4.2 gives the parameters for the lower and upper bound curves and briefly describes their derivation.

Then, the lower and upper bound curves, $POD_{UT,L}$ and $POD_{UT,U}$, are assumed to represent the two sigma bounds for a family POD curves (the variability within this family would be considered epistemic or reducible with further experimentation). To get a single realization of the POD curve, a standard normal deviate, z_{UT}, is sampled once per Monte Carlo realization (i.e., once per top head), and the following equation is used to simulate UT inspection of all cracks:

$$POD_{UT}\left(\frac{a}{t}\right)=\frac{POD_{UT,U}\left(\frac{a}{t}\right)+POD_{UT,L}\left(\frac{a}{t}\right)}{2}+z_{UT}\frac{POD_{UT,U}\left(\frac{a}{t}\right)-POD_{UT,L}\left(\frac{a}{t}\right)}{4} \qquad \text{[A-11]}$$

A maximum POD may be specified to truncate the POD curve, regardless of the crack size. This maximum POD can be enforced to account for operator error or other systematic error.

It is noted that UT detection of both axial and circumferential through-wall cracks is modeled using an effective crack depth equal to the penetration nozzle thickness, i.e., a through-wall fraction of one.

It is assumed for the purpose of the probabilistic model that any flaws located exclusively in the J-groove attachment weld are not detectable by UT inspection performed from the ID of the

nozzle. In reality, it is possible that flaws in the weld metal that extend close to the fusion line with the base metal might be detectable by the UT examination.

BMV inspections are given a constant POD (p_{BMV}) for leaking penetrations (i.e., RPVHPN with through-wall cracking to the nozzle annulus) and zero POD for non-leaking penetrations.

A.7.3 Detection and Repair Modeling

After a POD is calculated, detection is simulated by sampling a random value between zero and one, referred to as the detection sample. If the detection sample is less than or equal to the POD, the crack is predicted to be detected; if not, the crack is predicted to be undetected for the current examination.

If the detection sample is sampled independently of previous samples, it reflects the premise that inspection success is uncorrelated, from examination to examination. Alternatively, the examination model allows for the correlation of successive detection samples for a given flaw. This is equivalent to assuming that each crack has some ambiguous (unmodeled) features which may make it harder or easier to detect than the general population.

If a crack is identified on a penetration, before or after the crack causes leakage, the entire penetration is considered to be repaired or removed from service. The head is assumed to stay in operation after this repair/removal, but no future degradation is assumed to occur on the repaired/removed penetration.

A.8 Nozzle Leakage and Ejection Criteria

At the end of each Monte Carlo realization, the probabilistic model stores a limited number of metrics related to the extent of flaw degradation in and the repair status of individual penetrations and the head as a whole. Most importantly, during each realization, incidences of leakage and ejection are catalogued by operational cycle and initial location of the offending crack. This section describes the criteria for determining leakage and ejection.

A.8.1 Ejection Criterion

The critical size for a through-wall crack on the circumference of a penetration nozzle is a model input, in degrees. The choice of critical size for penetration nozzle ejection is based on net section collapse calculations (see Section B.2.4.4).

Credit is taken for penetration nozzle incidence angle when converting between crack length and crack angle. Specifically, crack angle, θ, is calculated by the following equation:

$$\theta = \frac{2c}{2\pi R_m}\cos(\phi) \qquad \text{[A-12]}$$

where ϕ is the penetration nozzle angle of incidence with respect to the top head. It is noted that this results in a greater effective length for ejection for non-central nozzles.

A.8.2 Ejection Statistics

One metric of interest is the incremental ejection frequency (IEF) during a given cycle. This metric has precedent in MRP-105 [6] and MRP-335 Rev. 1 [30]. It is defined as the quotient of the number of realizations during which ejection occurred during a given cycle and the total number of realizations, as shown in Equation [A-13]. This is adjusted to a probability per year by dividing by the number calendar years per cycle. For cycles where no ejections are predicted to occur during a given cycle across all realizations, 0.5 ejections are assumed for the sake of Monte Carlo stability and conservatism in calculating the IEF.

$$IEF = \frac{\max\left\{\left(\text{Number of ejections predicted during cycle across all realizations}\right), 0.5\right\}}{\left(\text{Number of realizations}\right)\left(\text{Calendar years per cycle}\right)} \quad \text{[A-13]}$$

A second metric of interest is the average ejection frequency (AEF). It is defined as the average number of predicted ejections per reactor vessel head per year, as shown in Equation [A-14]. As with the IEF, 0.5 ejections are assumed to occur for cycles with no predicted ejections. As discussed in MRP-117 [7] and MRP-105 [6], the effect of nozzle ejection on nuclear safety can be assessed through multiplication of the frequency of nozzle ejection (i.e., the initiating event frequency) with an appropriate conditional core damage probability (CCDP) value. The resulting core damage frequency (CDF) is typically averaged over long-term operation and compared to the acceptance criteria of Regulatory Guide 1.174 [45]. Regulatory Guide 1.174 specifies an acceptable change in core damage frequency of 1×10^{-6} per reactor year for permanent changes in plant design parameters, technical specifications, etc.

$$AEF = \frac{\sum_{i}^{N_{cycle}} \max\left\{\left(\text{Number of ejections predicted during } i\text{th cycle across all realizations}\right), 0.5\right\}}{\left(\text{Number of realizations}\right)\left(\text{Total calendar years}\right)} \quad \text{[A-14]}$$

A third metric of interest is the cumulative probability of ejection (CPE) over all cycles. This quantifies the relative difference in ejection risk among the cases which were investigated, as shown in Equation [A-15]. Of particular importance are comparisons with the baseline Alloy 600 nozzle case inspected per N-729-1.

$$CPE = \frac{\left(\text{Total number of heads with at least 1 predicted ejection}\right)}{\left(\text{Number of realizations}\right)} \quad \text{[A-15]}$$

A.8.3 Leakage Criterion and Statistics

As discussed in Section A.3, a given flaw causes leakage if it propagates through the entire material thickness to breach the annulus above the weld before it is detected and repaired.

Two of the metrics of interest for ejection are analogously determined for leakage—incremental leakage frequency during a given cycle (ILF) and average frequency of leakage (ALF):

$$ILF = \frac{(\text{Number of initial leaks predicted during cycle across all realizations})}{(\text{Number of realizations})(\text{Calendar years per cycle})} \quad [A\text{-}16]$$

$$ALF = \frac{\sum_{i}^{N_{cycle}} (\text{Number of initial leaks predicted during } i\text{th cycle across all realizations})}{(\text{Number of realizations})(\text{Total calendar years})} \quad [A\text{-}17]$$

In addition to these statistics, the model also reports the proportion of leaks that occur in the wrought material, the HAZ, and the weld material. These values provide an indication of how varying inspections and FOIs affect the prevalence of large cracks.

B
INPUTS AND RESULTS OF PROBABILISTIC PWSCC MODEL

This appendix reports a set of results generated within the probabilistic framework to support alternative inspection regimes for top heads with RPVHPNs fabricated with Alloys 690/52/152. The probabilistic calculations presented in this appendix are designed to bound the conditions for such heads, so conclusions drawn from the results are generically applicable to heads with Alloy 690 RPVHPNs.

B.1 Modeling Assumptions and Simplifications

Several assumptions and simplifications are embedded in the probabilistic model used for this evaluation. Knowledge of the following simplifications is essential when interpreting the results given in this appendix; however, the conclusions drawn in this report are not expected to be dependent on these simplifications. It is noted that each of these key modeling assumptions is shared with the RPVHPN model described in the peening topical report, MRP-335 Rev. 1 [30].

- *Possible flaw locations.* It is assumed that multiple crack initiation on a single RPVHPN is adequately represented with six possible initiation sites: an axial flaw at the nozzle ID, an axial flaw at the nozzle OD below the weld, and a radial flaw in the weld material (each at the greatest uphill and greatest downhill locations, the locations of largest tensile residual stresses). To account for the cumulative risks of a top head, many RPVHPNs at different angles of incidence relative to the RPV head are modeled. The probability of initiation at any given site is assumed to be equal (i.e., the surface stress dependency of PWSCC initiation is not explicitly modeled).
- *Circumferential flaw initiation.* If any nozzle or weld flaw grows into the annulus above the J-groove weld, a circumferential flaw is assumed to initiate with an initial circumferential extent of 30°. This assumption is consistent with MRP-105 [6]. Flaw growth into the annulus is presumed to occur if an axial ID flaw or radial weld flaw grows to a depth exceeding the material thickness or if an axial OD flaw grows to a length such that its uppermost tip extends to the J-groove weld root.
- *Nozzle ejection threshold.* Ejection of a given RPVHPN is assumed to occur once the through-wall circumferential flaw reaches a specified threshold length. Cases presented in this section assume a conservative threshold length equivalent to 300° around the penetration, which is the same value used in MRP-105 [6] and is based on net section collapse (NSC) calculations presented in Appendix D of that report. The difference in ASME BPVC Section II-D minimum material properties between Alloy 600 and Alloy 690 only

changes the results of NSC calculations by approximately 1°.[20] Consequently, this value of 300° remains valid and conservative irrespective of the nozzle alloy.

- *Detectability by ultrasonic testing (UT) and bare metal visual (BMV) inspections.* For both Alloy 600 and Alloy 690 cases, UT examinations are assumed to be unable to detect flaws growing in the weld material. Also, the probability of detecting leakage by BMV examination is assumed to be a constant, independent of the leak rate. These modeling choices were also made in MRP-335 Rev. 1 [30].

B.2 Description of Model Inputs

The RPVHPN probabilistic model framework takes both deterministic and distributed inputs. The values of the distributed inputs are determined by sampling probability distributions during each Monte Carlo realization, potentially for each penetration or for each initiated crack. The inputs selected for use in the probabilistic model are discussed in Section B.2.1 through B.2.6.

B.2.1 General Inputs

The inputs for geometry, operating time, temperature, and loading are summarized in Table B-1 through Table B-3 and are detailed in this section. With the exception of a handful of sensitivity cases presented in Section B.2.6, these inputs are applied for all cases.

B.2.1.1 Reactor Vessel Head Nozzle Geometry

The penetration nozzle wall thickness and OD are taken as deterministic inputs, assumed constant across all penetration nozzles.

The nozzle thickness and OD that are applied for all penetration nozzles are the standard dimensions per MRP-48 [46] for CRDM nozzles in Westinghouse and B&W plant heads. The number of penetrations modeled and their angles of incidence relative to the RPVH is based on a specific design but is considered representative of the U.S. reactor fleet. The reactor vessel top head thickness is taken as 6.0 in., a length that is representative of heads in the U.S. fleet.

ICI nozzles are not considered to have geometries different from CEDM/CRDM nozzles in this analysis, despite their larger ODs and smaller thicknesses in practice. This simplification is not considered to be non-conservative because reviews of plant experience and inspection history have not uncovered any reports of PWSCC on ICI components [1].

As discussed in the modeling sections, crack initiation and growth are modeled through the J-groove weld region of the RPVHPNs. For various modeling aspects, certain J-groove weld geometries are required including: the distance from the weld toe to the weld root ("weld toe-to-root distance"), the distance from the weld surface to the weld root ("weld path length"), and the weld width halfway along the weld path length ("weld half-width") as depicted in Figure B-2 and Figure B-3. The variation of these geometries across penetrations was incorporated by fitting normal distributions to inputs for various J-groove weld FEA studies [42] (which span different

[20] The material flow strength used in this calculation is defined as the average of the yield and ultimate strengths in the ASME BPVC Section II-D (2011 edition) at 350°C (e.g., 370.5 MPa for Alloy 690 and 358 MPa for Alloy 600).

heads and penetration locations), at the uphill and downhill locations separately.[21,22] An example of such a fit (i.e., for the uphill weld path length) is given in Figure B-1. Lower and upper truncation limits were set based on engineering judgment and the extreme values from the FEA studies. The distribution parameters for all geometrical attributes are given in Table B-2.

B.2.1.2 Operating Time

Reactor vessel heads are simulated from head replacement until shutdown. Shutdown is considered to occur approximately 40 years after replacement (e.g., head replacement with less than 20 years remaining in the original license followed by a 20 year license renewal). In one sensitivity case, the effect of extending the total operational time of the head to 60 years is considered with all other parameters unchanged.

Both the Alloy 600 and Alloy 690 heads are simulated with 24-month operating cycles and assumed to have a capacity factor of 0.92, which is representative of US PWRs. For the case of the Alloy 600 head, UT inspections are simulated to occur on the most frequent schedule that has been applied in the U.S. for top heads with Alloy 600 nozzles, i.e., every fuel cycle, or 2 calendar years in the assumed case.[23]

B.2.1.3 Temperature

By the end of 2014, there are planned to be 42 reactor pressure vessel top heads with Alloy 690 penetration nozzles operating in the U.S. Of these 42 heads, four operate at cold-leg temperature (i.e., cold heads) and 38 operate at or above the upper threshold for cold-leg temperature (i.e., hot heads). The temperature of the hottest Alloy 690 top head (about 613°F or 323°C [2]) is used in this study. Variation in head temperature (due to temperature streaming or operating tolerances) is incorporated into the model by using a normal distribution with a standard deviation of 5°F (2.8°C).

The Alloy 600 base case, against which all Alloy 690 cases are compared, is also run at 613°F to allow for equivalent inputs save for differences in inspection schedule and assumed FOIs. This temperature is not considered implausible but is believed to be on the high end of historical operation of Alloy 600 heads.

The effect of reducing the mean head temperature from 613°F to 600°F (from 323°C to 316°C) is considered in a sensitivity case.

B.2.1.4 Operational Loads and Welding Residual Stresses

Results of FEAs of J-groove welding residual stresses [42] were used to estimate the total stresses in the same manner as described in MRP-335 Rev. 1 [30].

---

[21] The trends in weld geometry characteristics as a function of penetration incidence angle are not strong enough to justify in this modeling effort.

[22] The ratio of the weld path length and the weld half-width was found to be approximately constant across penetration nozzles and accordingly was treated as a deterministic input.

[23] For the assumed head temperature of 613°F (323°C) and an assumed capacity factor of 0.92, the RIY accumulated between simulated UT inspections is RIY = 2.54. This is slightly greater than the RIY = 2.25 interval of Code Case N-729-1 [3].

Stress profiles on six vectors of interest (shown in Figure A-4) were synthesized from results of J-groove weld FEA analyses [42]. Equation [A-4] describes the second-order polynomial form fit to FEA results. The coefficients of the polynomial stress profile along each vector of interest are solved to satisfy the constraint that the total stress curve passes through sampled stresses at three locations: x/D=0, x/D=1, and x/D=0.5, where:

- x/D=0 is defined as the location where cracks are expected to initiate: the ID above the weld for ID axial cracks, the OD below the weld for OD axial cracks, or the weld surface center for weld cracks.
- x/D=1 is defined as the location toward which cracks are expected to grow: the OD above the weld for ID axial cracks, the ID below the weld for OD axial cracks, or the weld root for weld cracks.
- x/D=0.5 is defined as being halfway between the previous two locations.

Equation [B-1] gives parameterized equations for the sampled stresses at x/D=0, x/D=1, and x/D=0.5:

$$\begin{aligned}
&\sigma_{tot,loc}(x/D=0) = \sigma_{0,tot,loc} \\
&\sigma_{tot,loc}(x/D=1) = R_{1,loc}\sigma_{0,tot,loc} \\
&\sigma_{tot,loc}(x/D=0.5) = \left(\frac{\sigma_{0,tot,loc} + R_{1,loc}\sigma_{0,tot,loc}}{2}\right) R_{0.5,loc}
\end{aligned} \qquad \text{[B-1]}$$

Uncertainty inherent in data, as well as the uncertainty due to unknown variation of missing data, is incorporated through distributed inputs for the parameters in Equation [B-1]: the surface stress, $\sigma_{0,tot}$, the gradient quantifier, $R_{1,tot}$, and the curvature quantifier, $R_{0.5,tot}$.

For each location of interest, parameter distributions were estimated to give a family of stress profile curves bounding of FEA results with an adequate excess of uncertainty to account for variation not captured across the FEA studies. These parameter distributions are summarized in Table B-3. Conservatively, a minimum no less than zero is used for all parameters to ensure tensile hoop stresses at the three interpolated depths.

Based on these parameter distributions, fifty instances of the stress profile through the downhill weld, together with corresponding FEA results, are shown in Figure B-4. Equivalent figures for each of the other locations of interest are given in Figure B-11 through Figure B-15 in MRP-335 Rev. 1 [30].

Table B-1
Summary of General Model Inputs

Symbol	Description	Source	Units	Distrib. Parameter	Value for Base Case
	Number of operating cycles	Selected to yield desired cumulative operating time	Nondim		20
	Nominal cycle length	Upper end cycle length for US PWR	yr		2.0
CF	Operating capacity factor	Reasonable capacity factor for US PWR	Nondim		0.92
	UT inspection frequency	Varied for investigation purposes; see "Summary of Inspection Scheduling Cases" table in this report	$(\#\ \text{cycles})^{-1}$		
	BMV inspection frequency	Varied for investigation purposes; see "Summary of Inspection Scheduling Cases" table in this report	$(\#\ \text{cycles})^{-1}$		
T	Operating temperature	Believed to be an upper bound for operating Alloy 690 hot heads in service	°F	type	Normal
				mean	613.0
				stdev	5.0
				min	583.0
				max	643.0
P_{op}	Normal operating pressure	Representative normal operating pressure	MPa		15.5

Table B-2
Model Geometry Inputs

Symbol	Description	Source	Units	Distrib. Parameter	Value for Base Case
N_{pen}	Number of modeled penetrations	Selected based on properties of unit serving as characteristic hot head	Nondim		89
	Incidence angles for penetrations	Selected based on properties of unit serving as characteristic hot head	degrees	type	discrete list
				average	34.1
				min	0.0
				max	56.1
t	Nozzle thickness	Representative of CEDM nozzle thickness of unit serving as characteristic hot head	m		0.0158
D_o	Nozzle outer diameter	Representative of CEDM nozzle OD of unit serving as characteristic hot head	m		0.1016
t_{head}	Reactor head thickness	Representative of industry PWRs	m		0.152
	Representative length from weld surface to weld root, uphill	Inputs to previous finite element analyses of J-groove weld residual stresses; valid across various penetration geometries	in	type	Normal
				mean	1.05
				stdev	0.18
				min	0.5
				max	1.7
	Representative length from weld surface to weld root, downhill	Inputs to previous finite element analyses of J-groove weld residual stresses; valid across various penetration geometries	in	type	Normal
				mean	0.97
				stdev	0.23
				min	0.5
				max	1.7
	Representative length from weld toe to weld root, uphill	Inputs to previous finite element analyses of J-groove weld residual stresses; valid across various penetration geometries	in	type	Normal
				mean	1.38
				stdev	0.30
				min	0.8
				max	2.9
	Representative length from weld toe to weld root, downhill	Inputs to previous finite element analyses of J-groove weld residual stresses; valid across various penetration geometries	in	type	Normal
				mean	1.36
				stdev	0.37
				min	0.8
				max	2.9
	Ratio of weld path length to weld half-width, uphill	Inputs to previous finite element analyses of J-groove weld residual stresses; valid across various penetration geometries	Nondim		1.62
	Ratio of weld path length to weld half-width, downhill	Inputs to previous finite element analyses of J-groove weld residual stresses; valid across various penetration geometries	Nondim		1.24

Table B-3
Summary Total Stress Profile Parameters

Symbol	Description	Source	Units	Distrib. Parameter	Value for Base Case
$\sigma_{0,tot,1}$	Total hoop stress at penetration ID above weld, uphill	Finite element analyses of J-groove weld residual stresses (14 independent analyses)	MPa	type	Normal
				mean	282.6
				stdev	50.6
				min	0.0
				max	586.2
$\sigma_{0,tot,2}$	Total hoop stress at penetration OD below weld, uphill	Finite element analyses of J-groove weld residual stresses (14 independent analyses)	MPa	type	Normal
				mean	370.8
				stdev	68.4
				min	0.0
				max	781.2
$\sigma_{0,tot,3}$	Total hoop stress at weld surface center, uphill	Finite element analyses of J-groove weld residual stresses (14 independent analyses)	MPa	type	Normal
				mean	413.5
				stdev	39.5
				min	176.5
				max	650.5
$\sigma_{0,tot,-1}$	Total hoop stress at penetration ID above weld, downhill	Finite element analyses of J-groove weld residual stresses (14 independent analyses)	MPa	type	Normal
				mean	297.7
				stdev	57.2
				min	0.0
				max	640.9
$\sigma_{0,tot,-2}$	Total hoop stress at penetration OD below weld, downhill	Finite element analyses of J-groove weld residual stresses (14 independent analyses)	MPa	type	Normal
				mean	462.5
				stdev	73.1
				min	23.9
				max	901.1
$\sigma_{0,tot,-3}$	Total hoop stress at weld surface center, downhill	Finite element analyses of J-groove weld residual stresses (14 independent analyses)	MPa	type	Normal
				mean	426.0
				stdev	39.8
				min	187.2
				max	664.8

Table B-3
Summary Total Stress Profile Parameters (Continued)

Symbol	Description	Source	Units	Distrib. Parameter	Value for Base Case
$R_{1,tot,1}$	Gradient quantifier at penetration ID above weld, uphill	Finite element analyses of J-groove weld residual stresses (14 independent analyses)	Nondim	type	Normal
				mean	1.11
				stdev	0.24
				min	0.00
				max	2.55
$R_{1,tot,2}$	Gradient quantifier at penetration OD below weld, uphill	Finite element analyses of J-groove weld residual stresses (14 independent analyses)	Nondim	type	Normal
				mean	0.84
				stdev	0.14
				min	0.00
				max	1.68
$R_{1,tot,3}$	Gradient quantifier at weld surface center, uphill	Finite element analyses of J-groove weld residual stresses (14 independent analyses)	Nondim	type	Normal
				mean	0.89
				stdev	0.32
				min	0.00
				max	2.81
$R_{1,tot,-1}$	Gradient quantifier at penetration ID above weld, downhill	Finite element analyses of J-groove weld residual stresses (14 independent analyses)	Nondim	type	Normal
				mean	0.60
				stdev	0.41
				min	0.00
				max	3.06
$R_{1,tot,-2}$	Gradient quantifier at penetration OD below weld, downhill	Finite element analyses of J-groove weld residual stresses (14 independent analyses)	Nondim	type	Normal
				mean	0.51
				stdev	0.13
				min	0.00
				max	1.29
$R_{1,tot,-3}$	Gradient quantifier at weld surface center, downhill	Finite element analyses of J-groove weld residual stresses (14 independent analyses)	Nondim	type	Normal
				mean	0.36
				stdev	0.17
				min	0.00
				max	1.38

Table B-3
Summary Total Stress Profile Parameters (Continued)

Symbol	Description	Source	Units	Distrib. Parameter	Value for Base Case
$R_{0.5,tot,1}$	Curvature quantifier at penetration ID above weld, uphill	Finite element analyses of J-groove weld residual stresses (14 independent analyses)	Nondim	type	Normal
				mean	1.08
				stdev	0.09
				min	0.54
				max	1.62
$R_{0.5,tot,2}$	Curvature quantifier at penetration OD below weld, uphill	Finite element analyses of J-groove weld residual stresses (14 independent analyses)	Nondim	type	Normal
				mean	0.87
				stdev	0.13
				min	0.09
				max	1.65
$R_{0.5,tot,3}$	Curvature quantifier at weld surface center, uphill	Finite element analyses of J-groove weld residual stresses (14 independent analyses)	Nondim	type	Normal
				mean	1.21
				stdev	0.12
				min	0.49
				max	1.93
$R_{0.5,tot,-1}$	Curvature quantifier at penetration ID above weld, downhill	Finite element analyses of J-groove weld residual stresses (14 independent analyses)	Nondim	type	Normal
				mean	1.46
				stdev	0.13
				min	0.68
				max	2.24
$R_{0.5,tot,-2}$	Curvature quantifier at penetration OD below weld, downhill	Finite element analyses of J-groove weld residual stresses (14 independent analyses)	Nondim	type	Normal
				mean	0.78
				stdev	0.09
				min	0.24
				max	1.32
$R_{0.5,tot,-3}$	Curvature quantifier at weld surface center, downhill	Finite element analyses of J-groove weld residual stresses (14 independent analyses)	Nondim	type	Normal
				mean	1.47
				stdev	0.19
				min	0.33
				max	2.61

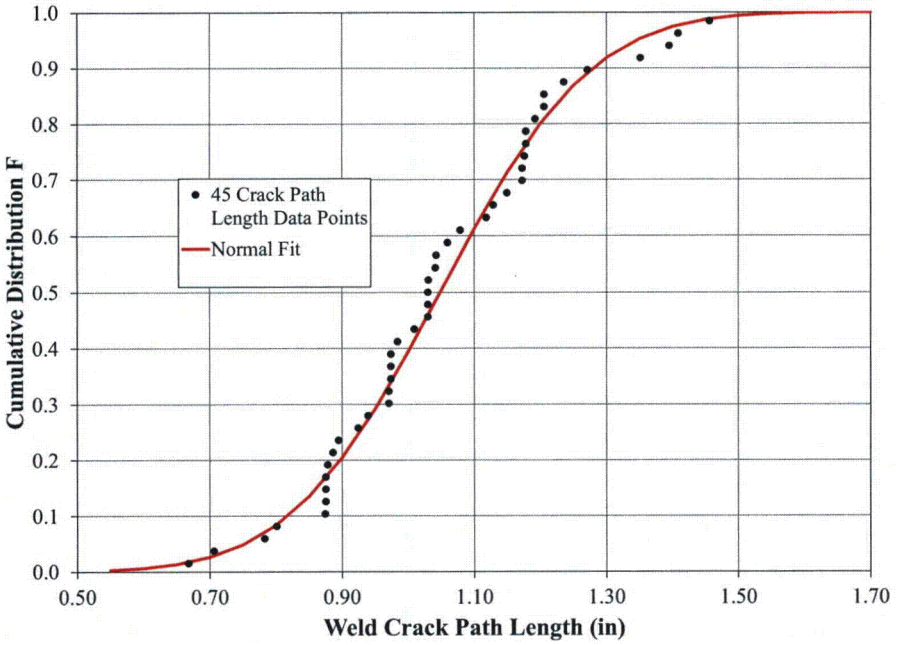

Figure B-1
Example of Normal Distribution Fit to Geometry Data Varying Across Penetration Nozzle Incidence Angles: Uphill Weld Path Length [30]

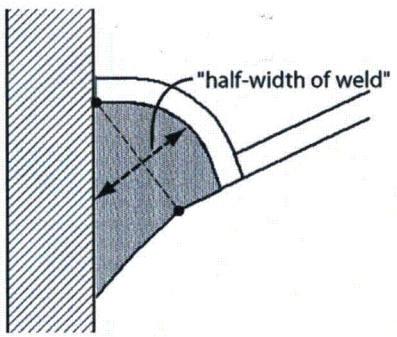

Figure B-2
Description of Weld Half-Width [30]

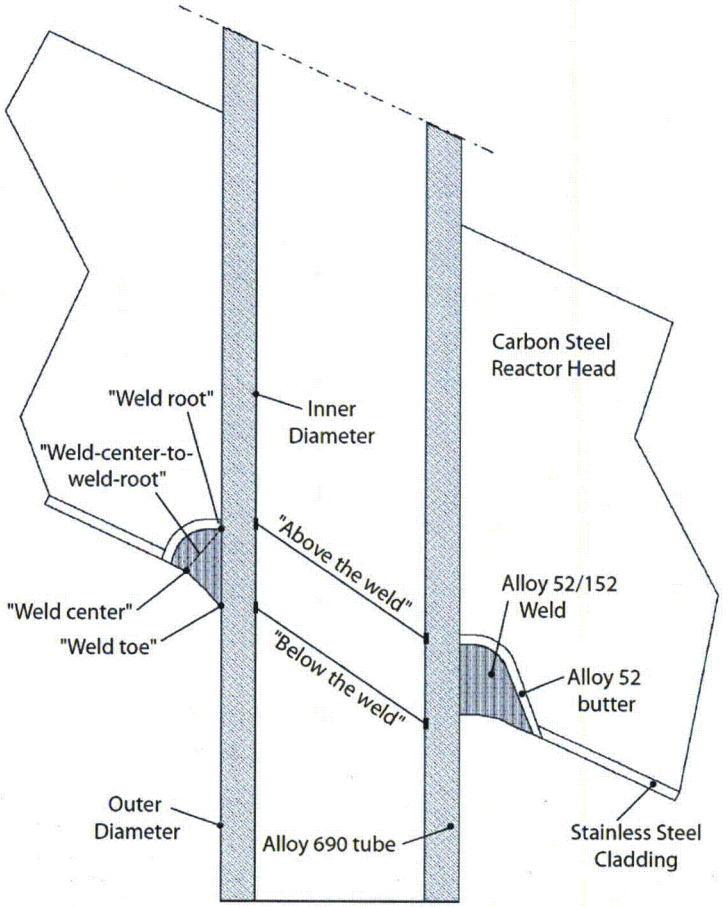

Figure B-3
Summary of General RPVHPN Geometry and Terminology

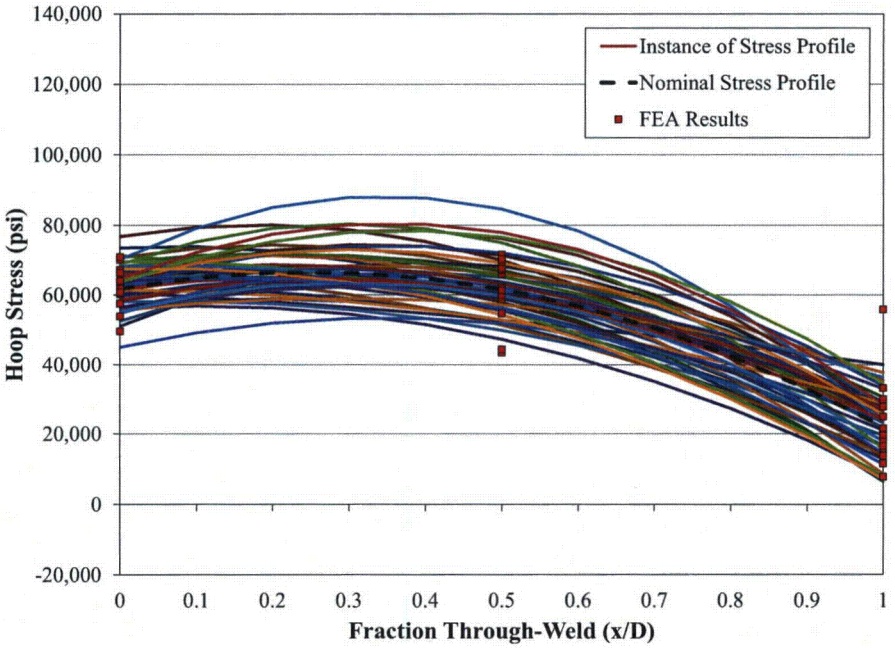

Figure B-4
Stochastic Family (50 instances) of Curves and FEA Results for the Total Stress Profile between the Weld Center and the Weld Root, Downhill Side [30]

B.2.2 Crack Initiation Inputs

The set of inputs for the RPVHPN PWSCC initiation model is detailed in the following subsections and is summarized in Table B-4.

B.2.2.1 Industry Weibull used to Develop Initiation Model

Plant inspection data for RPVHPNs fabricated from Alloy 600 with J-groove welds fabricated from Alloys 82 and 182 were evaluated in MRP 2011-034 [2]. Figure B-5 shows the detected cracking indications that were used in this report but also reflects indication data from more recent experience.

To fit a Weibull model to the time of first PWSCC initiation on each head, a multiple flaw Weibull slope of 3 [2] was assumed to address instances of multiple cracking indications. Multiple indications are typically discovered on heads with Alloy 600 nozzles during inspections where at least a single indication is detected. The assumption of a multiple flaw Weibull slope allows the projection from the time of multiple flaw detection to an estimate for the time of first initiation.

Figure B-5 shows an example Weibull distribution fit to the industry experience with RPVHPNs fabricated from Alloy 600 with welds from Alloys 82 and 182. The leakage and ejection times were adjusted to a common reference temperature of 600°F (315.6°C) using a thermal activation energy of 184 kJ/mole (the mean value given for PWSCC initiation in thick-walled components in Section B.2.2.2). Table B-5 summarizes the estimated Weibull parameters.

B.2.2.2 Uncertainty in Weibull Model Parameters

Uncertainty in Weibull Slope (β)

The uncertainty in the Weibull slope is modeled with a normal distribution having the mean and standard deviation values estimated from data. The best-fit Weibull slope and the standard error on this slope are determined with ordinary least-squares [47] and are provided in Table B-5.

Uncertainty in Anchor Point Time (t_1)

Based on data presented in Figure B-5, a value of 0.01 was selected as the value of the failure fraction associated with the anchor point, F_1. The best-fit value for t_1, the time to PWSCC initiation in 1% of the RPVH population, is estimated to be 0.827. Figure B-5 shows that this combination of failure fraction and time provides a reasonable representation of the earlier failures observed in the field.

Uncertainty in the anchor point time is incorporated using the following procedure for each Monte Carlo realization:

- Determine the characteristic time, θ, using the value of F_1 and the best-fit values of β and t_1.
- Determine the best-fit vertical intercept parameter, c, using the best-fit value of β and the value of θ determined in the previous step.
- Sample the value of c from a normal distribution using the best-fit vertical intercept parameter determined in the previous step and the standard error (σ_c) given in Table B-4. The estimator for this standard error is determined with ordinary least-squares regression of the data.
- Determine the anchor point time for the current realizations using the sampled vertical intercept parameter from the previous step and the best-fit value of β.

Uncertainty in Multiple Flaw Weibull Slope

As discussed in the modeling section, a second Weibull model is used to predict the initiation of multiple flaws on a single head. The key input to this model is the Weibull slope.

The slope of the multiple flaw Weibull model, β_{flaw}, quantifies the rate at which flaws occur after the initiation of the first flaw. An analytical data fitting procedure, as was done for the time to first initiation model, was not considered appropriate to fit β_{flaw} given several complexities. Instead, a mean value of 2 was selected for β_{flaw}. This value has a precedent in probabilistic modeling of SCC in steam generators [48]. A normal distribution with a mean of 2 and a standard deviation of 0.5 is employed to incorporate uncertainties due to material and manufacturing disparities. A lower truncation bound of 1 was selected to prevent a multiple flaw Weibull model in which the PWSCC initiation rate at the remaining initiation sites decreases over time. A sensitivity case that considers a greater multiple flaw initiation slope is included to compare with the base cases of this report.

A benchmarking experiment was run in MRP-335 Rev. 1 [30] with a value of 2 for β_{flaw} in order to demonstrate the resulting number of cracks per head, given distributed parameter values similar to those discussed in this report. The results presented in Figure B-18 and Figure B-19 of that report indicate that the probabilistic model predicts a similar number of flaws, for heads that that have at least one flaw, compared to industry data.

Uncertainty in Initial OD Axial Flaw Location

As discussed in the modeling section, an initial flaw location is required for OD axial flaws. For each initiated OD axial flaw, the flaw center location is uniformly sampled between the weld toe and the location where the residual stresses in the penetration nozzle fall below 80% of yield stress.

The distance from the weld toe to the 80% yield location (the "80% yield stress length") is taken as a distributed input. The variation in the 80% yield stress length is due to process variation and geometrical variation across different penetration nozzle incidence angles. The trend in the 80% yield stress length versus incidence angle is not strong enough to justify its implementation in this study.

This distribution for this length has been estimated from results of FEA of J-groove welding residual stresses [42] at both the uphill and downhill sides of the penetration. The resulting fits are shown in Figure B-6 and Figure B-7; the distribution parameters are given in Table B-4.

Uncertainty in Initial Flaw Depth

The initial through-wall fraction for each flaw is sampled at the time of flaw initiation. A log-normal distribution with a median of 5% through-wall and an upper 95% confidence bound of 10% through-wall is used. For the penetration nozzle thickness presented earlier (15.8 mm) this results in a median absolute initiation depth of 0.8 mm. This distribution has the following desirable qualities:

- The PWSCC initiation time model has been developed from industry detection data. Appropriately, this distribution reflects depths of flaws that could reasonably be detected with UT inspection of RPVHPNs.
- Distributions with positive skewness (e.g., mass concentration at low values, long-tail extending to high values) like the log-normal distribution have been found to be appropriate for modeling initial depths measured in practice.
- This distribution is in approximate agreement with the 0.4 - 2.0 mm range defined for initial cracks in Reference [49].
- This distribution accurately bypasses earlier stages of short crack development—which are difficult to model accurately, and in fact represent an area of active research—and allows growth to begin from flaws of engineering significance.

A lower truncation limit of 0.5 mm is defined to prevent the initiation of very small flaws for which the stress intensity factor (based on the input distributions of the surface welding residual stress) would be significantly less than the minimum stress intensity factors (about 15 – 20 MPa-$m^{1/2}$ or 14 – 18 ksi-$in^{1/2}$) evaluated in the laboratory studies used to define the flaw propagation models used in this work.

Uncertainty in Flaw Aspect Ratio

As in MRP-335 Rev. 1, a log-normal distribution is fit to yield a mode of 4 and a 99% confidence (one-sided) interval upper bound of 10 for the aspect ratio distribution. Not enough data is available for initial RPVHPN crack sizes to allow a distribution to be fit for aspect ratio.

Uncertainty in Temperature Effect

Uncertainty in the apparent activation energy for PWSCC crack initiation is treated by defining a distributed input. As shown in Table B-4, a normal distribution is assumed to describe the uncertainty in the activation energy.

An experimentally based value of 184.2 kJ/mole has been determined for Alloy 600 CRDM nozzle (i.e., thick-wall) material [50]. Based on evaluations of PWSCC in Alloy 600 steam generator tubing [51], an activation energy of 209.4 kJ/mole is a standard value applied for the initiation of PWSCC in Alloy 600 components [52]. Based on this discussion and a separate review of laboratory and field data [51], 184.2 kJ/mole was selected as the mean of the distribution and the standard deviation was selected such that the 95% confidence bound of the distribution would be 209.4 kJ/mole.

Table B-4
Summary of Crack Initiation Submodel Inputs

Symbol	Description	Source	Units	Distrib. Parameter	Value for Base Case
Q_i	Thermal activation energy for PWSCC flaw initiation	Q distribution based on laboratory data and judgment from experience with Weibull analysis	kJ/mole	type	Normal
				mean	184.2
				stdev	12.8
				min	107.3
				max	261.1
β	Weibull slope for PWSCC flaw initiation on RPVPNs	Flaw initiation data assessed in this report	Nondim	type	Normal
				mean	1.393
				stdev	0.078
				min	0.924
				max	1.862
F_1	Failure fraction selected to define Weibull PWSCC initiation function	Selected to reflect failure fractions observed for early plant experience	Nondim		0.01
t_1	Time at which failure fraction F_1 is reached on RPVPNs	Flaw initiation data assessed in this report	EDY	type	Normal
				mean	0.827
				stdev	see σ_c
				min	0.405
				max	1.690
σ_c	Standard error in intercept of linearized Weibull fit	Linearized Weibull fit to flaw initiation data assessed in this report	ln(EDY)		0.166
β_{flaw}	Weibull slope for PWSCC multiple flaw initiation on RPVPNs	Based on representative value for formation of PWSCC at multiple locations in industry SGs	Nondim	type	Normal
				mean	2.0
				stdev	0.5
				min	1.0
				max	5.0
T	Component operating temperature	See model inputs table in this report			
$T_{ref,i}$	Reference temperature to normalize PWSCC flaw initiation data	Temperature used to adjust flaw initiation data assessed in this report	°F		600.0

Table B-4
Summary of Crack Initiation Submodel Inputs (Continued)

Symbol	Description	Source	Units	Distrib. Parameter	Value for Base Case
a_0	Initial depth assigned to newly initiated flaw	Consistency with initial through-wall fractions of MRP–335R1	m	type	Log-Normal
				linear μ	8.44E-04
				log-norm μ	-7.14
				log-norm σ	0.35
				min	5.00E-04
				max	0.0158
AR	Initial aspect ratio assigned to newly initiated flaw	Engineering judgment and aspect ratios for cracks at other locations	Nondim	type	Log-Normal
				linear μ	4.77
				log-norm μ	1.50
				log-norm σ	0.34
				min	0.575
				max	35.2
	Distance from weld toe to location where welding residual stress is equal to 80% of yield stress, uphill side	Finite element analyses of J-groove weld residual stresses; valid across various units and penetration geometries	in	type	Normal
				mean	0.25
				stdev	0.13
				min	0.00
				max	1.03
	Distance from weld toe to location where welding residual stress is equal to 80% of yield stress, uphill side	Finite element analyses of J-groove weld residual stresses; valid across various units and penetration geometries	in	type	Normal
				mean	0.25
				stdev	0.06
				min	0.00
				max	0.61

Table B-5
Summary of Head Initiation Weibull Distribution Parameters

Fitting Method	β	θ (EDY)	Standard Error in Weibull Slope	Standard Error in Vertical Intercept (ln(EDY))
Linearized Least Squares	1.39	22.5	0.078	0.166

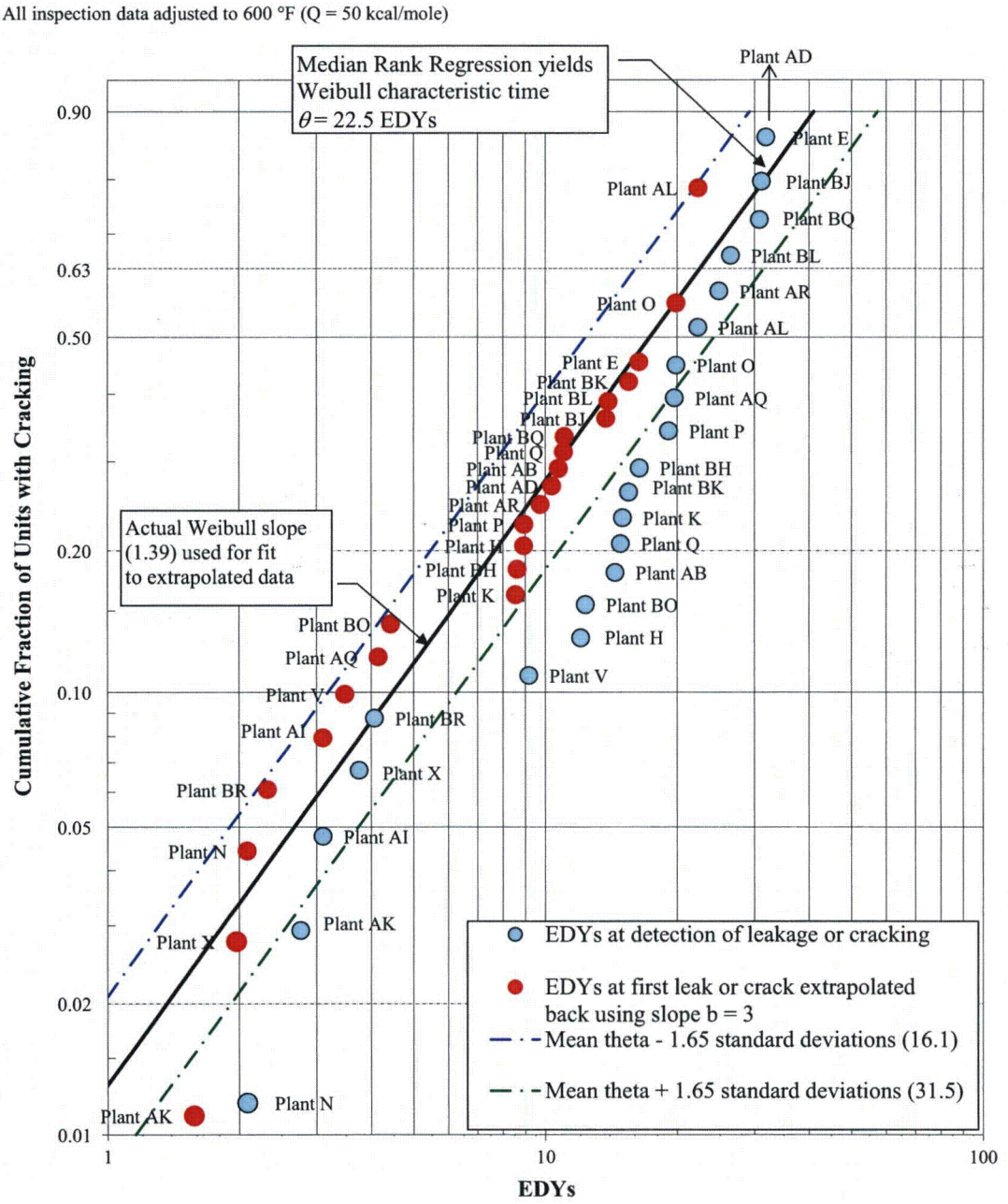

Figure B-5
Data Used to Generate Parameters and Resulting Fit for PWSCC Initiation Weibull Model

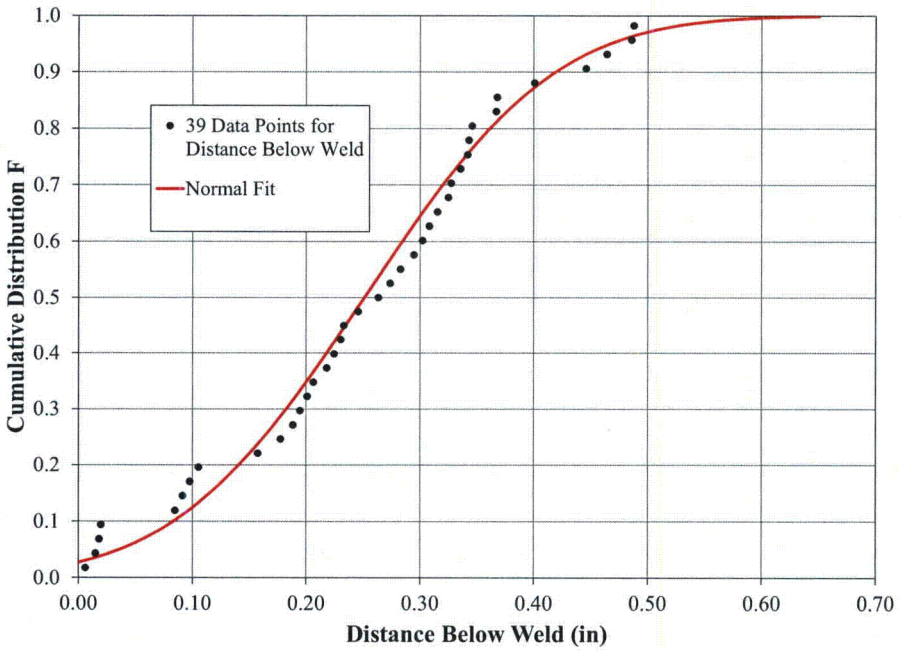

Figure B-6
Normal Distribution Fit to 80% Yield Stress Length on Uphill Side of Penetration Predicted by Different FEA Studies [30]

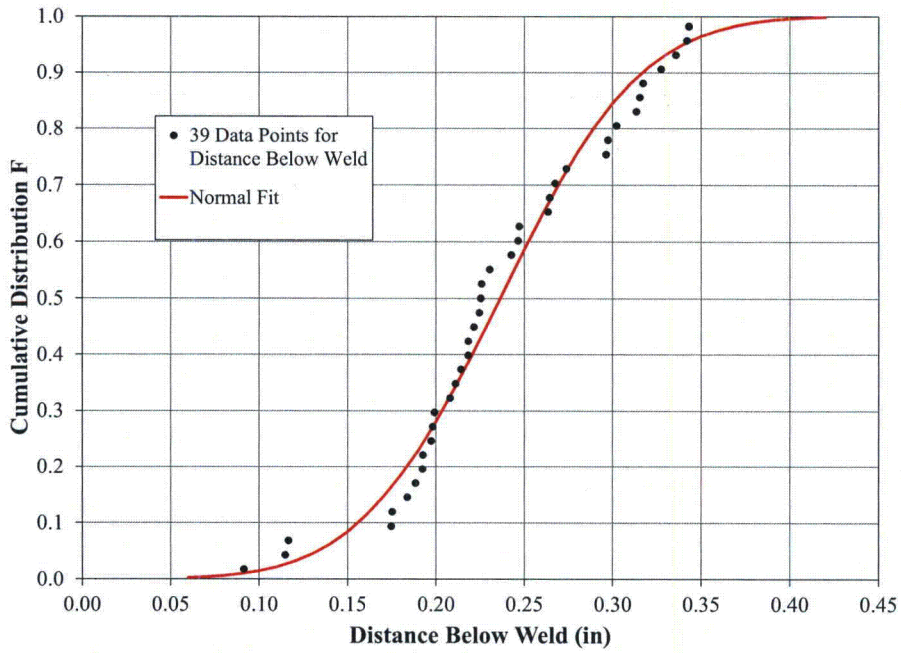

Figure B-7
Normal Distribution Fit to 80% Yield Stress Length on Downhill Side of Penetration Predicted by Different FEA Studies [30]

B.2.3 Crack Growth Inputs

The set of inputs for the PWSCC propagation model is described in Table B-6 at the end of this section, including deterministic and distributed inputs. Various inputs are detailed in the following subsections. As discussed previously, the FOIs for growth of Alloys 690/52/152 are applied after calculating the growth rate based on Alloys 600/82/182. Consequently, the parameter fits in this section utilize data for Alloys 600/82/182.

B.2.3.1 Empirical Growth Parameters

The general equations used in this study to calculate flaw propagation rate in Alloys 600/82/182 is given as Equation [A-8].

The flaw propagation rate constant for growth in Alloy 82/182, α_{weld}, is based on the 50th percentile (best-fit) value estimated in MRP-115 [14] and reported in Appendix F of MRP-263 [53]. Likewise, the stress intensity factor threshold and stress intensity factor exponent (for growth in Alloys 82/182) are based on values regressed in MRP-115.

The empirical growth parameters for Alloy 600 are based on the crack growth data compiled and presented in MRP-55 [29]. Instead of using a crack growth curve with a stress intensity factor threshold of 9 MPa$\sqrt{m}$—as suggested in MRP-55—a more bounding curve with a stress intensity factor threshold of 0 has been fit to the data. The fitted parameters are provided in Table B-6.

A comparison of the CGR curves used in this report with the 50th and 75th percentile curves from each of MRP-55 and MRP-115 is shown in Figure B-12.

B.2.3.2 Growth Variation Factors

Alloy 82/182 (Used for Alloy 52/152)

The uncertainty in the probabilistically calculated flaw propagation in the weld material is principally characterized by the f_{weld} and f_{ww} parameters in the flaw propagation rate equation described Section A.6.

The weld-to-weld parameter (f_{weld}) is a common factor applied to all specimens fabricated from the same weld to account for effects of the weld wire/stick heat processing and of weld fabrication. For this study, a log-normal distribution is fit to the weld factors for the set of laboratory test welds assessed in MRP-115 (see Figure B-8).

A within weld factor (f_{ww}) is included to describe the variability in flaw propagation rate for different weld specimens fabricated from the same weld. The within weld factor distribution describes the scatter in the flaw propagation rate data that remains after all model effects are accounted for and the weld-to-weld variation is reconciled. A log-normal distribution is utilized to describe the within weld variability exhibited by the data generated in MRP-115 (see Figure B-9).

Because there is a physical upper limit to the rate at which PWSCC crack propagation can proceed, an upper truncation limit is applied when sampling the weld-to-weld or within-weld factors. These factors are bound by the higher of two quantities: the 95th percentile of the respective distribution or the maximum factor exhibited by the data. The lower bound is imposed

in a similar manner, using the 5th percentile of the distribution or the minimum factor exhibited by the data.

Note that the product of the upper truncation limits for the two weld variability factors prescribes the maximum flaw propagation rate that can be applied. That maximum flaw propagation rate is assured to be greater than the maximum flaw propagation rate actually observed in any of the laboratory tests under analogous conditions.

Alloy 600 (Used for Alloy 690)

Similar to the way growth uncertainty is accounted for in the weld material, the uncertainty of flaw propagation in Alloy 600 data is characterized by heat-to-heat and within-heat parameters.

The heat-to-heat parameter (f_{heat}) is a common factor applied to all specimens fabricated from the same raw material to account for the effects of manufacturing variation. For this study, a log-normal distribution is fit to the heat factors for 26 laboratory heat specimens assessed in MRP-55 (see Figure B-10).

The within-heat factor (f_{wh}) describes the variability in flaw propagation rate for cracks in the same raw material (heat). The within-heat factor distribution describes the scatter in the flaw propagation rate data that remains after all model effects are accounted for and the weld-to-weld variation is reconciled. A log-normal distribution has been developed to describe the variability in the within-heat factor for the data presented in MRP-55. For this study, a log-normal distribution is fit to the heat factors for 140 laboratory crack specimens assessed in MRP-55 (see Figure B-11).

The lower and upper bounds for the Alloy 600 growth variability factors are set in the same manner as described for Alloy 82/182 growth variation factors.

In addition to the heat-to-heat and within-heat variation terms, other forms of uncertainty are incorporated for the growth of circumferential through-wall cracks, as discussed in the modeling section. First, a multiplicative factor is used to scale the FEA-derived *K* curves; a triangular distribution with a minimum and mode of 1 and a maximum of 2 is used. This results in a modestly increased *K* curve to account for any non-conservative bias in the FEA results.

Second, an environmental factor is used to scale the growth rate for circumferential flaws growing along the J-groove weld; again, a triangular distribution with a minimum and mode of 1 and a maximum of 2 is used. Based on the consensus of the international PWSCC expert panel convened by EPRI in 2001-2002, the crack growth rate for flaws connected to the OD annulus environment is most likely not significantly accelerated by chemical concentration effects. However, as documented in MRP-55 [29], the expert panel conservatively recommended an environmental factor of 2 for deterministic calculations of growth of circumferential flaws in contact with the annulus environment. The triangular distribution described above was selected based on this work.

B.2.3.3 Uncertainty in Temperature Effect

The temperature dependence of the flaw propagation process is modeled using an Arrhenius relationship. A normal distribution is used to describe the uncertainty in the activation energy for PWSCC growth. A mean of 130 kJ/mole and a standard deviation of 5 kJ/mole are assumed

based on empirically estimated values reported by various investigators for the Alloy 600 wrought material.

A reference temperature of 617°F (325°C) is chosen for the crack growth model. The uncertainty in the activation energy accounts for the uncertainty in the temperature effect between 617°F and the operating temperature.

B.2.3.4 Correlation Between Flaw Initiation and Propagation

It is generally accepted by PWSCC experts [14] that components that are more susceptible to PWSCC flaw initiation than other components tend to have higher flaw propagation rates than those other components. The main challenge in correlating the time to initiation and the flaw propagation rate in a probabilistic PWSCC assessment is that there is a general lack of data with which to choose an appropriate correlation coefficient. In the absence of data to select an appropriate correlation coefficient, the correlation is only invoked for sensitivity cases; the correlation coefficient is set to zero for the base case analysis. It is noted that MRP-105 [6] assumed a correlation of -0.8 between flaw initiation and propagation for its case studies.

Table B-6
Summary of Crack Growth Submodel Inputs

Symbol	Description	Source	Units	Distrib. Parameter	Value for Base Case
Q_g	Thermal activation energy for PWSCC flaw propagation	Q values from MRP-115; stdev based on judgment as used in MRP-335R1	kJ/mole	type	Normal
				mean	130
				stdev	5
				min	100
				max	160
T	Component operating temperature	See general inputs table in this report			
f_{weld}	Weld factor: common factor applied to all specimens fabricated from the same weld to account for weld wire/stick heat processing and for weld fabrication	By definition, the median within weld factor is one; Distributions from fits shown in figures of this document	Nondim	type	Log-Normal
				linear μ	1.19
				log-norm μ	0.00
				log-norm σ	0.5892
				min	0.313
				max	2.64
f_{ww}	Within Weld factor: factor accounting for the variability in crack growth rate for different specimens fabricated from the same weld	By definition, the median within weld factor is one; Distributions from fits shown in figures of this document	Nondim	type	Log-Normal
				linear μ	1.12
				log-norm μ	0.00
				log-norm σ	0.4807
				min	0.309
				max	3.24
f_{heat}	Heat factor: common factor applied to all specimens fabricated from the same material to account for manufacturing variations	Fit to heat factors from MRP-55	Nondim	type	Log-Normal
				linear μ	1.68
				log-norm μ	0.00
				log-norm σ	1.016
				min	0.143
				max	5.32
f_{wh}	Within Heat factor: factor accounting for the variability in crack growth rate for different specimens fabricated from the same raw material	Fit to within-heat factors from MRP-55 after normalizing for heat factors	Nondim	type	Log-Normal
				linear μ	1.18
				log-norm μ	0.00
				log-norm σ	0.5695
				min	0.208
				max	3.68
$T_{ref,g}$	Absolute reference temperature to normalize PWSCC flaw propagation data	MRP-115	°F		617
Δt	Time step size for crack increment	See convergence analysis in this report	yr		1/4

Note:
Δt for Alloy 600 case and all cases with a FOI of 1 is 1/12 years.

Table B-6
Summary of Crack Growth Submodel Inputs (Continued)

Symbol	Description	Source	Units	Distrib. Parameter	Value for Base Case
ρ_{weld}	Correlation coefficient for PWSCC initiation and propagation of all cracks in Alloy 182/82 weld	No basis for selection of non-zero base case value	Nondim		0.0
ρ_{heat}	Correlation coefficient for PWSCC initiation and propagation of all cracks in Alloy 600	No basis for selection of non-zero base case value	Nondim		0.0
α_{weld}	Flaw propagation rate equation power law constant for Alloy 182/82 weld	MRP-115, as reported in Table F-2 of MRP-263	$(m/s)/(MPa\text{-}m^{0.5})^{1.6}$		9.82E-13
b_{weld}	Flaw propagation rate equation power law exponent for Alloy 182/82 weld	Best fit per MRP-115	Nondim		1.6
$K_{ith,weld}$	Stress intensity factor threshold for Alloy 182/82	MRP-115	$MPa\text{-}m^{0.5}$		0.0
α_{heat}	Flaw propagation rate equation power law constant for Alloy 600	Derived from MRP-55 data with power law constant of 1.6 and stress intensity factor threshold of 0	$(m/s)/(MPa\text{-}m^{0.5})^{1.6}$		1.97E-13
b_{heat}	Flaw propagation rate equation power law exponent for Alloy 600	Derived to MRP-55 data with stress intensity factor threshold of 0	Nondim		1.6
$K_{ith,heat}$	Stress intensity factor threshold for Alloy 600	Assumed threshold such that all cracks in tensile field have positive growth	$MPa\text{-}m^{0.5}$		0.0
$K_{circ,mult}$	Circumferential through-wall crack K curve multiplier	Assumed to assure conservative application of FEA-predicted K curves	Nondim	type mode min max	Triangular 1.0 1.0 2.0
$c_{circ,mult}$	Circumferential through-wall crack environmental factor	Based on anecdotal information about environment effects on circumferential through-wall cracks	Nondim	type mode min max	Triangular 1.0 1.0 2.0
K_{90}	Stress intensity factor at deepest point on crack front	SIF model	$MPa\text{-}m^{0.5}$		calculated by SIF models
K_0	Stress intensity factor at surface point on crack front	SIF model	$MPa\text{-}m^{0.5}$		calculated by SIF models

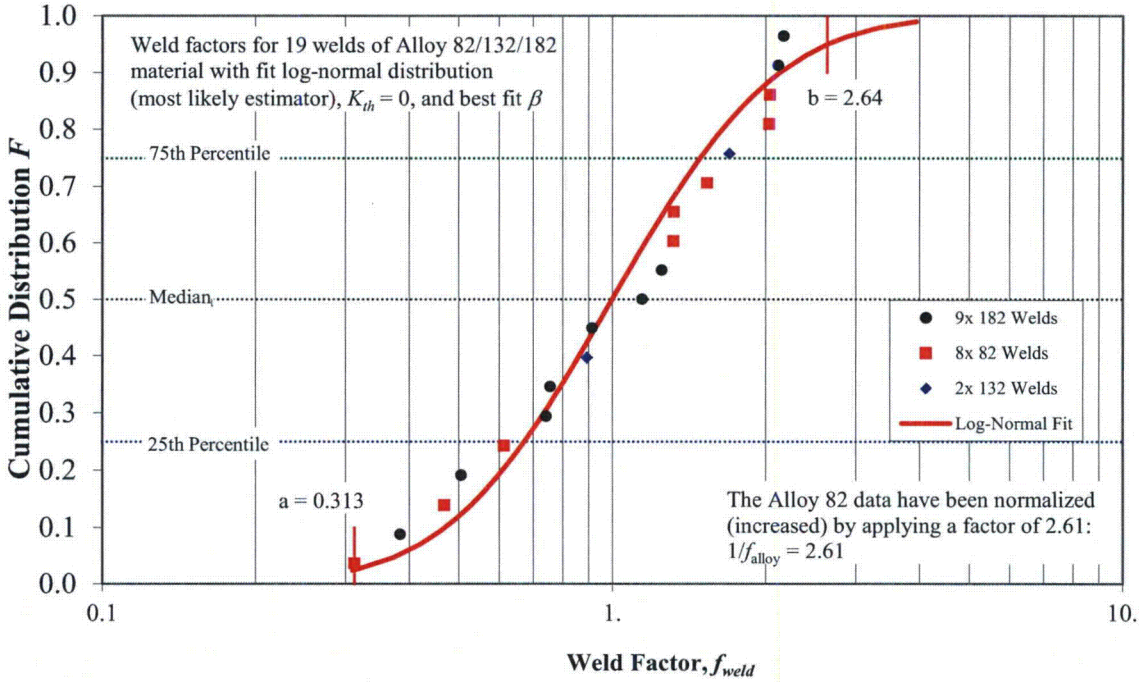

Figure B-8
MRP-115 Weld Factor f_{weld} Distribution with Log-Normal Fit for Alloys 82/182/132 [14]

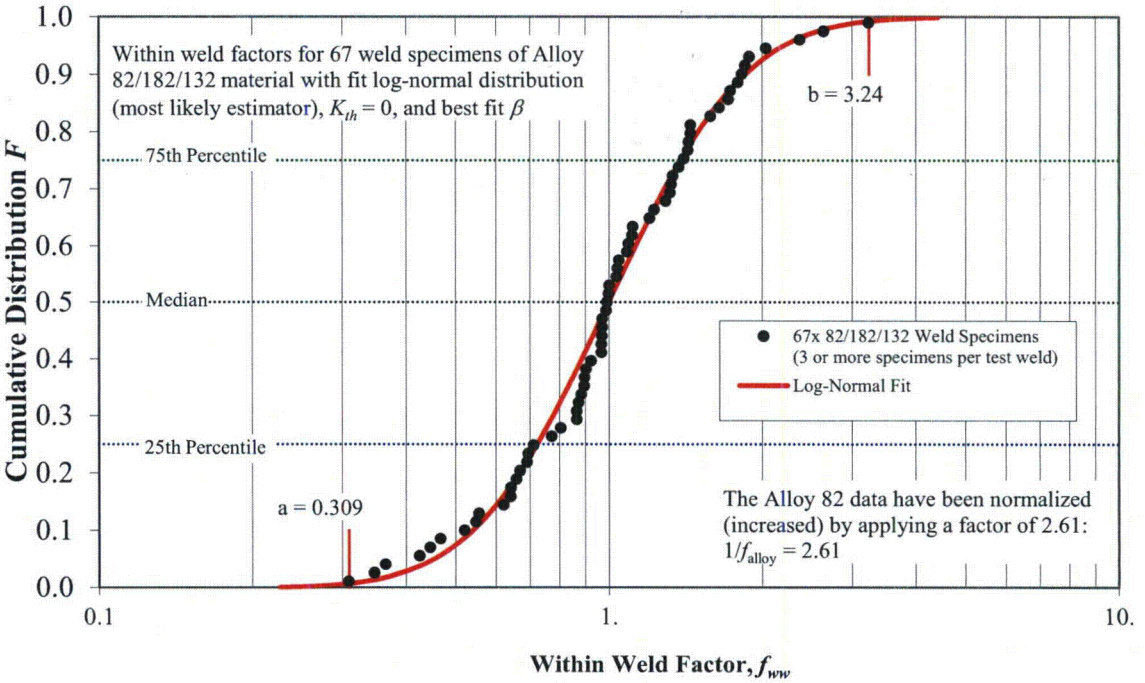

Figure B-9
MRP-115 Within Weld Factor f_{ww} Distribution with Log-Normal Fit for Alloys 82/182/132 [40]

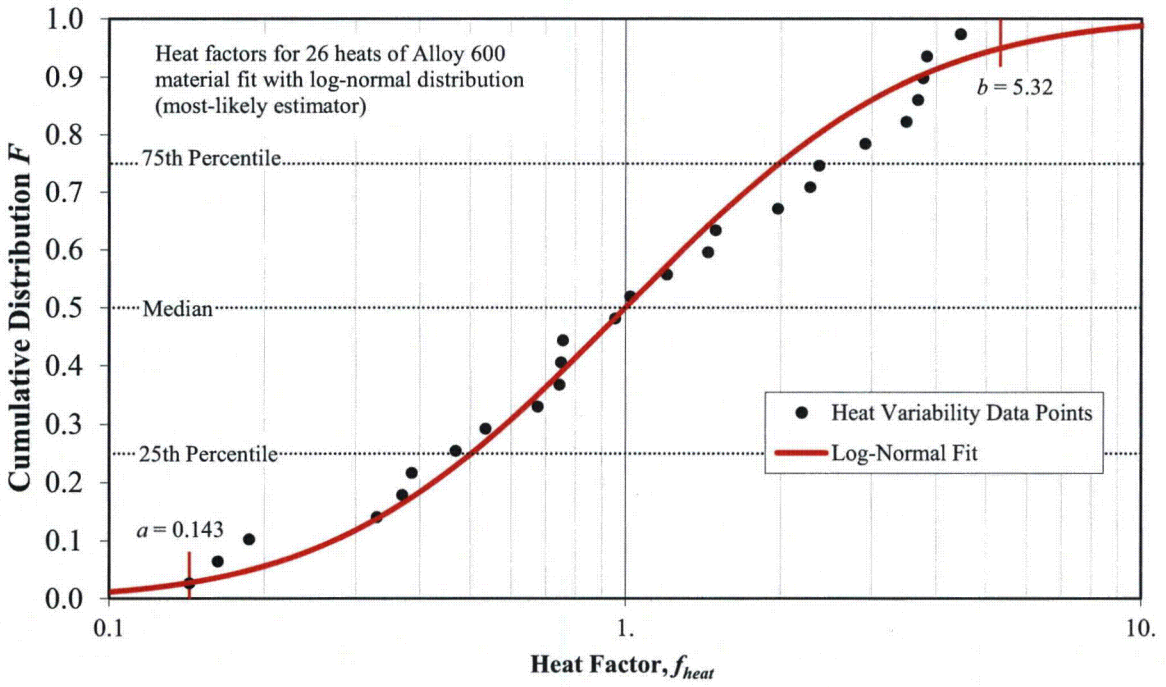

Figure B-10
Heat Factor f_{heat} Distribution with Log-Normal Fit for MRP-55 Alloy 600 Data [30]

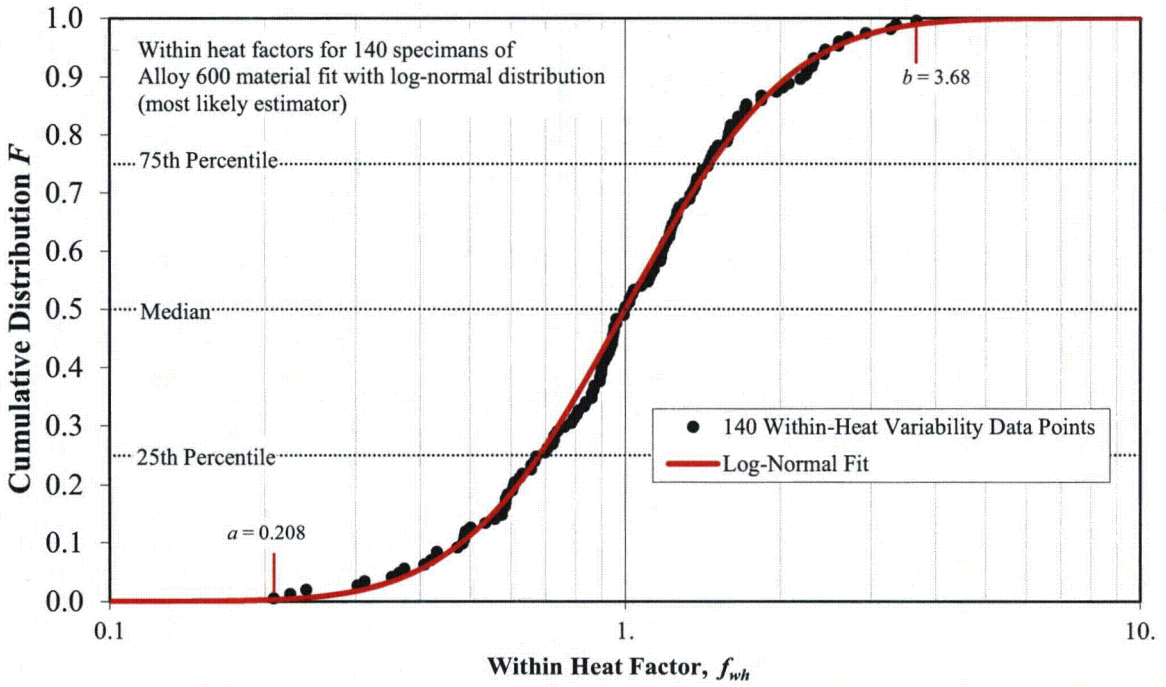

Figure B-11
Within-Heat Factor f_{wh} Distribution with Log-Normal Fit for MRP-55 Alloy 600 Data [30]

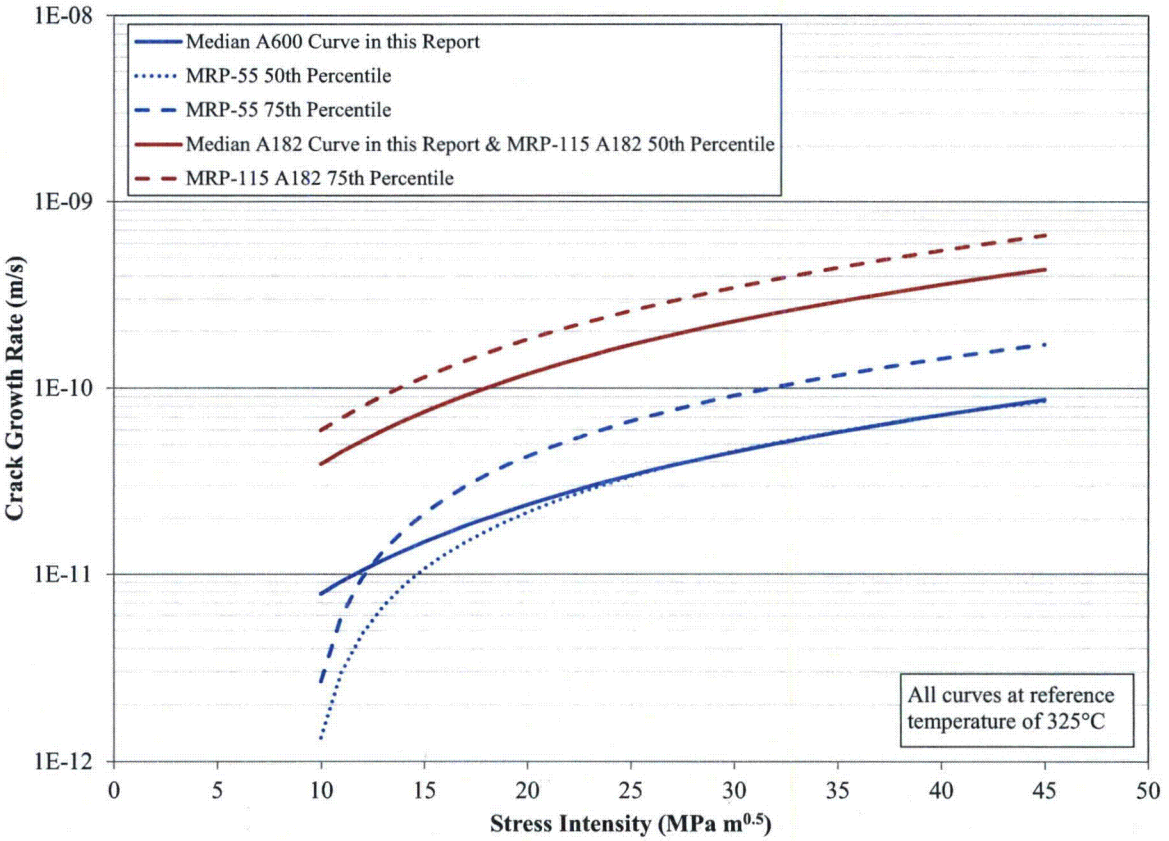

Figure B-12
Comparison of Stress Intensity Factor Dependence of CGR Models Against MRP-55 and MRP-115

B.2.4 Flaw Inspection, Detection, and Stability Submodel

The sets of inputs for the flaw examination and stability models are described in Table B-7, Table B-8, and Table B-9. Various inputs are detailed in the following subsections.

B.2.4.1 Examination Scheduling

Various UT and BMV inspection scheduling intervals are examined to determine the relative risk of extending inspection intervals for Alloy 690. Table B-7 describes the different UT and BMV inspection intervals investigated for Alloy 690 RPVHs in this work. These inspection intervals are variations on the intervals specified in Code Case N-729-1 [3] for Alloy 690 RPVHPNs. Note that each unique case in this report is assigned a two character identifier with the first character (letter) identifying the inspection interval (per Table B-7) and the second character (number) identifying the assumed FOIs.

The UT inspection cases considered for Alloy 690 include the current N-729-1 required interval (inspection schedule A), a moderately extended UT interval to 20 years (inspection schedules B and C), and an extension of the UT interval to beyond the 40-year service period of the top head (inspection schedule D).

For all but one Alloy 690 inspection case, BMV inspection intervals are in accordance with the N-729-1 frequency of the lesser of every third RFO or every 5 calendar years (i.e., every two cycles for the assumed 24-month refueling cycle). The other Alloy 690 inspection case (inspection schedule C) uses a BMV inspection interval of every 10 calendar years to better understand the importance of this inspection requirement.

The benchmark Alloy 600 case uses inspection intervals in accordance with Code Case N-729-1 for a newly replaced head. The UT inspection interval is once every RFO while BMV inspection interval is dependent on the cumulative service period for the top head—the frequency of BMV inspections for the first 8 EDY is the lesser of every third RFO or every 5 calendar years, and once every cycle thereafter. Code Case N-729-1 requires tighter inspection intervals after detection of certain flaws; however, because all flaws are repaired upon detection in the framework developed for this report, this provision is not included.

B.2.4.2 UT Probability of Detection

The probabilistic UT POD model is described by Equation [A-10] and [A-11]. The model is generated from upper and lower POD curves which each represent a two standard deviation offset from the mean POD curve. The upper bound (favorable) curve was chosen such that there is an 80% POD for cracks 20% through-wall and a 95% POD for cracks 40% through-wall. The lower bound (unfavorable) curve was chosen such that there is a 65% POD for cracks 40% through-wall and a 90% POD for cracks 70% through-wall. Finally, a maximum POD of 95% is used to account for human/equipment error or other factors. The lower, upper, and mean POD curves are shown in Figure B-13.

This curve is based in part on 10 CFR 50.55a(g)(6)(ii)(D), which requires an 80% flaw detection rate on mockup test blocks for qualification testing of UT procedures and personnel used to inspect RPVHPNs. Under the assumption that the test crack sizes are uniformly distributed between 10% and 90%, the mean curve given in Figure B-13 would give a 78% success rate, slightly below a worst-case qualified UT detection process.

A correlation coefficient relating the results of successive inspections can be included to simulate an increasing likelihood of non-detection for a crack that has already been missed in a previous inspection. Because this value has not been experimentally determined, a modest correlation coefficient of 0.5 is used for base cases.

B.2.4.3 BMV Probability of Detection

The BMV inspection model employs a constant POD, irrespective of leak rate or the duration of leakage. A value of 90% is used based on engineering judgment and is considered conservatively low based on plant experience that through-wall cracking of CRDM and CEDM nozzles is accompanied by boric acid deposits that are reliably detected during direct visual examinations of the intersection of the nozzle with the upper surface of the reactor pressure vessel top head [1].

A strong correlation coefficient, 0.95, is used to correlate successive inspections of the same leaking penetration. It can be shown numerically that this results in approximately a 21%, 17%, and 14% POD for a leaking nozzle at the first, second, and third inspections, respectively, following an original inspection in which a leaking nozzle was not detected.

B.2.4.4 Flaw Stability

The two key inputs to the flaw stability model presented in this report are the initial size of a circumferential through-wall crack and the critical crack length at which ejection is predicted to occur. Both are deterministic inputs and are presented in Table B-9.

Consistent with the precedent set in MRP-105 for Alloy 600 [6], circumferential through-wall cracks along the weld contour are assumed to initiate with a length equivalent to 30° around the weld contour. Together with the immediate transition to through-wall growth on the weld contour after leakage, this is expected to result in conservative estimates for the time to ejection following leakage.

The critical crack length for ejection, or net section collapse, is based on calculations presented in MRP-110 (Appendix D of Reference [1]). The result of these calculations repeated for Alloy 690, using ASME BPVC Section II-D material properties, varied by less than 1% from Alloy 600 results. As in MRP-110 and MRP-105, a length equivalent to 300° around the weld contour is used for all base case analyses in this report in order to bound the critical flaw angles projected for CRDM and CEDM nozzles under standard design pressure.

Table B-7
Summary of Inspection Scheduling Cases

Inspection Schedule Identifier	Description	Inspection Interval (No. of two year cycles)	
		UT	BMV
A600	A600 Hot Head per N-729-1[(1)]	1	1
A	A690 per N-729-1	5	2
B	A690, 20 yr UT	10	2
C	A690, 10 yr BMV & 20 yr UT	10	5
D	A690, No UT	20[(2)]	2

Notes:
1. BMV every 2 cycles for first 8 EDY per N-729-1.
2. No UT inspections occur for the duration of most "D" cases, but an inspection occurs after 40 years of operation (20 cycles) for the 60 year sensitivity case.

Table B-8
Summary of Probability of Detection Parameters

Symbol	Description	Source	Units	Distrib. Parameter	Value for Base Case
$(a/t_{U,1,UT}, p_{U,1,UT})$	First defined coordinate for favorable UT POD curve	Engineering judgment, NDE experts, literature	Nondim		(0.2,0.8)
$(a/t_{U,2,UT}, p_{U,2,UT})$	Second defined coordinate for favorable UT POD curve	Engineering judgment, NDE experts, literature	Nondim		(0.4,0.95)
$(a/t_{L,1,UT}, p_{L,1,UT})$	First defined coordinate for unfavorable UT POD curve	Engineering judgment, NDE experts, literature	Nondim		(0.4,0.65)
$(a/t_{L,2,UT}, p_{L,2,UT})$	Second defined coordinate for unfavorable UT POD curve	Engineering judgment, NDE experts, literature	Nondim		(0.7,0.9)
$p_{max,UT}$	Maximum probability of detection for UT inspection	Engineering judgment	Nondim		0.95
$\rho_{insp,UT}$	Correlation coefficient for successive UT inspections	Engineering judgment	Nondim		0.50
p_{BMV}	Probability of detection for visual inspection of leaking nozzle	Engineering judgment, NDE experts, literature	Nondim		0.90
$\rho_{insp,BMV}$	Correlation coefficient for successive BMV inspections	Engineering judgment	Nondim		0.95

Table B-9
Summary of Stability Parameters

Symbol	Description	Source[1]	Units	Distrib. Parameter	Value for Base Case
$\theta_{circ,init}$	Initial angle for circumferential through-wall cracks immediately following leaks	MRP-105	degrees		30
$\theta_{circ,crit}$	Critical flaw angle for nozzle ejection	MRP-110	degrees		300

Notes:
1. The critical flaw size for Alloy 600 and Alloy 690 components was evaluated by limit load analysis and shown to be within 1° using respective material property values from BPVC II-D.

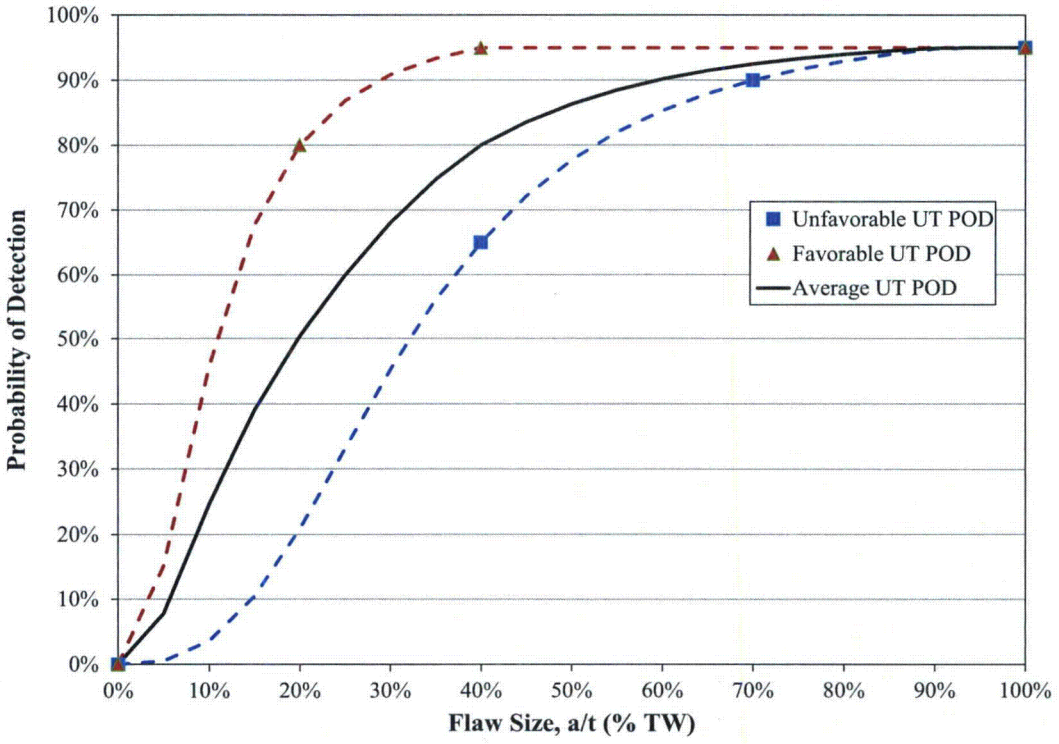

Figure B-13
Modeled POD Curves for Favorable, Unfavorable, and Mean Conditions

B.2.5 Factors of Improvement

A key facet of the probabilistic model is the adjustment of model predictions based on more comprehensive Alloy 600 data to achieve predictions for Alloy 690 based on a factor of improvement (FOI). Distinct FOIs are applied for predicting crack initiation times and growth rates; furthermore, distinct FOIs are applied at the different locations shown in Figure A-3, resulting in four distinct FOIs:

- The FOI for initiation in wrought Alloy 690 material compared to Alloy 600 material
- The FOI for initiation in Alloy 52/152 weld material compared to Alloy 182 material and Alloy 690 HAZ material compared to Alloy 600 material[24]
- The FOI for growth rates of cracks in wrought Alloy 690 material compared to that in Alloy 600 material
- The FOI for growth rates of cracks in Alloy 52/152 weld material compared to that in Alloy 182 material and growth rates of cracks Alloy 690 HAZ material compared to that in Alloy 600 material[24]

[24] The use of the same FOI for the Alloy 690 HAZ and weld material was a conservative modeling choice given the general concern for potentially elevated crack growth rates in the base metal HAZ in comparison to that for bulk Alloy 690 base metal.

In recognition of the uncertainty associated with FOI values, various FOI sets are applied for different cases in this study. Two primary sets of FOIs are considered in significant detail while other variations are included as comparative cases. The first primary set of FOIs uses 1 for initiation in all materials, 20 for growth in wrought Alloy 690 materials, and 10 for growth in Alloy 690 HAZ and Alloy 52/152 weld material (Case 4). The second primary set of FOIs uses 1 for initiation in all materials, 10 for growth in wrought Alloy 690 materials, and 5 for growth in Alloy 690 HAZ and Alloy 52/152 weld materials (Case 2). The conservative basis for the use of these FOIs is described in Section 3.

Table B-10 provides a full summary of the FOI inputs for the cases considered in B.3.2.3, each of which is assigned a number. Note that each unique case in this report is assigned a two character identifier with the first character (letter) identifying the inspection interval and the second character (number) identifying the FOI case (per Table B-10).

Table B-10
Summary of FOI Case Inputs

FOI Set Identifier	Description	Growth FOI		Initiation FOI	
		Wrought	Weld & HAZ	Wrought	Weld & HAZ
1 A600	Growth FOI 1[(1)] (Effectively A600 RPVHPN)	1	1	1	1
2	Growth FOI 10/5	10	5	1	1
3	Growth FOI 10/5 Initiation FOI 5/5	10	5	5	5
4	Growth FOI 20/10	20	10	1	1
5	Growth FOI 20/10 Initiation FOI 5/5	20	10	5	5
6	Growth FOI 100/10	100	10	1	1
7	Growth FOI 100/10 Initiation FOI 10/10	100	10	10	10

Notes:
1. Duration of time loop sub-cycle (Δt) is 1/12 year for this case.

B.2.6 Inputs for Model Sensitivity Cases

In addition to studies investigating different inspection intervals and different assumed FOIs, several other sensitivity cases are studied to understand the sensitivity of predicted leakage and nozzle ejection risks (and dependent conclusions) to less substantiated inputs or key model assumptions. Relevant cases presented in Section B.9.3 and Figure B-38 of MRP-335 Rev. 1 [30] that demonstrated a significant effect on the predicted risk are repeated in this report along with other studies predicted to cause significant differences.

Table B-11 provides a listing of the base case inputs compared with those of the sensitivity cases. The identifier for the model sensitivity cases consists of an "M" and a reference number. The sensitivity case identifiers are appended to the inspection schedule and FOI set identifier (e.g., B2-M3 is the third sensitivity case applied with inputs otherwise equivalent to the B2 base case).

Table B-11
Summary of Alloy 690 Sensitivity Case Inputs

Case Number	Description	Parameter	Units	Distrib. Parameter	Base Case Value	Sensitivity Case Value
M1	Increased Reactor Head Lifetime	Number of operating cycles	Nondim		20	30
M2	Reduced Operating Temperature	T Operating temperature	°F	type	Normal	Normal
				mean	613	600
				stdev	5	5
				min	583	570
				max	643	630
M3	Earlier Time to First Initiation	t_1 Time at which failure fraction F_1 is reached	EDY	type	Normal	Normal
				mean	0.827	0.1654
				min	0.405	0.081
				max	1.690	0.338
M4	More Rapid Acceleration of Multiple Initiations After First Initiation	β_{flaw} Weibull slope for PWSCC multiple flaw initiation	Nondim	type	Normal	Normal
				mean	2.0	3.0
				stdev	0.5	0.5
				min	1.0	1.0
				max	5.0	6.0
M5	Correlated Initiation and Growth	ρ_{weld} Correlation coefficient for PWSCC initiation and propagation of all cracks in weld material	Nondim		0.0	-0.8
		ρ_{heat} Correlation coefficient for PWSCC initiation and propagation of all cracks in nozzle material	Nondim		0.0	-0.8
M6	Decreased Maximum UT POD	$p_{max,UT}$ Maximum probability of detection for UT inspection	Nondim		0.95	0.9
M7	Decreased Critical Flaw Size	$\theta_{circ,crit}$ Critical flaw angle for nozzle ejection	degrees		300	275
M8	MRP-55 Crack Growth Rate Model Parameters	$K_{ith,heat}$ K_I Stress intensity factor threshold for Alloy 600	MPa-$m^{0.5}$		0.0	9.0
		α_{heat} Flaw propagation rate equation power law constant for Alloy 600	(m/s)/ (MPa-$m^{0.5}$)$^{1.6}$		1.97E-13	1.34E-12
		b_{heat} Flaw propagation rate equation power law exponent for Alloy 600	Nondim		1.6	1.16

B.2.7 Inputs for Benchmarking Cases

The probabilistic RPVH model published in MRP-105 [6] in 2004 is a key part of the technical basis for the current set of inspection requirements for RPVHs with Alloy 600 nozzles. Thus, a benchmarking exercise was performed comparing the model developed for this study of RPVHs with Alloy 690 nozzles versus the model published in MRP-105. The benchmarking exercise provides continuity between the MRP-105 technical basis and the present study, and provides a measure of validation of the current model.

In order to confirm that the two models produced similar results for similar inputs, the benchmarking cases are chosen to correlate as closely as possible to the values in MRP-105. The cases chosen are Case 11 and Case 19 in Table 8-1 of MRP-105, which correspond to heads operating at 600°F and 580°F (316°C and 304°C), respectively, and inspected by UT roughly every 4 EDY. The key inputs common to the models were matched:

- The scheduling of inspections in EFPY
- Operating and reference temperatures for the model
- Basic nozzle dimensions
- Initiation Weibull parameters (head initiation model)
- Correlation between distributed parameters for initiation and growth submodels
- UT probability of detection

  Per the practice of MRP-105, the probability of detection for successive UT inspections was treated independently (i.e., zero correlation of the POD for successive examinations of the same flaw). In addition, the UT POD curve in Figure B-13 is scaled by 80% to simulate the incomplete inspection coverage modeled in MRP-105.

- Stress intensity factor and crack growth rate for circumferential through-wall cracking

  The bounding uphill and downhill SIF values for the MRP-105 cases are used. These are found in Figures 3-12 and 3-13 of MRP-105. In addition, the factor to account for the possibility of higher stress intensity factors was not applied (i.e., it was set to one), and the factor accounting for the possibility of increased crack growth rate due to concentration of primary water in the nozzle annulus was not applied (i.e., it was also set to one). In the base case runs of this study, these factors result in increased rates of growth of the through-wall circumferential flaws assumed to be produced immediately after leakage occurs.

In addition to the items above, all FOIs are set to one to model the behavior of Alloys 600/82/182. The inputs to these cases that differ from the Alloy 600 base case are shown in Table B-12. Some component loading, initiation, growth, and examination submodels and inputs differ between the benchmarking cases in this report and the cases in MRP-105. These differences arise from systematic differences in the detailed modeling approaches of the two reports and are discussed along with the results in Section B.3.3.3.

Table B-12
Summary of Inputs Representing MRP-105 [6] Benchmarking Cases

Parameter	Units	Distrib. Parameter	Alloy 600 Base Case Value	MRP-105 Case 11 / 19
Number of realizations	Nondim		1.0E+06	1.0E+06
CF Plant capacity factor	Nondim		0.92	1.00
Cycle duration	Years		2.0	2.0 / 1.5
Number of cycles	Nondim		20	15 / 26
i1st Cycle of first UT inspection	Nondim		1	6 / 18
icyc UT inspection interval	Nondim		1	2/6
icycBMV BMV inspection interval	Nondim		1 after 8 EDY	No BMV
T Operating temperature	°F	type	Normal	Normal
		mean	613	600 / 580
		stdev	5	5
		min	583	570 / 550
		max	643	630 / 610
N_{pen} Number of Penetrations	Nondim		89	69
t Nozzle thickness	m		0.0158	0.0157
OD Nozzle outer diameter	m		0.1016	0.1016
t_{head} Reactor head thickness	m		0.152	0.168
Incidence angles for penetrations	degrees	type	discrete list	discrete list
		average	34.1	28.8
		min	0.0	0.0
		max	56.1	43.0
σ_c Standard error in intercept of linearized Weibull fit	ln(EDY)		0.166	See t_1
t_1 Time at which failure fraction F_1 is reached on RPVPNs	EDY	type	Normal	Triangular
		mean (mode)	0.827	(3.550)
		stdev	see σ_c	-
		min	0.405	2.546
		max	1.690	4.953

Table B-12
Summary of Inputs Representing MRP-105 [6] Benchmarking Cases (Continued)

Parameter	Units	Distrib. Parameter	Alloy 600 Base Case Value	MRP-105 Case 11
β Weibull slope for PWSCC flaw initiation	Nondim	type	Normal	Constant
		mean	1.393	3.0
		stdev	0.078	
		min	0.924	
		max	1.862	
Q_i Activation Energy for Initiation	kJ/mole	type	Normal	Constant
		mean	184.23	209
		stdev	12.82	
		min	107.32	
		max	261.13	
ρ_{weld} Correlation coefficient for PWSCC initiation and propagation of all cracks in Alloy 182/82 weld	Nondim		0.00	-0.80
ρ_{heat} Correlation coefficient for PWSCC initiation and propagation of all cracks in Alloy 600	Nondim		0.00	-0.80
a_0 Initial depth assigned to newly initiated flaw	m	type	Log-Normal	Normal
		linear μ	8.44E-04	5.00E-03
		linear σ	-	1.30E-04
		log-norm μ	-7.14	-
		log-norm σ	0.35	-
		min	5.00E-04	5.00E-04
		max	0.0158	0.0158
$K_{circ,mult}$ Circumferential through-wall crack K curve multiplier	Nondim	type	Triangular	Constant
		mode	1.0	1.0
		min	1.0	
		max	2.0	
$c_{circ,mult}$ Circumferential through-wall crack environmental factor	Nondim	type	Triangular	Constant
		mode	1.0	1.0
		min	1.0	
		max	2.0	

Table B-12
Summary of Inputs Representing MRP-105 [6] Benchmarking Cases (Continued)

Parameter	Units	Distrib. Parameter	Alloy 600 Base Case Value	MRP-105 Case 11
$p_{max,UT}$ Maximum probability of detection for UT inspection	Nondim		0.95	0.76
$\rho_{insp,UT}$ Correlation coefficient for successive UT inspections	Nondim		0.50	0.00
Defined coordinates for favorable UT POD curve	Nondim	$(a/t_{H,1,UT}, p_{H,1,UT})$	(0.2,0.80)	(0.2,0.64)
	Nondim	$(a/t_{H,2,UT}, p_{H,2,UT})$	(0.4,0.95)	(0.4,0.76)
Defined coordinates for unfavorable UT POD curve	Nondim	$(a/t_{L,1,UT}, p_{L,1,UT})$	(0.4,0.65)	(0.4,0.52)
	Nondim	$(a/t_{L,2,UT}, p_{L,2,UT})$	(0.7,0.90)	(0.7,0.72)

B.3 Probabilistic Model Results

This section presents the results generated by the probabilistic model introduced in Appendix A using inputs specified in Section B.2. This section is organized as follows:

- Section B.3.1 provides a results overview.
- Section B.3.2 provides detailed comparisons of predictions for Alloy 600 and Alloy 690 RPVHs; cases with varying inspection schedules; and case with varied assumed FOIs.
- Section B.3.3 provides model validation studies including sensitivity cases, convergence analysis, and benchmarking.

B.3.1 Overview of Results

B.3.1.1 Interpreting Results

First, the reader is directed to Section B.1, which catalogues the main model simplifications and assumptions in view of which all results should be interpreted. Other important considerations when interpreting results are given below.

Relative versus absolute comparison: Because various assumptions and simplifications are involved in the development of the integrated probabilistic model, the absolute magnitudes of predicted risks may include substantial biases. However, these biases are expected to be largely similar (in magnitude and direction) across cases. Accordingly, the more vital conclusions are drawn from the relative differences between risks predicted for different cases (e.g., between the

risks presented for a head with Alloy 600 RPVHPNs inspected per N-729-1 and a head with Alloy 690 RPVHPNs inspected under a modified inspection interval).

Convergence and precision of results: Ejection frequencies for certain cases are below the statistical convergence achieved with Monte Carlo simulation, i.e., the number of Monte Carlo realizations in some cases is not sufficient to provide precision within the absolute value of the predicted frequency. To help stabilize results and to provide added conservatism, cycles for which zero ejections are predicted across all Monte Carlo realizations (i.e., null results) are replaced with a total of 0.5 ejections. To further help assess convergence of results, ejection versus time plots generally include annotation to indicate a frequency below which results are not well-converged.[25] Finally, convergence analyses of Section B.3.3.2 may be consulted to better understand the precision of results.

Time-varying risks: It is important to consider the time-varying characteristics of risks, in addition to the time-averaged risks, in order to understand how concentrated the risk may be over particular spans of time and if there are particular cycles with considerably higher risk. Averaged statistics such as AEF do not provide information about risk concentrations or trends, e.g., increasing rates of leakage or ejection between initial start-up and first inspections due to some physically limiting incubation period for PWSCC initiation and growth. To address this, plots demonstrating ILF or IEF versus time are generally provided throughout this results section; furthermore, maximum incremental risks are reported in the summarized results in the next subsection.

Per head versus per penetration risks: Unless otherwise specified, the results presented in this appendix are given on a penetration frequency per head basis. That is events are counted for each independently simulated penetration. This is contrasted with a head frequency basis where only the first leaking penetration and the first ejected nozzle are counted for each head.

Case naming conventions: Each case presented in this section is assigned a two character identifier with the first character, a letter, identifying the inspection interval from Table B-7 and the second character, a number, identifying the FOI case from Table B-10. Table B-13 provides a matrix denoting the combinations of inspection schedule and FOIs that are represented by cases in this appendix.

A numeric code appended to the case numbers described above indicates sensitivity test cases, convergence tests, and benchmarking tests:

- For sensitivity test cases that vary model parameters other than inspection timing and FOIs, a second code of the form "M#" is appended, where the numeric value for "#" is defined in Table B-11.
- For numerical integration convergence tests, a second code of the form "N#" is appended, where the numeric value for "#" quantifies the number of integration time steps per year used to simulate PWSCC growth and crack transitioning.

[25] Given the extremely rare instances of multiple ejections on the same head, the frequency of ejection statistic can be thought of as a Bernoulli random variable with a very low probability of occurrence that is estimated via Monte Carlo simulation. The convergence of the Monte Carlo estimate is therefore assessed with the central limit theorem applied to the binomial distribution. Based on this approximation, at least 10 instances of ejection are required to give reasonable convergence (±30% relative standard error).

- For Monte Carlo convergence tests, a second code of the form "P#" is appended, where the numeric value for "#" quantifies the number of independent runs of the Monte Carlo simulation that are used to develop convergence statistics.
- For benchmarking tests, a second code of the form "Q#" is appended, where the numeral for "#" quantifies the case number in MRP-105 against which benchmarking is performed.

Furthermore, to simplify presentation of the results in this section without having to refer back to Table B-10 frequently, a naming convention for distinguishing FOIs is used:

$$\text{FOI Identifer} = \text{g}\left(FOI_{wrought}\right)/\left(FOI_{HAZ\&weld}\right)\,\text{i}\left(FOI_{wrought}\right)/\left(FOI_{HAZ\&weld}\right)$$

where *g* indicates growth FOIs and *i* indicates initiation FOIs. $FOI_{wrought}$ is applied to the wrought nozzle material (with respect to the Alloy 600 predictions), and $FOI_{HAZ\&weld}$ is applied to the HAZ nozzle material (with respect to the Alloy 600 predictions) and the weld material (with respect to the Alloy 182 predictions). For example, g10/5 i2/1 indicates a growth FOI of 10 on the wrought material and of 5 on the HAZ and weld material with an initiation FOI of 2 on the wrought material and of 1 on the HAZ and weld material.

Table B-13
Matrix of Cases Presented in this Appendix (See Table B-7 and Table B-10 for the Meaning of Case Identifiers)

Inspection Schedule Identifier	FOI Set Identifier						
Case Number	A600 1	2	3	4	5	6	7
A600 (N-729-1)	X						
A		X		X			
B	X	X	X	X	X	X	X
C		X		X			
D	X	X	X	X	X	X	X

Note: Solid fill indicates base cases from which all other cases are derived.

B.3.1.2 Full Set of Results

Table B-14 presents the results for all the cases described in this report. It includes the base cases, FOI variation cases, inspection variation cases, and model validation cases. The benchmarking case results are included but are intended only for comparison with MRP-105 results.

Figure B-14 presents the first Alloy 690 base case (B2) and its associated variations; results are presented as AEFs standardized to reflect their variation relative to the base case. Similarly, Figure B-15 presents the second Alloy 690 base case (D4) and its associated variations. Across all cases, the cases with the greatest average risks of nozzle ejection reflect an Alloy 600 hot head with an inspection interval of two RFOs for BMV and ten or more RFOs for UT (in contrast with essentially every RFO for an Alloy 600 hot head per N-729-1).

The subsequent subsections further analyze these results.

Table B-14
Summary of All Case Results

	FOI on Wrought/Weld&HAZ		Inspection Interval (2 yr cycles)			Statistics			
Case ID	Growth	Initiation	BMV	UT	Other	AEF	ALF	Max IEF	Max ILF
A600	1/1	1/1	1	1		5.13E-05	2.00E-01	7.10E-05	2.29E-01
B2	10/5	1/1	2	10		6.24E-06	1.96E-01	4.39E-05	3.32E-01
D4	20/10	1/1	2	20		3.07E-06	1.46E-01	1.99E-05	2.91E-01
B1	1/1	1/1	2	10		6.82E-03	3.63E-01	1.54E-02	4.82E-01
B3	10/5	5/5	2	10		7.05E-07	2.69E-02	5.30E-06	5.14E-02
B4	20/10	1/1	2	10		1.00E-07	1.23E-01	4.00E-07	2.57E-01
B5	20/10	5/5	2	10		5.25E-08	1.63E-02	1.00E-07	3.70E-02
B6	100/10	1/1	2	10		5.00E-08	1.25E-01	5.00E-08	2.52E-01
B7	100/10	10/10	2	10		5.00E-08	6.54E-03	5.00E-08	1.44E-02
D1	1/1	1/1	2	20		1.17E-02	4.01E-01	2.12E-02	4.97E-01
D2	10/5	1/1	2	20		1.01E-04	2.25E-01	4.25E-04	3.62E-01
D3	10/5	5/5	2	20		1.20E-05	3.02E-02	5.26E-05	5.50E-02
D5	20/10	5/5	2	20		3.38E-07	1.90E-02	2.10E-06	4.13E-02
D6	100/10	1/1	2	20		5.00E-08	1.39E-01	5.00E-08	2.74E-01
D7	100/10	10/10	2	20		5.00E-08	7.10E-03	5.00E-08	1.53E-02
A2	10/5	1/1	2	5		2.68E-07	1.69E-01	1.40E-06	2.71E-01
A4	20/10	1/1	2	5		5.00E-08	1.05E-01	5.00E-08	2.10E-01
C2	10/5	1/1	5	10		1.18E-05	1.96E-01	8.41E-05	3.32E-01
C4	20/10	1/1	5	10		9.00E-08	1.23E-01	6.00E-07	2.57E-01
A600-M1	1/1	1/1	1	1	Extended simulation time to 60 years	5.02E-05	1.97E-01	6.70E-05	2.30E-01
A600-M2	1/1	1/1	1	1	Mean Temperature of 600°F	6.80E-06	1.13E-01	1.65E-05	1.36E-01
A600-M3	1/1	1/1	1	1	Decreased Initiation Ref. Time Parameters	1.15E-04	6.66E-01	1.90E-04	1.13E+00
A600-M5	1/1	1/1	1	1	Correlated Initiation & Growth	1.46E-04	2.15E-01	3.72E-04	2.42E-01
B2-M1	10/5	1/1	2	10	Extended simulation time to 60 years	7.55E-06	2.20E-01	4.39E-05	3.32E-01
B2-M2	10/5	1/1	2	10	Mean Temperature of 600°F	6.00E-07	9.50E-02	4.50E-06	1.84E-01
B2-M3	10/5	1/1	2	10	Decreased Initiation Ref. Time Parameters	3.30E-05	8.51E-01	1.91E-04	1.38E+00
B2-M4	10/5	1/1	2	10	Increased Multiple Flaw Initiation Slope	1.75E-05	4.18E-01	1.23E-04	6.77E-01
B2-M5	10/5	1/1	2	10	Correlated Initiation & Growth	5.85E-05	2.35E-01	3.70E-04	3.45E-01
B2-M6	10/5	1/1	2	10	Decreased Max POD for UT	7.27E-06	1.96E-01	4.81E-05	3.32E-01
B2-M7	10/5	1/1	2	10	Decreased Critical Flaw Size	1.06E-05	1.96E-01	6.88E-05	3.32E-01
B2-M8	10/5	1/1	2	10	Use MRP-55 curve for Alloy 690, 50%tile	4.48E-06	1.95E-01	3.14E-05	3.29E-01
D4-M1	20/10	1/1	2	20	Extended simulation time to 60 years	2.31E-06	1.75E-01	2.24E-05	2.91E-01
D4-M2	20/10	1/1	2	20	Mean Temperature of 600°F	1.93E-07	6.13E-02	1.10E-06	1.43E-01
D4-M3	20/10	1/1	2	20	Decreased Initiation Ref. Time Parameters	2.63E-05	7.31E-01	1.59E-04	1.13E+00
D4-M4	20/10	1/1	2	20	Increased Multiple Flaw Initiation Slope	9.44E-06	3.30E-01	6.06E-05	6.30E-01
D4-M5	20/10	1/1	2	20	Correlated Initiation & Growth	5.23E-05	2.01E-01	2.78E-04	3.16E-01
D4-M6	20/10	1/1	2	20	Decreased Max POD for UT	3.17E-06	1.45E-01	2.12E-05	2.91E-01
D4-M7	20/10	1/1	2	20	Decreased Critical Flaw Size	5.35E-06	1.46E-01	3.34E-05	2.91E-01
D4-M8	20/10	1/1	2	20	Use MRP-55 curve for Alloy 690, 50%tile	2.25E-06	1.44E-01	1.46E-05	2.88E-01
B4-M6	20/10	1/1	2	10	Decreased Max POD for UT	9.50E-08	1.23E-01	6.00E-07	2.57E-01
B2-6BMV	10/5	1/1	3	10		7.64E-06	1.96E-01	5.56E-05	3.32E-01
D4-6BMV	20/10	1/1	3	20		3.95E-06	1.46E-01	2.64E-05	2.91E-01
A600-N24	1/1	1/1	1	1	24 time steps per year for crack growth	5.60E-05	2.02E-01	7.45E-05	2.32E-01
A600-N6	1/1	1/1	1	1	6 time steps per year for crack growth	4.26E-05	1.97E-01	5.80E-05	2.27E-01
B2-N12	10/5	1/1	2	10	12 time steps per year for crack growth	6.82E-06	1.98E-01	4.74E-05	3.33E-01
B2-N2	10/5	1/1	2	10	2 time steps per year for crack growth	5.71E-06	1.93E-01	4.41E-05	3.31E-01
B2-N8	10/5	1/1	2	10	8 time steps per year for crack growth	6.67E-06	1.97E-01	4.67E-05	3.32E-01
D4-N12	20/10	1/1	2	20	12 time steps per year for crack growth	3.31E-06	1.47E-01	2.00E-05	2.92E-01
D4-N2	20/10	1/1	2	20	2 time steps per year for crack growth	2.79E-06	1.43E-01	1.71E-05	2.90E-01
D4-N8	20/10	1/1	2	20	8 time steps per year for crack growth	3.31E-06	1.47E-01	2.24E-05	2.92E-01
A600-P10	1/1	1/1	1	1	Base case, mean over 10 runs	5.05E-05	2.00E-01	6.43E-05	2.30E-01
B2-P10	10/5	1/1	2	10	Base case, mean over 10 runs	6.33E-06	1.96E-01	4.37E-05	3.32E-01
D4-P10	20/10	1/1	2	20	Base case, mean over 10 runs	3.12E-06	1.46E-01	2.00E-05	2.91E-01

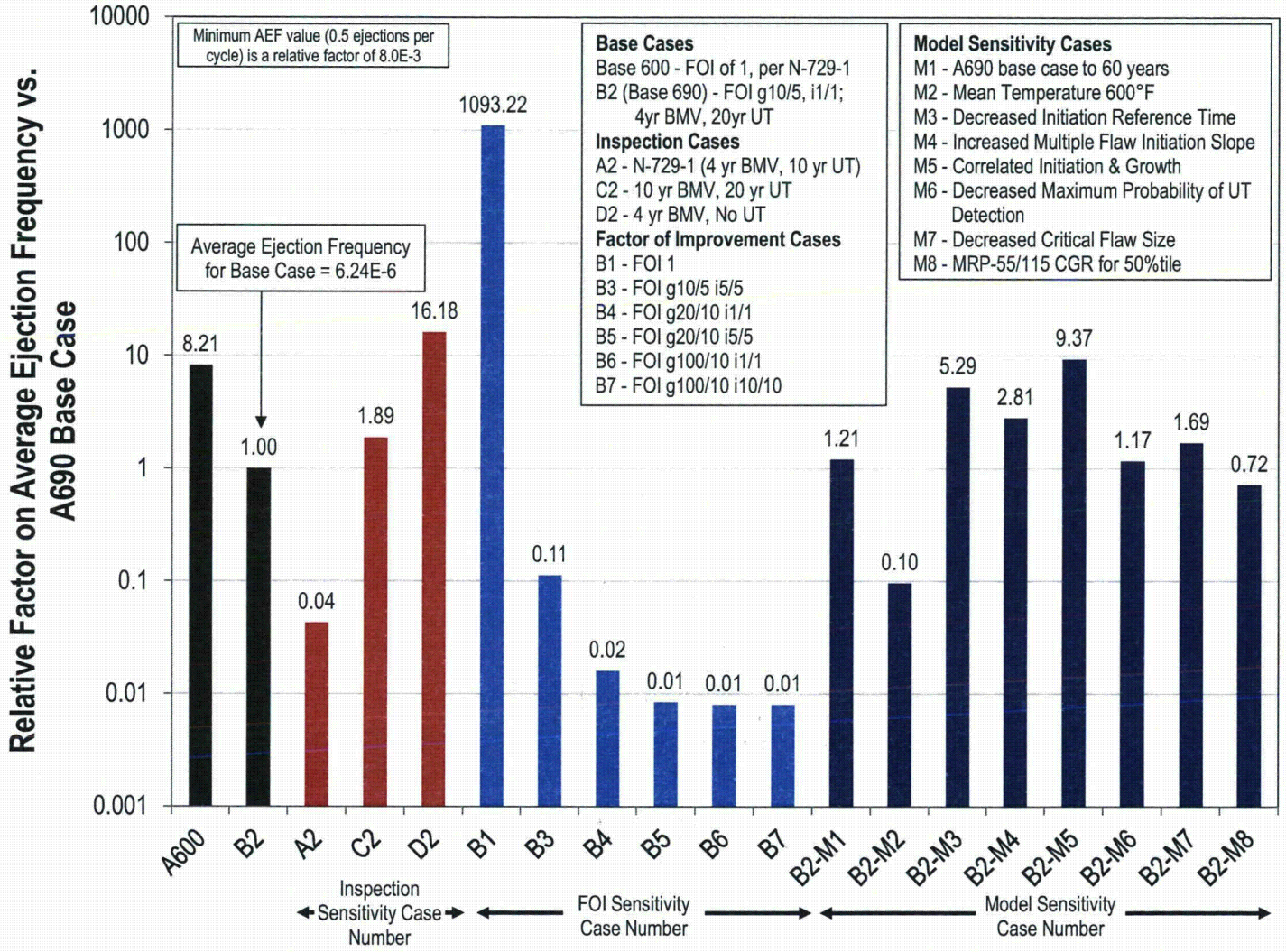

Figure B-14
Comparison of Cases Based on the Alloy 690 Case with a FOI Set of g10/5 and UT Inspections Every 10 Cycles (Presented as the Average Ejection Frequency Normalized by the Base Case)

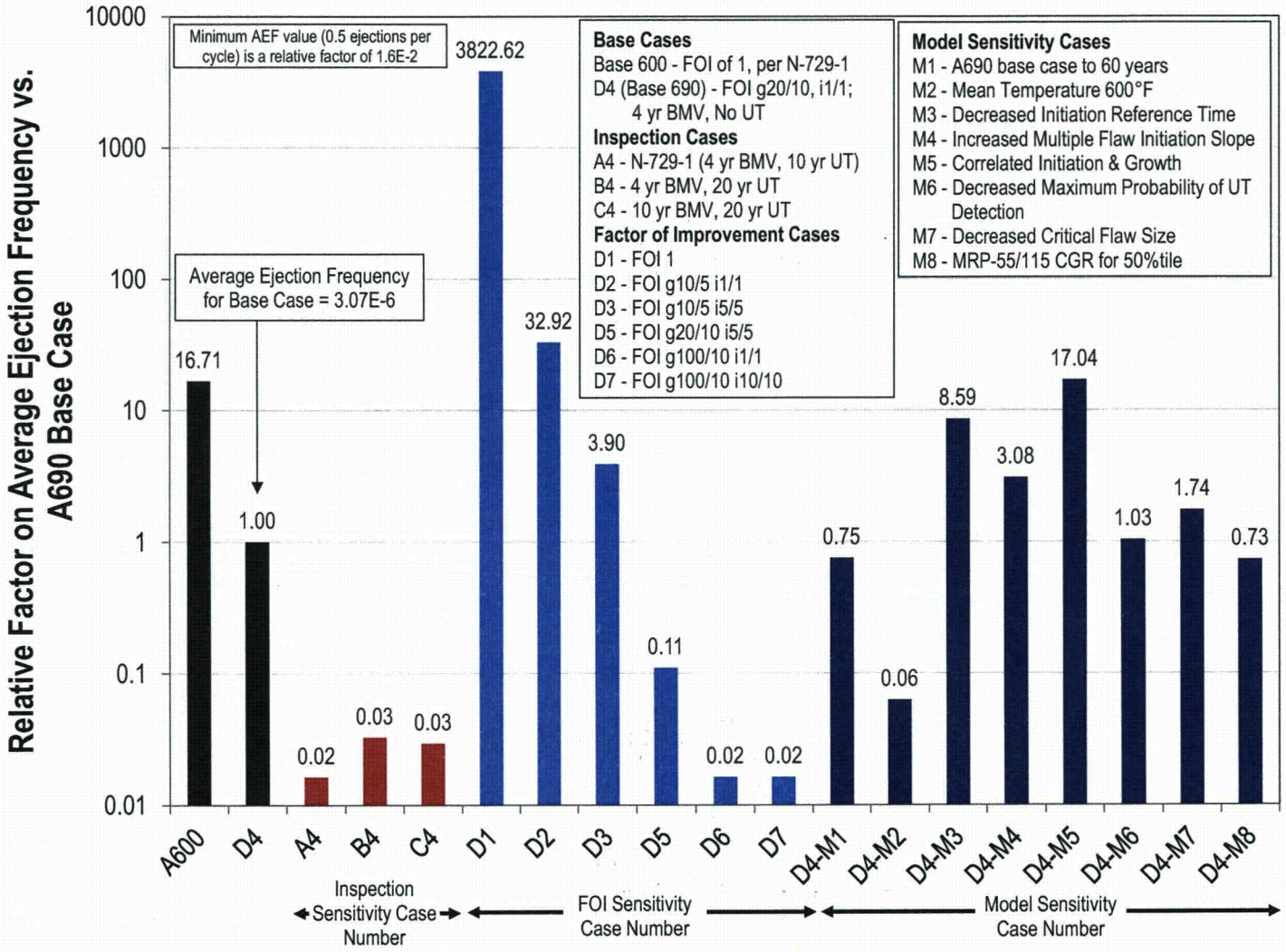

Figure B-15
Comparison of Cases Based on the Alloy 690 Case with a FOI Set of g20/10 and No UT Inspections Over 40 Years (Presented as the Average Ejection Frequency Normalized by the Base Case)

B.3.2 Main Results

This section presents detailed results for many of the cases summarized in the previous section. Section B.3.2.1 presents the two Alloy 690 base cases and contrasts their risk predictions against those of the Alloy 600 base case. The following subsections then examine the effect of changing the inspection intervals assumed for the base cases (Section B.3.2.2) and changing the FOI values assumed for the base cases (Section B.3.2.3).

B.3.2.1 Base Cases

Using the inputs specified in Sections B.2.1 through B.2.5, results were generated for the base cases of an Alloy 600 head inspected per N-729-1 and two Alloy 690 heads.

Comparisons of the IEF and ILF versus time for all three base cases over the expected RPVH service period (40 years; 36.8 EFPY) are provided in Figure B-16 and Figure B-17.[26]

Alloy 600/82/182 Base Case (Case A600)

The Alloy 600 base case is generated by setting all FOI values to 1 and performing inspections in accordance with N-729-1 for a head with penetration nozzles fabricated with Alloy 600/82/182.

Leakage predictions for the Alloy 600 base case indicate that the incremental likelihood of leakage increases rapidly over the first ten years of operation before essentially leveling out. The deceleration and eventual decline in the rate of leakage is believed to occur because the penetrations with the highest PWSCC susceptibility (i.e., earlier sampled initiation times; higher sampled growth rates) have already begun to leak or have been repaired.

As with leakage, the IEF remains level after about 10 years with the use of both BMV and UT inspections every outage.

The cumulative probability of having any nozzle ejections on a given head is predicted to be 1.9E-3 at the end of 40 years—an AEF of 5.1E-5 penetrations per year per head. This cumulative probability is consistent with the absence of any PWSCC-related ejection incidences in Alloy 600 PWR top heads to date. The cumulative probability of any leakage occurring on a given head is predicted to be 79%—an ALF of 0.20 new leaking penetrations per head per year. This result supports the conservative nature of the modeling assumptions made. A detailed assessment of top head Alloy 600 nozzle experience for U.S. PWRs [54] shows that there have been no reports of nozzle leakage for times subsequent to the time that all nozzles were first examined by non-visual NDE. In other words, all the cases of reports of top head nozzle leakage occurred prior to the time that the head was placed into a program of periodic in-service non-visual examinations of all nozzles.

Alloy 690/52/152 Base Case with Growth FOI of 10/5 and UT Interval of 20 years (Case B2)

The base case with a growth FOI of 10 on the wrought material and 5 on the weld and HAZ material (g10/5 i1/1) demonstrates, from a relative risk standpoint, that the higher resistance to PWSCC growth—although conservative in comparison to best estimates for FOIs based on most

[26] The low constant values of IEF for early operation in the Alloy 690 cases are artifacts of assuming a minimum of 0.5 ejections across all head realizations for each cycle and represent the minimum resolution of the ejection risk statistic.

laboratory studies (see Section 3)—supports extending the UT inspection interval to 20 years. Table B-15 presents the results of this base case and the variations thereof.

The cumulative probability of having any nozzle ejections on a given head is predicted to be 2.4E-4 at the end of 40 years—an AEF of 6.2E-6 penetrations per year per head. The cumulative probability of any leakage occurring on a given head is predicted to be 69% —an ALF of 0.20 new leaking penetrations per head per year. That is an AEF more than eight times lower than the Alloy 600 case and an ALF that is roughly equivalent.

At the time of UT inspection scheduled at 20 years (18.4 EFPY), there is a marked decline in the leakage frequency and a sharp decline in the ejection rate for the subsequent cycles penetration repairs. As predicted in Section B.3.2.3, lower maximum incremental frequencies are safely maintained with the 20 year UT inspection interval with the selection of initiation and growth FOIs that are more appropriate relative to laboratory data (see Case B5).

Alloy 690/52/152 Base Case with Growth FOI of 20/10 and UT Inspections in 40 Years (Case D4)

The base case with a growth FOI of 20 on the wrought material and 10 on the weld and HAZ material (g20/10 i1/1) demonstrates, from a relative risk standpoint, that the higher resistance to PWSCC growth—consistent if not conservative with respect to the average consensus across laboratory studies—support extending the UT inspection interval to 40 years. Table B-16 presents the results of this base case and the variations thereof.

The cumulative probability of having any nozzle ejections on a given head is predicted to be 1.1E-4 at the end of 40 years—an AEF of 3.1E-6 penetrations per year per head. The cumulative probability of any leakage occurring on a given head is predicted to be 56%—an ALF of 0.15 new leaking penetrations per head per year. That is an AEF that is a factor of almost 17 less than the Alloy 600 case and an ALF that is approximately 30% lower.

Comparing the two Alloy 690 base cases, the leakage frequency is not changed substantially by varying the inspection interval and growth FOI. This is believed to result from the assumptions that UT examinations do not detect part-depth flaws in the weld material and that flaws are equally likely to initiate at any nozzle location. Consequently, it is typical for more than 90% of leakage events to occur due to a flaw in the weld material growing to the weld root.

It is noted that the leakage predictions for Alloy 690 base cases are inconsistent with operational experience in which zero instances of leakage through Alloy 690 have occurred. In Section B.3.2.3, it is shown that taking credit for a moderate FOI on initiation significantly affects the leakage frequency to bring the probability of leakage into better agreement with current operating experience.

Table B-15
Summary of Results for Base Case with Growth FOI of g10/5 and UT Interval of 20 years

Case ID	FOI on Wrought / (Weld&HAZ)		Inspection Interval [years]		Other Variation	Average Yearly Frequency		Cumulative Probability of Any Ejection on a Head
	CGR	Initiation	BMV	UT		Leaking Penetrations (ALF)	Ejected Penetrations (AEF)	
A600	1/1	1/1	2	2		0.200	5.13E-05	1.95E-03
B2	10/5	1/1	4	20		0.196	6.24E-06	2.39E-04
A2	10/5	1/1	4	10		0.169	2.68E-07	9.60E-06
C2	10/5	1/1	10	20		0.196	1.18E-05	4.44E-04
D2	10/5	1/1	4	40		0.225	1.01E-04	3.00E-03
B1	1/1	1/1	4	20		0.363	6.82E-03	1.19E-01
B3	10/5	5/5	4	20		0.027	7.05E-07	2.72E-05
B4	20/10	1/1	4	20		0.123	1.00E-07	2.40E-06
B5	20/10	5/5	4	20		0.016	5.25E-08	2.00E-07
B6	100/10	1/1	4	20		0.125	5.00E-08	0.00E+00
B7	100/10	10/10	4	20		0.007	5.00E-08	0.00E+00
B2-M1	10/5	1/1	4	20	60 yr Service Life	0.220	7.55E-06	4.39E-04
B2-M2	10/5	1/1	4	20	600°F Mean Temp.	0.095	6.00E-07	2.24E-05
B2-M3	10/5	1/1	4	20	Decreased Initiation t_{ref}	0.851	3.30E-05	1.27E-03
B2-M4	10/5	1/1	4	20	Increased β_{flaw}	0.418	1.75E-05	6.68E-04
B2-M5	10/5	1/1	4	20	Correlated Init. & Growth	0.235	5.85E-05	2.08E-03
B2-M6	10/5	1/1	4	20	Decreased $POD_{max,UT}$	0.196	7.27E-06	2.80E-04
B2-M7	10/5	1/1	4	20	Decreased $\theta_{circ,crit}$	0.196	1.06E-05	4.01E-04
B2-M8	10/5	1/1	4	20	MRP-55 Curve	0.195	4.48E-06	1.74E-04

Table B-16
Summary of Results for Base Case with Growth FOI of 20/10 and No UT Inspections over 40 Years

Case ID	FOI on Wrought / (Weld&HAZ)		Inspection Interval [years]		Other Variation	Average Yearly Frequency		Cumulative Probability of Any Ejection on a Head
	CGR	Initiation	BMV	UT		Leaking Penetrations (ALF)	Ejected Penetrations (AEF)	
A600	1/1	1/1	2	2		0.200	5.13E-05	1.95E-03
D4	20/10	1/1	4	40		0.146	3.07E-06	1.14E-04
A4	20/10	1/1	4	10		0.105	5.00E-08	0.00E+00
B4	20/10	1/1	4	20		0.123	1.00E-07	2.40E-06
C4	20/10	1/1	10	20		0.123	9.00E-08	2.00E-06
D1	1/1	1/1	4	40		0.401	1.17E-02	1.76E-01
D2	10/5	1/1	4	40		0.225	1.01E-04	3.00E-03
D3	10/5	5/5	4	40		0.030	1.20E-05	3.58E-04
D5	20/10	5/5	4	40		0.019	3.38E-07	1.14E-05
D6	100/10	1/1	4	40		0.139	5.00E-08	0.00E+00
D7	100/10	10/10	4	40		0.007	5.00E-08	0.00E+00
D4-M1	20/10	1/1	4	40	60 yr Service Life	0.175	2.31E-06	1.29E-04
D4-M2	20/10	1/1	4	40	600°F Mean Temp.	0.061	1.93E-07	6.20E-06
D4-M3	20/10	1/1	4	40	Decreased Initiation t_{ref}	0.731	2.63E-05	9.63E-04
D4-M4	20/10	1/1	4	40	Increased β_{flaw}	0.330	9.44E-06	3.44E-04
D4-M5	20/10	1/1	4	40	Correlated Init. & Growth	0.201	5.23E-05	1.85E-03
D4-M6	20/10	1/1	4	40	Decreased $POD_{max,UT}$	0.145	3.17E-06	1.20E-04
D4-M7	20/10	1/1	4	40	Decreased $\theta_{circ,crit}$	0.146	5.35E-06	1.94E-04
D4-M8	20/10	1/1	4	40	MRP-55 Curve	0.144	2.25E-06	8.24E-05

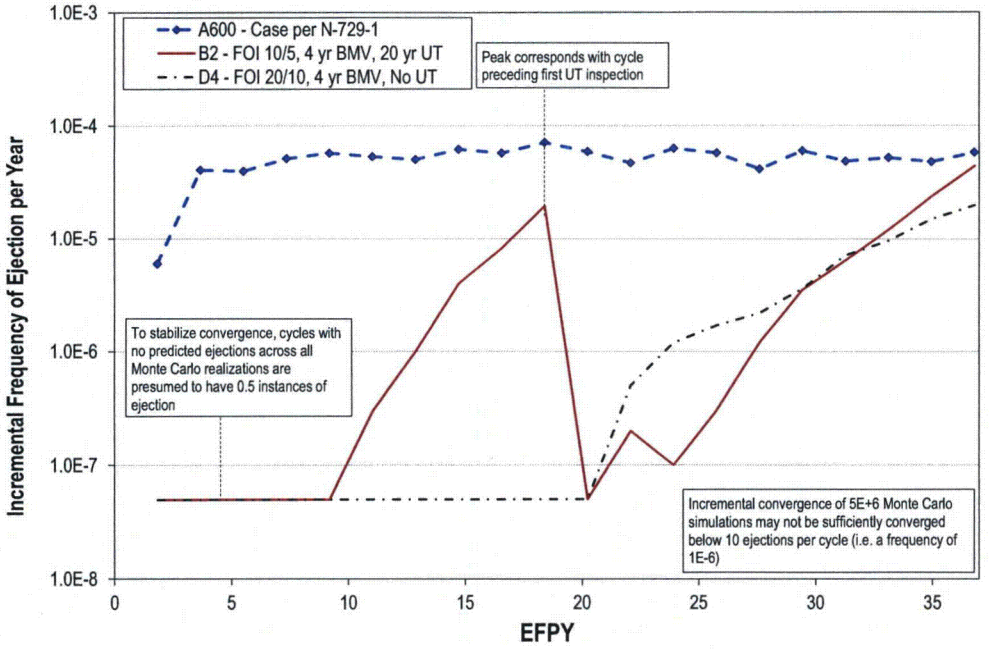

Figure B-16
Incremental Frequency of Ejection vs. Time for Base Cases

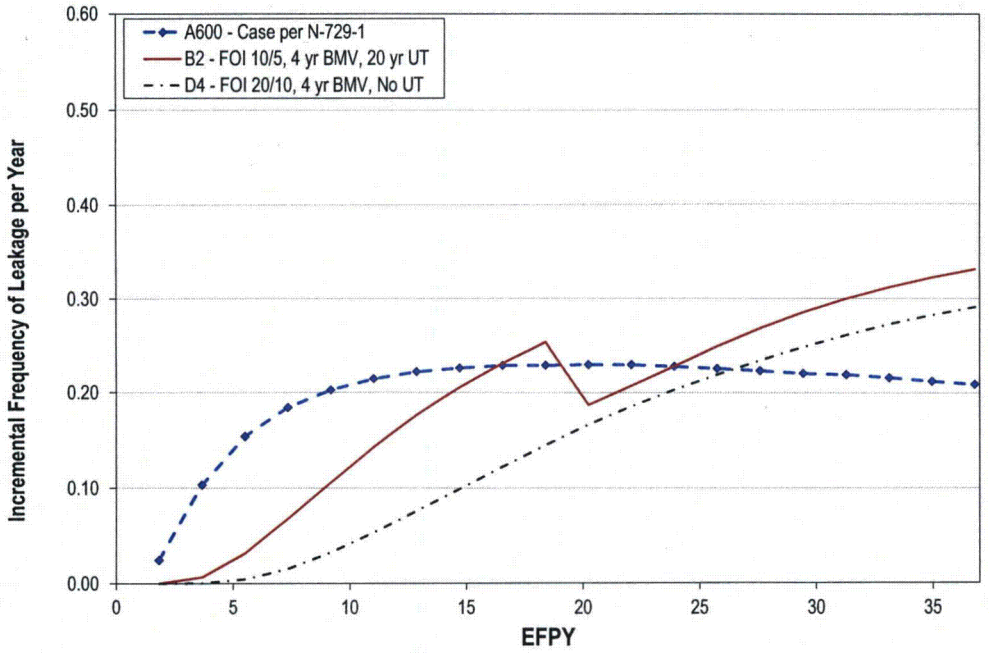

Figure B-17
Incremental Frequency of Leakage vs. Time for Base Cases

B.3.2.2 Varying Inspection Intervals

Variations in inspection interval are simulated for both of the base cases presented in B.3.2.1. The current N-729-1 examination requirements are evaluated in addition to extensions of both the BMV and UT examination intervals. The IEF and ILF versus time for various the inspection intervals from the B2 base case (g10/5 i1/1) are presented in Figure B-18 and Figure B-20, respectively. The IEF and ILF versus time for various inspection intervals from the D4 base case (g20/10 i1/1) are presented in Figure B-19 and Figure B-21, respectively. Remarks and conclusions are provided below.

For both of the Alloy 690 base cases, a variation with BMV inspections every three RFOs (i.e., 6 calendar years) was evaluated. There was negligible change in the ALF because BMV inspections do not detect part-depth flaws. The modified B2 run produced a 22% increase in AEF relative to the base case (a change equivalent to 3% of the Alloy 600 base case AEF), and the modified D4 case resulted in a similar change to the AEF. Even for the B2 case with BMV inspections every 6 years, the AEF remains a factor of about 7 lower than that for the Alloy 600 case.

A – Alloy 690 with Inspections per N-729-1

This case models inspections at the intervals specified by current N-729-1 requirements for nozzles and welds fabricated from PWSCC resistant material. For a refueling cycle of 24 months, this corresponds to BMV examinations every 4 years and UT examinations every 10 years. Applied with FOIs representative of Alloy 690, this inspection regime is predicted to be orders of magnitude more conservative than the Alloy 600 RPVs examined in accordance with N-729-1, as measured by probability of ejection.

Inspection scheduling per N-729-1 decreases the predicted AEF by over 95% relative to each of the Alloy 690 base cases. For assumed growth FOIs of g20/10 and g10/5, performing UT inspection in accordance with N-729-1 results in an AEF over the 40-year head service period that is less than 1% of that predicted for Alloy 600 heads inspected per N-729-1. This is considered excessive given that the base cases with extended UT inspection intervals already predicted lower ejection risks than the Alloy 600 base case by a considerable margin.

Inspection scheduling per N-729-1 results in an ALF that is 16% and 48% less than the Alloy 600 base case for the g10/5 and g20/10 growth FOI assumptions, respectively.

B – Alloy 690 with UT Exams Every 10 RFOs

This case (B4) considers the extension of the UT inspection interval requirement from 10 to 20 years, under the assumed FOI set of g20/10. Relative to case A4, which simulates inspection in accordance with N-729-1, this case predicts a twofold increase in AEF. However, this predicted AEF is still over 500 times less than that predicted for the Alloy 600 base case.

The corresponding inspection case for g10/5 is covered as base case B2 in Section B.3.2.1.

C – Alloy 690 with BMV Exams Every 5 RFOs and UT Exams Every 10 RFOs

This case simulates an extension of the BMV inspection interval to ten years and an extension of the UT inspection interval to 20 years. This case is used to examine the importance of the BMV inspection interval through comparison with the inspection schedule B cases (which use the same UT inspection interval, but with a BMV interval of every four years).

Under the assumed FOI set of g10/5, the predicted AEF approximately doubles when the BMV interval is extended from every 2 cycles to every 5 cycles. The resulting AEF is still over four times less than that predicted for the Alloy 600 base case. Under the assumed FOI set of g20/10, no statistical change is predicted.

The leakage prediction is not affected in this case because BMV inspections are not able to detect part-depth flaws.

D – Alloy 690 Case with No UT Exams over 40 Years

This case (D2) considers delaying the UT inspection interval requirement until after 40 years, under the assumed FOI set of g10/5. Relative to case B2, which simulates inspection at 20 years, this case predicts a factor of approximately 16 increase in AEF. This predicted AEF is about two times greater than that predicted for the Alloy 600 base case. The predicted ALF is also greater than that predicted for the Alloy 600 base case.

Consequently, in this case, relying solely on BMV inspections every other refueling outage is considered insufficient from a relative risk perspective. However, this case gives no credit to lower susceptibility to PWSCC initiation (i.e., it assumes the same rate of initiation observed in Alloy 600 heads). Furthermore, the assumed growth FOI set of g10/5 is considered low in comparison to most laboratory CGR testing data.

The corresponding inspection case for g20/10 is covered as base case D4 in Section B.3.2.1.

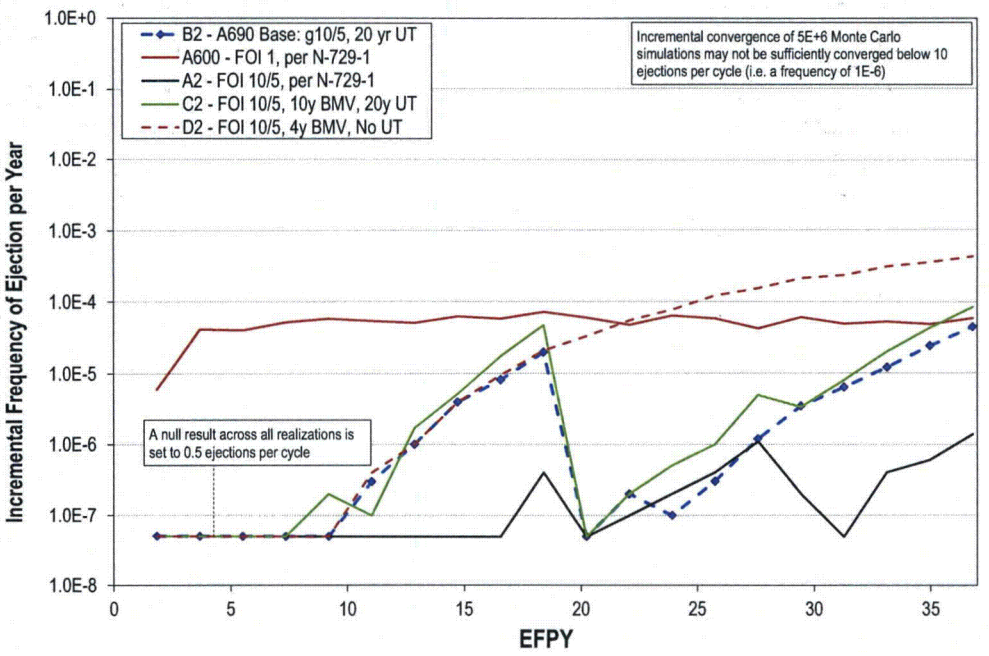

Figure B-18
Incremental Frequency of Ejection vs. Time for Different Inspection Regimes (Variations on Base Case B2)

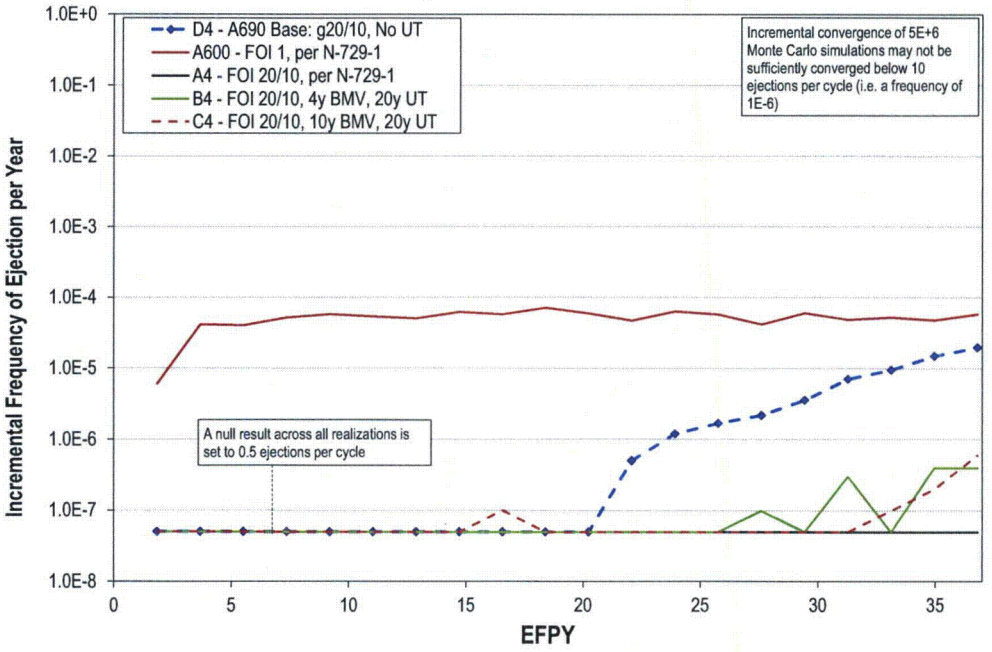

Figure B-19
Incremental Frequency of Ejection vs. Time for Different Inspection Regimes (Variations on Base Case D4)

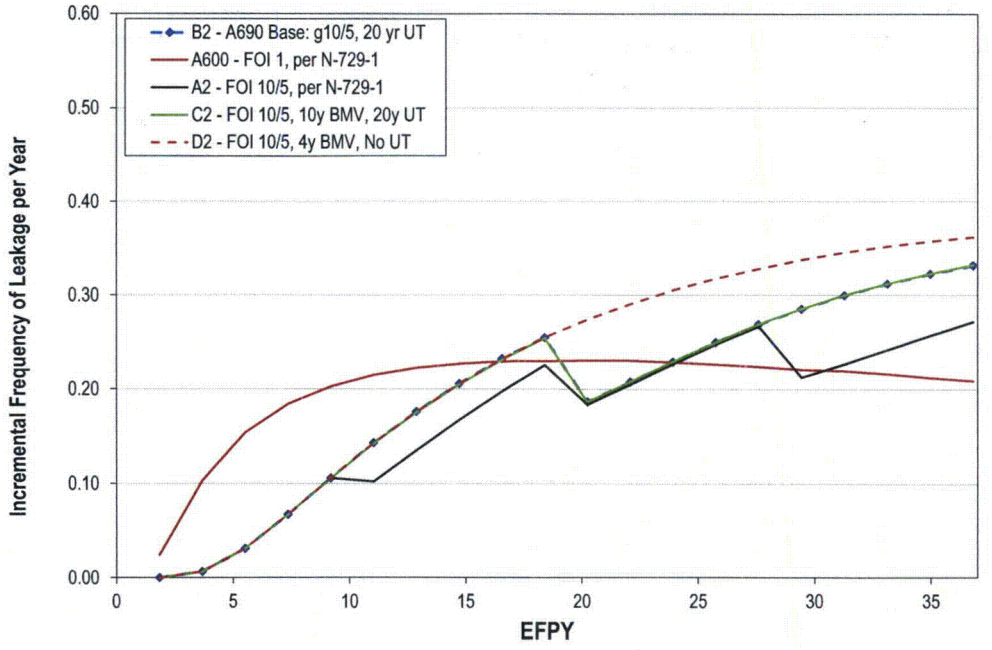

Figure B-20
Incremental Frequency of Leakage vs. Time for Different Inspection Regimes (Variations on Base Case B2)

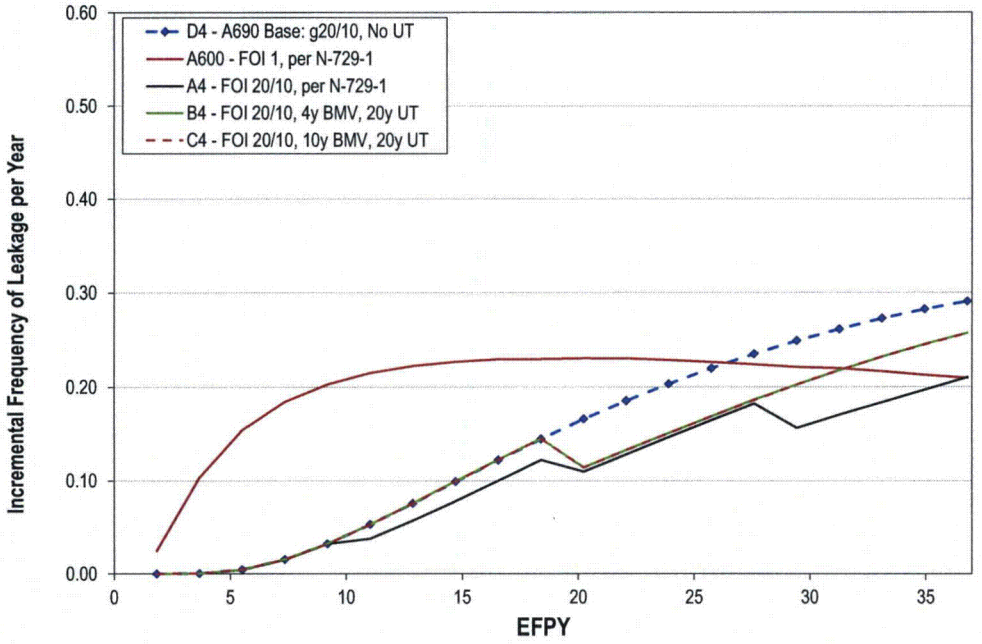

Figure B-21
Incremental Frequency of Leakage vs. Time for Different Inspection Regimes (Variations on Base Case D4)

B.3.2.3 Varying Factors of Improvement (FOI)

This section explores the impact of varying assumed FOIs for initiation and growth in Alloys 690/52/152 relative to Alloys 600/182. The FOIs for the various cases presented in this section are defined in Table B-10. The IEF and ILF versus time for all cases with the type B inspection intervals (UT inspection every 20 years; BMV inspection every 4 years) are presented in Figure B-22 and Figure B-24, respectively, while all cases with type D inspection intervals (UT inspection every 40 or more years; BMV inspection every 4 years) are presented in Figure B-23 and Figure B-25, respectively. AEF results are contrasted against the results of the associated base case (i.e., cases B2 or D4) in Figure B-14 and Figure B-15.

FOI sets 1, 2, 4, and 6 consider the effect of changing growth FOIs on the risk of leakage and ejection. FOI sets 3, 5, and 7 consider the effect of changing initiation FOIs; results of these cases can be respectively compared to results for FOI sets 2, 4, and 6 to demonstrate the effect of taking credit for PWSCC initiation resistance in Alloy 690/52/152.

The following general conclusions are drawn by investigating all different FOI cases:

- Increasing the initiation FOI decreases the leakage frequency by a factor slightly larger than the change in FOI.
- Increasing the initiation FOI decreases the frequency of ejection by a factor on the same order as the change in FOI.
- Increasing the growth FOI typically decreases the ejection frequency by a factor much larger than increasing the initiation FOI.

- Increasing the growth FOI on weld and HAZ material modifies the leakage frequency by a factor less than the change in FOI.
- However, increasing the growth FOI for wrought material beyond more than double that of the weld and HAZ material does not substantially alter the leakage frequency. This suggests that leakage frequencies may be governed by cracking near adverse material conditions (e.g., HAZ, weld dilution zones, excessive cold work) and that further improved bulk nozzle material may not significantly limit leakage frequency if other susceptible locations are not also improved.

1 – Alloy 690 Base Case with a FOI of g1/1 i1/1

This case considered the Alloy 690 base cases with a FOI of one at all locations. Effectively, this simulates an Alloy 600 RPVH with inspection intervals extended to durations permissible for Alloy 690 RPVHs. Consequently, risks are significantly greater than those of the base cases.

These cases are the only cases that predict an average of more than two ejections for each head with at least one ejected penetration nozzle.

The results of this particular case are purely hypothetical and are only relevant as points of comparison in this study. These cases are not expected to be applicable to any scenarios encountered in practice.

2 – Alloy 690 Base Case with a FOI of g10/5 i1/1

These cases compare the use of a growth FOI of g10/5 against no growth FOI (i.e., Alloy 600). Assuming UT inspection at 20 years, the AEF is reduced by three orders of magnitude, sufficient to provide an AEF that is factor of eight lower than the Alloy 600 base case. Assuming no UT inspection, the AEF is reduced by two orders of magnitude, but remains a factor of two greater than that predicted for the Alloy 600 base case. The ALF for both inspection schedules is comparable to (within 15% relative to) the Alloy 600 base case.

3 – Alloy 690 Base Case with a FOI of g10/5 i5/5

These cases take some modest credit (i5/5) for reduced PWSCC initiation susceptibility of Alloy 690 materials with the also modest credit (g10/5) for reduced PWSCC growth susceptibility.

These cases are characterized by dramatically lower leakage frequencies when compared against their base cases, which give no credit to initiation improvement. Specifically, increasing the initiation FOI from 1 to 5 decreases the predicted ALF by a factor of approximately seven.

Since leakage is a prerequisite for ejection (as modeled in this report), the ejection risk was expected to be reduced by a factor similar or greater than the leakage improvement. In fact, increasing the initiation FOI from 1 to 5 decreases the predicted AEF by a factor of about nine.

4 – Alloy 690 Base Case with a FOI of g20/10 i1/1

These cases compare the use of a growth FOI of g20/10 versus g10/5. Assuming UT inspection at 20 years, the AEF is reduced by a factor of about 62; assuming no UT inspection, the AEF is reduced by a factor of about 33. These are very significant benefits for an increase in the growth FOI by only a factor of two. The rate of leakage is also somewhat lower (e.g., between 30-40% depending on the assumed inspection schedule).

5 – Alloy 690 Base Case with a FOI of g20/10 i5/5

These cases take some modest credit for reduced PWSCC initiation susceptibility of Alloy 690 materials with a more representative credit (g20/10) for reduced PWSCC growth susceptibility.

Again, these cases are characterized by dramatically lower leakage frequencies when compared against their base cases, which give no credit to initiation improvement. Specifically, increasing the initiation FOI from 1 to 5 decreases the predicted ALF by a factor of approximately eight and decreases the predicted AEF by a factor of about two or nine, depending on whether UT inspection is performed at 20 years or not performed at all.

6 – Alloy 690 Base Case with a FOI of g100/10 i1/1

These cases assume a FOI of 100 for PWSCC growth in Alloy 690 wrought material in comparison to Alloy 600. This FOI is applied for circumferential cracks growing above the J-groove weld. This FOI is consistent with some laboratory testing of Alloy 690 with limited cold work (e.g., as received materials). A conservative FOI of 10 for Alloy 690 HAZ and Alloy 52/152 is maintained to evaluate how only increasing the wrought Alloy 690 FOI affects leakage predictions.

No ejections are predicted to occur in these cases and 100% of leakage occurs through flaws in the weld material.

Because leakage at the lower FOI cases with g20/10 is already predicted to occur overwhelmingly (~95%) through cracks in welds, the increase in the FOI for growth in wrought material does not substantially change the ALF.

7 – Alloy 690 Base Case with a FOI of g100/10 i10/10

These cases assume a FOI of 100 for PWSCC growth in Alloy 690 wrought material, a FOI of 10 in Alloy 690 HAZ and Alloy 52/152 weld material, and a FOI of 10 for initiation at all locations on RPVHPNs fabricated with Alloy 690/52/152 materials.

As mentioned in conjunction with the previous cases, no ejections are predicted with a growth FOI of 100 for wrought Alloy 690 material because it applies to the growth of circumferential cracks above the J-groove weld.

As with the previous set of cases, 100% of the leakage is predicted to occur through the weld. However, the addition of a FOI of 10 on multiple crack initiation leads to an ALF of 0.007 new leaks per head per year. This is more than a factor of 20 lower than the ALF for the base cases (B2 and D4).

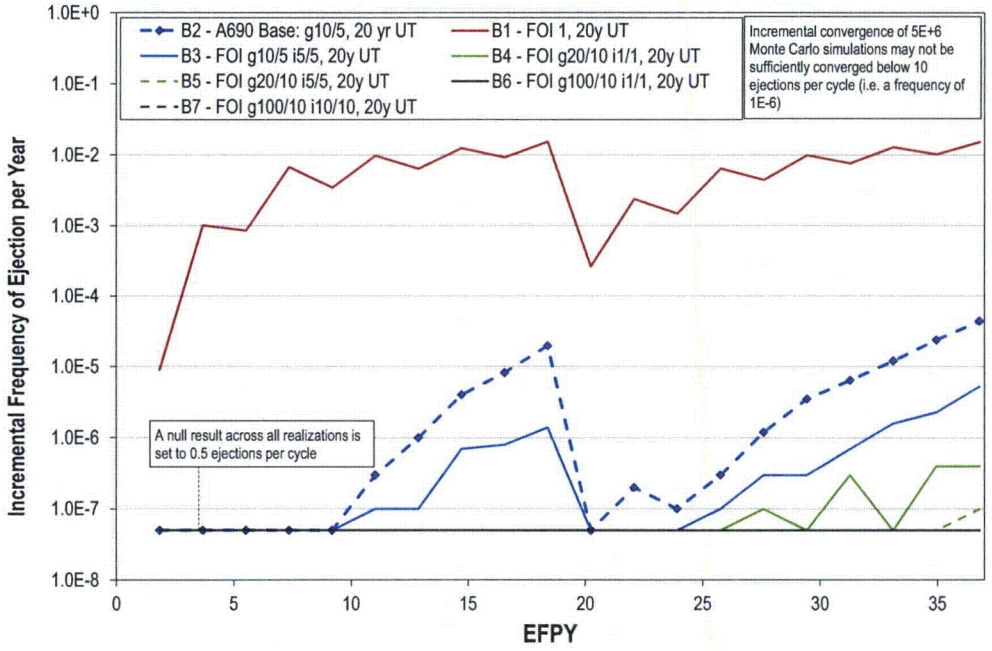

Figure B-22
Incremental Frequency of Ejection vs. Time for Varying FOIs (Variations on Case B2)

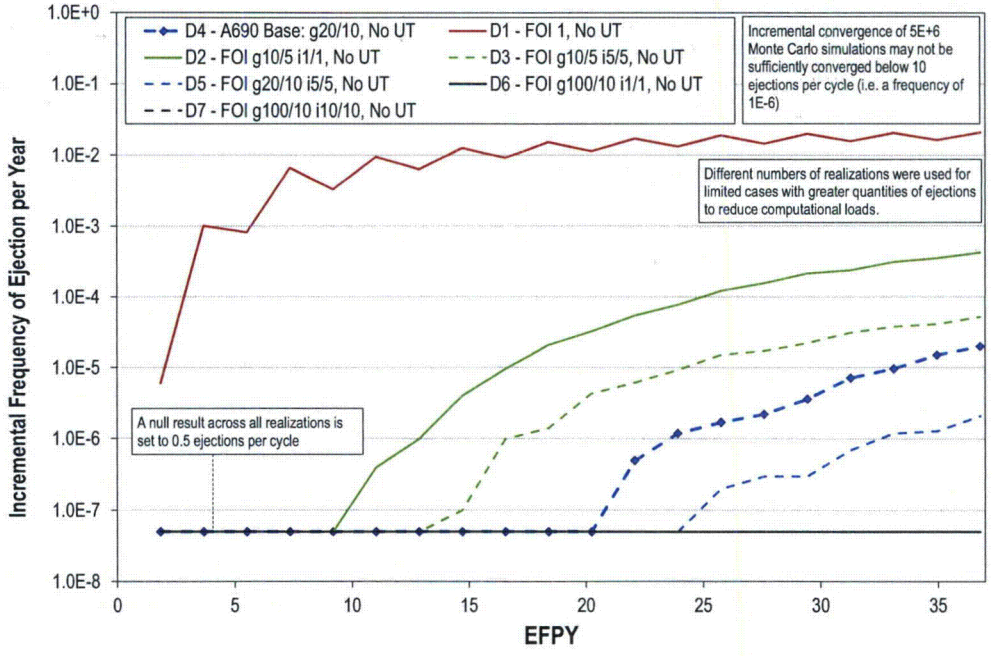

Figure B-23
Incremental Frequency of Ejection vs. Time for Varying FOIs (Variations on Case D4)

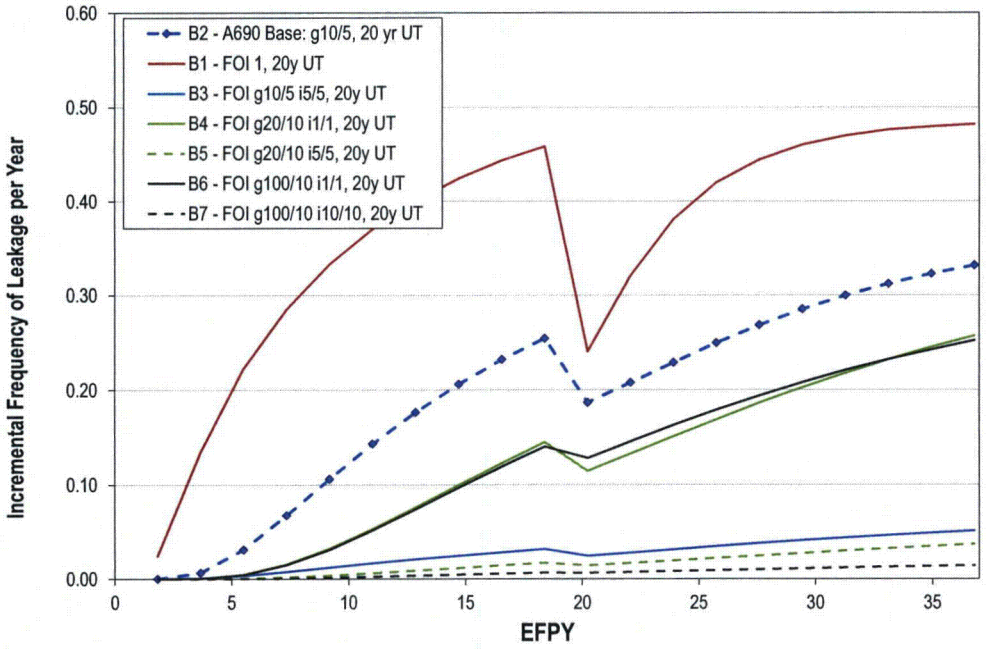

Figure B-24
Incremental Frequency of Leakage vs. Time for Varying FOIs (Variations on Case B2)

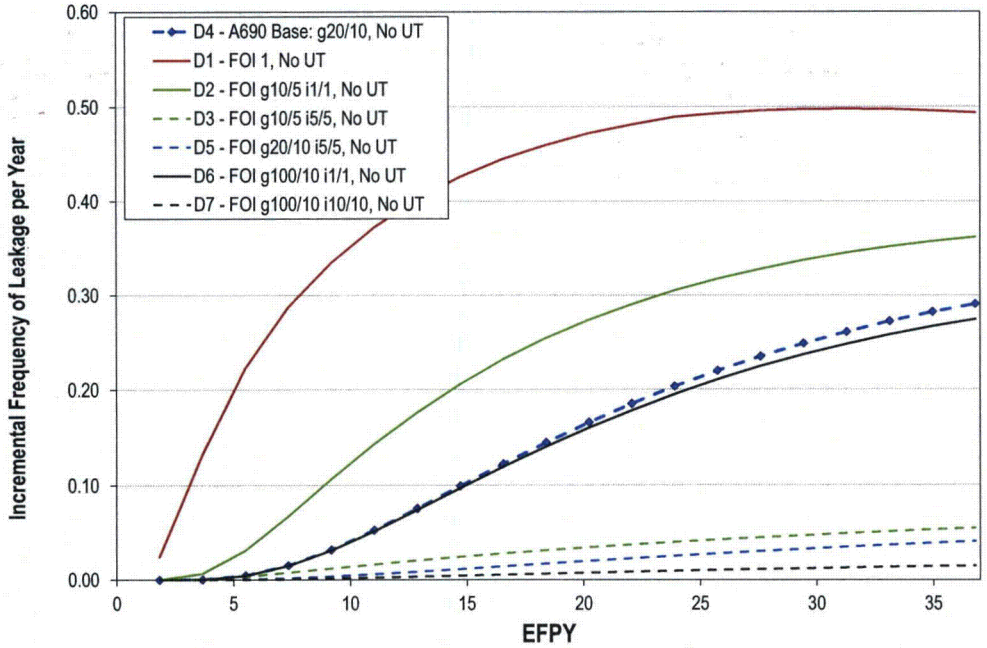

Figure B-25
Incremental Frequency of Leakage vs. Time for Varying FOIs (Variations on Case D4)

B.3.3 Model Validation Test Results

This section describes methods to validate earlier results including the investigation of modeling assumptions through sensitivity tests (Section B.3.3.1), convergence analyses (Section B.3.3.2), and benchmarking studies (Section B.3.3.3).

B.3.3.1 General Sensitivity Test Cases

Various sensitivity cases with the RPVHPN probabilistic model were examined in order to demonstrate the relative change in the predicted results given one or more changes to modeling assumptions. The inputs that vary for each case are presented in Table B-11 in Section B.2.6.

These results are presented in several forms:

- Comparisons of predicted AEFs relative to the base case are presented in Figure B-14 for the B2 base case (FOI g10/5; 20 year UT inspection interval) and in Figure B-15 for the D4 base case (FOI g20/10; 40 year UT inspection interval).
- Numerical results for each sensitivity case are presented in Table B-15 and Table B-16 for the B2 and D4 cases, respectively.
- The IEF and ILF versus time for model sensitivity tests of the B2 base case are presented in Figure B-27 and Figure B-29, respectively. The IEF and ILF versus time for model sensitivity tests of the D4 base case are presented in Figure B-28 and Figure B-30, respectively.

The results are further discussed below.

Case M1 – Increased Reactor Vessel Head Operating Period

This sensitivity case investigated the effect of a 20 year license renewal on the results and conclusions discussed in earlier sections. Under this condition, a UT investigation occurs at the 40-year mark for both the case with UT inspections every 20 years and the case with UT inspections every 40 years. By increasing the reactor vessel head operating period, the PWSCC degradation manifested toward the end of the 40 year cycle in the previously examined cases is given additional time to progress. The incremental results for this case are presented in Figure B-26.

The increased operating period leads to a 21% increase in the AEF over the B2 base case (with UT inspections every 20 years)—that corresponds to an increase from 2.4E-04 to 4.4E-04 in the CPE in the head operating period. Similarly, the cumulative probability of one or more leaks on a given head over its operating period increases from 69% to 86%.

For the slower growth of the D4-M1 case (g20/10), the UT examination at 40 years causes the IEF to decrease significantly. The increased operating period led to a 25% decrease relative to the base case and the greatest maximum IEF is the last cycle before the UT inspection (the cumulative probability of ejection occurring on a head only increases from 1.2E-4 to 1.3E-4 over the last 20 years of the case). The ALF increases 20% relative to the D4 base case, and the probability of leakage on the head increases from 56% to 78%.

Case M2 – Reduced Operating Temperature

Reducing the head temperature from 613°F to 600°F (323°C to 316°C) reflects that most Alloy 690 hot heads operate below 613°F (323°C), with a majority operating between 590°F and 600°F (310°C to 316°C). The reduced temperature decreases the thermally activated PWSCC flaw initiation and growth processes (i.e., through the Arrhenius relation in the model).

Reducing the head temperature leads to a more than tenfold reduction in AEF. Similarly, the frequency of leakage is decreased to less than half its base case value.

Case M3 – Earlier Time to First Initiation

This case explored the shifting of the head initiation model to earlier times, compensating for the fact that undetected cracks cannot be included to fit the initiation time model. Specifically, the time estimated from data at which 1% of all RPVHs are expected to initiate PWSCC is reduced by a factor of five.

The shorter time to initiation leads to a marked increase in the ALF for both cases (B2-M3 and D4-M3[27]) by a factor of approximately five. As a consequence, there is also a roughly sevenfold increase in the AEF. However, AEF for these sensitivity cases remain below the Alloy 600 base case and about a factor of four below the equivalent Alloy 600 sensitivity case.

The average time to the first predicted ejection does not change by an appreciable amount from the base case because the flaw growth rate is not modified and the unmodified initiation model already predicted 1% initiation prior to the end of the first operating cycle (i.e., ejection is limited by the minimum incubation time for significant PWSCC). However, once ejection risks begin to manifest, they manifest at higher rates due to the greater number of flaws initiated early in the modeled life of the RPVH.

Case M4 – More Rapid Acceleration of Multiple Initiations after First Initiation

Increasing the mean multiple flaw initiation slope from 2 to 3 directly increases the rate at which additional flaws initiate on a given head after the first flaw initiation. For instance, this would correspond to a head with more uniform material condition and operating conditions across all penetrations.

The increased multiple flaw initiation slope increases the average leakage and ejection rates by a factor of two to three. As with the case above exploring an earlier time to first initiation, average time to the onset of ejection risk is not altered significantly.

The results of this and the previous case suggest that the conclusions of this report hold for more severe assumptions about PWSCC initiation in Alloy 690.

Case M5 – Correlated Initiation and Growth

The concept of correlating flaw initiation and flaw growth is based on the expectation that components and locations that are more susceptible to PWSCC initiation tend to have higher flaw propagation rates, even after accounting for temperature and stress effects [14].

---

[27] Fewer realizations of this case were modeled than the other cases. This is due to dramatically increased runtimes associated with tracking a much greater number of flaws.

Adding this correlation between the initiation and growth models increased the AEF by an order of magnitude for both cases (B2-M5 and D4-M5) and ALF by a factor of 20% to 40%. The resulting AEFs become roughly equivalent to those of the Alloy 600 base case (which assumes no correlation). To address this, the Alloy 600 base case was rerun with the correlation, resulting in threefold increase in ejection risk (maintaining a factor of about three over the Alloy 690 sensitivity cases). These results considered together are deemed acceptable because there is no technical basis to assume that the relationship between initiation and growth in Alloy 690 would be starkly different for Alloy 600. Therefore, the Alloy 690 cases still have a large risk margin in comparison to analogous Alloy 600 cases.

Case M6 – Decreased Maximum UT POD

Decreasing the maximum probability of detection by UT examination reflects less effective inspection capability and/or more gross error. In this case, the effect of changing the maximum UT probability of detection from 95% to 90% is considered. Since this is a trivial sensitivity for D4, the base case without UT inspection, the lower POD was applied to case B4, which applies a 20-year UT interval and a growth FOI set of g20/10.

For all the cases, the small absolute change of the results relative to the convergence limit means the results are not statistically significant (change of less than 20% in the AEF).

The results of this case suggest that the conclusions of this report hold even for marginally poorer UT inspectability of Alloy 690 RPVHPNs.

Case M7 – Decreased Critical Flaw Size

In this study, the critical size is deceased from 300° to 275° to represent a more conservative assumption about RPVHPN stability. Changing the critical flaw size has no effect on the leakage probability, but rather reduces the threshold at which a circumferential crack is judged to cause net section collapse.

The decreased critical flaw size leads to a roughly 70% increase in AEF with respect to the Alloy 690 base cases. The resulting AEFs are still well below the AEF associated with the Alloy 600 base case.

The results of this case suggest that the conclusions of this report hold even for a case with compromised stability. It is noted that net section collapse calculations, specifically those of MRP-110 Appendix D, predict negligibly different critical flaw thresholds for Alloy 600 and Alloy 690 penetrations of the same geometry.

Case M8 – MRP-55 Crack Growth Rate Model Parameters

The Alloy 600 PWSCC growth model used in this report is based on MRP-55 CGR data, but is fit assuming no stress intensity factor threshold for growth, which results in a different fitted power law parameters. This sensitivity case examines the effect of using the MRP-55 CGR parameters (i.e., the 50^{th} percentile power law coefficient, a 9 MPa$\sqrt{m}$ stress intensity factor threshold, and a stress intensity factor exponent of 1.16) to predict Alloy 600 growth rates (which are then adjusted by FOI to represent Alloy 690).

This modification to the Alloy 690 growth model results in negligible changes to leakage frequency predictions because weld flaws—the drivers of leakage probability per the assumed model—are unaffected. This modification results in slight reductions in the AEF (roughly 30%)

due to the increased possibility that some very small initial flaws do not grow or grow extremely slowly.

The results of this case confirm that the modified CGR equation used in this report is more conservative than the median MRP-55 curve.

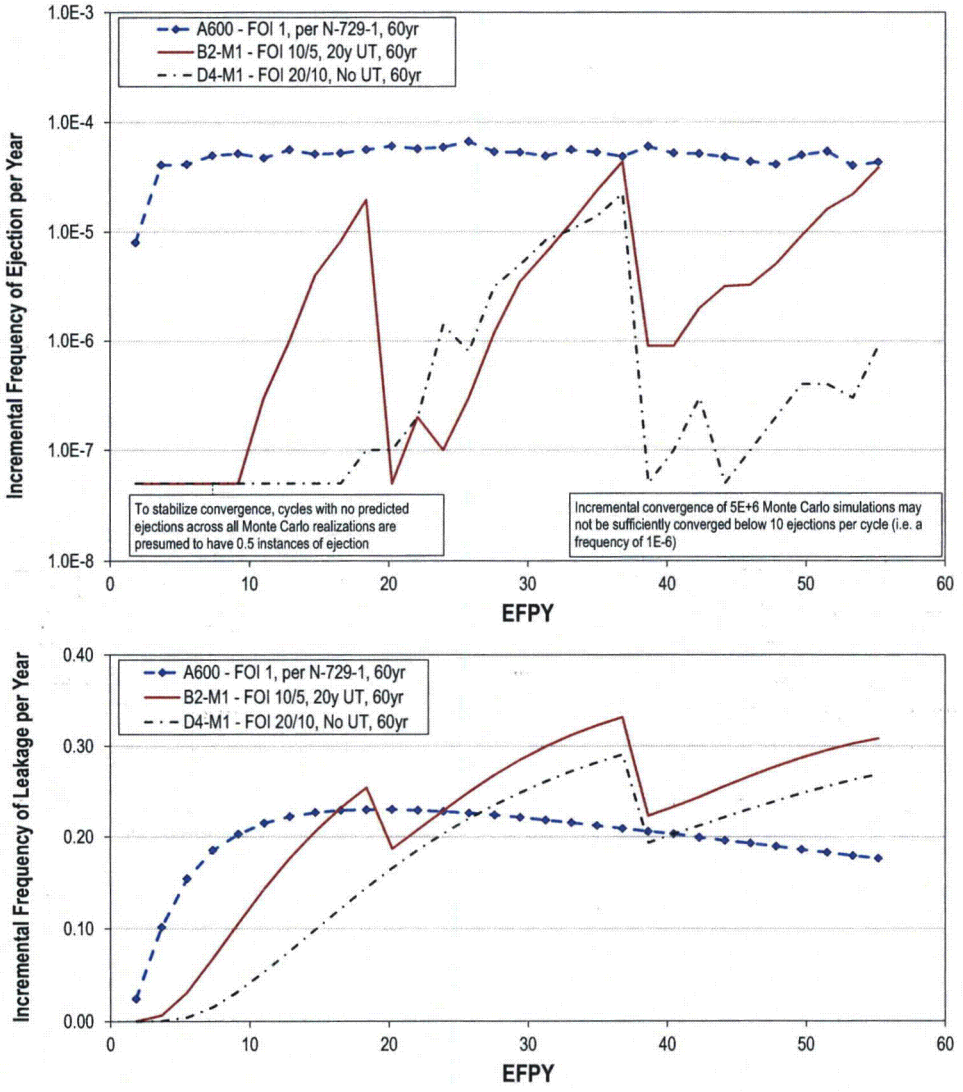

Figure B-26
IEF (top) and ILF (bottom) vs. Time for Extended Operating Period Sensitivity Cases

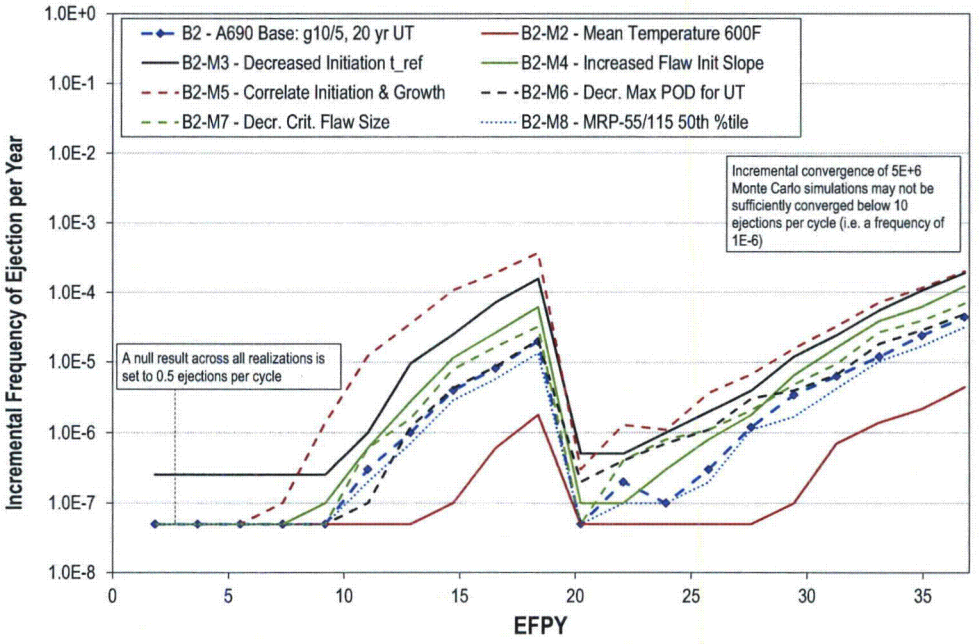

Figure B-27
Incremental Frequency of Ejection vs. Time for Sensitivity Cases (Variations on Base Case B2)

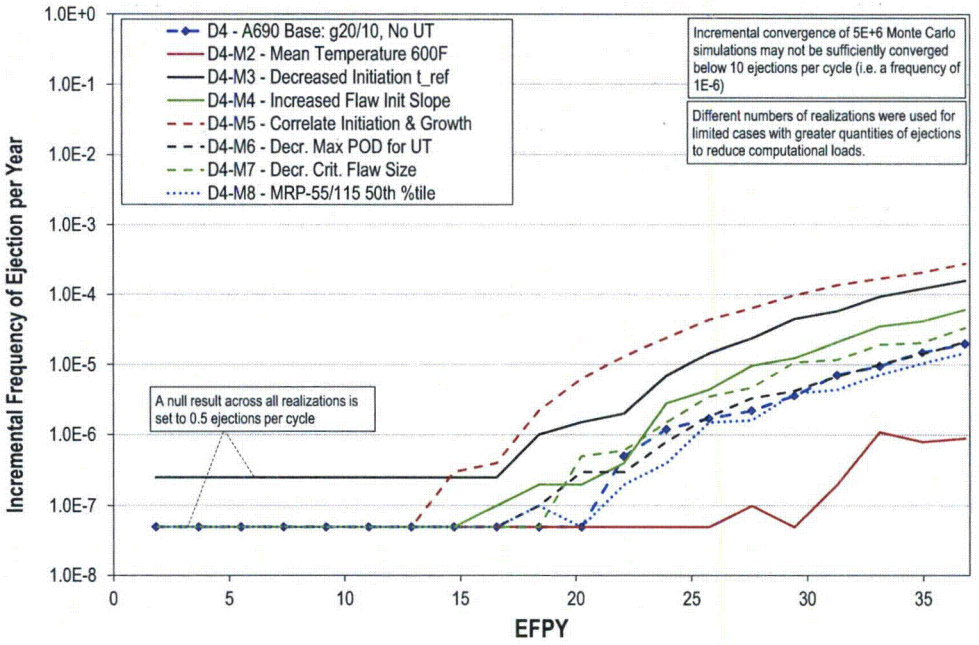

Figure B-28
Incremental Frequency of Ejection vs. Time for Sensitivity Cases (Variations on Base Case D4)

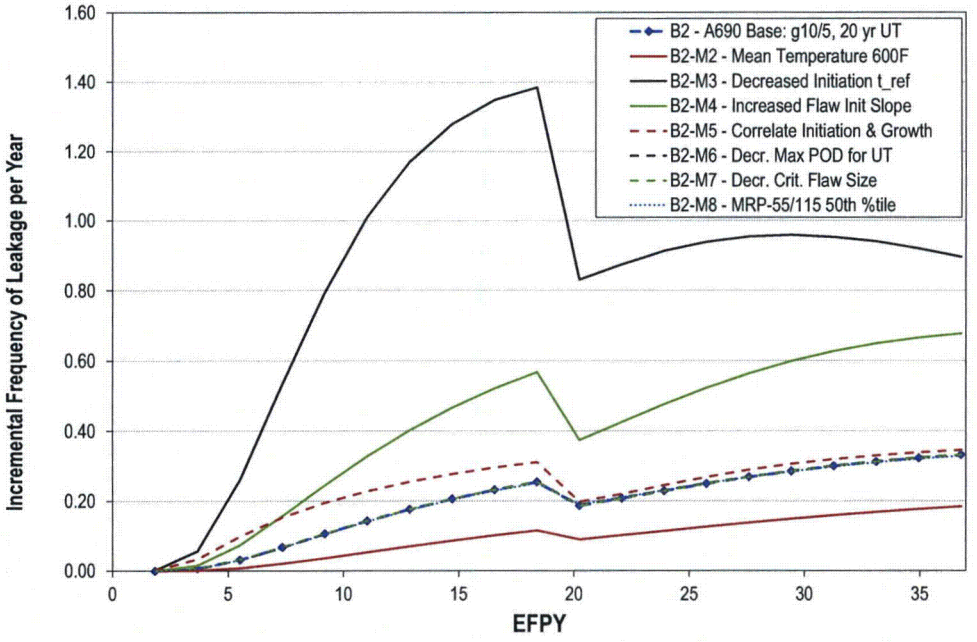

Figure B-29
Incremental Frequency of Leakage vs. Time for Sensitivity Cases (Variations on Base Case B2)

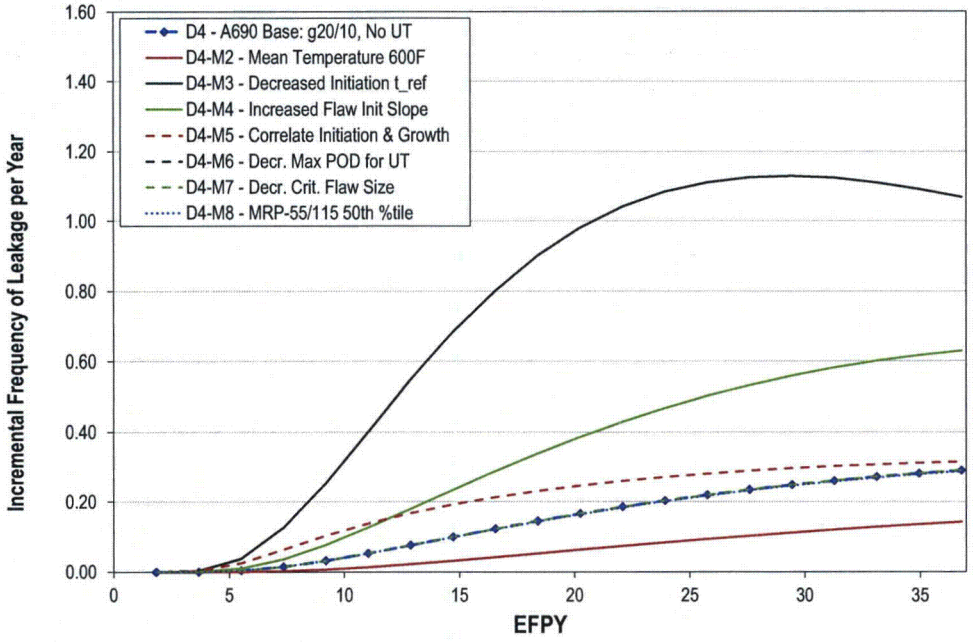

Figure B-30
Incremental Frequency of Leakage vs. Time for Sensitivity Cases (Variations on Base Case D4)

B.3.3.2 Convergence Tests

Two key modeling parameters affect the convergence of the probabilistic framework: the number of Monte Carlo realizations and the number of flaw growth steps per year.

Monte Carlo Realization Convergence Analysis: The number of realizations affects the convergence of statistical results, i.e., the precision of statistical results or the deviation between independent cases that may be considered statistically significant.

The comparatively large number of leaks that occur for a given number of realizations leads to rapid convergence of leakage statistics while the lower number of ejections (e.g., 1000 times less frequent) necessitate more realizations. To investigate the convergence of ejection statistics, the statistics reported from ten independent runs of the probabilistic framework with the same inputs are analyzed together.

For larger FOIs and more frequent inspection regimes, for which there are fewer ejections during the head operating period, the convergence of ejection results is slower. Due to this variation in convergence from case to case, all three base cases are investigated for convergence.

Based on the results presented in Table B-17, 5E+06 realizations are sufficient to provide converged statistics of both leakage and ejection for Alloy 690 cases while 1E+06 realizations are sufficient for the Alloy 600 base case.

Number of Growth Steps per Year Convergence Analysis: The number of growth steps per year determines the error of the discrete Euler integration approximation to the ordinary differential equations defining crack growth and transitioning throughout the RPVH. More steps per year provide more converged results. However, the number of growth steps per year can greatly increase the computational cost.

Convergence of the numerical integration is not assessed for singular realizations. Instead, convergence analysis is performed by comparing the Monte Carlo statistics across runs with different growth steps per year. The deviation in statistics between these runs helps quantify convergence.

The required number of growth steps per year varies depending on the average rate of growth. For instance, deterministic calculations for growth of a single crack indicate convergence is achieved with longer integration time steps when a FOI of 10 is applied. As such, all three base cases are investigated independently for convergence.

MRP-335 Rev. 1 determined that 12 growth steps per year provided sufficient convergence of Monte Carlo statistics for Alloy 600 RPVHs; Table B-18 shows that the Alloy 600 leakage and ejection results in this report are accurate to within ±1% and ±10%, respectively, with 12 growth steps per year.

Based on the results presented in Table B-19 and Table B-20, the use of 4 growth steps per year provides sufficient convergence for both Alloy 690 base cases. Due to the sometimes very low rate of ejection in Alloy 690 components, precision is stated as a ratio of the less accurate Alloy 690 case results and as a ratio of the Alloy 600 case results. The latter statistic is considered the more critical toward conclusions made in this report.

Also, a plot of AEF versus the integration step size is provided in Figure B-31. This plot indicates that bias due to lack of integration convergence is not significant and, at 4 growth steps per year, is probably outweighed by deviation between independent Monte Carlo realizations.

Table B-17
Summary of Monte Carlo Realization Convergence Case Results

Statistic	Mean Across 10 Trials	Standard Deviation Across 10 Trials	Precision of Mean (2 * stdev / mean)
Case A600-P10 *(1E+6 Realizations)*			
Average Yearly Frequency of Leakage on Head	2.00E-01	2.04E-04	0.2%
Cumulative Probability of any Nozzle Ejection	1.92E-03	3.95E-05	4.1%
Average Yearly Frequency of Ejection (0 = 0.5)	5.05E-05	1.05E-06	4.2%
Case B2-P10 *(5E+6 Realizations)*			
Average Yearly Frequency of Leakage on Head	1.96E-01	1.64E-04	0.2%
Cumulative Probability of any Nozzle Ejection	2.44E-04	8.56E-06	7.0%
Average Yearly Frequency of Ejection (0 = 0.5)	6.33E-06	2.24E-07	7.1%
Case D4-P10 *(5E+6 Realizations)*			
Average Yearly Frequency of Leakage on Head	1.46E-01	1.72E-04	0.2%
Cumulative Probability of any Nozzle Ejection	1.15E-04	5.55E-06	9.6%
Average Yearly Frequency of Ejection (0 = 0.5)	3.12E-06	1.38E-07	8.8%

Table B-18
Summary of Integration Convergence Case Results for the Alloy 600 Base Case

Statistic	Absolute Difference	Percent Difference
6 to 12 Substeps per year (Case A600-N6 to A600-N12)		
Average Yearly Frequency of Leakage on Head	+2.90E-03	+1.4%
Cumulative Probability of any Nozzle Ejection	+3.19E-04	+16.4%
Average Yearly Frequency of Ejection (0 = 0.5)	+8.67E-06	+16.9%
12 to 24 Substeps per year (Case A600-N12 to A600-N24)		
Average Yearly Frequency of Leakage on Head	+2.39E-03	+1.2%
Cumulative Probability of any Nozzle Ejection	+1.59E-04	+7.6%
Average Yearly Frequency of Ejection (0 = 0.5)	+4.73E-06	+8.4%

Table B-19
Summary of Integration Convergence Case Results for Case B2

Statistic	Absolute Difference	Percent Difference	Difference as Percent of A600 Statistic
2 to 4 Substeps per year (Case B2-N2 to B2-N4)			
Average Yearly Frequency of Leakage on Head	+2.89E-03	+1.5%	+1.4%
Cumulative Probability of any Nozzle Ejection	+1.70E-05	+7.1%	+0.9%
Average Yearly Frequency of Ejection (0 = 0.5)	+5.33E-07	+8.5%	+1.0%
4 to 8 Substeps per year (Case B2-N4 to B2-N8)			
Average Yearly Frequency of Leakage on Head	+1.41E-03	+0.7%	+0.7%
Cumulative Probability of any Nozzle Ejection	+1.72E-05	+6.7%	+0.9%
Average Yearly Frequency of Ejection (0 = 0.5)	+4.30E-07	+6.4%	+0.8%

Table B-20
Summary of Integration Convergence Case Results for Case D4

Statistic	Absolute Difference	Percent Difference	Difference as Percent of A600 Statistic
2 to 4 Substeps per year (Case D4-N2 to D4-N4)			
Average Yearly Frequency of Leakage on Head	+2.27E-03	+1.6%	+1.1%
Cumulative Probability of any Nozzle Ejection	+1.02E-05	+9.0%	+0.5%
Average Yearly Frequency of Ejection (0 = 0.5)	+2.78E-07	+9.0%	+0.5%
4 to 8 Substeps per year (Case D4-N4 to D4-N8)			
Average Yearly Frequency of Leakage on Head	+1.16E-03	+0.8%	+0.6%
Cumulative Probability of any Nozzle Ejection	+8.40E-06	+6.9%	+0.4%
Average Yearly Frequency of Ejection (0 = 0.5)	+2.43E-07	+7.3%	+0.5%

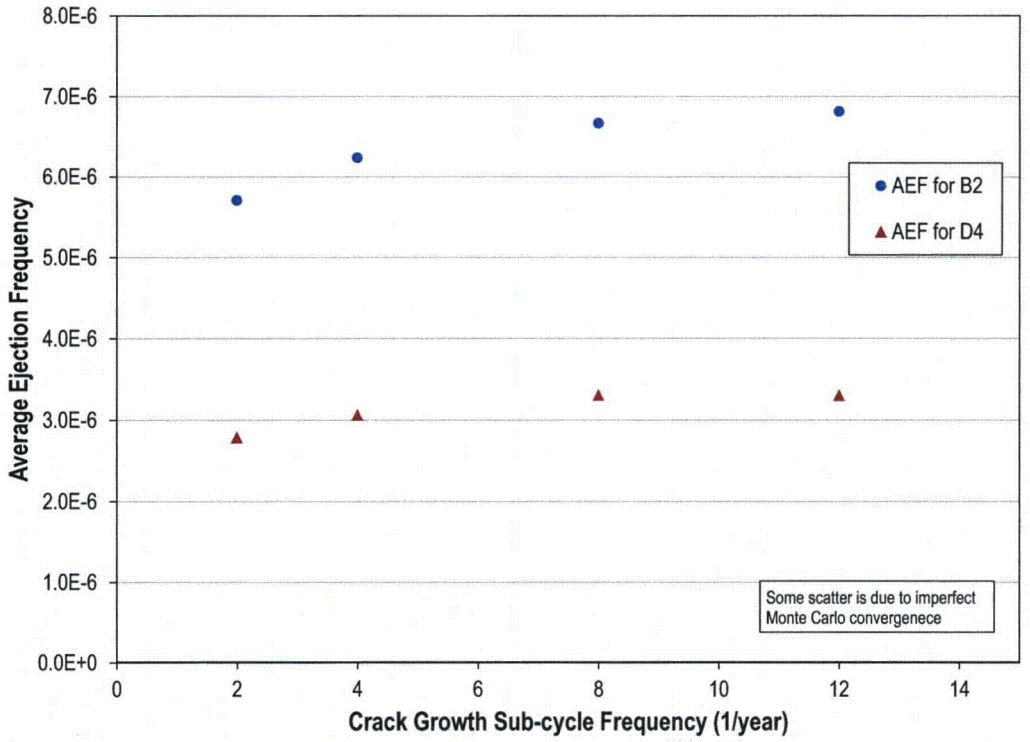

Figure B-31
Average Ejection Frequency vs. Sub-Cycle Steps per Year

B.3.3.3 Benchmarking Cases

The probabilistic RPVH model published in MRP-105 [6] in 2004 is a key part of the technical basis for the current set of inspection requirements for RPVHs with Alloy 600 nozzles. Thus, a benchmarking exercise was performed comparing the model developed for this study of RPVHs with Alloy 690 nozzles versus the model published in MRP-105. The benchmarking exercise provides continuity between the MRP-105 technical basis and the present study, and provides a measure of validation of the current model.

Specifically, two cases presented in MRP-105 [6] are compared against simulations performed using the probabilistic model presented in this report with inputs chosen to closely match those in MRP-105 (see Section B.2.7). Based on the results presented in MRP-105, the statistic of incremental ejection frequency (per year) versus time is compared. This statistic is compiled on a per-head basis such that only the first instance of ejection is counted per realization. In MRP-105, this statistic is presented in graphical form.

A graphical comparison of the results is presented in Figure B-32. The incremental probabilities of ejection of the benchmarking cases show reasonable agreement with MRP-105 values. The modeled UT inspections result in comparable reductions in IEF for MRP-105 and MRP-375 models. The degree of deviation between the results for the two models reflects the detailed differences in the modeling approaches and assumptions.

Deviation between the results of this report and MRP-105 arises from recognized differences in the detailed model approximations and model inputs, several of which are noted below:

- MRP-105 assumes constant rate growth of surface flaws not based on any stress calculations while this report more accurately bases part-depth crack growth on post-weld residual stresses per FEA studies and uses the influence coefficient method to determine the stress intensity factors at cracks tips.
- While MRP-105 models flaw initiation at uphill and downhill locations, this report separately models flaws originating on the nozzle ID, nozzle OD, and weld surfaces. Instead of assuming incomplete examination coverage, this allows explicit modeling volumetric inspections of the nozzle base metal without crediting detection of flaws located in the weld material, resulting in examinations more characteristic of those performed in the field.
- BMV inspections are not modeled in the results presented in Figure B-32, but they are modeled differently for the cases in which they are used in the respective reports. The POD curve for BMV inspections in MRP-105 is characterized in terms of the initial interference fit between the nozzle and reactor pressure vessel head as a means to consider the probable leak rates. This study uses a conservatively low constant POD value for BMV inspections considering the lack of data to correlate such a relationship.

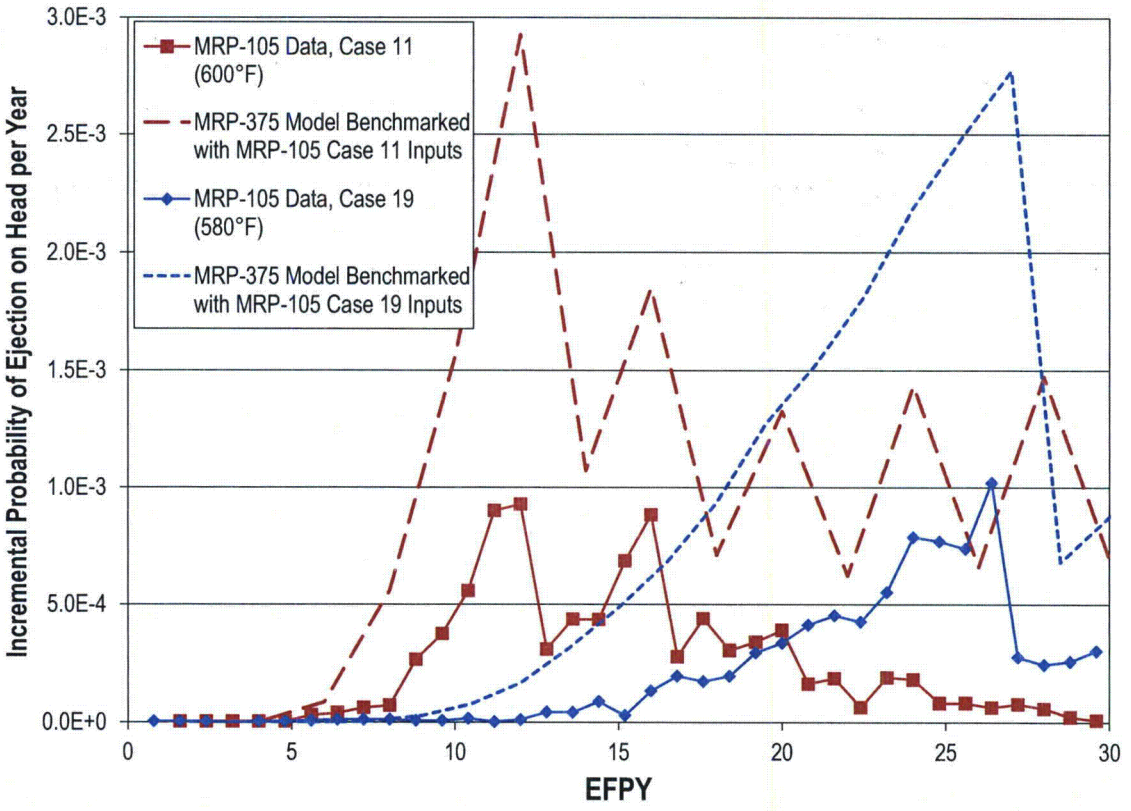

Figure B-32
Comparison of Incremental Probability of Ejection Prediction with MRP-105 [6] Results

Export Control Restrictions

Access to and use of EPRI Intellectual Property is granted with the specific understanding and requirement that responsibility for ensuring full compliance with all applicable U.S. and foreign export laws and regulations is being undertaken by you and your company. This includes an obligation to ensure that any individual receiving access hereunder who is not a U.S. citizen or permanent U.S. resident is permitted access under applicable U.S. and foreign export laws and regulations. In the event you are uncertain whether you or your company may lawfully obtain access to this EPRI Intellectual Property, you acknowledge that it is your obligation to consult with your company's legal counsel to determine whether this access is lawful. Although EPRI may make available on a case-by-case basis an informal assessment of the applicable U.S. export classification for specific EPRI Intellectual Property, you and your company acknowledge that this assessment is solely for informational purposes and not for reliance purposes. You and your company acknowledge that it is still the obligation of you and your company to make your own assessment of the applicable U.S. export classification and ensure compliance accordingly. You and your company understand and acknowledge your obligations to make a prompt report to EPRI and the appropriate authorities regarding any access to or use of EPRI Intellectual Property hereunder that may be in violation of applicable U.S. or foreign export laws or regulations.

The Electric Power Research Institute, Inc. (EPRI, www.epri.com) conducts research and development relating to the generation, delivery and use of electricity for the benefit of the public. An independent, nonprofit organization, EPRI brings together its scientists and engineers as well as experts from academia and industry to help address challenges in electricity, including reliability, efficiency, affordability, health, safety and the environment. EPRI also provides technology, policy and economic analyses to drive long-range research and development planning, and supports research in emerging technologies. EPRI's members represent approximately 90 percent of the electricity generated and delivered in the United States, and international participation extends to more than 30 countries. EPRI's principal offices and laboratories are located in Palo Alto, Calif.; Charlotte, N.C.; Knoxville, Tenn.; and Lenox, Mass.

Together...Shaping the Future of Electricity

Programs:

Nuclear Power

Materials Reliability

3002002441

Electric Power Research Institute
3420 Hillview Avenue, Palo Alto, California 94304-1338 • PO Box 10412, Palo Alto, California 94303-0813 USA
800.313.3774 • 650.855.2121 • askepri@epri.com • www.epri.com